On the Lagrangian Theory of Structure Formation in Relativistic Cosmology : intrinsic Perturbation Approach and Gravitoelectromagnetism

Fosca Al Roumi

Thèse

présentée devant

l'Université Claude Bernard Lyon - I

École Doctorale de Physique et d'Astrophysique

pour l'obtention du

DIPLÔME de DOCTORAT

Spécialité : Physique Théorique / Cosmologie

(arrêté du 7 août 2006)

par

Fosca Al Roumi

Théorie Lagrangienne Relativiste de la Formation des Grandes Structures : Description Intrinsèque des Perturbations et Gravitoélectromagnétisme

A soutenir publiquement le 18 Septembre 2015 devant la Commission d'Examen :

Prof.	P.	Salati	*Président du jury*	-	LAPTH, Annecy le Vieux
Prof.	B.	Roukema	*Rapporteur et examinateur*	-	Torún Centre for Astronomy, Torún
Prof.	R.	Sussman	*Rapporteur et examinateur*	-	Instituto de Ciencias Nucleares, México, D. F.
Prof.	R.	Triay	*Examinateur*	-	CPT, Marseille
Prof.	R.	Walder	*Examinateur*	-	CRAL, Lyon
Prof.	T.	Buchert	*Directeur de thèse*	-	CRAL, Lyon

PHD THESIS of the UNIVERSITY of LYON

Delivered by the UNIVERSITY CLAUDE BERNARD LYON 1

Subject:

THEORETICAL PHYSICS / COSMOLOGY

submitted by

Ms FOSCA AL ROUMI

for the degree of

DOCTOR OF THEORETICAL PHYSICS

On the Lagrangian Theory of Structure Formation in Relativistic Cosmology: Intrinsic Perturbation Approach and Gravitoelectromagnetism

---

To be defended 18 September 2015 in front of the following Examining Committee:

Prof.	P.	Salati	*President*	-	LAPTH, Annecy le Vieux
Prof.	B.	Roukema	*Reviewer and examiner*	-	Torún Centre for Astronomy, Torún
Prof.	R.	Sussman	*Reviewer and examiner*	-	Instituto de Ciencias Nucleares, Mexico City
Prof.	R.	Triay	*Examiner*	-	CPT, Marseille
Prof.	R.	Walder	*Examiner*	-	CRAL, Lyon
Prof.	T.	Buchert	*Supervisor*	-	CRAL, Lyon

Acknowlegments / Remerciements

First of all I would like to thank my mentor, Thomas Buchert. It will take me many years to realize how lucky I've been to work under your direction. Thank you for all your scientific skills, your patience and your rigor. But most of all, thank you for your sense of humor, your creativity and for being so open-minded. I hope I took some of your qualities during these three years.

I wish to thank Gilles Chabrier for his fruitful remarks during seminars and for hosting us at CRAL-ENS.

My thanks to Herbert Wagner and Martin Kerscher, with whom I worked in Munich on gravitoelectromagnetism. Your help, remarks and advices have been very important for my work on this topic. This student exchange was supported by the French–Bavarian Cooperation Center, BFHZ Munich http://www.bayern-france.org/.

Special thanks to Xavier Roy, who helped me a lot throughout the PhD. Thank you for the detailed answers to my questions, for all the explanations on foliation of space-time and differential geometry and for all the useful advices you gave me on the manuscript. Thank you also for all the non-scientific discussions we had. They have been crucial to me.

My thanks to Alexander Wiegand for the fruitful discussions, the nice work we did together, for you time and advices.

Thanks to Léo Brunswic for all the work we achieved on topology and Hodge decomposition. Your mathematical skills have been really precious for this work.

I wish also to thank Alexandre Alles for the help and the useful discussions on the blackboard.

My thanks to Boud Roukema for the useful discussions on topology and for his very interesting work on inhomogeneous cosmology. Thank you for your time and help!

Thanks to Frank Steiner for sharing his great knowledge on cosmic topology.

Martin France, thank you for all the nice discussions we had on the CMB.

Thanks to Rolf Walder for the nice remarks and discussions we had during the seminars.

I would also like to thank Roberto Sussman and Boud Roukema for having accepted to be reviewer of my thesis and spending some of your precious time on reading my thesis and writing a report.

I also want to thank Pierre Salati for being the president of my examining committee, for the very interesting discussions we had on the scalar model for dark matter at the beginning of my PhD and at Cargèse last september. Thank you also for all the help gave me in my research career.

I also want to thank Roland Triay and Rolf Walder for having accepted to be examiner of my thesis.

Thanks to Jan Ostrowski for everything: from physics to beers and ping-pong.

Thanks also to Pierre Mourier for the scientific discussions and the nice time we had together. Good luck with your PhD!

Thanks to Thomas Buchert, Martin France, Boud Roukema, Rolf Walder, Frank Steiner, Léo Brunswick, Jan Ostrowski, Tomek Kazimierczak and Pierre Mourier for the really nice dinners we had together. It is a pleasure to talk about science or something else around a glass of wine!

Je voudrais aussi remercier Stephanie Vignier, Sylvie Réa and Sylvie Flores pour avoir rendu tous les aspects administratifs bien plus simples. C'est toujours avec grand plaisir que je suis allée vous poser des questions et vous demander de l'aide. Merci pour votre patience et votre bonne humeur!

Vielen Dank an Marie von München. Les quelques jours de rédaction à Munich ont étés un vrai plaisir!

Merci à tous mes amis lyonnais, qui m'ont fait passer d'excellents moments pendant ces trois ans! Merci à Julien, Catherine, Martin, Elisa, Tatjana, Camille, Grégoire, Lila, Elsa, Thiago, Mariana, Mirella et Matei.

Un grand merci à mes colocs adorés, Matteo et Lucy. Quel bonheur d'avoir partagé avec vous le même toit!

Martin, merci aussi pour tous tes conseils sur la rédaction de la thèse! Tatjana, merci de m'avoir acceuillie après cette longue période de rédaction à Milano, la ville qui ne se couche jamais. Julien, merci de m'avoir aidée à certains moments particulièrement délicats!

Merci aussi à mes amis parisiens! Julia, Fanny et Victoria, les moments que nous avons passés ensemble et les fous rires que nous avons eus ont grandement participé à mon équilibre mental. Merci aussi à Daniel, Louison, Olivier, Léo. J'espère vous voir plus souvent maintenant.

Merci enfin à Mohamad et Amélie pour avoir toujours étés là pour moi. Vous m'avez beaucoup aidée. Merci aussi à mon frère Meyar pour m'avoir prêté son coffret Paradjanov. Constance, il faudrait un chapitre entier pour te remercier. Alors, je préfère le faire de vive voix dans un bon restaurant!

Sans ces rencontres et ces échanges, mon travail de thèse n'aurait pas été possible. Je vous remercie donc sincèrement.

Abstract

The dynamics of structure formation in the Universe is usually described by Newtonian numerical simulations and analytical models in the frame of the Standard Model of Cosmology. The structures are then defined on a homogeneous and isotropic background. Such a description has major drawbacks since, to be self-consistent, it entails a large amount of dark components in the content of the Universe.

Different strategies are considered to solve this enigma. Particle physicists have been searching for some exotic sources of the stress-energy tensor to account for these dark components. Nevertheless, no direct evidence of these 26% of dark matter and 69% of dark energy has yet been given. Therefore, some alternative theories to General Relativity are explored.

To address the problem of dark matter and dark energy, we will neither suppose that exotic sources contribute to the content of the Universe, nor that General Relativity is obsolete. We will develop a more realistic description of structure formation in the frame of General Relativity and thus no longer assume that the average model is a homogeneous-isotropic solution of the Einstein equations, as claimed by the Standard Model of Cosmology.

During my work under the supervision of Thomas Buchert, I contributed to the development of the perturbative formalism that enables a more realistic description of space-time dynamics. In the framework of the intrinsic Lagrangian approach, which avoids defining physical quantities on a flat background, I contributed to the building of relativistic solutions to the gravitoelectric part of the Einstein equations from the generalization of the Newtonian perturbative solutions. Moreover, the gravitoelectromagnetic approach I worked with has provided a new understanding of the dynamics of the analytical solutions to the field equations. Finally, treating globally the spatial manifold, I used powerful mathematical tools and theorems to describe the impact of topology on the dynamics of gravitational waves.

Résumé

La dynamique de formation des structures de l'Univers est habituellement décrite dans le cadre du modèle standard de Cosmologie par des simulations numériques newtoniennes et des modèles analytiques. Les structures sont alors associées à des grandeurs définies sur un fond homogène et isotrope. Cependant, pour que les observations cosmologiques soient cohérentes avec le modèle standard, il est nécessaire de supposer l'existance d'une grande proportion d'éléments de nature inconnue dans le contenu de l'Univers.

Différentes stratégies sont envisagées pour déterminer la nature de ces éléments. En effet, les physiciens des particules cherchent des particules exotiques, qui pourraient alors rendre compte des 26% de matière noire et 69% d'énergie sombre. Cependant, aucune mesure expérimentale n'ayant pour l'instant démontré l'existence de ces éléments, des théories de gravitation alternatives à la relativité générale sont actuellement envisagées.

Pour tenter de résoudre ce problème, nous ne considèrerons pas d'autres sources dans le contenu de l'Univers que celles ordinaires et resterons dans le cadre de la Relativité Générale. Nous développerons néanmoins une description plus réaliste de la formation de structures dans le cadre de la théorie d'Einstein. Ainsi, contrairement au modèle standard de Cosmologie, nous ne supposerons pas que l'Univers moyenné est une solution homogène et isotrope des équations d'Einstein.

Lors de mon travail sous la direction de Thomas Buchert, j'ai participé au développement d'un formalisme perturbatif permettant une description plus réaliste de la dynamique de l'espace-temps. J'ai également contribué à l'obtention de solutions relativistes à la partie gravitoélectrique des équations d'Einstein en généralisant les solutions perturbatives newtoniennes. Ces travaux ont été réalisés dans le cadre d'une approche lagrangienne intrinsèque, évitant ainsi de définir les grandeurs physiques sur un fond plat. L'approche gravitoélectromagnétique que j'ai adoptée m'a permis une interprétation nouvelle et performante des solutions des équations d'Einstein. Enfin, j'ai étudié l'impact de la topologie sur la dynamique des ondes gravitationelles à l'aide d'une description globale de l'hypersurface spatiale, permise par des théorèmes mathématiques puissants.

"Put your hand on a hot stove for a minute,
and it seems like an hour.
Sit with a pretty girl for an hour,
and it seems like a minute.
That's relativity!"

Albert Einstein

Contents

Motivation

Determining the nature of what surrounds us and its history has been one of the most ambitious project that human kind has dared to undertake. Through time, the precision of the observations of the Universe has improved. Combined with philosophical and theoretical developments, they led to changes of paradigms which finally resulted in our current idea of the Universe. The representation of the Universe shared by most of the observational cosmologists is the Standard Model of Cosmology, namely the ΛCDM model (Cold Dark Matter model with a cosmological constant modeling dark energy). This model gives the evolution of the Universe and its constituents, from the inflation to the formation of large scale structures, and assumes a decoupling of the dynamics of the small structures with respect to the global evolution of space-time, which is described as being locally isotropic and hence homogeneous on all scales.

For the cosmological observations to be consistent with this model, a large amount of unknown constituents has to be postulated. Indeed, at most 5% of the energy budget of the Universe can be explained using the matter content of the standard particle physics while $\sim 69\%$ of the content of the Universe is attributed to dark energy and 26% to dark matter, which are both of hypothetical origin.

Different strategies are considered to determine the true nature of these dark components. Particle physicists have been searching for some exotic sources of the stress-energy tensor in order to account for these dark components. Even if many candidates for dark matter and dark energy have been considered, no direct evidence has yet been obtained. Doubting of the success of the detection experiments undertaken by astroparticle physicists, alternative theories to General Relativity are now being explored [111, 12].

To address the problem of dark matter and dark energy, the strategy we will adopt will neither suppose that exotic sources contribute to the content of the Universe, nor that General Relativity is obsolete. We will develop a more realistic description of structure formation that takes into account the inhomogeneities of the distribution of matter in the theoretical framework of Einstein's theory. Thus, we will go beyond the ΛCDM model and no longer assume that the average model is a homogeneous-isotropic solution of the Einstein equations [103, 102]. The inhomogeneous approach allows a refined description of the dynamics of the Universe and takes into account, through a term named backreaction, the coupling between the matter content and the geometry of the Universe. Inhomogeneities of the distribution of matter and geometry will have an impact on the history of structure formation and, according to some models, may even be capable of replacing the dark matter and dark energy in the dynamics of the Universe, then solving one of the major mysteries of modern physics.

In order to quantify the effects of the backreaction term on the dynamics of the Universe Thomas Buchert has proposed an averaging formalism [30, 29]. During my three-year work under the direction of Thomas Buchert, I contributed to the development of the intrinsic Lagrangian perturbation formalism, which defines perturbations locally in a relativistic way, without the need for a global background. I adopted in most of my work the irrotational dust matter model, which accounts for the impact of large-scale structures on the average properties of the Universe down to scales of rich galaxy clusters ($2-3\,h^{-1}$ Mpc), irrespective of whether we assume "dust" to be the dark matter component or ordinary matter, since pressure-, dispersion- and vorticity-effects become important only on smaller scales [1] .

My PhD builds on two previous works on the Lagrangian theory of structure formation in relativistic cosmology. The first one, accomplished by Thomas Buchert and Matthias Ostermann [35] presents the Lagrangian framework for the description of structure formation in General Relativity and defines the relativistic generalization of the Zel'dovich approximation [161]. The second one, by Thomas Buchert, Charly Nayet and Alexander Wiegand [36], averages the inhomogeneous cosmological equations for an irrotational dust matter model and evaluates the backreaction term in the relativistic Zel'dovich approximation.

During my three-year work, I contributed to the building of relativistic solutions to the gravitoelectric part of the Einstein equations from the generalization of the Newtonian perturbation and solution schemes at any order of the perturbations, published by Alexandre Alles, Thomas Buchert, Fosca Al Roumi and Alexander Wiegand [4]. The gravitoelectromagnetic approach I worked with has provided me with a new understanding of the dynamics of the analytical solutions to the field equations. It shed a new light on the complementary part to the gravitoelectric solution, which, at first-order, contains the propagative dynamics: gravitational waves. To determine the propagative solutions, elliptic equations had to be solved, thus needing boundary conditions, provided by a global treatment of the spatial manifold. In order to do so, I used powerful mathematical tools and theorems to describe the impact of topology on the dynamics of gravitational waves.

To present what I accomplished during my three-years PhD under the supervision of Thomas Buchert, I divided the manuscript into three parts:

- **Part 1:**
  This part of the thesis settles the framework of the investigations I led during my PhD. In the first part, I present Einstein's theory of General Relativity and explain why it as a true revolution in the representation and treatment of spacetime. Afterwards, I discuss on which observational grounds the Standard Model of Cosmology is built and which assumptions it implies on the matter distribution of the Universe. I then sum up the full Big Bang scenario of the history of the Universe, from inflation to late times in a short review. The next chapter is dedicated to the Lagrangian description of large scale structure formation, first in the Newtonian frame then in the relativistic one. The approach and the formalism that is then

1. We could alternatively describe the effect of backreaction at the different structure scales with a multiscale model [155].

presented will be the one developed in the next parts. In the last chapter of this part, I provide the deep motivations for the inhomogeneous approach we develop. The additional term that appears in our formalism with respect to the standard model, namely backreaction, may overcome the failures of the standard model.

- **Part 2:**
  Part two is subdivided into two chapters. In the first one, I present the main features of the gravitoelectromagnetic approach of General Relativity. I first present the 3+1 decomposition of the Einstein equations for general foliations and matter models. I then specify these equations for an irrotational dust matter model and a flow orthogonal foliation. Thereafter, I discuss how GEM can provide us with a new insight into the physics of the Einstein equations and will focus on the formulation of General Relativity in terms of the electric and magnetic parts of the Weyl tensor. A formal analogy between the Newtonian equations of gravity formulated in the Lagrangian framework and the gravitoelectric part of the Einstein equations will be discussed. Furthermore, I will present the Minkowski Restriction, which is a mathematical tool that will enable us to go from a tensorial to a vectorial gravitation theory and under certain conditions from Einstein's General Relativity to Newton's theory. The inverse Minkowski Restriction will be used to obtain relativistic solutions of the gravitoelectric part of the Einstein equations from the Newtonian perturbative solutions at order n . This scheme will be the subject of the second chapter of this part.
- **Part 3:**
  The solution obtained from the generalization of the Newtonian perturbative solution to order n does not contain the propagative dynamics. Indeed, up to first-order, gravitational waves are contained in the complementary part of this solution. To obtain the full first-order solutions, elliptic equations have to be solved. Their solutions depend strongly on the topology of the spatial sections. For this reason, one of the main aspects of this part will be to study the impact of topology on the dynamics of these gravitational waves with the help of powerful mathematical tools available on closed manifolds, e.g. the Hodge theorem.

Throughout the manuscript, without further specification, the equation numbers will refer to equations in the same part.

Part I

Introduction

Chapter 1

General Relativity and the Standard Model of Cosmology

Contents

During medieval times, the Universe was considered to be something fixed, with the Earth at its center. The Universe was geocentric and the Moon, the Sun, the other planets and the stars moved in circles around the Earth. However, by placing the sun at the center of the Universe and not the Earth, Copernicus drastically changed the representation of the Universe that was shared by most of the physicists. As the observational techniques developed and improved, the center of the Universe was shifted further away. Thanks to his refracting telescope, in 1610 Galileo Galilei discovered that the Milky way was composed of a big number of stars. Nevertheless, until the beginning of the XXth century, the advances in the representation of the Universe were motivated by some hypothetical and philosophical ideas. Around 1755, Kant postulated that the Milky Way was made of a huge number of stars and that the visible nebulae could be some other island universes like the Milky Way.

The idea of island-universe only reappeared thanks to the photography of a supernova made by Herber Curtis in 1917. The luminosity of this exploding star was fainter than usual and the distance was estimated to 150 kpc, far beyond the limit of our island-universe. Even if his discovery was controversial at that time, Curtis was convinced that this object was not in the Milky Way. It was during this debate period that the term of galaxy was first used. Thanks to his reflective telescope, Edwin Hubble in 1923 managed to observe in detail several Cepheids [81, 82]. This enabled him to determine more precisely the distance between the Earth and these objects.

General Relativity was born in this context. Within the two years after its birth, Einstein realized that his theory could be applied to the dynamics of the whole Universe. When he applied his equations to cosmology in order to find a solution to describe the Universe, Einstein realized that it could be a dynamical entity. He then rejected this idea and inserted a term, the cosmological constant Λ, into the equations in order to obtain a static universe. However, in 1929 Edwin Hubble observationally verified that the Universe was expanding [1].

In this part, we will first discuss the theoretical framework of General Relativity and explain why it is so innovative and powerful. In order to do so, we will present the different stages of its development and will end up with its mathematical formulation. Then, we will explain how the Standard Model of Cosmology (*SMC*) has emerged from it and which approximations it entails. Finally, we will give an overview of the history of structure formation from inflation to the large scale structure formation, that will be the subject of Chapter I.2.

1.1 Einstein's theory of General Relativity

In this section, I present the conceptual path which led to General Relativity. I explain how Einstein abandoned the notion of absolute space and time to build an intrinsic gravitation theory, where matter tells space-time how to curve, and space-time tells matter how to move. I then introduce the mathematical formalism of the Einstein's equations,

1. Lemaître was actually the first to conclude this from Slipher's observations (*cf* Section I.1.2.1).

which relate the Ricci curvature tensor to the matter content of the Universe, represented by the stress-energy tensor. This discussion is inspired by the excellent books [130, 74].

1.1.1 From Newtonian gravity to General Relativity

Newton's theory of gravity

Newton's first assumption was the existence of a reference frame with an absolute space and an absolute time passing at the same rate everywhere in space. He postulated an instantaneous action-at-a-distance force that violated the idea shared by physicists at that time, namely that interactions could only happen between entities in contact:

$$F = G\,\frac{m_1\,m_2}{d^2}\;. \tag{1.1}$$

The force is a function of d the distance between the two masses, m_1 and m_2 their mass and G the gravitational constant.

Newton's theory was a total success. Moreover, he defined a class of non-rotating reference frames moving uniformly in an absolute space. He called them the Galilean reference frames. Relative to these Galilean reference frames, all mechanical systems behave according to Newton's laws. This is the Galilei-Newton principle of relativity.

Einstein observed a formal similarity between Newton's force and Coulomb's force and concluded that Newton's theory could be the static limit of a dynamical field theory. Moreover, gravitational interaction could share the same property as the electromagnetic interaction: i.e. not to be instantaneous. These ideas guided him in the search for a more general gravitation theory.

Special Relativity

Einstein noticed that Maxwell's electromagnetic theory was not Galilean invariant. Therefore, Newtonian equivalence principle of the Galilean frames could not be extended straightforwardly to electromagnetism. Indeed, applying the Galilean coordinate transformation to Maxwell's electromagnetic theory, one found that Maxwell's equations were not invariant. Furthermore, there was only one Galilean frame in which electromagnetic waves had an isotropic velocity.

The Michelson-Morley experiment [110] was designed to measure the velocity of the Earth with respect to this preferred frame [2] but demonstrated that the notion of absolute space had no physical legitimacy.

Furthermore, Einstein was convinced that, despite the apparent contradiction, the physics was the same in all moving inertial frames and that the Maxwell equations were correct. He realized that, by dropping the prejudice on the temporal structure of time i.e. that simultaneity is well defined in a manner independent from the observer, and by accepting the fact that temporal ordering of distant events may have no meaning,

2. Michelson-Morley experiment was supposed to measure the velocity of the Earth with respect to the "ether", a materialization of Newton's absolute space. It failed and Newton's idea of an absolute space had no physical grounds.

the picture could be consistent again. Einstein had overcome the contradiction and built Special Relativity.

He then looked for the field theory that gave (1.1) in the static limit. In order to do so, he based his work on what Faraday and Maxwell did with the Coulomb force to obtain Maxwell theory of electromagnetism.

Relativity of motion

Einstein was convinced that Newton's idea of an absolute space was wrong. According to him, only relative motions could be physically meaningful.

In Newton's bucket experiment [3], when the water rotates, it results in the concavity of its surface. If the water rotated with respect to the rotating bucket that surrounds it, then the surface of the water would be flat. For Newton, the rotation was with respect to the absolute space whereas for Einstein, the water rotates with respect to a local physical entity: the gravitational field.

Galilei proved that the gravitational and inertial mass were the same for all bodies by demonstrating that freely falling bodies moved in the same way, regardless of their mass and of their composition. As a consequence, Newton asserted that the laws of physics should be the same in the Galilean frames (i.e. in the regions far from mass distributions, where there are no gravitational fields) and in frames falling freely in a gravitational field (for which inertial forces compensate gravitational ones). Nevertheless, Newton distinguished the Galilean frames in absence of gravity and free falling non-inertial frames. Einstein dropped this distinction, which referred to the existence of a global frame, and realized that each mass at a given space-time point had its own local inertial reference frame. Since these local inertial frames were defined by the absence of inertial effects, Einstein understood that it is gravity that specifies at each point the inertial motion and thus determines the local inertial frames.

General covariance

Around 1912, the field equations for the gravitational field were still missing. At first, Einstein demanded the field equations for the gravitational field to be generally covariant on the space-time manifold. This meant that the laws of physics should be the same in all coordinate systems. But then, he realized that general covariance did not only imply invariance of the theory with respect to passive diffeomorphisms (i.e. coordinate transformations). The consequences were far more important. Indeed, a deterministic prediction was no longer possible for a given space-time point. Predictions were only possible at locations determined by the dynamical elements of the theory themselves [4].

3. In this experiment, we consider a bucket full of water that starts rotating. First, the bucket rotates with respect to us and the water remains still. The surface of the water is flat. Then, the motion of the bucket is transmitted to the water by friction and thus the water starts rotating together with the bucket. At some time, the water and the bucket rotate together. The surface of the water is concave [130].

4. It was the "Hole" argument which made Einstein first renounce to the general covariance. He struggled for three years and finally understood that the notion of a space-time point had to be abandoned. For an explanation of the "Hole" argument, see [130].

It followed that localization on the manifold has no physical meaning. The background space-time Newton believed in was eliminated in this new understanding of the dynamics. Reality is not made by particles and fields on space-time: it is made by particles and fields that can only be localized with respect to one another.

1.1.2 Einstein's field equations

Einstein's theory of General Relativity was a true revolution in the representation of space-time since it gave up the idea of a gravitational force and an absolute frame [59]. Newton's motion of a particle under the influence of a gravitational force was replaced by free motion along the geodesic curves in a curved space-time. The Einstein field equations formalize the coupling between the matter content of the Universe and its geometry. According to Einstein's field equations, matter tells space-time how to curve, and space-time tells matter how to move. Space-time is a four dimensional manifold $\mathcal{M}$ on which the metric bilinear form $\mathbf{g}$ with signature $(-,+,+,+)$ acts.

The matter and energy local content is encoded into the stress-energy tensor, which is a symmetric tensor $\mathbf{T}$. To ensure the conservation of the energy and momentum of the continuum of matter and energy, its covariant divergence has to vanish. The stress-energy tensor being coupled to the geometry of space-time, a symmetric divergence-free tensor had to be built from the following geometrical quantities: the metric, the Ricci curvature tensor $\mathbf{R}$ associated with the metric $\mathbf{g}$ and its trace: the Ricci scalar $\mathcal{R}$. The Einstein tensor $\mathbf{G}$ fulfills these conditions.

The dynamics of $(\mathcal{M}, \mathbf{g})$ is linked to the matter content of the Universe $\mathbf{T}$ via the Einstein equations:

$$\mathbf{G} = 8\,\pi\,G\,\mathbf{T} \quad , \quad \mathbf{G} = \mathbf{R} - \frac{1}{2}R\,\mathbf{g} + \Lambda\,\mathbf{g}\,, \tag{1.2}$$

where G is the gravitational constant. The tensor formulation of the Einstein equations ensures the covariance of the theory. The projection of these equations on a basis gives[5]:

$$G_{\mu\nu} = 8\,\pi\,G\,T_{\mu\nu} \quad , \quad G_{\mu\nu} = R_{\mu\nu} - \frac{1}{2}R\,g_{\mu\nu} + \Lambda\,g_{\mu\nu}\,. \tag{1.3}$$

The Einstein equations determine the dynamics of cosmological objects of different size such as black holes, galaxies or even the whole Universe. For example, to describe a star or a static spherical symmetric black hole, the Schwarzschild metric is considered [134]. For a spherical symmetric rotating object, the Kerr metric will have to be considered [86]. Moreover, the LTB metric [145] is the one adopted to describe an inhomogeneous spherical symmetric object.

The next section will give a short introduction to standard cosmology. The curious reader may find a detailed introduction to cosmology in one of these excellent works [90, 98] or in [151] for an additional introduction to General Relativity.

5. The greek indices represent space-time coordinates, they run in $\{0,1,2,3\}$. The latin indices run in $\{1,2,3\}$ and correspond to the spatial coordinates. Einstein summation convention on repeated indices is adopted and we consider that $c = 1$. Furthermore, the Einstein tensor $G_{\mu\nu}$ is not related to the Gram tensor of the coframes G_{ab} that we introduce in the third chapter of this part.

1.2 Homogeneous and Isotropic Cosmology

Once he had built General Relativity, Einstein realized that he could apply it to the full Universe as a single object. Thereafter, cosmologists quickly developed a cosmological model based on strong hypothesis: spatial homogeneity and isotropy. This model is the Standard Model of Cosmology (*SMC*).

In this section, will first present the observational grounds on which the homogeneous isotropic and expanding universe model is based. The spatial length above which the Universe can be considered as homogeneous and isotropic is indeed still debated. Then, we will explain how Hubble's observations (or actually Lemaître's observational analysis) combined with Slipher's redshift data led to the idea of an expanding universe. Afterwards, we will give the adapted metric to describe a homogeneous isotropic space-time in polar coordinates, namely the FLRW metric. We will show how the Hubble parameter is linked to the scale factor and obtain from the Einstein equations and the Bianchi identities the conservation of the energy and momentum and the Friedmann equations. Then, we will introduce the cosmological parameters, which are the parameters of the *SMC* .

1.2.1 The Cosmological Principle and the Hubble law

The Cosmological Principle

The first solutions of Einstein's equations were obtained for homogeneous and isotropic universe models. The homogeneity and isotropy hypothesis are based on the following cosmological observations. When we observe galaxies, looking in different directions of the sky, the galaxies are evenly distributed at large scales. Large scales in this context are neither galactic scales nor galactic clusters scales. They are scales greater than a certain spatial length beyond which the Universe is statistically homogeneous and isotropic. This scale is estimated to be in the interval of $100\,h^{-1}$ Mpc [6] [159, 142, 95] and $700\,h^{-1}$ Mpc. As the observation technics and statistical treatments improved, fluctuations were shown to have an impact on large scales as $200\,h^{-1}$ Mpc found in [87, 77] or even $700\,h^{-1}$ Mpc in the paper by Wiegand et al. [156]. Most of the estimations are based on lower order statistical properties, whereas the larger results are extracted from Minkowski functionals and higher order perturbations. The baryon acoustic oscillation (BAO) scale has been shown to be inhomogeneous at the $100\,\mathrm{Mpc}^{-1}$ scale [128].

The cosmological principle asserts that there exists a spatial length beyond which the Universe is statistically homogeneous and isotropic. However, the *SMC* extrapolates from these global observations a *local* isotropy, resulting in global homogeneity. The simplest cosmological model, the homogeneous and isotropic cosmological model, results from these very strong assumptions.

6. with the dimensionless factor $h = (H/100)\ km.s^{-1}.\mathrm{Mpc}^{-1}$ where H is Hubble constant and will be presented later

Expanding Universe and the Hubble law

Hubble published in 1929 a study based on 18 galaxies (in which cepheids could be seen) which showed that the speed of galaxies along the line of sight, or equivalently, their redshift, was proportional to their distance. To do so, he combined the relation between the luminosity of the cepheids and their distance to the recessional velocities of the galaxies in which these cepheids were. This quantity was calculated by Vesto Slipher through the use of the redshift. However, Georges Lemaître was actually the first one to obtain these conclusions. His article was published in French two years before Hubble's and was based on Slipher's same redshift data and Hubble's calculated distances. The coefficient of proportionality, H, is called the Hubble parameter.

In 1998, two teams, the Supernova Cosmology Project [118], and the High-z Supernova Search team [124], reported that, interpreting their data within the *SMC* , the Universe is not only expanding, but also accelerating. As we will see in the next part, within the *SMC* , the acceleration of the expansion of the Universe requires the mass-energy density of the Universe to be dominated at the present time by a gravitationally repulsive component: the cosmological constant Λ.

1.2.2 Homogeneous and isotropic universe models

Spatial homogeneity and isotropy allows a simple foliation of space-time. A scalar parameter that is called cosmic time t labels the spatial sections. The time direction can be represented by the time-like vector $\mathbf{e}_t$. It is possible to build spatial sections Σ_t such that $\mathbf{e}_t$ is everywhere orthogonal to them. As was found by Friedmann, Lemaître, Robertson and Walker in the 1920's and 1930's [70, 97, 125, 150], for such a high symmetry space-time, we can choose the following line-element [7]:

$$ds^2 = dt^2 - a(t)^2 \left(\frac{dr^2}{1 - kr^2} + r^2(d\theta^2 + \sin^2\theta d\phi^2) \right) \quad . \tag{1.4}$$

This metric is called the Friedman-Lemaître-Robertson-Walker (FLRW) metric. The variables r, θ, ϕ are polar coordinates. All physical length scales are multiplied by $a(t)$, the scale factor that describes a homogeneous expansion of the Universe. k is a constant number that represents the spatial curvature.

If we assume that the space sections of the Universe are simply connected, then, for $k = 0$ the Universe is Euclidean (flat universe: hyperplane), for $k > 0$ the Universe is closed and has a spherical topology and for $k < 0$ the Universe is open and has a hyperboloid topology. Nevertheless, Einstein's field equations are local and thus do not constrain the global topology of the Universe. A multi-connex topology could also be a good candidate for the description of the space sections. A hypertorus topology, for example, can be flat (its curvature is zero everywhere) and closed (compact without boundaries) at the same time. Cosmic topology will be the subject of Section III.3.1 and Thurston's geometrization conjecture will be presented in Section III.3.2.1.

7. The FLRW metric is cited in a form that contains a coordinate singularity at the equator in the $k > 0$ case. This could be avoided by considering another set of coordinates.

For an FLRW metric, the dynamics are then encoded in the evolution of $a(t)$. The rate of change of a is called the expansion rate, or the Hubble parameter:

$$H(t) := \frac{1}{a}\frac{da}{dt} = \frac{\dot{a}}{a} \quad . \tag{1.5}$$

The value of the Hubble parameter today H_0 is often expressed as $H_0 = h \times 100\,\mathrm{kms^{-1}Mpc^{-1}}$. Its measured value today is roughly $h \sim 0.7$. The evolution of $a(t)$ depends on the matter content of the Universe and can be calculated using Einstein's field equations (1.3). The most general form of the stress-energy tensor which is compatible with homogeneity and isotropy, is the stress-energy tensor of the form:

$$T_{\mu\nu} = (p+\rho)u_\mu u_\nu + p g_{\mu\nu} \quad . \tag{1.6}$$

In the fluid restframe, it has the following matrix form:

$$T^\mu_{\ \nu} \quad = \quad \begin{pmatrix} \rho & 0 & 0 & 0 \\ 0 & -p & 0 & 0 \\ 0 & 0 & -p & 0 \\ 0 & 0 & 0 & -p \end{pmatrix} \quad , \tag{1.7}$$

where ρ is the mass density, p is the pressure of the cosmological fluid, $u_\mu = (-1,0,0,0)$ and $u^\mu = (1,0,0,0)$. Homogeneity implies that the pressure and density should be position-independent on the spatial hypersurfaces Σ_t. Hence, they can only be time-dependent. If the 4–velocity of the fluid has a spatial component, then the assumption of spatial isotropy is violated. Thus the vector u_μ has only a time component and the fluid flow is orthogonal to the hypersurfaces.

When we insert the metric given by (1.4) into the Einstein equations (1.3), we get the following Friedmann equations in the presence of a cosmological constant:

$$H^2 = \left(\frac{\dot{a}}{a}\right)^2 = \frac{8\pi G}{3}\rho - \frac{k}{a^2} + \frac{\Lambda}{3} \quad , \tag{1.8}$$

$$3\frac{\ddot{a}}{a} = 4\pi G(\rho + 3p) + \Lambda \quad . \tag{1.9}$$

One sees that only a positive curvature term decreases the expansion of the Universe, all other terms enhance the expansion rate.

Bianchi identities give the energy momentum conservation for a fluid with energy momentum tensor given in equation (1.7) in an expanding universe

$$u_\beta \nabla_\alpha T^{\alpha\beta} \quad \Rightarrow \quad \dot{\rho} = -3\frac{\dot{a}}{a}(\rho + p) \quad , \tag{1.10}$$

where ∇_α is the Levi-Civita connexion on $\mathcal{M}$ [8].

The cosmological constant was introduced as a geometrical quantity in (1.3). It can also be interpreted as a uniform and stationary fluid with pressure and density:

$$\rho_\Lambda = \frac{\Lambda}{8\,\pi\,G} \quad ; \quad p_\Lambda = -\frac{\Lambda}{8\,\pi\,G} \quad . \tag{1.11}$$

8. It thus has no torsion: for any scalar field ψ, $\nabla_\alpha\nabla_\beta\psi = \nabla_\beta\nabla_\alpha\psi$ and is associated to the metric $\mathbf{g}$.

To determine the evolution of the scale factor $a(t)$, we have to consider an equation of state for the fluid. Most of the time, we consider it of the form:

$$p(t) = w(t)\rho(t) \ . \tag{1.12}$$

If $w(t)$ is constant, then the conservation of the energy (1.10) gives $\rho \propto a^{-3(1+w)}$. As will be detailed in Section I.1.3, after inflation, the Universe was consecutively dominated by radiation, matter and by the cosmological constant Λ. The global evolution of the size of the Universe can be determined by solving the system of equations (1.8), (1.9) and (1.10).

- The equation of state of radiation is obtained for $w = 1/3$ and consequently the radiative energy $\rho_r \propto a^{-4}$. Therefore the size of the Universe grows as $a(t) \propto t^{1/2}$ during the radiation domination era. Not only the number density gets diluted but also the energy per particle is redshifted when the Universe expands. Both effects sum up to a faster dilution of an ultra-relativistic fluid such as radiation compared to a non-relativistic fluid such as pressureless matter.
- After the radiation domination era, expansion is due to the non-relativistic pressureless matter, for which $w = 0$, $\rho_m \propto a^{-3}$ and the size of the Universe grows as $a(t) \propto t^{2/3}$.
- Finally, due to the cosmological constant Λ, expansion accelerates . Then $w = -1$ and the scale factor is $a(t) \propto t^{(\Lambda/3)^{1/2}t}$.

- During a potential domination of curvature, the Universe would be expanding linearly with time: $H^2 \propto R^{-2} \quad \Rightarrow \quad a(t) \propto t$.

In the model of evolution of the Universe that is considered by most cosmologists nowadays, at some moment in the past, the scale factor was equal to zero. This initial singularity is called the "Big Bang". However, at times smaller than the Planck time, General Relativity is no longer valid. Gravitational quantum effects should be taken into account. Therefore, the physical treatment that we used here no longer holds.

If we divide the Friedman equation by H_0^2 and define

$$\Omega_r := \frac{8\pi G}{3H_0^2}\rho_R(t_0) \ , \tag{1.13}$$

$$\Omega_m := \frac{8\pi G}{3H_0^2}\rho_M(t_0) \ , \tag{1.14}$$

$$\Omega_k := -\frac{k}{R_0^2 H_0^2} \ , \tag{1.15}$$

$$\tag{1.16}$$

$$\Omega_\Lambda := \frac{\Lambda}{3H_0^2} \ , \tag{1.17}$$

the Friedman equation today now reads

$$1 = \Omega_r + \Omega_m + \Omega_k + \Omega_\Lambda \ . \tag{1.18}$$

In order to get rid of the uncertainty of H_0, the energy densities of the components of the Universe are usually given as $\Omega_x h^2$. The content of the Universe is given by the 2015 publication of the PLANCK collaboration [2] and is obtained from the analysis of the temperature fluctuations in the Cosmic Microwave Background [9]. The Hubble expansion rate and the energy densities from the non-relativistic matter and the cosmological constant are given for 68 % confidence levels, supposing that the Universe is flat since the energy densities from the curvature term satisfies $|\Omega_k| < 0.005$:

$$\begin{aligned} H_0 &= 67.74 \pm 0.46 \text{ kms}^{-1}\text{Mpc}^{-1} \ , && (1.19) \\ \Omega_M &= 0.3089 \pm 0.0062 \ , && (1.20) \\ \Omega_\Lambda &= 0.6911 \pm 0.0062 \ . && (1.21) \end{aligned}$$

The baryon mass density and the dark matter density are:

$$\begin{aligned} \Omega_B h^2 &= 0.02230 \pm 0.00014 \ , && (1.22) \\ \Omega_{\text{DM}} h^2 &= 0.1188 \pm 0.0010 \ . && (1.23) \end{aligned}$$

The baryon mass density can be measured to be $\Omega_B h^2 = 0.02205 \pm 0.00028$ (1σ) which is only $\sim 15\%$ of the total non-relativistic matter density in the Universe. The dark matter density is $\Omega_{\text{DM}} h^2 = 0.1199 \pm 0.0027$ (1σ).

1.3 Standard Model of Cosmology: history of structure formation and observational evidences

The *SMC* does not only include the Einstein equations for a homogeneous isotropic space-time, it also contains the history of the Universe, in the Big Bang scenario. In this standard picture, that we will present here, the Universe is well described on average throughout its history by the *SMC* of Cosmology. We will present what are considered to be the strong observational evidences for the ΛCDM model. Nevertheless, the values of the cosmological parameters are not directly obtained from the observations: they are interpreted via the *SMC* . Moreover, to be self-consistent, the *SMC* has to assume that 95% of the content of the Universe is of unknown nature.

The following elements I give on the early Universe and the nucleosynthesis are inspired by the very good lecture on standard cosmology [98].

1.3.1 Early stages

There is no theory that has been approved by the majority of the scientific community that describes the earliest stages of the evolution of the Universe. We here do a short overview of the standard picture of that period.

9. Today, the average temperature of the CMB is $T = 2.7255$ K.

The Planck Era

Just after the Big Bang, the fluctuations are so significant that a quantum theory of gravity is needed to describe the physics of the Universe. This quantum description is necessary until t_{Pl}, the *Planck time*, which is

$$t_{Pl} = \sqrt{\frac{\hbar G}{c^3}} = 5.4 \cdot 10^{-44} s \ . \tag{1.24}$$

At the time before t_{Pl}, the Universe was filled with a plasma of relativistic elementary particles [10], including quarks, leptons, gauge bosons. We think that the Universe existed in a state of fluctuating chaos during this era. Time was not a well defined quantity, and the curvature and the topology of space fluctuated very much.

The Inflationary Era

Shortly after the Planck era, the Universe went through a phase of accelerated expansion, called inflation, during which the Universe was expanding exponentially:
$a(t) = \exp(H_{infl}\ t)$. During this era, the energy content of the Universe was dominated by the potential energy of the inflaton, a scalar field that has negligible kinetic energy. Inflation ended when the inflaton oscillated around its minimum of potential. It then decayed into the particles of the Standard Model of Particles, which were produced with high kinetic energy. After inflation, the Universe was dominated by radiation since the particles formed a thermal bath of relativistic particles. The inflationary era lasted $10^{-33}s$.

At this point, the particles have no mass and quickly interact with other particles. Quarks are free particles and are not confined into hadrons.

At $T \sim 100$ GeV, the electroweak symmetry is spontaneously broken and the particles acquire their mass. Heavy particles become quickly non-relativistic.

At $T \sim 100$ MeV the QCD phase transition occurs: quarks are confined into hadrons.

Baryonic asymmetry

If baryon number was conserved during inflation, the number of baryons and antibaryons would be the same. They would then annihilate into photons : $b + \bar{b} \leftrightarrow n\gamma$. Then, the Universe would be filled with radiation and no matter.

At temperatures bigger then the baryonic mass, photons have enough energy to produce pairs of $b\bar{b}$. When the temperature drops below it, photons no longer recreate $b\bar{b}$. The number of baryons and antibaryons drops since they annihilate. Baryon number must have been violated at some point since we observe baryonic matter in the Universe today. Nevertheless, the original asymmetry was very small: $\frac{n_b - n_{\bar{b}}}{n_b + n_{\bar{b}}} \simeq 10^{-9}$.

At a temperature $T \sim 10$ MeV, only the over-density of baryons is left. Non-relativistic protons and neutrons dominate the matter content and neutrons can decay into protons by β decay $n \rightarrow p + e^- + \nu_e$. The reverse process being possible, the ratio of protons and

10. The corresponding temperature is $T_{Pl} \simeq 10^{32}\ K$.

neutrons is constant. Furthermore, electrons and anti-electrons are still relativistic while neutrinos and antineutrinos are thermalized by the weak interaction.

As the temperature drops, the neutrinos decouple. From then on, their density gets only diluted by the expansion of the Universe. Then, electrons become non-relativistic and annihilate until their number density is equal to the proton number density from charge conservation. Photons are the only relativistic species in the bath and their temperature scales until today in the same way as the neutrino temperature.

Nucleosynthesis

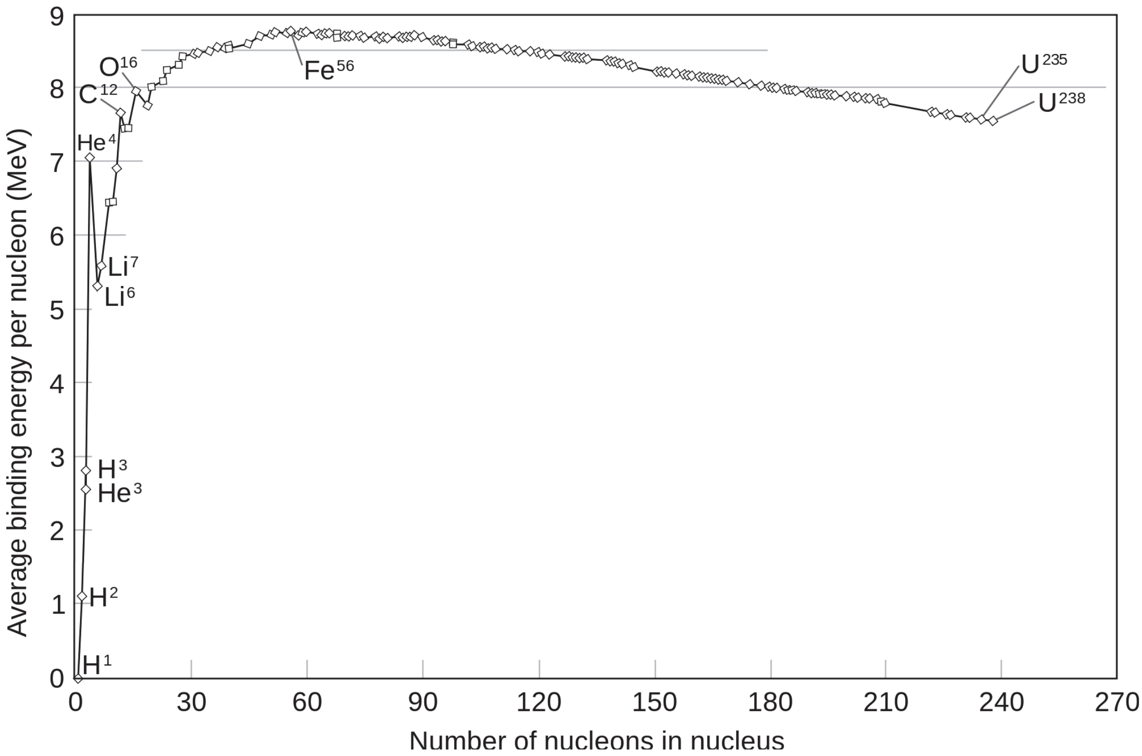

Figure 1.1: The average binding energy per nucleon in a nucleus as a function of the number of nucleons. The most strongly coupled nucleus is Fe^{56}. The picture was taken from https://commons.wikimedia.org/wiki/File:Binding_energy_curve_-_common_isotopes.svg, credits: Fastfission

The nucleosynthesis is the primordial formation of light elements and happens between $1s$ and $12\,mins$. Figure 1.1 presents the average binding energy per nucleon in a nucleus.

When temperature drops below the binding energy of deuterium $B_D \sim 2$ MeV (which is the first element having two nucleons in its nucleus: a proton and neutron) we would expect a formation of deuterium from the protons and neutrons since it is energetically more advantageous. However, there is still a large number of photons in the high energy tail of the photon distribution that can destroy the deuterium that was formed. It is only when $T \sim 0.07$ MeV that the formed deuterium is stable and that the nuclear reaction chain can take place:

$$\begin{aligned} p+n &\leftrightarrow \mathrm{D}+\gamma \\ \mathrm{D}+\mathrm{D} &\rightarrow {}^3\mathrm{He}+n \\ {}^3\mathrm{He}+\mathrm{D} &\rightarrow {}^4\mathrm{He}+p \end{aligned} \tag{1.25}$$

$$\cdots \tag{1.26}$$

Fe^{56} has the highest binding energy per nucleon but the number densities of intermediate nuclei are not high enough to form Fe^{56}. Nucleosynthesis stops around ^{4}He and only very few Li and heavier elements are formed because of the local maximum at ^{4}He [11] .

The next stage in the evolution of the Universe is the matter-radiation equality.

For $T \sim 1$ eV, the matter and radiation have comparable energy densities. When temperature lowers, matter begins to dominate.

After nucleosynthesis, photons, electrons, protons and ^{4}He are still in thermal equilibrium since they electromagnetically interact. Around $T \sim 0.25$ eV, there are not enough energetic photons to enable the ionization of hydrogen. Protons and electrons leave the thermal bath and combine into stable atoms. Thereafter, the Universe no longer contains charged particles. This stage is called recombination. At recombination, photons decouple since there are no more charged particles to interact with. The photon distribution is from that time on only changed by the expansion of the Universe. The remaining photons form a background radiation, still observable today with a temperature $T \approx 2.7$ K. This radiation is the Cosmic Microwave Background, that we discuss in the next part.

1.3.2 Decoupling and the CMB anisotropies

For a good historical introduction on the CMB, the reader may refer to [75]. The discovery of the Cosmic Microwave Background (CMB) is usually attributed to Arno Penzias and Robert Wilson in 1965 [116]. As they were trying to build an antenna for radio waves, they measured a uniform excess temperature. Simultaneously, Robert Dicke's group at Princeton had already realized that a hot Big Bang scenario could leave a blackbody radiation filling the Universe [49] of a few Kelvin today. Nevertheless, the CMB could be dated back to 1941, when McKellar interpreted some interstellar spectroscopic absorption lines to be due to some excitation radiation from a black body. The black body temperature required in order to explain the relative intensities of the observed lines was $2,3\ K$. Nevertheless, this result has never been properly discussed because of world war two. This discovery represents the most powerful observational constraint on the parameters of the *SMC* we have today.

As we have discussed in the previous section, before recombination, hydrogen and other elements were mostly ionized. At recombination, the Universe transitioned from this opaque state, to being mainly neutral, and therefore transparent. The photons then decoupled from matter, when Universe was about 380000 years old. If we assume that decoupling was a fast process, then the small fluctuations in the photon temperature

11. To cross the gap a three body reaction is needed $3 \times {}^4\mathrm{He} \rightarrow {}^{12}\mathrm{C}$.

before decoupling are frozen in. Photons propagate freely until today and their spectrum still contains the fluctuations of the primordial inhomogeneities in the matter repartition at the moment of decoupling.

The power spectrum of the initial perturbations characterizes the temperature fluctuations with respect to the angular scale of the anisotropies. With Planck data [1], the cosmological parameters of the ΛCDM model are being measured with percent level uncertainties. They are tuned in order to fit optimally the initial fluctuations obtained from the CMB statistical observations (*cf* Figure 37 in [1], showing the power spectrum obtained by the PLANCK collaboration) but also the brightness-redshift relation for supernovae, and the large-scale galaxy clustering. The CMB power spectrum can be obtained theoretically for scalar adiabatic perturbations taking into account the Sacks-Wolfe effect [12], the BAOs [13] and Silk damping [14].

In this chapter, I presented the historical context in which General Relativity emerged. I discussed the theoretical steps that led to this revolutionary theory, that abandons Newton's idea of absolute space and time and asserts that it is gravity that specifies at each point the inertial motion, thus determining the local inertial frames. Then, I explained how the equations for a homogeneous isotropic universe model can be obtained from Einstein's equations. These equations lie at the basis of the *SMC* , i.e. ΛCDM model. In the third part of this chapter, I presented the history of the Universe until recombination in the frame of the Big Bang scenario. This ended in a discussion of the Cosmic Microwave Background, which provides us with the observational constraint on the parameters of the *SMC* . In the next chapter, we will consider the next stage of the evolution of the Universe: the formation of large scale structures.

12. The photon spectrum is not only redshifted because of expansion. It also contains a shift due to the gravitational Doppler effect. The difference between the local value of the gravitational potential at emission and detection shifts the wavelength of photons. The gravitational Doppler effect is called the Sachs-Wolfe effect.

13. The modes that entered the horizon during radiation domination underwent acoustic oscillations because of the interplay of gravity and pressure. When the photon fluid decouples from baryons the oscillations remain frozen in the spectrum.

14. When we observe a photon from a given direction, it does not exactly carry the information from the same direction but from a point a little bit around it. When photons leave equilibrium, they can indeed still scatter elastically and change the direction of their trajectory. This implies that correlations on smaller scales are erased. The power spectrum drops asymptotically to zero for large wave number.

Chapter 2

Large Scale Structure Formation

Contents

In the last chapter, we explained how the Friedmann equations of the *SMC* were obtained from the Einstein equations, assuming a homogeneous isotropic universe. No exact solution of the Einstein equations can be obtained in general, except for highly symmetric density profiles. This is the case for the Schwarzchild metric of black holes for example.

In order to deal with more general cases, we have to build a perturbation theory for the gravitation equations.

In this chapter, we will first consider Newtonian structure formation in the phase space. In Section 2.8, we will present the Vlasov-Newton system and then consider the case of a dust fluid model to obtain the Euler-Newton system. An Eulerian first-order perturbation solution will be then given in Section I.2.1.3. We will then discuss how numerical simulations, that mostly use Newtonian perturbation theory, give an interesting insight into the large scale structure formation (see Section I.2.1.4).

The next section will first present the Lagrangian description of structure formation (Section I.2.2.1) and then discuss how, in many respects, this approach is far more powerful then the Eulerian one (Section I.2.2.4).

This will be the major motivation for developing a relativistic Lagrangian perturbation theory. Therefore, we will discuss the generalization of the Newtonian Lagrangian perturbation approach to General Relativity in Section I.2.3. We will build the relativistic analogue of the deformation field and give the major tools that will enable us to develop this approach in the next part.

Since Newtonian gravity and General Relativity share several features, their perturbation schemes will exhibit strong similarities. These analogies will be the subject of Chapter II.2.

2.1 Vlasov equation and Newtonian Eulerian dynamics

2.1.1 The Vlasov-Newton system

Trajectories in phase space and mass conservation

In this section, we consider Newton's theory of gravity. We will follow the ideas presented in Thomas Buchert's M2 lecture course at ENS de Lyon [38] and in [13] to establish the fundamental equations for cosmological fluids. These equations are used in numerical simulations, as we will discuss in Section I.2.1.4. As we will see, phase space is more adapted then the Euclidean space $\mathbb{R}^3$ to describe fluids with pressure or velocity dispersion.

Fluid particles can either be described in an Eulerian way, where the reference frame is fixed with respect to the fluid flow, or in a Langrangian way, following the fluid flow. Contrary to the Eulerian coordinates ($\mathbf{w} = (\mathbf{x}, \mathbf{v})$, Eulerian position and velocity), the Lagrangian coordinates label the fluid ($\mathbf{W} = (\mathbf{X}, \mathbf{V})$, Lagrangian position and velocity). If N is the total number of particles in the volume Ω_t, $\mathrm{d}^6 w$ the infinitesimal Eulerian volume, $\varrho(\mathbf{x}, t)$ the density, m the mass of the particles, then the particle distribution function $\mathrm{e}(\mathbf{w},t)$ satisfies:

$$N = \int_{\Omega_t} \mathrm{e}(\mathbf{w},t)\,\mathrm{d}^6 w \quad \text{and} \quad \varrho(\mathbf{x},t) = m \int_{\Omega_t^v} \mathrm{e}(\mathbf{w},t)\,\mathrm{d}^3 v \ . \tag{2.1}$$

Ω_t^v being the restriction of Ω_t to the velocity space, the average velocity is defined by :

$$\overline{\mathbf{v}}(\mathbf{x},t) = \frac{\int_{\Omega_t^v} \mathrm{e}(\mathbf{w},t)\,\mathbf{v}\,\mathrm{d}^3 v}{\int_{\Omega_t^v} \mathrm{e}(\mathbf{w},t)\,\mathrm{d}^3 v} \ . \tag{2.2}$$

A diffeomorphism $\mathbf{k}$ mapping Lagrangian coordinates to the Eulerian ones in the phase space exists:

$$\begin{aligned} \mathbf{k} : \mathbb{R}^6 &\longrightarrow \mathbb{R}^6 \\ \mathbf{W} &\longmapsto \mathbf{w} = \mathbf{k}(\mathbf{W},t) \quad \text{thus} \quad \mathbf{W} = \mathbf{k}(\mathbf{w},t_i) \ . \end{aligned} \tag{2.3}$$

t_i is the initial time. The determinant of the Jacobian matrix for the Eulerian-to-Lagrangian coordinate transformation is

$$J^\Gamma = det\left(\frac{\partial k_i}{\partial W_k}\right) \quad \text{with} \quad \mathrm{d}^6 w = J^\Gamma(\mathbf{W},t)\,\mathrm{d}^6 W \ . \tag{2.4}$$

If we generalize the Lagrangian derivative to

$$\frac{D}{Dt} := \left.\frac{\partial}{\partial t}\right|_{\mathbf{W}} = \left.\frac{\partial}{\partial t}\right|_{\mathbf{w}} + \mathbf{s}\cdot\nabla_{\mathbf{w}} \ , \tag{2.5}$$

where $\mathbf{s}$ is the generalization of the velocity vector in the phase space:

$$\mathbf{s}(\mathbf{W},t) := \frac{D}{Dt}\,\mathbf{k}(\mathbf{W},t) = \left.\frac{\partial}{\partial t}\right|_{\mathbf{W}} \mathbf{k}(\mathbf{W},t) \ , \tag{2.6}$$

we can show that the conservation of the number of particles $\frac{D}{Dt}N = 0$ implies [1]:

$$\frac{D}{Dt}\mathrm{e} + \mathrm{e}\,\nabla_{\mathbf{w}}\cdot\mathbf{s} = 0 \ . \tag{2.7}$$

Vlasov-Newton equations

The gravitational field $\mathbf{g}(\mathbf{x},t)$ does not depend of the velocity field thus [2] $\nabla_{\mathbf{w}}\cdot\mathbf{s} = \frac{\partial v_i}{\partial x_i} + \frac{\partial g_k}{\partial v_k} = 0$ and the conservation of the number of particles (2.7) becomes:

$$\frac{D}{Dt}\mathrm{e} = \frac{\partial}{\partial t}\mathrm{e} + v_i\,\frac{\partial}{\partial x_i}\mathrm{e} + g_i\,\frac{\partial}{\partial v_i}\mathrm{e} = 0 \ , \tag{2.8}$$

1. This comes from the relation on the Jacobian:

$$\frac{D}{Dt}J^\Gamma = J^\Gamma\,\nabla_{\mathbf{w}}\cdot\mathbf{s} \ .$$

2. $\mathbf{x}$ and $\mathbf{v}$ are independent coordinates.

If we add to these equations the field equations of the gravitational field:

$$\nabla \times \mathbf{g} = \mathbf{0} \quad ; \quad \nabla \cdot \mathbf{g} = \Lambda - 4\,\pi\,G\,m \int_{\Omega_t^v} \mathrm{e}\,(\mathbf{w},t)\,\mathrm{d}^3 v \ , \tag{2.9}$$

we obtain the Vlasov-Newton system. A dust fluid matter model has neither velocity dispersion nor pressure. Its particle distribution function is:

$$\mathrm{e}^{\,dust}(\mathbf{x},\mathbf{v},t) = n(\mathbf{x},t)\,\delta(\mathbf{v} - \overline{\mathbf{v}}(\mathbf{x},t)) \ . \tag{2.10}$$

We recover the usual continuity equation, which, with the gravitational field equations gives the Euler-Newton system.

We now consider a homogeneous isotropic Universe filled with dust fluid. We can thus go back to the Euclidean space $\mathbb{R}^3$. We represent by $\mathbf{f}$ the diffeomorphism mapping the Lagrangian spatial coordinates $\mathbf{X}$ which label fluid elements, to the Eulerian ones $\mathbf{x}$, which are the positions of these elements in Eulerian space at the time t:

$$\begin{aligned} \mathbf{f} : \mathbb{R}^3 &\longrightarrow \mathbb{R}^3 \\ \mathbf{X} &\longmapsto \mathbf{x} = \mathbf{f}(\mathbf{X},t) \quad \text{and} \quad \mathbf{X} = \mathbf{f}(\mathbf{x},t_i) \ . \end{aligned} \tag{2.11}$$

The description in terms of the trajectory function $\mathbf{f}$ is only possible before shell-crossing. Once caustics have formed, $\mathbf{f}$ is no longer a diffeomorphism and this description breaks down.

A deeper physical interpretation of the specificity of Lagrangian coordinates will be given in the next section I.2.2.1.

Homogeneity and isotropy imply $\mathbf{f} = a(t)\mathbf{X}$ where $a(t)$ is a time dependent function called scale factor. Newton's second law implies $\mathbf{g} = \ddot{a}(t)\mathbf{X}$ where we denoted by an overdot $\dot{}$ the time derivative d/dt. Combining the mass conservation equation with the field equation (2.9), we get Friedmann's acceleration law:

$$\frac{\ddot{a}(t)}{a(t)} = \Lambda - 4\,\pi G \varrho_H \ . \tag{2.12}$$

ϱ_H is the homogeneous density. Integrating this equation gives the Friedmann expansion law, which is the fundamental equation of the ΛCDM model:

$$H^2 - \frac{8\,\pi\,G}{3}\varrho_H - \frac{\Lambda}{3} + \frac{k}{a^2} = 0 \ . \tag{2.13}$$

$H(t) = \dot{a}/a$ is Hubble expansion factor. We remark that we didn't use Einstein's theory of gravitation to derive this equation.

Let us now look at the moments of Vlasov equation. To do so, we define the following quantities:

$$\varrho(\mathbf{x},t)\overline{v}_i = m \int_{\Omega_t^v} v_i\,\mathrm{e}\,(\mathbf{w},t)\,\mathrm{d}^3 v \quad : \quad \varrho(\mathbf{x},t)\overline{v_i\,v_j} = m \int_{\Omega_t^v} v_i\,v_j\,\mathrm{e}\,(\mathbf{w},t)\,\mathrm{d}^3 v \ . \tag{2.14}$$

The 0^{th} moment gives:

$$\frac{\partial}{\partial t}\varrho + \frac{\partial}{\partial x_j}(\varrho \overline{v}_j) = 0 \ . \tag{2.15}$$

We define the velocity dispersion tensor $\pi_{ij} = \overline{(v_i - \overline{v}_i)(v_j - \overline{v}_j)}$ and $\Pi_{ij} = \varrho\,\overline{(v_i - \overline{v}_i)(v_j - \overline{v}_j)}$. Then the 1^{st} moment gives the Euler-Jeans equation:

$$\varrho \frac{d}{dt}\overline{v}_i = \varrho\, g_i - \frac{\partial}{\partial x_j}\Pi_{ij} \ . \tag{2.16}$$

The velocity dispersion, defined at each point $\mathbf{x}$ can be represented in terms of the eigenvectors and eigenvalues of the velocity dispersion tensor. If $\psi_i = \frac{1}{\varrho}\,\Pi_{ik,k}$, the Euler-Jeans equation can be rewritten:

$$\frac{\partial}{\partial t}\overline{v}_i + \overline{v}_k\,\overline{v}_{i,k} = g_i - \psi_i \ . \tag{2.17}$$

If we take the divergence of this equation, we get

$$\frac{d}{dt}\theta = \Lambda - 4\,\pi\varrho\, G - \frac{1}{3}\theta^2 + 2\,(\omega^2 - \sigma^2) - \psi_{i,i} \ , \tag{2.18}$$

where θ the expansion rate, ω the vorticity and σ the shear are defined locally. To obtain this equation, we didn't assume homogeneity, isotropy or any symmetry.

2.1.2 Structure formation, shell-crossing and velocity dispersion

The primordial fluctuations of the CMB I.1.3.2, amplified by gravity, have collapsed into the large scale structures of the present Universe. Over-dense regions have indeed attracted some matter and emptied under-dense regions. Voids got larger and larger and confined the matter into sheets. Sheets collapsed into filaments and filaments into clusters which virialized to give halos. We want to present the dynamics of a gravitational collapse and explain how, from a fluid without initial velocity dispersion, the several shell-crossings it will undergo will generate velocity dispersion.

The dynamics of the collapse are determined by the eigenvectors and eigenvalues of the Jacobian matrix of coordinate transformation $\mathbf{f}$ from Lagrangian coordinates to Eulerian ones. This is illustrated in the following figure.

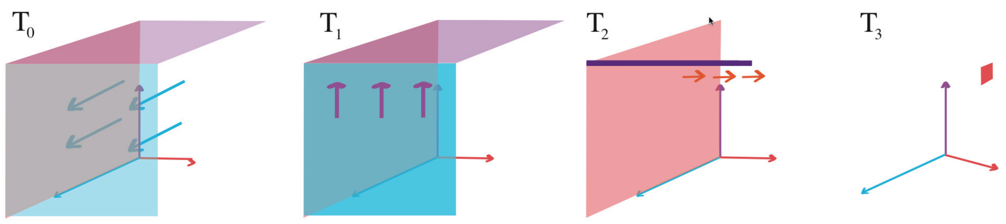

Figure 2.1: The eigenvectors of the Jacobian matrix are represented in blue, purple and red. We supposed that $|\lambda_1|$, $|\lambda_2|$, $|\lambda_3|$. The initially 3–dimensional fluid element collapses into a sheet, which collapses to a filament. The filament then collapses to a point.

Let us consider now $|\lambda_1| \gg |\lambda_{2,3}|$ and assume the following initial velocity:

$$\overline{v}_1(X_1, T_0) \propto \sin(X_1) \ . \tag{2.19}$$

The gravitational field generated by three streams is bigger then the one generated by one stream. Thus, the wave fronts will cross again, to generate five then seven streams and so on. As the number of streams increases, the ellipsoid of velocities, which was initially highly anisotropic, becomes more and more isotropic.

2.1.3 Eulerian perturbation scheme

We now consider a fluid without pressure and velocity dispersion. The 0^{th} and 1^{st} moments of the Vlasov equation associated to the field equations for the gravitational field give the Euler-Newton system:

$$\frac{\partial \mathbf{v}}{\partial t} + \mathbf{v} \cdot \boldsymbol{\nabla} \mathbf{v} = \mathbf{g} \ , \tag{2.20}$$

$$\frac{\partial \rho}{\partial t} + \boldsymbol{\nabla} \cdot (\rho \mathbf{v}) = 0 \ , \tag{2.21}$$

$$\boldsymbol{\nabla} \times \mathbf{g} = \mathbf{0} \ , \tag{2.22}$$

$$\boldsymbol{\nabla} \cdot \mathbf{g} = \Lambda - 4\pi G \rho \ . \tag{2.23}$$

From these equations, it is possible to obtain an evolution equation for the vorticity $\boldsymbol{\omega} = \frac{1}{2}\boldsymbol{\nabla} \times \mathbf{v}$. This equation is called Helmholtz transport equation for the vorticity:

$$\frac{d}{dt}\left(\frac{\boldsymbol{\omega}}{\rho}\right) = \left[\frac{\boldsymbol{\omega}}{\rho} \cdot \boldsymbol{\nabla}\right] \mathbf{v} \ . \tag{2.24}$$

Combining this equation with the continuity equation, we can show that the solution is

$$\boldsymbol{\omega} = \frac{\boldsymbol{\Omega} \cdot \boldsymbol{\nabla}_{\mathbf{0}} \mathbf{f}}{J} \quad ; \quad \boldsymbol{\Omega} := \boldsymbol{\omega}(\mathbf{X}, t_{\mathbf{i}}) \ , \tag{2.25}$$

where J is the determinant of the Eulerian-to-Lagrangian Jacobian matrix.

We introduce the comoving coordinates $\mathbf{q} = \mathbf{x}/a(t)$. They coincide with the Lagrangian coordinates when the fluid undergoes a homogeneous and isotropic expansion. In what follows, we consider inhomogeneous deformations of the form:

$$\mathbf{q} = \mathbf{X} + \mathbf{P}(\mathbf{X}, t) \ , \tag{2.26}$$

where the magnitude of $\mathbf{P}(\mathbf{X}, t)$ must not be small. In the Eulerian perturbation approach, we split the following fields into background fields, associated with the Hubble flow and solution of Friedmann's equations, and peculiar fields.

$$\rho(\mathbf{q}, t) \quad =: \quad \rho_H(t)(1 + \delta(\mathbf{q}, t)) \ , \tag{2.27}$$

$$\mathbf{v}(\mathbf{q}, t) \quad =: \quad \mathbf{v}_H + \mathbf{u}(\mathbf{q}, t) \quad ; \quad \mathbf{v}_H(t) := \dot{a}\ \mathbf{q} \ , \tag{2.28}$$

$$\mathbf{g}(\mathbf{q}, t) \quad =: \quad \mathbf{g}_H + \mathbf{w}(\mathbf{q}, t) \quad ; \quad \mathbf{g}_H(t) := \ddot{a}\ \mathbf{q} \ . \tag{2.29}$$

$\delta(\mathbf{q}, t)$, $\mathbf{u}$ and $\mathbf{w}$ are respectively the density contrast, the peculiar velocity and the peculiar acceleration. The Euler-Newton system can be split into the background dynamics and equations for peculiar fields. If we now assume that the deviation fields are first-order perturbations [3], the first-order equations for the peculiar fields are

$$\begin{aligned}
\frac{\partial}{\partial t}\Big|_{\mathbf{q}} \delta + \frac{1}{a}\nabla_{\mathbf{q}} \cdot \mathbf{u} &= 0 \ , &(2.30)\\
\frac{\partial}{\partial t}\Big|_{\mathbf{q}} \mathbf{u} + H\mathbf{u} &= \mathbf{w} \ , &(2.31)\\
\nabla_{\mathbf{q}} \times \mathbf{w} &= \mathbf{0} \ , &(2.32)\\
\nabla_{\mathbf{q}} \cdot \mathbf{w} &= -4\pi G a \rho_H \, \delta \ . &(2.33)
\end{aligned}$$

The Eulerian perturbation theory was first formalized by Peebles in [115]. The solutions to these equations for an Einstein-de-Sitter Universe ($k = 0$, $\Lambda = 0$) are:

$$\begin{aligned}
\mathbf{w} &= \frac{2}{3{t_{\mathbf{i}}}^2}\left(\frac{t}{t_{\mathbf{i}}}\right)^{-2/3} \mathbf{A}(\mathbf{q}) + \frac{2}{3{t_{\mathbf{i}}}^2}\left(\frac{t}{t_{\mathbf{i}}}\right)^{-7/3} \mathbf{B}(\mathbf{q}) \ , &(2.34)\\
\mathbf{u} &= \frac{2}{3t_{\mathbf{i}}}\left(\frac{t}{t_{\mathbf{i}}}\right)^{1/3} \mathbf{A}(\mathbf{q}) - \frac{1}{t_{\mathbf{i}}}\left(\frac{t}{t_{\mathbf{i}}}\right)^{-4/3} \mathbf{B}(\mathbf{q}) \ , &(2.35)\\
\delta &= -\left(\frac{t}{t_{\mathbf{i}}}\right)^{2/3} \nabla_{\mathbf{q}} \cdot \mathbf{A}(\mathbf{q}) - \left(\frac{t}{t_{\mathbf{i}}}\right)^{-1} \nabla_{\mathbf{q}} \cdot \mathbf{B}(\mathbf{q}) \ , &(2.36)
\end{aligned}$$

where

$$\begin{aligned}
\mathbf{A}(\mathbf{q}) &= \frac{3}{5}\mathbf{U}t_{\mathbf{i}} + \frac{9}{10}\mathbf{W}{t_{\mathbf{i}}}^2 \ , &(2.37)\\
\mathbf{B}(\mathbf{q}) &= -\frac{3}{5}\mathbf{U}t_{\mathbf{i}} + \frac{3}{5}\mathbf{W}{t_{\mathbf{i}}}^2 \ , &(2.38)
\end{aligned}$$

and

$$\mathbf{U} := \mathbf{u}(\mathbf{q}, t_{\mathbf{i}}) \quad ; \quad \mathbf{W} := \mathbf{w}(\mathbf{q}, t_{\mathbf{i}}) \ . \qquad (2.39)$$

Initial data is often given in terms of the Fourier transform of the initial density contrast.

2.1.4 Numerical simulations

A powerful insight into the physics of large scale structures is provided by numerical simulations. Cosmological simulations are based on the ΛCDM model and Newtonian gravity. They take into account the homogeneous expansion of the Universe and assume a given set of cosmological parameters.

Cosmological dark matter simulations don't consider baryonic matter since, according to the ΛCDM model, it is small with respect to the amount of dark matter. They use a dust fluid model for dark matter and are able to predict the evolution of large scale structures accurately up to the non-linear regime. They simulate systems from the cosmic scales ($\simeq$ 20 Gpc) to the cluster and galactic scales ($\simeq$ 10 pc) and involve until 5.10^{11} particles of dark matter, as is done in DEUS Full Universe Run simulation based on RAMSES code [17]. Simulations of the DEUS Full Universe Run for different

3. We see that, in the Eulerian perturbation theory, from the definition of the peculiar fields (2.29), we cannot describe high density contrast because the density field is a perturbed variable.

box sizes and redshifts can be found at http://www.deus-consortium.org/a-propos/dark-energy-universe-simulation-full-universe-run/.

Even if dark matter-only simulations are often used as a basis for semi-analytical models, their relevance ends when we go to galactic scales, where the baryonic effects are too important to be neglected. The baryonic effects could indeed have a strong impact on the distribution of dark matter in galactic halos. Furthermore, deviations from the mean-field approximation that is used by the solution of Poisson's equations, then become significant [32]. [94] is an excellent review on the state of the art in cosmological simulations.

Hydrodynamical simulations describe the baryonic component of the Universe. These simulations either solve Euler equations for a gas on a grid (which can be adaptative - Adaptative Mesh Refinement - as is done in RAMSES [140]) or can describe the gas as a set of particles, as is done in "Smooth Particle Hydrodynamics" SPH codes such as GADGET [137].

Once the initial conditions, coming from the CMB, are implemented, different methods can be used to solve Euler equations. The direct summation method, known as Particle-Particle method, evaluates the force on each particle by summing the interaction exerted by the neighbors. The tree-code method, used in RAMSES code, consists in decomposing hierarchically the influence of the neighboring structures and treating the influence of remote structures by a multipole expansion on clusters containing many particles. The expansion can thus be truncated at low order. Other methods exist, as is explained in [13].

The description of the evolution of structures is enriched by taking into account the radiative and thermal transfers (as is done in RAMSES [140] by Godunov method, a modern shock-capturing scheme that describes the thermal history of the fluid), the chemical reactions or the impact of magnetic fields on plasmas. Then, these simulations allow a good precision estimation of the baryonic mass-to-light function of galaxies. The submesh physics, which includes, for example, the stellar formation, supernovae explosions or the active galactic nucleus are usually described as an overall feedback.

Some cosmologists claim that analytical approaches have arrived at their limits while we will show that numerical and analytical approaches are complementary in the description of structure formation. The intrinsic Lagrangian analytical approach will give a powerful insight into the large-scale structure formation and shed a new light on the dynamics of the Universe.

2.2 Newtonian Lagrangian perturbation approach to describe structure formation

We here present a Lagrangian theory for self gravitational flows following [38] and [26]. Contrary to the Eulerian case, a single variable is needed to describe the gravitation dynamics: the trajectory function $\mathbf{f}$, presented in (2.11). Density and velocity are no longer dynamical variables and thus high density contrasts can be described by this method. We will derive the Lagrange-Newton system, which is a closed set of Lagrangian equations for the trajectory field $\mathbf{f}$ describing the gravitational dynamics of the self-gravitating flow. As we will show, we can go back to the Euler-Newton system from the Lagrange-

Newton system as long as the mapping $\mathbf{f}$ is invertible and non-singular. This condition will be expressed in terms of J, the determinant of the Jacobian matrix of the Eulerian-to-Lagrangian coordinate transformation.

2.2.1 Lagrangian description of structure formation

The trajectory field of fluid elements, also called deformation field, has been defined in (2.11). In the Lagrangian approach, the Eulerian position $\mathbf{f}(\mathbf{X},t)$ and time t are no longer independent variables. The independent variables are now $(\mathbf{X},t)$. The tensor of the first derivatives of the trajectory field with respect to the Lagrangian coordinates: $(f_{i|j})$, called the Jacobian matrix, measures the deformation of the fluid particle. Its determinant is given by:

$$J := \det\left(\frac{\partial f_i}{\partial X_j}(\mathbf{X},t)\right) = \frac{1}{6}\epsilon_{ijk}\epsilon^{klm} f^i_{\ |k} f^j_{\ |l} f^k_{\ |m} \quad . \tag{2.40}$$

We have denoted by a vertical slash $_{|j}$ the spatial derivative with respect to X_i, by an overdot $\dot{}$ the time derivative and have used Einstein summation convention on repeated indices: $u_i\, v^i = u_1\, v^1 + u_2\, v^2 + u_3\, v^3$ and $u_\mu\, v^\mu = u_0\, v^0 + u_1\, v^1 + u_2\, v^2 + u_3\, v^3$. ϵ_{ijk} is the Levi-Civita tensor. It is equal to 1 if $\{i,j,k\}$ are an even permutation of $\{1,2,3\}$, -1 if they are an odd permutation of $\{1,2,3\}$ and zero otherwise. We link the Eulerian position, velocity and acceleration to the trajectory function by:

$$\mathbf{x} := \mathbf{f}(\mathbf{X},t) \quad ; \quad \mathbf{v} := \dot{\mathbf{f}}(\mathbf{X},t) \quad ; \quad \mathbf{g} := \ddot{\mathbf{f}}(\mathbf{X},t) \quad . \tag{2.41}$$

In the Lagrangian perspective, the volume of the deformed fluid element is measured by the determinant of the Jacobian matrix $J(\mathbf{X},t) = \det(f_{i|j})$. The density must therefore be proportional to its inverse.

$$\rho(\mathbf{X},t) = \frac{\rho(\mathbf{X},t_{\mathbf{i}})}{J(\mathbf{X},t)} \quad . \tag{2.42}$$

This comes from the fact that the Jacobian is solution of the following equation:

$$\dot{J} = J\ \boldsymbol{\nabla}\mathbf{v} \quad . \tag{2.43}$$

It is initially equal to $J(\mathbf{X},t_{\mathbf{i}}) = 1$ since by definition, Eulerian coordinates initially coincide with Lagrangian ones.

The inverse map to $\mathbf{f}$ is defined by $\mathbf{h} = \mathbf{f}^{-1}$. It is possible to check that its gradient is given by [4]

$$\mathbf{X} = \mathbf{h}(\mathbf{x},t) \quad , \quad h^i_{\ ,j} = \frac{1}{2J}\epsilon_{jpq}\epsilon^{ilm} f^p_{\ |l} f^q_{\ |m} \quad . \tag{2.44}$$

We denoted by $_{,i}$ the Eulerian derivative with respect to x^i.

4. This can be easily proved in the 2–dimensionnal case, where the inverse Jacobian matrix is

$$J^{-1}_{ab}(2D) = \frac{1}{J(2D)}\begin{pmatrix} f_{2|2} & -f_{1|2} \\ -f_{2|1} & f_{1|1} \end{pmatrix}$$

where the Jacobian is $J(2D) = f_{2|2}f_{1|1} - f_{2|1}f_{1|2}$.

2.2.2 Lagrange-Newton System

In order to formulate Euler-Newton system in terms of the Lagrangian trajectory function, we introduce the following notation. We denote by $\mathcal{J}(A, B, C)$ the functional determinant of $A(\mathbf{X}, t)$, $B(\mathbf{X}, t)$ and $C(\mathbf{X}, t)$

$$\mathcal{J}(A, B, C) = \epsilon_{klm} A_{|k} B_{|l} C_{|m} \ . \tag{2.45}$$

From the composition of the derivatives and from (2.44), for any field a_i we have

$$a_{i,j} = a_{i|k} h^k{}_{,j} = \frac{1}{2J} \epsilon_{jpq} \mathcal{J}(a_i, f^p, f^q) \ . \tag{2.46}$$

We denote by $g_{[i,j]}$ the antisymmetric part of $g_{i,j}$: $g_{[i,j]} = \frac{1}{2}(g_{i,j} - g_{j,i})$. If we replace the gravitational field by the second time derivative of the trajectory function $\mathbf{f}(\mathbf{X}, t)$ (*cf* (2.41)) in the field equations, we get from (2.46) the following equations:

$$\begin{aligned} g_{[i,j]} = (\boldsymbol{\nabla} \times \mathbf{g})_k = \frac{1}{2J} \epsilon_{pq[j} \mathcal{J}(\ddot{f}_{i]}, f^p, f^q) = 0 \ , \\ g^i{}_{,i} = \frac{1}{2J} \epsilon_{ipq} \mathcal{J}(\ddot{f}^i, f^p, f^q) = \Lambda - 4\pi G \rho \ . \end{aligned} \tag{2.47}$$

The first one can be rewritten as

$$\epsilon_{pq[j} \mathcal{J}(\ddot{f}_{i]}, f^p, f^q) = 0 \quad \text{which is equivalent to} \quad \delta_{ij} \ddot{f}^i{}_{|[p} f^j{}_{|q]} = 0 \ . \tag{2.48}$$

Later, we will show that these equations have relativistic counterparts. The relativistic equations will no longer be expressed in terms of the 3 components of the trajectory function $\mathbf{f}$, but in terms of the nine components of the Cartan coframes.

2.2.3 Zel'dovich approximation

The Zel'dovich approximation [161] has been built from the observation that, for a sufficiently long time, a gravitational collapse exhibits a preferred direction. This direction corresponds to the eigenvector of the Jacobian matrix associated to the largest eigenvalue ($|\lambda_1|$ in Fig. 2.1). This collapse leads to the formation of flat structures (pancakes), then to filaments and finally to clusters. For each stage of the collapse, we can assume that the velocity and the acceleration fields are approximately collinear. A subclass of solutions can then be investigated [21]. The success of the Zel'dovich approximation in the Newtonian Lagrangian setup is a strong motivation to develop it in the relativistic frame. Nevertheless, since no relativistic numerical simulations exist, a relativistic Zel'dovich approximation has not yet been implemented.

2.2.4 Newtonian Lagrangian perturbation theory

Major differences exist between the Eulerian perturbation approach and the Lagrangian one. They are the motivations for developing the Lagrangian approach. First, the density field is not a perturbation variable, contrary to the Eulerian case. Second, the perturbed flow $\mathbf{f}$ is a function of the Lagrangian coordinates, which follow the flow whereas in the Eulerian case, the perturbations are expressed in the frame associated to the homogeneous flow. Deviations to the homogeneous flow may be small but the Eulerian fields evaluated along the perturbed flow can experience large changes as is represented and discussed in Figure 2 of [26].

The perturbed trajectory field is the sum of a homogeneous background trajectory field and of an inhomogeneous perturbation field:

$$\mathbf{f}(\mathbf{X},t) = a(t)\left(\mathbf{X} + \mathbf{P}(\mathbf{X},t)\right) \quad . \tag{2.49}$$

The inhomogeneous perturbations can be decomposed into different orders, order n being negligible with respect to order $n-1$. A discussion of the perturbation and solution scheme will be provided in Chapter II.2.

A reason for the strong success of analytical Lagrangian description of structure formation is that it intrinsically contains non-linear Eulerian terms. The efficiency of this approach has been discussed in [153], where the authors compare the density profile obtained from a particle-mesh Newtonian simulation, based on the iterative resolution of Poisson equations, to the density profile obtained from the second order solutions of the Lagrange-Newton system. Both are computed for a box of a size of $(200h^{-1}\ \mathrm{Mpc})^3$ and from the CMB initial data. The first method requires a numerical resolution whereas the second is just the plotting of analytical functions. Both are in very good agreement as discussed in [109].

Nevertheless, the Lagrangian scheme has an intrinsic limit: it is no longer accurate once the shell-crossing has taken place. In order to follow the perturbation scheme after that time, we have to truncate the high-frequency modes in the initial fluctuation spectrum. Thus, under a certain characteristic size ($\simeq$ galaxy group mass scale), the approach breaks down [108]. For further details on the Newtonian perturbation theory, the reader can refer to [27, 55].

2.3 Relativistic Lagrangian description of structure formation

In last section, we have presented the Newtonian Lagrangian perturbation theory. We have seen that the Lagrangian description is much more powerful then the Eulerian one, even when Lagrangian analytical perturbation solutions are compared to Eulerian numerical simulations. These outcomes strongly support the search for a relativistic generalization of the Lagrangian approach. Such a generalization was first suggested by Kasai [85] and was further investigated for the non-perturbative regime in [35] by Thomas Buchert and Matthias Ostermann, where they build a Lagrangian framework for the description of structure formation in General Relativity and define the relativistic generalization of the Zel'dovich approximation. Nevertheless, some work has still to be done for the development of the intrinsic Lagrangian perturbation formalism. In this chapter, I will give the basic mathematical notions of differential geometry needed to describe structure formation on a curved manifold.

I will try to give a physical intuition for the Cartan frames and explain how Cartan coframes can be obtained from them. Then, we will discuss why these coframes are the relativistic counterparts of the gradient of the trajectory function. The Cartan formalism will be the accurate one to describe the relativistic dynamics of space-time in the Lagrangian way.

2.3.1 Cartan formalism and the dynamics of space-time

We present the tools needed to understand the Cartan coframe formulation of General Relativity in the Lagrangian description. The reader seeking for a more detailed and complete introduction to the mathematical tools needed for General Relativity can find further information in these very good books [75] [74] [130].

Manifolds and charts

Space-time is a four dimensional manifold $\mathcal{M}$ to which is associated the metric bilinear form $\mathbf{g}$ with signature $(-,+,+,+)$. A 4-dimensional manifold $\mathcal{M}$ is a topological space that is locally homeomorphic to Euclidean space [5] [6] $\mathbb{R}^4$. This means that there exists a family of open neighborhoods U_i together with continuous one-to-one mappings $f_i : U_i \mapsto \mathbb{R}^4$ with a continuous inverse such that this family of open neighborhoods covers the whole manifold :

$$\bigcup_i U_i = \mathcal{M} \ . \tag{2.50}$$

If P is a point in $\mathcal{M}$ and U an open neighborhood of P, there exists a mapping $\phi : U \to \mathbb{R}^4$ such that $\phi(P) = (x^0, x^1, x^2, x^3)$ will be a vector in $\mathbb{R}^4$. This mapping ϕ is a coordinate system, also called coordinate chart.

Usually, it is not possible to cover a manifold with a single chart such that every point of space-time has a unique coordinate. For $\mathbb{S}^2$, the 2-sphere, 2-dimensional surface of the 3-dimensional sphere, the lines of constant coordinate must cross somewhere on $\mathbb{S}^2$. Therefore, at least two charts are required to cover it. At the overlapping of two charts, General Relativity requires that the mapping between the coordinates of the overlapping charts is at least doubly differentiable.

From coordinates to frames

Gravity can be seen as the field that determines at each point of space-time the preferred frame in which the motion is inertial. Consider now a particular event associated to the point A on the space-time manifold. Let $\mathbf{x}_A$ be its coordinates. Consider the local inertial frame around A and denote by ${}^A\boldsymbol{\chi}$ the coordinates it defines in some arbitrary coordinate map $\mathbf{x} = \{x^\mu\}$. Choose the origin such that ${}^A\boldsymbol{\chi}(A) = \mathbf{0}$. As explained in the Section I.1.1.1, the motion of an object in space-time has to be considered with respect to the frame determined by the gravitational field. Here, gravity in A can be seen as

5. A homeomorphism being a continuous map which has a continuous inverse map.

6. This means that a manifold is locally Euclidean, i.e. flat. To illustrate this idea, we could think of the Earth, which was thought to be flat in the ancient times. On the small scales that we see, Earth does indeed look flat. Any object that is nearly flat on small scales is a manifold.

the information of the change of coordinates that takes us to the inertial coordinates. It is contained in ${}^{A}\boldsymbol{\chi} = {}^{A}\boldsymbol{\chi}(\mathbf{x})$. The value of this function is only meaningful in a small neighborhood of A since, as we move away from A, the inertial reference frame will change and so will the coordinates attached to it. The first-order Taylor expansion gives

$$ {}^{A}\boldsymbol{\chi}(\mathbf{x}) = \left.\frac{\partial\, {}^{A}\boldsymbol{\chi}}{\partial\, x^{\mu}}\right|_{\mathbf{x}_A} x^{\mu} = {}^{A}\mathbf{e}_{\mu}(\mathbf{x}_A)\; x^{\mu} \ . \tag{2.51} $$

The construction can be done for any point of the space-time manifold. The gravitational field is therefore the Jacobian matrix of the change of coordinates [130] from $\mathbf{x}$ to the coordinates that are locally inertial at the space-time point defined by $\mathbf{x}$:

$$ \mathbf{e}_{\mu}(\mathbf{x}) = \left.\frac{\partial\, \boldsymbol{\chi}}{\partial\, x^{\mu}}\right|_{\mathbf{x}} \ . \tag{2.52} $$

The $\mathbf{e}_{\mu}$ are called tetrad fields or Cartan frames. They live in the tangent space at the point that is considered on the manifold. If we had only one inertial frame for the whole space-time, then the Cartan frames would be equal to the inertial coordinate basis. But this is not the case since the inertial frame is a local concept. These frames are defined on the space-time manifold independently of the existence of a metric $\mathbf{g}$.

We have seen that they represent the gravitational field and are, by construction, attached to the local inertial frame. If we add to the manifold a metric structure, then, from Gram-Schmidt orthonormalization procedure we can build some orthonormal frames. This point will be explained in the next paragraph.

Differential forms and Cartan coframes

At any point P of the manifold $\mathcal{M}$ it is possible to define a cotangent space that has $\{\mathbf{d}X^{i}\}$ as a basis. Let $\boldsymbol{\phi}$ be a $k-$differential form (k is an integer smaller that the dimension of the manifold). Its coefficients can be expressed in the exact basis of the cotangent space according to

$$ \boldsymbol{\phi} = \phi_{i_1\ i_2\ \ldots\ i_k} \mathbf{d}X^{i_1} \wedge \mathbf{d}X^{i_2} \wedge \ldots \wedge \mathbf{d}X^{i_k} \ , \tag{2.53} $$

where $\wedge$ is the Wedge operator.

The exterior differential is defined to be the unique mapping from the k-forms to the $(k+1)$-forms satisfying the following properties:

1. $\mathbf{d}$ is additive: $\mathbf{d}(\boldsymbol{\alpha}+\boldsymbol{\beta}) = \mathbf{d}\boldsymbol{\alpha} + \mathbf{d}\boldsymbol{\beta}$,
2. If α^0 is a scalar, $\mathbf{d}\alpha^0$ is the usual differentiation of the function α^0,
3. $\mathbf{d}(\boldsymbol{\alpha}^p \wedge \boldsymbol{\beta}^q) = \mathbf{d}\boldsymbol{\alpha}^p \wedge \boldsymbol{\beta}^q + (-1)^p \boldsymbol{\alpha}^p \wedge \mathbf{d}\boldsymbol{\beta}^q$,
4. $\forall\, \boldsymbol{\alpha}$, $\mathbf{d}(\mathbf{d}\boldsymbol{\alpha}) = 0$.

We can equivalently define it on a local coordinate chart $(X^1, \ldots, X^n)$. On the $k-$form $\boldsymbol{\phi}$

$$ \begin{aligned} \mathbf{d}\boldsymbol{\phi} = \mathbf{d}\left(\phi_{\nu_1\ldots\nu_p}\ \mathbf{d}X^{\nu_1} \wedge \ldots \wedge \mathbf{d}X^{\nu_p}\right) &= \mathbf{d}\phi_{\nu_1\ldots\nu_p} \wedge \mathbf{d}X^{\nu_1} \wedge \ldots \mathbf{d}X^{\nu_p} \\ &= \phi_{\nu_1\ldots\nu_p|\,i}\ \mathbf{d}X^{i} \wedge \mathbf{d}X^{\nu_1} \wedge \ldots \mathbf{d}X^{\nu_p} \ , \end{aligned} \tag{2.54} $$

where $\phi_{\nu_1 \dots \nu_p | i} = \partial_{X^i}(\phi_{\nu_1 \dots \nu_p})$. A $k-$form $\boldsymbol{\phi}$ is exact if and only if it is equal to the exterior derivative of a $(k-1)-$form $\boldsymbol{\psi}$:

$$\boldsymbol{\phi} \text{ exact} \quad \Longleftrightarrow \quad \exists\, \boldsymbol{\psi} \ / \ \boldsymbol{\phi} = \mathbf{d}\, \boldsymbol{\psi} \quad . \tag{2.55}$$

We will work with coframes rather than frames since this description will be closer to the Newtonian Lagrangian formalism. The coframes are the duals of the frames and therefore are 1−forms that live in the cotangent space. They satisfy

$$\boldsymbol{\eta}^{\mu}(\mathbf{e}_{\nu}) = \delta^{\mu}_{\ \nu} \ . \tag{2.56}$$

We will see later that they can be chosen in such a way to both encode the dynamics of the fluid and the geometry of the manifold, via the metric bilinear form.

2.3.2 $3+1$ foliation of space-time in a Lagrangian approach

In the following, we briefly present the 3+1 foliation of space-time in order to introduce and discuss the decomposition of the metric in terms of the Cartan coframes. More details on the $3+1$ foliation and on the decomposition of the Einstein equations will be given in the Chapter II.1.

In General Relativity, an absolute space and an absolute time do not exist. Nevertheless, a $3+1$ splitting of space-time is often considered in order to have a more intuitive understanding of the dynamics of matter and geometry. For an excellent introduction to the $3+1$ formalism, I recommend the reader the following lecture [73].

The Einstein equations, which are 4-dimensional equations, can be split into evolution equations and constraint equations, defined on 3-dimensional space-like hypersurfaces[7]. The $3+1$ foliation of space-time is only possible if space-time is globally hyperbolic. This means that spatial hypersurfaces Σ in $\mathcal{M}$ are Cauchy surfaces, i.e. each causal (i.e. timelike or null) curve without end point intersects Σ once and only once. We introduce a smooth and regular scalar field $\hat{t}$ on $\mathcal{M}$ such that each hypersurface is a level surface of this scalar field.

$$\forall t \in \mathbb{R} \ , \ \Sigma_t := \{p \in \mathcal{M} \,, \hat{t}(p) = t\} \ . \tag{2.57}$$

For different times t and t', the hypersurfaces Σ_t and $\Sigma_{t'}$ do not intersect because $\hat{t}$ is regular.

We call the class of observers that move freely the inertial observers. The tetrad fields associated with a reference frame $\mathcal{R}$ are such that $\mathbf{e}_0$ is the normal vector to the hypersurfaces: $\mathbf{e}_0 = \mathbf{n}$. We here choose the special foliation for which $\mathbf{n} := \mathbf{u}$ is the unit tangent vector field of the world lines of the fundamental observers in $\mathcal{R}$, i.e. the 4–velocity field of these observers. The rest-space of an observer is defined as the local 3-dimensional space orthogonal to the 4-velocity $\mathbf{u}$ of the observer.

If the matter model that we consider is a fluid with vorticity, it is not possible to synchronize globally the clocks associated to the local rest-spaces of all the inertial observers. In other words, a single space of simultaneity encompassing the rest spaces of all the inertial observers does not exist.

7. R. L. Arnowitt, S. Deser and C. W. Misner were the first ones to perform this splitting [6].

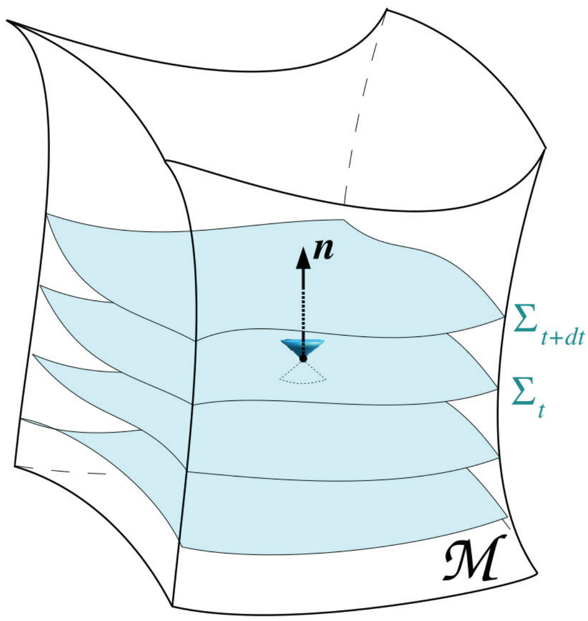

Figure 2.2: The space-time $\mathcal{M}$ is foliated by a family of spacelike hypersurfaces Σ_t. The unit vector $\mathbf{n}$ is normal to the hypersurface. Here we choose the foliation such that $\mathbf{n}$ coincides with the 4–velocity of the fluid flow. The image is taken from[73].

Nevertheless, for a dust fluid without vorticity, such a global space of simultaneity exists. We can indeed choose the hypersurfaces to be everywhere orthogonal to the 4–velocity of the inertial observers. In Chapter II.1, we will explain how we obtain from the general $3+1$ decomposition of the Einstein equations the equations in the flow-orthogonal foliation for the dust fluid without vorticity matter model.

We will refer to spatial quantities with indices $a, b, ...$ going from 1 to 3. Moreover, the 4−coframes $\boldsymbol{\eta}^\mu$ will be split into:

- $\boldsymbol{\eta}^0$, the cotangent field along the worldlines of the inertial observers, i.e. in this splitting, in the direction of time,
- $\boldsymbol{\eta}^a$, a running from 1 to 3, the spatial coframes.

In the foliation we have chosen, the 4−metric is:

$$^{(4)}\mathbf{g} = -\mathbf{d}t \otimes \mathbf{d}t + {}^{(3)}\mathbf{g} \ . \tag{2.58}$$

From a given symmetric tensor G_{ab} that may depend of the point of the manifold that we consider and with the help of Gram-Schmidt process, we can build a frame basis in which the spatial 3−metric is:

$$^{(3)}\mathbf{g} = G_{ab}\ \boldsymbol{\eta}^a \otimes \boldsymbol{\eta}^b \ , \tag{2.59}$$

where a and b run from 1 to 3. We may want to consider the orthonormal coframes, that satisfy the following identity:

$$^{(3)}\mathbf{g} = \delta_{ab}\ \tilde{\boldsymbol{\eta}}^a \otimes \tilde{\boldsymbol{\eta}}^b \ . \tag{2.60}$$

Nevertheless, we consider the coframes adapted to $G_{ab} \neq \delta_{ab}$ in order to encode in this term the initial deviation fields. This will be discussed in Section II.2.1.1.

As in the Newtonian case, we will consider Lagrangian coordinates. These coordinates cover the spatial sections and are constant along the flow lines. For the dust fluid that we consider, they are thus transported along the geodesics. More information on the Lagrangian description will be given for general foliations and matter models in Section II.1.1.2.

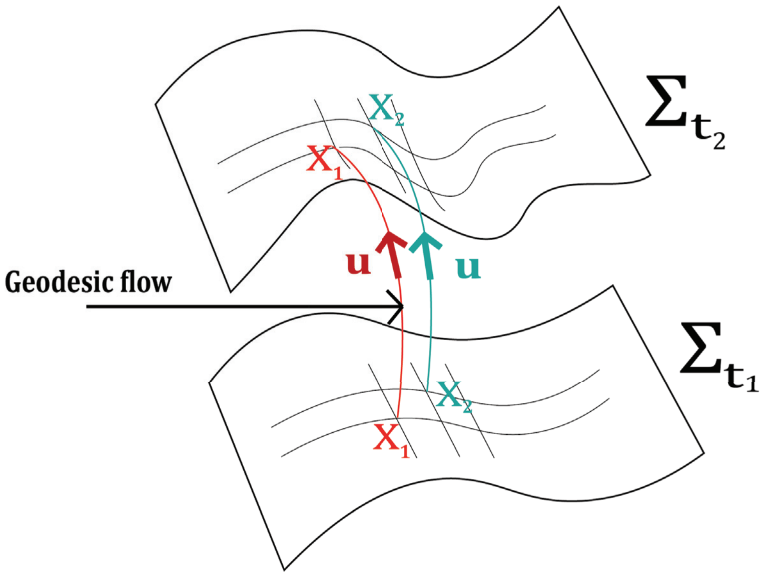

Figure 2.3: The Lagrangian coordinates, which cover the spatial hypersurfaces Σ_t, label the fluid particles. They are thus constant along the trajectories of the fluid flow, which are here geodesics since we consider an irrotational dust fluid.

From (2.59), we get:

$$ {}^{(3)}\mathbf{g} = g_{ij}\ \mathbf{d}X^i \otimes \mathbf{d}X^j = G_{ab}\ \eta^a{}_i \eta^b{}_j \mathbf{d}X^i \otimes \mathbf{d}X^j\ . \tag{2.61} $$

This implies[8], in the Lagrangian coordinate basis $\{\mathbf{d}X^i\}$:

$$ g_{ij} = G_{ab}\ \eta^a{}_i \eta^b{}_j\ . \tag{2.62} $$

It is possible to show that, if the coframes are integrable forms, $\boldsymbol{\eta}^a \longrightarrow \mathbf{d}f^a$, then, as discussed in Section II.1.5.2, we only have one inertial frame for the whole space-time. It is remarkable to note that the appearance of a global frame couples with the fact that a part of the Einstein equations will give back the Lagrange-Newton-System. This will be discussed in Section II.1.5.

8. G_{ab} is the Gram tensor for the coframes $\boldsymbol{\eta}^a$ and not the Einstein tensor.

Chapter 3

Inhomogeneous Cosmology

Contents

The *SMC* is based on the cosmological principle: global homogeneity and isotropy. But, as it assumes that the average Universe is described by a homogeneous and isotropic model, it implies that global and local dynamics are decoupled. This assertion goes far beyond the cosmological principle.

In this chapter, we first show that for most of the interesting scales, the Universe is not homogeneous. Taking into account these inhomogeneities will lead, both in Newtonian gravity and in General Relativity, to an additional term contributing to the global dynamics of the Universe. Nevertheless, in the Newtonian case, inhomogeneities have no impact on the global dynamics.

We will consider the relativistic case and explain how the non-linearity of the Einstein equations results in a difference between the dynamics of an initially averaged space-time and the averaged dynamics of space-time. The backreaction term quantifies this difference. Afterwards, we will consider the Einstein equations in the $3+1$ foliation. The averaging process that will be introduced is the accurate formalism to determine the impact of the inhomogeneities of the matter distribution on the evolution of the Universe. Once averaged, the Einstein equations will be analogous to the ones of the *SMC* , except for the additional backreaction term, that will encode the coupling of the evolution of the fluid to the geometry of space-time. Finally, we will discuss how the backreaction may replace the dark matter and dark energy that the *SMC* needs to be self-consistent.

3.1 Inhomogeneities and their consequences on the global dynamics

Our galaxy is at the edge of a local void in a filamentary sheet [149] that joins us to Virgo Cluster. Furthermore, some surveys estimate that 40 to 50 % of the volume of the Universe is contained in voids of diameter 30 h^{-1} Mpc [79, 80]. Nevertheless, the *SMC* assumes that the averaged Universe can be described by a homogeneous and isotropic model. Are the inhomogeneities really negligible? If so, above which scale can we neglect them?

3.1.1 Hierarchical structures and their density contrast

The density contrast within structures is the dimensionless excess density over the mean density : $\delta := (\rho - \overline{\rho})/\overline{\rho}$. Its volume average increases as we consider smaller scales in the Universe:

— for a region of about 10 Mpc, $\langle\delta\rangle \simeq 1$,
— for a typical rich cluster of galaxies, $\langle\delta\rangle \simeq 10$,
— for a galaxy, $\langle\delta\rangle \simeq 10^5$,
— for a star, $\langle\delta\rangle \simeq 10^{28}$.

Nevertheless, the cosmological principle asserts that there exists a spatial length, lying somewhere between 100 h^{-1} Mpc and 700 h^{-1} Mpc, beyond which the Universe is statistically homogeneous and isotropic as discussed in Section I.1.2.1. The next step consists in assuming that this homogeneity and isotropy at large scales allows us to describe the Universe at these scales with the FLRW metric tensor (1.4). This assumption decouples the local dynamics from the global dynamics. Nevertheless, we cannot neglect the global contribution of inhomogeneities on the dynamics of the averaged space-time [103, 102].

3.1.2 A first insight into averaging and backreaction

We consider the physical space-time described by $(\mathcal{M}, g_{\mu\nu})$ and an averaged space-time $(\langle\mathcal{M}\rangle, \langle g_{\mu\nu}\rangle)$, where we did not specify the averaging procedure $\langle\cdot\rangle$. The averaged Einstein equations (1.3) are then:

$$\langle G_{\mu\nu}\rangle = 8\,\pi\,G\,\langle T_{\mu\nu}\rangle \quad , \quad \langle G_{\mu\nu}\rangle = \langle R_{\mu\nu}\rangle - \frac{1}{2}\,\langle R\,g_{\mu\nu}\rangle + \Lambda\,\langle g_{\mu\nu}\rangle \ . \tag{3.1}$$

In the same spirit as perturbation theory, we decompose the metric tensor as average and deviations from the average:

$$g_{\mu\nu} = \overline{g}_{\mu\nu} + \delta g_{\mu\nu} \ , \tag{3.2}$$

where we have denoted $\langle g_{\mu\nu}\rangle$ by $\overline{g}_{\mu\nu}$. We remark that if we do the same thing for $g^{\mu\nu}$, i.e.

$$g^{\mu\nu} = \overline{g}^{\mu\nu} + h^{\mu\nu} \ , \tag{3.3}$$

then $\overline{g}^{\mu\nu} \neq \langle g^{\mu\nu}\rangle$ and $h^{\mu\nu} \neq \delta g^{\mu\nu}$. We denote by $\overline{X}$ all the geometrical quantities build from $\overline{g}_{\mu\nu}$, that caracterize $\langle\mathcal{M}\rangle$.

Averaged Einstein equations can be reformulated in the following way [65]:

$$\langle G_{\mu\nu}\rangle = \overline{G}_{\mu\nu} + \Delta G_{\mu\nu} = 8\,\pi\,G\,\langle T_{\mu\nu}\rangle \ . \tag{3.4}$$

Einstein's theory is non-linear. Thus the averaging process and the construction of the Einstein tensor do not commute. The averaged dynamics of space-time is not equal to the dynamics of the averaged space-time. This is nevertheless what the standard model assumes when stating that Einstein's equations on $\langle\mathcal{M}\rangle$ are:

$$\overline{G}_{\mu\nu} = 8\,\pi\,G\,\langle T_{\mu\nu}\rangle \ . \tag{3.5}$$

$\Delta G_{\mu\nu}$, the backreaction term, will be non-zero as long as the inhomogeneities in the physical space can act on the dynamics of the averaged space-time. The open question is to understand if this term is big enough to account for dark energy and dark matter. The standard model of cosmology, by neglecting this term, assumes that the dynamics of structures at small scales do not influence the global dynamics, at scales larger then the homogeneity scale.

3.2 Backreaction and spatial average of the Einstein equations

In the last section, we had a first insight in the origins of backreaction. We will here work with the $3+1$ formulation of the Einstein equations, first obtained by [6] and that we will determine in Chapter II.1. Then, we will give a definition for the spatial averaging operation we consider. When compared with the equations of the standard model, the averaged inhomogeneous Einstein equations exhibit an additional term, the backreaction. It is the sum of two terms, the first being linked to the shear, the vorticity and the expansion rate of the fluid while the second is the curvature term.

We are looking for a covariant averaging process for tensors in order to preserve the covariance of Einstein's equations. Nevertheless, this averaging procedure has not yet been found and seems to involve a complex hierarchy of averaging processes [158, 43, 65], that goes beyond the two scale model proposed by Zalaletdinov [160]. A way to avoid this difficulty is to only average scalar fields and not tensors. Therefore, we will not consider the averaged Einstein equations in their tensorial form but rather the scalar equations that they contain [1].

In the following sections, we present the 3+1 decomposition of the Einstein equations. Then, we define the averaging operation on scalar fields for any spatial domain. Thereafter, we build the averaged evolution equations of an inhomogeneous universe, according to Buchert's formalism.

3.2.1 Einstein equations in the $3+1$ formalism

As we will discuss in detail in Section II.1.1.1, the irrotational dust fluid matter model has the following stress-energy tensor:

$$T_{\mu\nu} = \rho \; u_\mu u_\nu \quad , \tag{3.6}$$

where the 4–velocity is normalized: $u_\mu u^\mu = -1$. We choose a flow orthonormal foliation: the hypersurfaces of constant time Σ_t are normal to the 4–velocity of the fluid flow $\mathbf{u}$. Then, the 4–metric and the 4–velocity have the following form in the Lagrangian coordinate basis [2], also called Gaussian normal coordinate basis $\{\mathbf{d}X^i\}$:

$$g_{\mu\nu} = diag(-1, g_{ij}) \quad ; \quad u_\mu = (-1, \mathbf{0}) \quad ; \quad u^\mu = (1, \mathbf{0}) \;, \tag{3.7}$$

where g_{ij} is the metric on the hypersurface. The 4-dimensional line element in these coordinates is:

$$ds^2 = -dt^2 + g_{ij}\, \mathrm{d}X^i \mathrm{d}X^j \;. \tag{3.8}$$

In the special foliation that we considered for the irrotational dust fluid, the Einstein equations and the conservation equation can be expressed in terms of the expansion tensor [3], which is a symmetric spatial tensor:

$$\Theta_{ij} = \frac{1}{3}\theta\delta_{ij} + \sigma_{ij} \quad \text{where} \quad \sigma_{ij} = \Theta_{(ij)} - \frac{1}{3}\theta\delta_{ij} \;. \tag{3.10}$$

1. The resulting averaged Einstein's equations will only cover the full dynamical degrees of freedom in the case of locally rotationally symmetric spacetimes. In fact, in that case, Einstein's equations can be fully reduced to the dynamics of their covariant scalars [67].
2. The Strong Lagrangian description will be introduced in Section II.1.1.2.
3. The expansion tensor is initially a 4–dimensional object, defined by:

$$\Theta_{\mu\nu} := f^{\alpha}_{\;\;\mu} f^{\beta}_{\;\;\nu} \nabla_\beta u_\alpha \;, \tag{3.9}$$

where $f^{\alpha}_{\;\;\mu}$ is the projector on the rest-frames of the fluid, defined by (1.16), and ∇_β denotes the 4–dimensional covariant derivative.

θ is the trace of Θ_{ij}, i.e. the expansion rate and σ_{ij} is the shear. Then, the conservation of the stress-energy tensor reads:

$$\dot{\rho} + \theta\rho = 0 \ . \tag{3.11}$$

The full projection of the Einstein equations onto the hypersurfaces Σ_t gives the evolution equation of the extrinsic curvature:

$$\dot{\Theta}^i{}_j + \theta\Theta^i{}_j = (4\pi G\rho + \Lambda)\delta^i{}_j - \mathcal{R}^i{}_j \ . \tag{3.12}$$

The full projection perpendicular to the hypersurface (i.e. along the 4–velocity field) gives the Hamilton constraint:

$$\mathcal{R} + \theta^2 - \Theta^i{}_j\Theta^j{}_i = 16\pi G\rho + 2\Lambda \ . \tag{3.13}$$

The mixed projection gives the momentum constraint equation:

$$\theta_{|i} - \Theta^j{}_{i\|j} = 0 \ . \tag{3.14}$$

The details of the derivation of these equations will be given in Section II.1.1.3. From these equations, we will extract some scalar equations, which will be averaged in Section I.3.2.2.

3.2.2 Dynamics of a compact domain from the averaged Einstein equations

We here define the averaging operator on scalar fields for any domain. This operator will enable us to obtain the averaged scalar Einstein equations for the averaged evolution of an inhomogeneous universe [29].

Averaging scalars

We consider a compact and simply connected domain in the spatial hypersurfaces Σ. This domain $\mathcal{D}$ will follow the fluid during its evolution: it will follow the flow lines of the fluid elements. The total rest-mass of the fluid contained in the domain will be conserved. We use Lagrangian coordinates to parametrize the position on Σ_t.

$$\langle\phi\rangle_{\mathcal{D}}(t) := \frac{1}{V_{\mathcal{D}}}\int_{\mathcal{D}} \phi(t, \mathbf{X})\sqrt{g(t, \mathbf{X})}\ \mathbf{d}^3X \ , \tag{3.15}$$

$$V_{\mathcal{D}} := \int_{\mathcal{D}} \sqrt{g(t, \mathbf{X})}\ \mathbf{d}^3X \ , \tag{3.16}$$

is the volume of the domain and g is the determinant of the spatial metric tensor g_{ij}. Lagrangian coordinates index each particle of fluid and are thus comoving with the fluid. Furthermore, with these definitions, we can show that

$$\langle\theta\rangle_{\mathcal{D}} = \frac{\dot{V}_{\mathcal{D}}}{V_{\mathcal{D}}} \ . \tag{3.17}$$

Finally, from these definitions and identities, we get the non-commutation rule:

$$\langle \phi \rangle_{\mathcal{D}}^{\cdot} - \left\langle \dot{\phi} \right\rangle_{\mathcal{D}} = \langle \theta \rangle_{\mathcal{D}} \langle \phi \rangle_{\mathcal{D}} - \langle \theta\, \phi \rangle_{\mathcal{D}} \ . \tag{3.18}$$

We conclude that spatial averaging and time evolution do not commute. In the standard approach, the fluctuations of the CMB are averaged out to obtain the FLRW metric. This averaged universe is then evolved in time. According to (3.18), this is not equivalent to first evolving the inhomogeneous fields until present time and then spatially averaging them to obtain their final averaged values e.g. averaged density field or cosmological parameters.

Averaging scalar equations: Buchert's equations

We consider the following three scalar equations. The Hamilton constraint equation (3.19) can be rewritten:

$$\frac{1}{3}\theta^2 = 8\pi G\rho - \frac{1}{2}\mathcal{R} + \sigma^2 + \Lambda \ , \tag{3.19}$$

where $\sigma^2 = \frac{1}{2}\sigma_{ij}\sigma^{ij}$. The Raychaudhuri equation is obtained by replacing the Ricci scalar in the Hamilton constraint by its expression obtained by the trace of (3.12),

$$\dot{\theta} = -4\pi G\rho + \Lambda + \frac{1}{3}\theta^2 - 2\sigma^2 \ . \tag{3.20}$$

The last scalar equation we consider is the conservation of mass (3.11). We define the averaged scale factor

$$a_{\mathcal{D}}(t) = \left(\frac{V_{\mathcal{D}}}{V_{\mathcal{D}_\mathbf{i}}}\right)^{1/3} \ , \tag{3.21}$$

$\mathcal{D}_\mathbf{i}$ represents the initial domain and $a_{\mathcal{D}}(t)$ is linked to the averaged expansion rate according to

$$\langle \theta \rangle_{\mathcal{D}} = 3\frac{\dot{a}_{\mathcal{D}}}{a_{\mathcal{D}}} \ . \tag{3.22}$$

The Buchert's equations are obtained by combining (3.18) and (3.22) to average (3.19), (3.20) and (3.11):

$$3\left(\frac{\dot{a}_{\mathcal{D}}}{a_{\mathcal{D}}}\right)^2 = 8\pi G \langle \rho \rangle_{\mathcal{D}} - \frac{1}{2}\left(\mathcal{R}_{\mathcal{D}} + \mathcal{Q}_{\mathcal{D}}\right) + \Lambda \ , \tag{3.23}$$

$$3\frac{\ddot{a}_{\mathcal{D}}}{a_{\mathcal{D}}} = -4\pi G \langle \rho \rangle_{\mathcal{D}} + \mathcal{Q}_{\mathcal{D}} + \Lambda \ , \tag{3.24}$$

$$\langle \rho \rangle_{\mathcal{D}}^{\cdot} + 3\frac{\dot{a}_{\mathcal{D}}}{a_{\mathcal{D}}} \langle \rho \rangle_{\mathcal{D}} = 0 \ , \tag{3.25}$$

where we have defined

$$\mathcal{R}_{\mathcal{D}} := \langle \mathcal{R} \rangle_{\mathcal{D}} \quad , \quad \mathcal{Q}_{\mathcal{D}} := \frac{2}{3}\left\langle (\theta - \langle \theta \rangle_{\mathcal{D}})^2 \right\rangle_{\mathcal{D}} - 2\left\langle \sigma^2 \right\rangle_{\mathcal{D}} \ . \tag{3.26}$$

$\mathcal{Q}_\mathcal{D}$ is the kinematical backreaction. The time-derivative of the averaged Hamiltonian constraint (3.23) is equal to the averaged Raychaudhuri equation (3.24) if the following integrability condition is satisfied:

$$\frac{1}{a_\mathcal{D}^6}\left(\mathcal{Q}_\mathcal{D}\, a_\mathcal{D}^6\right)^{\cdot} + \frac{1}{a_\mathcal{D}^2}\left(\mathcal{R}_\mathcal{D}\, a_\mathcal{D}^2\right)^{\cdot} = 0 \ . \tag{3.27}$$

This equation has no Newtonian analogue and states that the averaged intrinsic and extrinsic curvature are dynamically coupled.

3.3 Can backreaction replace Dark Matter and Dark Energy?

To be self-consistent, the *SMC* has to assume a large amount of dark sources, namely Dark Matter and Dark Energy. The averaged Einstein equations for an inhomogeneous universe are analogous to the ones of the *SMC* but exhibit an additional term: $\mathcal{Q}_\mathcal{D}$, called backreaction, that has an impact on the dynamics of the domain considered $\mathcal{D}$. From (3.24), we conclude that

- if $\mathcal{Q}_\mathcal{D} > 0$, it contributes to the acceleration of the expansion of the domain and behaves like dark energy.
- if $\mathcal{Q}_\mathcal{D} < 0$, it will slow down the expansion of the domain and thus behave like dark matter.

Furthermore, the backreaction behaves like Dark Matter on the small scales and like Dark Energy on the large scales [154]. Moreover, it has been shown that, for an LTB model [139], backreaction can mimic the cosmological constant. Nevertheless, a precise evaluation of the backreaction has still to be achieved for more general inhomogeneous density profiles. Finally, the observational data should be entirely reinterpreted in the framework of inhomogeneous cosmology [43] in order to be fully consistent with this approach. A complete discussion of the effects of the inhomogeneities on the dynamics of the Universe can be found in the following reviews [65, 34, 91, 123, 158].

Part II

Insight into General Relativity via Electromagnetism Analogy

Chapter 1

Gravitoelectromagnetism and Gravitoelectric Part of the Einstein Equations

Contents

Gravitoelectromagnetism is an analogy between the equations of Newtonian or relativistic gravity and electromagnetism. This approach of gravity allows a special understanding of Einstein's theory of General Relativity. In this chapter, we will give a brief historical presentation of the development of this analogy and illustrate it in the case of the Newtonian gravitation theory. Thereafter, we will discuss the formulation of the Einstein equations in terms of the electric and magnetic parts of the Weyl tensor. As we will see, this formulation exhibits strong similarities with the Maxwell equations. Furthermore, we will show that the part of the Einstein equations, namely the gravitoelectric part, is the non-integrable counterpart of the Lagrange-Newton-System. Exploiting this formal analogy will be the subject of Chapter II.2, where a relativistic generalization of the Newtonian perturbation solutions to order n will be presented. The GEM analogy, as well as the perturbation scheme that we will discuss in the next chapters, is based on the 3+1 decomposition of the Einstein equations. Even if in most of the work that I carried out during my PhD, we considered the irrotational dust fluid as a matter model for the content of the Universe, some results for the perfect fluid matter model will be given in Appendix A.

In this chapter, I first present the general $3+1$ foliation of space-time and introduce the geometrical quantities that parametrize the foliation. We will explain how these quantities can be constrained in order to build a foliation adapted to the fluid flow, namely a comoving synchronous foliation. The Einstein equations will be given in the $3+1$ decomposition. The extrinsic curvature and expansion tensor will be expressed in terms of the physical and geometrical quantities we will define. These general results will then be specified on the case of the irrotational dust fluid matter model and for the perfect fluid matter model in Appendix A. Most of the results presented here are discussed in [129]. With permission of the authors, I present the following introductory notes here, since my work is based on some of these non-published results (in particular, appendix A).

1.1 Preparatory remarks: $3+1$ decomposition of the Einstein equations

1.1.1 Description of the fluid flow and foliation of space-time

In this section, we explain how we can relate the fluid flow to the foliation of space-time. Then, we present the general space-time foliations for an arbitrary set of coordinates and discuss how the degrees of freedom associated to the choice of the coordinate system, namely the lapse α and the shift $\boldsymbol{\beta}$, are related to the physical quantities of the fluid flow. Thereafter, we define the rest-frame of the fluid flow and give the expression of the stress-energy tensor of a perfect fluid in this frame.

$3+1$ foliation of space-time and description of the fluid flow

Fluid flow and hypersurfaces

We consider a globally hyperbolic 4–dimensional manifold, endowed with the pseudo-Riemannian metric tensor $\mathbf{g}$. We foliate this 4–dimensional manifold into space-like hypersurfaces for a given time t. We will denote by $\mathbf{n}$ the normal vector to the hypersurfaces [73] [135].

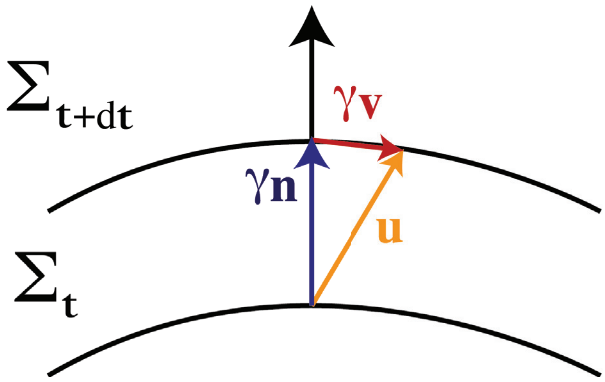

Figure 1.1: The unitary vector $\mathbf{n}$ is orthonormal to the spatial hypersurface Σ_t. It is tangent to the integral curves of the Eulerian frames. $\mathbf{u}$, the time-like 4–velocity unit vector, is tangent to the congruence of the fluid. It is not equal to $\mathbf{n}$ in general. The tilt vector $\mathbf{v}$ measures the difference between $\mathbf{n}$ and $\mathbf{u}$.

If we call $\mathbf{u}$ the time-like 4–velocity unit vector of the fluid flow, then, we can decompose it in the following way, as illustrated by the Figure 1.1:

$$\mathbf{u} = \gamma(\mathbf{n} + \mathbf{v}) \ , \tag{1.1}$$

where

$$\mathbf{g}(\mathbf{n}, \mathbf{v}) = 0 \quad \text{and} \quad \gamma = (1 - \mathbf{g}(\mathbf{v}, \mathbf{v}))^{-1/2} = -\mathbf{n} \cdot \mathbf{u} \ . \tag{1.2}$$

$\mathbf{v}$ is the spatial velocity of the fluid relative to the Eulerian frames, called tilt. $\mathbf{v}$ vanishes when $\mathbf{n}$ and $\mathbf{u}$ are identified. The quantities that we have defined here are independent of the choice of coordinates.

Local coordinate system

We define on the 4–dimensional manifold a local system of coordinates $x^\mu = (t, x^i)$. The corresponding coordinate basis is $\{\boldsymbol{\partial}_{x^\mu}\} = \{\boldsymbol{\partial}_t, \boldsymbol{\partial}_{x^i}\}$. Furthermore, we define $\boldsymbol{\nabla} t$ as the dual of the one-form $\mathbf{d}t$. The normal vector to the hypersurfaces is proportional to $\mathbf{n} = -\alpha\, \boldsymbol{\nabla} t$ where[1] $\alpha = (- < \mathbf{d}t, \boldsymbol{\nabla} t >))^{-1/2}$. We introduce the normal evolution vector $\mathbf{m} = \alpha \mathbf{n}$ that satisfies $< \mathbf{d}t, \mathbf{m} >= 1$. Since $< \mathbf{d}t, \boldsymbol{\partial}_t >$ is also equal to 1, the vector $\boldsymbol{\beta} = \boldsymbol{\partial}_t - \mathbf{m}$ is tangent to the hypersurfaces Σ_t. α is called the lapse function and $\boldsymbol{\beta}$ the shift vector. The useful geometrical objects are represented in Figure 1.2.

1. We denote by $< \underline{\mathbf{w}}, \mathbf{y} >$ the scalar product between the 1-form $\underline{\mathbf{w}}$ and the vector $\mathbf{y}$: $w_\mu\, y^\mu$

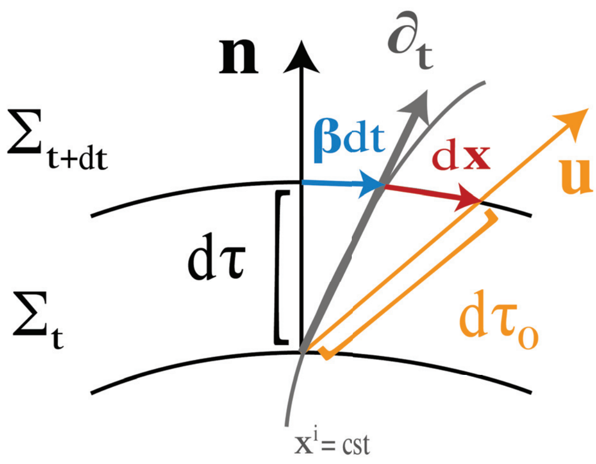

Figure 1.2: On this figure, we have represented schematically the normal vector $\mathbf{n}$ to the hypersurfaces, $\mathbf{u}$ the 4-velocity of the fluid, $\boldsymbol{\partial}_t$ the time-oriented vector of the coordinate basis which is tangent to the integral curves (of constant spatial coordinates $x^i = cst$). For the fluid congruence, the time that has elapsed between the two hypersurfaces is $d\tau_0$ whereas for the Eulerian observers, it is $d\tau$. γ measures their ratio : $d\tau/d\tau_0 = \gamma$.

In the coordinate basis that we have chosen, the normal vector to the hypersurfaces has the following coordinates:

$$n^\mu = \frac{1}{\alpha}(1, -\beta^i) \ . \tag{1.3}$$

The dual form of $\mathbf{n}$, $\underline{\mathbf{n}}$ has the following components:

$$n_\mu = -\alpha\,(1, 0) \ . \tag{1.4}$$

We define the spatial coordinate velocity $\mathbf{V}$ by:

$$\mathbf{V} := \frac{d\,\mathbf{x}}{d\,t} \ \text{ with } \ \mathbf{g}(\mathbf{n}, \mathbf{V}) = 0 \ . \tag{1.5}$$

$\mathbf{V}$ explicitly depends on the choice of coordinates which is not the case of $\mathbf{v}$.

Different times can be considered in the description of the dynamics of the fluid. τ_0 is the time associated to the comoving observers, i.e. measured by the Lagrangian observers along their flow lines whereas t is the time coordinate, depending on our choice of foliation of space-time. τ is the time associate to the Eulerian observers, attached to the foliation (*cf* Figure 1.2). It is possible to show that for any tensor field $\mathcal{F}$:

$$u^\mu \nabla_\mu \mathcal{F} = \frac{d\,\mathcal{F}}{d\tau_0} = \frac{\gamma}{\alpha}\frac{d\,\mathcal{F}}{dt} \ , \tag{1.6}$$

since $\alpha = d\tau/dt$ and $\gamma = d\tau/d\tau_0$. Furthermore,

$$\frac{d\,\mathcal{F}}{dt} = \left.\frac{\partial\,\mathcal{F}}{\partial t}\right|_{X^i} = \left.\frac{\partial\,\mathcal{F}}{\partial t}\right|_{x^i} + V_i\,\frac{\partial\,\mathcal{F}}{\partial x^i} \ . \tag{1.7}$$

From now on, we will denote $\frac{d\mathcal{F}}{d\tau_0}$ by $\dot{\mathcal{F}}$.

Furthermore, for $d\boldsymbol{\lambda} = \boldsymbol{\beta}dt + d\mathbf{x}$, we show the useful equality:

$$\mathbf{v} = \frac{d\boldsymbol{\lambda}}{d\tau} = \frac{dt}{d\tau}(\mathbf{V} + \boldsymbol{\beta}) = \frac{1}{\alpha}(\mathbf{V} + \boldsymbol{\beta}) \ . \tag{1.8}$$

For (1.1) and (1.8) we conclude that the 4–velocity of the fluid can be expressed as:

$$\mathbf{u} = \frac{\gamma}{\alpha}\left(\alpha\mathbf{n} + \boldsymbol{\beta} + \mathbf{V}\right) \ . \tag{1.9}$$

Thus, the components of the fluid flow vector and its dual are:

$$u^\mu = \frac{\gamma}{\alpha}\left(1, V^i\right) \quad , \quad u_\mu = \frac{\gamma}{\alpha}\left(-\alpha^2 + \beta^k(\beta_k + V_k), \beta_i + V_i\right) \ . \tag{1.10}$$

If we define the projector on the spatial hypersurfaces as:

$$h_{\mu\nu} = g_{\mu\nu} + n_\mu n_\nu \ , \tag{1.11}$$

it satisfies the following equalities:

$$h_{\mu\nu}n^\mu = 0 \ , \qquad h^\mu_\alpha\, h^\alpha_\nu = h^\mu_\nu \ , \qquad h^{\mu\nu}h_{\mu\nu} = 3 \ . \tag{1.12}$$

The components of the metric on the coordinate basis are:

$$g_{\mu\nu} = \begin{pmatrix} -\alpha^2 + \beta_k\beta^k & \beta_j \\ \beta_i & h_{ij} \end{pmatrix} \qquad ; \qquad g^{\mu\nu} = \begin{pmatrix} -\frac{1}{\alpha^2} & \frac{\beta^j}{\alpha^2} \\ \frac{\beta^i}{\alpha^2} & h^{ij} - \frac{\beta^i\beta^j}{\alpha^2} \end{pmatrix} \ . \tag{1.13}$$

Thus, the 4–dimensional line element can be decomposed as:

$$ds^2 = g_{\mu\nu}dx^\mu dx^\nu = -(\alpha^2 - \beta^k\beta_k)dt^2 + \beta_i dt\, dx^i + h_{ij}dx^i dx^j \ . \tag{1.14}$$

Stress-energy tensor for the general foliation

In the rest-frame of the fluid, the stress-energy tensor for a general matter model can be decomposed relative to the 4–velocity $\mathbf{u}$ as:

$$T_{\mu\nu} = \epsilon\, u_\mu u_\nu + q_\mu u_\nu + q_\nu u_\mu + p\, f_{\mu\nu} + \pi_{\mu\nu} \ , \tag{1.15}$$

where ϵ is the relativistic energy density, q^μ the relativistic momentum density, p the isotropic pressure, $\pi_{\mu\nu}$ the trace-free anisotropic pressure. We have defined the projector on the rest-frames of the fluid:

$$f_{\mu\nu} = g_{\mu\nu} + u_\mu u_\nu \ , \tag{1.16}$$

which satisfies the following equalities:

$$f_{\mu\nu}u^\mu = 0 \ , \qquad f^\mu_\alpha\, f^\alpha_\nu = f^\mu_\nu \ , \qquad f^{\mu\nu}f_{\mu\nu} = 3 \ . \tag{1.17}$$

In the rest-frame of the fluid, the stress-energy tensor of the perfect fluid is obtained for $q^\mu = \pi_{\mu\nu} = 0$:

$$T_{\mu\nu} = \epsilon\, u_\mu u_\nu + p\, f_{\mu\nu} \ . \tag{1.18}$$

Furthermore, for pressure-free matter, called dust matter model (which is the one used to model the Cold Dark Matter), the stress-energy tensor becomes:

$$T_{\mu\nu}^{dust} = \epsilon\, u_\mu u_\nu \ . \tag{1.19}$$

The stress-energy tensor for general matter models can also be described in this foliation using a foliation-dependent decomposition:

$$T_{\mu\nu} = E\, n_\mu n_\nu + 2\, n_{(\mu} J_{\nu)} + S_{\mu\nu} \ , \tag{1.20}$$

where E, the energy density, J_μ the momentum density and $S_{\mu\nu}$ the stress density, are all evaluated in the Eulerian frames i.e. the ones transported along the integral curves of $\mathbf{n}$:

$$E = n^\alpha n^\beta\, T_{\alpha\beta} \ , \quad J_\nu = -h^\alpha{}_\mu n^\beta T_{\alpha\beta} \ , \quad S_{\mu\nu} = h^\alpha{}_\mu h^\beta{}_\nu T_{\alpha\beta} \ . \tag{1.21}$$

For a perfect fluid matter model, the energy density, the momentum density and the stress density evaluated in the Eulerian frames can be expressed as functions of ϵ the relativistic energy and the pressure p:

$$E = \gamma^2 \epsilon + (\gamma^2 - 1) p \ , \qquad J_\mu = \frac{\gamma^2}{\alpha} (\epsilon + p)(\beta_\mu + V_\mu) \ , \tag{1.22}$$

$$S_{\mu\nu} = \frac{\gamma^2}{\alpha^2} (\epsilon + p)(\beta_\mu + V_\mu)(\beta_\nu + V_\nu) + p\, h_{\mu\nu} \ , \tag{1.23}$$

$$S = (\gamma^2 - 1)\epsilon + (\gamma^2 + 2) p \ . \tag{1.24}$$

Now that we have built all the quantities needed to describe both the fluid flow and the geometry of space sections, we are able to formulate the Einstein equations for this $3+1$ foliation of space-time. But before, we present the relativistic generalization of the Lagrangian description.

1.1.2 Lagrangian descriptions

We here generalize the Newtonian notion of Lagrangian description and introduce two Lagrangian descriptions: the Weak and the Strong descriptions, for which the observer follows the fluid flow. The Weak Lagrangian description of the fluid is obtained for a shift vector $\boldsymbol{\beta}$ attached to the fluid flow and the coordinate velocity is then zero:

$$\boldsymbol{\beta} = \alpha\, \mathbf{v} \Leftrightarrow \mathbf{V} = \mathbf{0} \ . \tag{1.25}$$

Furthermore, if the lapse function is equal to the Lorentz factor, $\alpha = \gamma$, then the hypersurfaces of constant t are also hypersurfaces of constant fluid proper time τ_0. This description is the Strong Lagrangian description. The two Lagrangian descriptions consider spatial Lagrangian coordinates (*cf* Section I.2.2.1) and provide us with a relativistic generalization of the Newtonian Lagrangian formalism.

The 4–velocity can then be expressed as:

$$u^\mu = (1, \mathbf{0}) \quad \text{and} \quad u_\mu = (-1, \boldsymbol{\beta}) \ . \tag{1.26}$$

The Strong Lagrangian description thus defines a comoving synchronous slicing of space-time. From (1.6), we can show that in this description for any tensor field $\mathcal{F}$,

$$\frac{d\,\mathcal{F}}{dt} = \left.\frac{\partial\,\mathcal{F}}{\partial t}\right|_{X^i} = \frac{d\,\mathcal{F}}{d\tau_0} \ , \tag{1.27}$$

i.e. all the time derivatives are equal.

Since the Lorentz factor γ and the shift α are equal, from (1.2) we conclude that $\gamma = \left(1 - \frac{\beta_k\beta^k}{\alpha^2}\right)^{-1/2}$ and therefore we obtain the equality:

$$\alpha^2 - \beta_k\beta^k = 1 \ . \tag{1.28}$$

This equality, which is a scalar constraint connecting the lapse and the shift, was discussed by H. Asada and M. Kasai [2] in [7].

1.1.3 $3+1$ decomposition of the Einstein equations

We here determine the $3+1$ decomposition of the Einstein equations in terms of the kinematical and geometrical quantities that we introduced in last section. We project the Ricci curvature tensor and the stress-energy tensor either on the normal vector to the hypersurfaces $\mathbf{n}$ or on the tangent space Σ_t [73] [73] [135].

The full projection of the Einstein equations on the spatial hypersurface Σ_t gives the *evolution equation for the extrinsic curvature*:

$$\begin{aligned} \partial_t|_{x^i}\mathcal{K}^i{}_j = \alpha\left(\mathcal{R}^i{}_j + \mathcal{K}\mathcal{K}^i{}_j - \delta^i_j\Lambda + 4\pi G[(S-E)\delta^i_j] - S^i{}_j\right) \\ -\alpha^{|i}{}_{|j} + \beta^k\mathcal{K}^i{}_{j|k} + \mathcal{K}^i{}_k\beta^k{}_{|j} - \mathcal{K}^k{}_j\beta^i{}_{|k} \ , \end{aligned} \tag{1.29}$$

where $\mathcal{K}^i{}_j = -h^\alpha_i h^\beta_j \nabla_\alpha n_\beta$ is the extrinsic curvature tensor of the hypersurface, ∇_α is the four-covariant derivative. $_{\|i}$ is the three-covariant derivative and $_{|i}$ is the simple three-derivative equal to ∂_{x^i}. $\partial_t|_{x^i}$ is the time derivative along the integral curves, for which the coordinates x^i are held fixed.

The full projection along $\mathbf{n}$ gives the *Hamilton constraint*:

$$\mathcal{R} + \mathcal{K}^2 - \mathcal{K}^i{}_j\mathcal{K}^j{}_i = 16\pi GE + 2\Lambda \ . \tag{1.30}$$

while the mixed projection

$$\mathcal{K}^k{}_{j|k} - \mathcal{K}_{|i} = 8\pi GJ_i \ , \tag{1.31}$$

gives the *momentum constraint*.

With the lapse function α and the shift vector $\boldsymbol{\beta}$ that we defined in last section, we express the extrinsic curvature $\mathcal{K}^i{}_j$ in terms of metric [73]:

$$\partial_t|_{x^i}h_{ij} = -2\alpha\mathcal{K}_{ij} + 2\beta_{(i\|j)} \ . \tag{1.32}$$

2. H. Asada and M. Kasai took another convention for the metric signature: $(+,-,-,-)$. They therefore get $\alpha^2 - \beta_k\beta^k = -1$ instead of $\alpha^2 - \beta_k\beta^k = 1$.

From equation (1.7) and (1.32), we obtain:

$$\mathcal{K}^i{}_j = \frac{1}{2}\left(\frac{1}{\alpha}(V^l h^{ik} h_{kj|l} + \beta^i{}_{\|j} + \beta_j{}^{\|i}) - \frac{h^{ik}\dot{h}_{kj}}{\gamma}\right) \quad , \tag{1.33}$$

its trace being

$$\mathcal{K} = \frac{1}{2}\left(\frac{1}{\alpha}(V^l h^{ik} h_{kj|l} + 2\beta_i{}^{\|i}) - \frac{h^{ik}\dot{h}_{ki}}{\gamma}\right) \quad . \tag{1.34}$$

(1.33) and (1.34) can be inserted into (1.29), (1.31) and (1.30) to obtain the evolution equations for the geometry of the spatial hypersurfaces. In the Strong Lagrangian description, these expressions become:

$$\mathcal{K}^i{}_j = \frac{1}{2\alpha}\left(-h^{ik}\dot{h}_{kj} + \beta^i{}_{\|j} + \beta_j{}^{\|i}\right) \quad ; \quad \mathcal{K} = \frac{1}{2\alpha}\left(-h^{ik}\dot{h}_{ki} + 2\beta_i{}^{\|i}\right) \quad . \tag{1.35}$$

The four-covariant derivative of $\mathbf{u}$ contains the kinematical information of the fluid flow. We consider the spatial components of the projection onto the hypersurfaces of the 4–velocity gradient $\nabla_\nu u_\mu$:

$$\mathcal{L}_{ij} := h^\mu{}_i h^\nu{}_j \, \nabla_\nu u_\mu = \Theta_{ij} + \omega_{ij} - u_j a_i = u_{i|j} - \Gamma^\alpha_{ij} u_\alpha \quad . \tag{1.36}$$

a_i is the acceleration: $a_i := u^\mu \nabla_\mu u_i$, Θ_{ij} is the expansion tensor, θ its trace, also called expansion rate. σ_{ij} is the symmetric traceless part of Θ_{ij} and is called the shear tensor while ω_{ij} is the vorticity of the fluid. In terms of the quantities that we defined, we get:

$$\mathcal{L}_{ij} = \frac{\gamma}{\alpha}(\beta_i + V_i)_{\|j} - \frac{\gamma}{\alpha^3}\left(-\alpha^2 + \beta_k\beta^k + \beta^k V_k\right)\left(\frac{1}{2}\frac{\partial}{\partial t}\Big|_{X^i} h_{ij} - \beta_{(i\|j)}\right) \quad . \tag{1.37}$$

With condition (1.28), in the Strong Lagrangian description, $\mathcal{L}_{ij}$ becomes :

$$\mathcal{L}_{ij} = \frac{\dot{h}_{ij}}{2\alpha^2} + (1 - \frac{1}{\alpha^2})\beta_{(i\|j)} + \beta_{[i|j]} \quad . \tag{1.38}$$

We here derived the $3+1$ decomposition of the Einstein equations for a general matter model in the Strong Lagrangian description. Now, we will determine what these equations become for the dust matter model. We will express these equations in terms of the Cartan coframes, that were defined in Section I.2.3.2. As we have seen, the Cartan coframes can indeed be connected to the spatial metric by (2.59).

1.1.4 Lagrangian formulation of Einstein's equations for an irrotational dust fluid matter model

Since we consider an irrotational flow, it is possible to choose a foliation for which the normal vector $\mathbf{n}$ coincides with the 4–velocity $\mathbf{u}$ of the fluid flow [3]. In such a foliation,

3. If the fluid flow has vorticity, the local rest-frames do not form a global hypersurface. A $3+1$ foliation for which $\mathbf{n} = \mathbf{u}$ cannot be built. The description of a non–zero vorticity will indeed require a $1+3$ threading of spacetime [68].

the acceleration vanishes since the trajectories are geodesics and, furthermore, $\gamma = 1$. Moreover, if we consider the Strong Lagrangian description, then

$$\boldsymbol{\beta} = \mathbf{0} \quad ; \quad \alpha = 1 \ . \tag{1.39}$$

Θ_{ij}, the expansion tensor, and $\mathcal{K}_{ij}$, the extrinsic curvature tensor, have now the following form:

$$\Theta_{ij} = \frac{\dot{g}_{ij}}{2} \quad ; \quad \mathcal{K}_{ij} = -\Theta_{ij} = -\frac{\dot{g}_{ij}}{2} \ , \tag{1.40}$$

where we now use the notation g_{ij} instead of h_{ij}. Furthermore, we now also have $h^{ij} = g^{ij}$ in this foliation.

As was shown in [35], we now insert the expression of the metric in terms of the Cartan coframes (2.59) and (2.62) into the Einstein equations to obtain the following system of equations, called the Lagrange-Einstein-System:

$$G_{ab}\, \ddot{\eta}^a_{[i}\eta^b{}_{j]} = 0 \ ; \tag{1.41}$$

$$\frac{1}{2J}\epsilon_{abc}\epsilon^{ikl}\left(\dot{\eta}^a{}_j\eta^b{}_k\eta^c{}_l\right)^{\cdot} = -\mathcal{R}^i{}_j + \left(4\pi G\varrho + \Lambda\right)\delta^i{}_j \ ; \tag{1.42}$$

$$\frac{1}{2J}\epsilon_{abc}\epsilon^{mjk}\dot{\eta}^a{}_m\dot{\eta}^b{}_j\eta^c{}_k = -\frac{\mathcal{R}}{2} + \left(8\pi G\varrho + \Lambda\right) \ ; \tag{1.43}$$

$$\left(\epsilon_{abc}\epsilon^{ikl}\dot{\eta}^a{}_j\eta^b{}_k\eta^c{}_l\right)_{||i} = \left(\epsilon_{abc}\epsilon^{ikl}\dot{\eta}^a{}_i\eta^b{}_k\eta^c{}_l\right)_{|j} \ , \tag{1.44}$$

The system $\{(1.41) - (1.44)\}$ consists of 13 equations. The equations are, respectively, the symmetry of the metric (1.41) (3 equations), the equation of motion (1.42) (i.e. the evolution equation for the extrinsic curvature) (6 equations), the energy constraint (1.43) (1 equation) and the momentum constraints (1.44) (3 equations). Thus, the first 9 equations furnish evolution equations for the 9 coefficient functions of the 3 Cartan coframe fields.

The double vertical slash denotes the covariant spatial derivative with respect to the 3–metric and the spatial connection is assumed to be symmetric. The first equation can be replaced by the irrotationality condition:

$$G_{ab}\, \dot{\eta}^a_{[i}\eta^b{}_{j]} = 0 \ . \tag{1.45}$$

Furthermore, the trace of the equation of motion and the energy constraint leads to the Raychaudhuri equation:

$$\frac{1}{2J}\epsilon_{abc}\epsilon^{ik\ell}\ddot{\eta}^a{}_i\eta^b{}_k\eta^c{}_\ell = \Lambda - 4\pi G\varrho \ . \tag{1.46}$$

The above system is equivalent to the results developed in [35] in a different coframe basis: in the first paper the choice of the standard orthonormal coframes has been made, whereas, from [36] on, the choice of the adapted coframes is preferred because it allows a formally closer Newtonian analogy.

The Lagrange-Einstein-System can also be expressed in a coordinate-independent way, using differential geometry (*cf* Section I.2.3.1). We then obtain the following set of equations [4], equivalent to the one expressed in the coordinate basis $\{\mathbf{d}X^i\}$:

$$G_{ab}\,\ddot{\boldsymbol{\eta}}^a \wedge \boldsymbol{\eta}^b = \mathbf{0}\ ; \tag{1.47}$$

$$\frac{1}{2}\epsilon_{dbc}\left(\dot{\boldsymbol{\eta}}^a \wedge \boldsymbol{\eta}^b \wedge \boldsymbol{\eta}^c\right)^{\cdot} = \left(-\mathcal{R}^a{}_d + (4\pi G\varrho + \Lambda)\,\delta^a{}_d\right) J\mathbf{d}^3X\ ; \tag{1.48}$$

$$\epsilon_{abc}\,\dot{\boldsymbol{\eta}}^a \wedge \dot{\boldsymbol{\eta}}^b \wedge \boldsymbol{\eta}^c = (16\pi G\varrho + 2\Lambda - \mathcal{R})\,J\mathbf{d}^3X\ ; \tag{1.49}$$

$$\epsilon_{abc}\,\left(\mathbf{d}\dot{\boldsymbol{\eta}}^a \wedge \boldsymbol{\eta}^b + \boldsymbol{\omega}^a{}_d \wedge \dot{\boldsymbol{\eta}}^d \wedge \boldsymbol{\eta}^b\right) = \mathbf{0}\ . \tag{1.50}$$

The combination of the trace of the equation of motion and the energy constraint straightforwardly leads to the Raychaudhuri equation:

$$\frac{1}{2}\epsilon_{abc}\ddot{\boldsymbol{\eta}}^a \wedge \boldsymbol{\eta}^b \wedge \boldsymbol{\eta}^c = (\Lambda - 4\pi G\varrho)\,J\mathbf{d}^3X\ . \tag{1.51}$$

To derive the above equations we have implicitly used the Cartan connection one–form and the curvature two–form that we do not need explicitly in what follows:

$$\boldsymbol{\omega}^a{}_b := \gamma^a{}_{cb}\boldsymbol{\eta}^c, \tag{1.52}$$

$$\boldsymbol{\Omega}^a{}_d := \frac{1}{2}\mathcal{R}^a{}_{bcd}\boldsymbol{\eta}^c \wedge \boldsymbol{\eta}^d\ , \tag{1.53}$$

with the connection and curvature coefficients $\gamma^a{}_{cb}$ and $\mathcal{R}^a{}_{bcd}$ in the non-exact basis, respectively. The 3–Ricci tensor can be expressed through the curvature two–form:

$$\mathcal{R}^a{}_d\boldsymbol{\eta}^d \wedge \boldsymbol{\eta}^b \wedge \boldsymbol{\eta}^c = \delta^{db}\boldsymbol{\Omega}^a{}_d \wedge \boldsymbol{\eta}^c - \delta^{dc}\boldsymbol{\Omega}^a{}_d \wedge \boldsymbol{\eta}^b\ . \tag{1.54}$$

We here explained how space-time can be foliated in the $3+1$ approach. Moreover, we established the $3+1$ decomposition of the Einstein equations for a general matter model and introduced the Strong Lagrangian description to generalize the Lagrangian approach presented in the Newtonian case. The geometrical parameters of the foliation could then be constrained in order to build a foliation adapted to the dynamics of the fluid. Since the major part of my work considers the irrotational dust matter model, I gave the Einstein equations for this matter model, in the Strong Lagrangian description, formulated in terms of the Cartan coframes. These equations are at the basis of the work I achieved during most of my PhD. Finally, a discussion of the perfect fluid matter model and some results at first order in the Strong Lagrangian description are provided in Appendix A.

We will now present a brief history of the GEM analogy. Before going to General Relativity, we will present in detail the GEM analogy for Newtonian gravity. We will see that Newtonian gravity could be the limit where c goes to infinity of a Maxwellian theory of gravity. Furthermore, we will show that it is possible to recover the Maxwell equations by doing a manipulation in the spirit of what Faraday did for electromagnetism.

In the frame of General Relativity, a way to achieve this analogy is to consider a formulation of the Einstein equations for which the Ricci tensor is no longer the main geometrical quantity. The Weyl curvature tensor becomes the fundamental geometrical quantity. It can be split into an electric and a magnetic part, in a way that is analogue to what is done in electrodynamics. Einstein equations are then inserted into the contracted Bianchi identities in order to obtain new field equations in terms of these electric and magnetic parts: the Maxwell-Weyl equations.

Finally, we include in the electric part of the Weyl tensor a part of the Einstein equations, as can be done with the Newtonian tidal tensor and Newtonian gravity equations. The absence of trace and the symmetry of the electric part, that before were satisfied by construction, will now give back the Einstein equations that we inserted. This new tensor, the Einstein electric tensor, will thus coincide with the electric tensor only if these equations are satisfied.

We should keep in mind that the GEM analogy has some limits since General Relativity and electromagnetism are, in many aspects, very different. On the one hand, General Relativity is a non-linear, diffeomorphism invariant field theory which can be formulated in terms of tensors. On the other hand, electromagnetism is a linear vector field theory which is Lorentz invariant. Any attempt to distort gravity in order to make it formally equal to electrodynamics in a restrictive sense will thus fail. Nevertheless, we can use the existing similarities in order to translate some of the ideas and results coming from electromagnetism to gravitation.

1.2 Historical introduction to GEM

Gravitoelectromagnetism (*GEM*) consists in finding a formal analogy between the theory of gravitation and electromagnetism. Such an analogy would enable us to transpose the results that have been established for electromagnetism to gravity. This analogy has many applications. Indeed, it would also allow us to take into account retardation effects in numerical simulations due to the finite value of the speed of light c (information does not travel instantaneously as in Newtonian theory of gravitation). Moreover, electromagnetism has been quantized in the frame of QED, so some similarities between the two theories could give us a new insight into the quantization of General Relativity. Finally, since electromagnetism is a propagation theory, finding an analogy with gravity should help us understand the physics of gravitational waves. This aspect will be discussed in detail in the part on Maxwell-Weyl equations obtained from the electric and magnetic parts of the Weyl tensor.

In 1870, Holzmüller and Tisserand first postulated that the gravitational force exerted by the sun on the planets could have a magnetic contribution [78] [141]. Few years later, in 1893, O. Heaviside published an article which is considered to be the foundation of GEM [76]. In this article, he built the basis of the formal analogy between electromagnetism and Newtonian gravity and postulated the existence of small terms that would enable a complete analogy.

In 1917, Lense and Thirring solved the problem of the rotating sphere and identified the gravitational analogue of a Coriolis force [104]. More recently, the gravitational counterpart of the Aharonov-Bohm effect was measured by [52], in the COW experiment. It proved that gravitomagnetic field could, as the magnetic field, be coupled to the quantum degrees of freedom of particles such as neutrons.

There are many ways to build a *GEM* analogy. By comparing the gravitational tidal tensors to the electric and magnetic fields, it is possible to build a covariant *GEM* analogy formulated in terms of tidal tensors. This analogy, that is very convincing for static fields, is still limited by the fact that gravitational tidal tensors are non-linear, spatial and symmetric whereas electromagnetic tensors are linear and generically non-symmetric and non-spatial [46].

Another approach is based on Fermi-Walker transport. This approach, that consists in saying that the analogue of the Lorentz force would come from some non-inertial fields is based on the 1+3 threading of space-time and Fermi-Walker transport (*FWT*). *FWT* defines locally nonrotating axes along the wordline of the comoving observers [84]. Nevertheless, the magnetic part of the Lorentz force has no physical counterpart in gravity since we compare a physical magnetic force to an artifact of reference frames.

Furthermore, we can linearize the metric tensor with respect to a flat background and consider weak gravitational fields and slowly moving gravitational objects: $v/c \ll 1$.

The propagation theory that we obtain in this post-newtonian approximation then formally gives the Maxwell equations and the Newtonian limit of the Lorentz force. This approach will be presented in Section III.1.2.3.

Finally, we could also cite the *GEM* analogy based on inertial frame dragging. This approach is discussed extensively in [157].

1.3 Maxwellian formulation of the Euler-Newton-System

We here consider the Euler–Newton–System (2.20) which gives the evolution equations governing the motion of self–gravitating dust in the Eulerian picture. The gravitational field is curl-free. Therefore, a gravitational potential Φ such that $\mathbf{g} =: -\boldsymbol{\nabla}\Phi$ exists.

The Euler–Newton–System can either be thought as vector equations on the field $\mathbf{g}$ or as a system of equations on the scalar field Φ. As we will see later, the limit of the Einstein equations on a flat space-time will exhibit some similarities with the Euler–Newton–System, expressed in its vector form. Thus, we are here interested in looking for a Maxwellian counterpart of the Euler–Newton–System.

We are looking for a mathematical operation that should bring the Einstein equations into a space in which they can be written as Maxwell's equations. We already know that for any point P of space-time, it is possible to define an inertial set of coordinates associated to the tangent space at that point for which the metric is Minkowskian and the laws of physics are ruled by special relativity.

The mathematical restriction has a link with the Newtonian limit, consisting in taking the geometrical limit of the equations and sending c to infinity.

In the following discussion, which is based on Thomas Buchert's M2 lecture at ENS de Lyon [38] and on the published work [33], we get an insight into the gravitoelectromagnetic analogy from Newtonian evolution equations. We identify some gravitoelectric and gravitomagnetic fields and predict their field equations in the case c is not sent to infinity.

Scalar and vector potentials of the current density

We introduce the current density $\mathbf{j} := \varrho\mathbf{v}$ for the fluid flow. Using the continuity equation and the relation between the restmass density and the divergence of the field strength, we find:

$$\frac{\partial}{\partial t}\varrho = -\boldsymbol{\nabla}\cdot\mathbf{j} \quad \text{and} \quad -4\pi G\frac{\partial}{\partial t}\varrho = \boldsymbol{\nabla}\cdot\frac{\partial}{\partial t}\mathbf{g} \quad , \tag{1.55}$$

so, we conclude:

$$\boldsymbol{\nabla}\cdot[\,\frac{\partial}{\partial t}\mathbf{g} - 4\pi G\mathbf{j}\,] \;=\; \mathbf{0} \quad \Rightarrow \quad \frac{\partial}{\partial t}\mathbf{g} - 4\pi G\mathbf{j} \;=:\; \boldsymbol{\nabla}\times\boldsymbol{\tau} \quad , \tag{1.56}$$

with $\boldsymbol{\tau}$ being the *vector potential* of the current density.

Since we have no equation for the divergence of $\boldsymbol{\tau}$, we may employ the transverse gauge condition $\boldsymbol{\nabla}\cdot\boldsymbol{\tau} = 0$ [4].

Using this gauge condition, we find the simple relationship:

$$4\pi G\,\boldsymbol{\nabla}\times\mathbf{j} = -\boldsymbol{\nabla}\times(\boldsymbol{\nabla}\times\boldsymbol{\tau}) = \Delta\boldsymbol{\tau} - \boldsymbol{\nabla}(\boldsymbol{\nabla}\cdot\boldsymbol{\tau}) = \Delta\boldsymbol{\tau} \quad . \tag{1.57}$$

We conclude that the vector fields $\mathbf{g}$ and $\boldsymbol{\tau}$ obey the Poisson equations:

$$\Delta\mathbf{g} \;=\; -4\pi G\boldsymbol{\nabla}\varrho \quad ; \quad \Delta\boldsymbol{\tau} \;=\; 4\pi G\boldsymbol{\nabla}\times\mathbf{j} \quad . \tag{1.58}$$

Kinematical intuition for the vector potential

In order to obtain some kinematical intuition for $\boldsymbol{\tau}$, we notice that $\boldsymbol{\tau}$ is a harmonic vector field for a class of motions that may be specified by the vanishing of the source in the equation

$$\Delta\boldsymbol{\tau} \;=\; 4\pi G\boldsymbol{\nabla}\times\mathbf{j} = 4\pi G[\,\varrho\boldsymbol{\nabla}\times\mathbf{v} + \boldsymbol{\nabla}\varrho\times\mathbf{v}\,] \quad . \tag{1.59}$$

We infer that, e.g., for irrotational flows, $\boldsymbol{\nabla}\times\mathbf{v} = \mathbf{0}$, together with the requirement that the integral curves of the velocity are orthogonal to isodensity surfaces, the source vanishes. Thus, a non–trivial $\boldsymbol{\tau}$ causes deviations from such a class of motion.

Lorentz–covariant generalization of Newton's theory

As we have seen, a Lorentz–covariant gravitational theory in the Minkowski space can be easily constructed. Indeed, including the source term $-1/c^2\,\partial/\partial t\,\boldsymbol{\tau}$ into Newton's field equations would render them Lorentz–covariant, while without this term they are

4. It is always possible to require this condition according to the following reasoning: the curl of the vector field $\boldsymbol{\tau}$ remains unchanged, if we add to $\boldsymbol{\tau}$ the gradient of an arbitrary scalar field, $\boldsymbol{\tau'} := \boldsymbol{\tau} + \boldsymbol{\nabla}\psi$; the divergence of $\boldsymbol{\tau}$ itself is not specified by the Euler–Newton system, so we can find ψ such that $\boldsymbol{\nabla}\cdot\boldsymbol{\tau} = 0$ from the following equation:

$$\Delta\psi = \boldsymbol{\nabla}\cdot\boldsymbol{\tau'} \quad .$$

If the spatial average of the source of Poisson's equation vanishes there is a solution to this equation. Nevertheless, the fact that the divergence of the magnetic field vanishes is not a freedom of the electromagnetic theory: it is a constitutive equation. The analogy is therefore only formal.

just Galilei–invariant. If we add this term into the Euler–Newton–System, we get the following equations:

$$\begin{aligned} \boldsymbol{\nabla}\cdot\mathbf{g} &= \Lambda - 4\pi G\varrho \quad ; \quad \boldsymbol{\nabla}\cdot\boldsymbol{\tau} = 0 \ ; \\ \boldsymbol{\nabla}\times\mathbf{g} &= -\tfrac{1}{c^2}\tfrac{\partial}{\partial t}\boldsymbol{\tau} \quad ; \quad \boldsymbol{\nabla}\times\boldsymbol{\tau} = \frac{\partial}{\partial t}\mathbf{g} - 4\pi G\mathbf{j} \ . \end{aligned} \tag{1.60}$$

They give back the Newtonian theory when we flatten out the light cone, i.e. that we send the speed of light c to infinity.

A way to obtain these equations is to follow Faraday's idea and dynamically couple $\mathbf{g}$ to $\boldsymbol{\tau}$ via their potentials. We no longer assume that $\mathbf{g}$ is curlfree:

$$\mathbf{g} = -\boldsymbol{\nabla}V - \frac{\partial\mathbf{A}}{\partial t} \ , \tag{1.61}$$

and we define $\boldsymbol{\tau}$ as

$$\boldsymbol{\tau} = c^2\boldsymbol{\nabla}\times\mathbf{A} \ . \tag{1.62}$$

Then, we get by construction:

$$\boldsymbol{\nabla}\times\mathbf{g} = -\frac{1}{c^2}\frac{\partial}{\partial t}\boldsymbol{\tau} \ . \tag{1.63}$$

The Lorentz gauge condition:

$$\frac{1}{c^2}\frac{\partial V}{\partial t} + \boldsymbol{\nabla}\cdot\mathbf{A} = 0 \ , \tag{1.64}$$

now has the following wave equation form:

$$-\frac{1}{c^2}\frac{\partial^2 V}{\partial t^2} + \Delta V = \Lambda - 4\pi G\varrho \ . \tag{1.65}$$

We now have obtained the equations analogous to the Maxwell equations. The gravitoelectric field $\mathbf{g}$ is the analogue of the electric field $\mathbf{E}$ and the gravitomagnetic field $\boldsymbol{\tau}$ is the analogue of the magnetic field $\mathbf{B}$. We here sum up the analogies existing in this Lorentz–covariant formulation of gravitation in the case $\Lambda = 0$:

$$\mathbf{E} \leftrightarrow \mathbf{g} \ ; \tag{1.66}$$

$$\mathbf{B} \leftrightarrow \frac{\boldsymbol{\tau}}{c^2} \ ; \tag{1.67}$$

$$\rho_{el} \leftrightarrow -\rho \ ; \tag{1.68}$$

$$\mu_0 \leftrightarrow -\frac{4\pi G}{c^2} \ ; \tag{1.69}$$

$$\epsilon_0 \leftrightarrow -\frac{1}{4\pi G} \ . \tag{1.70}$$

In order for the theory to be really analogue to electrodynamics, we should also have the gravitational analogue of the Lorentz force:

$$\mathbf{F}_G = m_G\left(\mathbf{g} + \mathbf{v}\times\frac{1}{c^2}\boldsymbol{\tau}\right) \ . \tag{1.71}$$

This assumption was first formulated by [76]. We can argue that, since the additional term arising from the equations is proportional to $\frac{1}{c^2}$, it may not be easy to detect. This may be responsible for the fact that we previously ignored it.

Moreover, we could generalize the Poisson equation as in [56] or previously discussed in [144] taking into account pressure for a perfect fluid:

$$\nabla \cdot \mathbf{g} = \Lambda - 4\pi G \left(\varrho + \frac{3p}{c^2} \right) \ . \tag{1.72}$$

The additional term is once again proportional to $\frac{1}{c^2}$.

1.4 Decomposition of the Weyl tensor and Maxwell-Weyl equations

1.4.1 Newtonian dynamics, tidal tensor and relativistic generalization

We consider again the Euler-Newton-System and we spatially derive once Newton's second law to get:

$$g_{i,j} = \frac{dv_{i,j}}{dt} + v_{i,k} v_{k,j} \ . \tag{1.73}$$

We now define the Newtonian tidal tensor as :

$$\mathcal{E}_{ij} = g_{i,j} - \frac{1}{3} g_{k,k} \delta_{ij} \ . \tag{1.74}$$

The kinematical decomposition of the velocity gradient $v_{i,j}$ is:

$$v_{i,j} = \frac{1}{3}\theta\delta_{ij} + \sigma_{ij} + \omega_{ij} \quad \text{where} \quad \sigma_{ij} = \Theta_{(ij)} - \frac{1}{3}\theta\delta_{ij} \quad \text{and} \quad \omega_{ij} = \Theta_{[ij]} \ . \tag{1.75}$$

Then (2.23) is equivalent to Raychaudhuri equation:

$$\dot{\theta} = -\frac{1}{3}\theta^2 - 2\sigma^2 + (\Lambda - 4\pi G\rho) \ . \tag{1.76}$$

If there is no vorticity, the tidal tensor $\mathcal{E}_{ij}$ can be rewritten

$$\mathcal{E}_{ij} = \frac{2}{3}\theta\sigma_{ij} + \sigma_{ik}\sigma_{kj} - \frac{2}{3}\sigma^2\delta_{ij} - \dot{\sigma}_{ij} \ . \tag{1.77}$$

We now define $\mathcal{F}^i{}_j$, the relativistic counterpart of the gradient of the gravitation field. To do so, we replace the velocity gradient by the expansion tensor $\Theta_{ij} = \delta_{ab}\, \eta^a{}_i \dot{\eta}^b{}_j$. The analogue of (1.73) is then:

$$\mathcal{F}^i{}_j = \dot{\Theta}^i{}_j + \Theta^i{}_k \Theta^k{}_j \ . \tag{1.78}$$

As will be discussed later, Raychaudhuri equation (1.76) and the absence of vorticity can be expressed as the following conditions on $\mathcal{F}^i{}_j$:

$$\mathcal{F}^k{}_k = \dot{\theta} + \Theta^l{}_k \Theta^k{}_l = \Lambda - 4\pi G\rho \ ; \tag{1.79}$$

$$\mathcal{F}_{[ij]} = \dot{\Theta}_{[ij]} = 0 \ . \tag{1.80}$$

We will show that the electric part of the Weyl tensor is [5] $E^i{}_j = -\mathcal{F}^i{}_j + \frac{1}{3}\delta^i_j \mathcal{F}^k{}_k$.

1.4.2 Electric and magnetic parts of the Weyl tensor

The full Riemann curvature tensor has 20 independent components. It can be split into

- its trace part, the Ricci tensor, which has 10 independent components linked to the matter content of the Universe by the Einstein field equations ,
- its traceless part, the Weyl tensor, containing the remaining 10 independent components and having, in addition to a zero trace, the same symmetry properties of Riemann tensor:

$$C_{\mu\rho\nu\sigma} = C_{\nu\sigma\mu\rho} \ , \ C_{\mu\rho\nu\sigma} = -C_{\rho\mu\nu\sigma} \ , \ C_{\mu[\rho\nu\sigma]} = 0 \ . \tag{1.81}$$

Since the Weyl tensor is the traceless part of the 4-Riemann curvature tensor [64, 74], it has the following expression:

$$C^{\mu\nu}{}_{\rho\sigma} = {}^{(4)}R^{\mu\nu}{}_{\rho\sigma} - 2\,\delta^{[\mu}_{[\rho}\,{}^{(4)}R^{\nu]}{}_{\sigma]} + \frac{1}{3}\delta^{[\mu}_{[\rho}\delta^{\nu]}_{\sigma]}\,{}^{(4)}R \ . \tag{1.82}$$

It is a traceless tensor so any contraction of two indices vanishes:

$$C^{\mu}{}_{\rho\mu\sigma} = 0 \ . \tag{1.83}$$

The Einstein equations only involve the Ricci tensor. Hence the Weyl tensor represents the part of the gravitational field that is not directly coupled to the matter content of the Universe. Furthermore, the Weyl tensor vanishes for dimensions less then 4. In particular, all the information of the 3-Riemann tensor will be contained in the 3-Ricci tensor since the 3-Weyl tensor is zero.

Let u^μ be the 4–velocity of the fluid. The Weyl tensor can be split in an irreducible way into an electric and a magnetic part, corresponding to two symmetric and traceless tensors, each of them containing 5 independent components of the Weyl tensor. The electric part is

$$E_{\mu\nu} = C_{\mu\rho\nu\sigma}\, u^\rho u^\sigma \ , \tag{1.84}$$

and the magnetic part is

$$H_{\mu\nu} = \frac{1}{2}\sqrt{|{}^{(4)}g|}\,\epsilon_{\alpha\beta\rho(\mu}\, C^{\alpha\beta}{}_{\nu)\sigma}\, u^\rho u^\sigma \ , \tag{1.85}$$

where ${}^{(4)}g$ represents the determinant of the 4-metric tensor ${}^{(4)}\mathbf{g}$ and $\epsilon_{\rho\mu\alpha\beta}$ is the 4-dimensional Levi-Civita tensor. ${}^{(4)}g$ coincides in our case with g, the determinant of the 3-metric tensor so that we will use the latter in the following. The electric and the magnetic parts satisfy by construction the following identities:

$$E^\mu{}_\mu = 0 \ ; \ E_{\mu\nu} = E_{(\mu\nu)} \ ; \ E_{\mu\nu}u^\mu = 0 \ , \tag{1.86}$$

$$H^\mu{}_\mu = 0 \ ; \ H_{\mu\nu} = H_{(\mu\nu)} \ ; \ H_{\mu\nu}u^\mu = 0 \ . \tag{1.87}$$

5. Note the conventional sign change between the gravitoelectric part of the spatially projected Weyl tensor $E^i{}_j$ and the Newtonian tidal tensor $\mathcal{E}^i{}_j$.

They represent the free gravitational field that enables gravitational action at a distance: tidal forces and gravitational waves. The Weyl tensor can also be expressed from the electric and magnetic parts as follows:

$$\begin{aligned} C_{\mu\nu\kappa\lambda} &= \left(g_{\mu\nu\alpha\beta}g_{\kappa\lambda\gamma\delta} - \varepsilon_{\mu\nu\alpha\beta}\varepsilon_{\kappa\lambda\gamma\delta}\right) u^\alpha u^\gamma E^{\beta\delta} \\ &+ \left(\varepsilon_{\mu\nu\alpha\beta}g_{\kappa\lambda\gamma\delta} + g_{\mu\nu\alpha\beta}\varepsilon_{\kappa\lambda\gamma\delta}\right) u^\alpha u^\gamma H^{\beta\delta} , \end{aligned} \tag{1.88}$$

where $g_{\mu\nu\alpha\beta} \equiv g_{\mu\alpha}g_{\nu\beta} - g_{\mu\beta}g_{\nu\alpha}$ and $\varepsilon_{\mu\nu\kappa\lambda} = \sqrt{-^{(4)}g}\ \epsilon_{\mu\nu\kappa\lambda}$.

1.4.3 Maxwell-Weyl equations

An alternative formulation of General Relativity, where the Weyl curvature tensor becomes the fundamental geometrical quantity, exists. It is obtained from the contracted Bianchi identities, which link the covariant derivatives of the Weyl tensor to the ones of the Ricci curvature tensor:

$$\nabla^\kappa C_{\mu\nu\kappa\lambda} = \nabla_{[\mu}R_{\nu]\lambda} + \frac{1}{6}g_{\lambda[\mu}\nabla_{\nu]}R^\kappa{}_\kappa \ . \tag{1.89}$$

If we insert in this equation the Einstein field equations and replace the Ricci curvature tensor by its expression in terms of the stress-energy tensor, we get:

$$\nabla^\kappa C_{\mu\nu\kappa\lambda} = 8\pi G\left(\nabla_{[\mu}T_{\nu]\lambda} + \frac{1}{3}g_{\lambda[\mu}\nabla_{\nu]}T^\kappa{}_\kappa\right) \ . \tag{1.90}$$

We now assume that matter is a perfect fluid for which $T_{\mu\nu} = (\rho + p)u_\mu u_\nu + pg_{\mu\nu}$ with u^μ being the fluid 4-velocity, ρ its density and p its pressure in the fluid frame. We decompose the velocity gradient into the acceleration 4-vector a_ν, the expansion scalar $\Theta = \nabla_\mu u^\mu$, the shear tensor $\sigma_{\mu\nu}$, and the vorticity tensor $\omega_{\mu\nu} = \varepsilon_{\mu\nu\alpha\beta}u^\alpha\omega^\beta$:

$$\nabla_\mu u_\nu = -u_\mu a_\nu + \frac{1}{3}\Theta f_{\mu\nu} + \sigma_{\mu\nu} + \omega_{\mu\nu} \ , \tag{1.91}$$

where $f_{\mu\nu}$ is the projection tensor on the rest-frame of the fluid, as defined in (1.16). We here denote by $d/d\tau_0 = u^\mu\nabla_\mu$ the derivative along the fluid wordline (*cf* (1.6)). We extract from (1.90) some equations on the electric $E_{\mu\nu}$ and magnetic parts $H_{\mu\nu}$ projected on the rest-frameof the fluid [14]:

$$\begin{aligned} &(\text{div E}):\ f^\mu{}_\alpha f^\nu{}_\beta \nabla_\nu E^{\alpha\beta} + \varepsilon^{\mu\nu\alpha\beta}u_\nu\sigma_{\alpha\gamma}H^\gamma{}_\beta - 3H^\mu{}_\nu\omega^\nu = \frac{8\pi}{3}G\ f^{\mu\nu}\nabla_\nu\rho \ , \\ &(\text{div H}):\ f^\mu{}_\alpha f^\nu{}_\beta \nabla_\nu H^{\alpha\beta} - \varepsilon^{\mu\nu\alpha\beta}u_\nu\sigma_{\alpha\gamma}E^\gamma{}_\beta + 3H^\mu{}_\nu\omega^\nu = -8\pi G(p+\rho)\omega^\mu \ , \\ &(\text{dE}/\text{d}\tau_0):\ f^\mu{}_\alpha f^\nu{}_\beta \frac{d}{d\tau_0}E^{\alpha\beta} + f^{\alpha(\mu}\varepsilon^{\nu)\beta\gamma\delta}u_\beta\nabla_\gamma H_{\alpha\delta} + 2u_\alpha a_\beta H_\gamma{}^{(\mu}\varepsilon^{\nu)\alpha\beta\gamma} \\ &\qquad + \Theta E^{\mu\nu} + f^{\mu\nu}(\sigma^{\alpha\beta}E_{\alpha\beta}) - 3E^{\alpha(\mu}\sigma^{\nu)}_\alpha + E^{\alpha(\mu}\omega^{\nu)}_\alpha = -4\pi G(\rho+p)\sigma^{\mu\nu} \ , \\ &(\text{dH}/\text{d}\tau_0):\ f^\mu{}_\alpha f^\nu{}_\beta \frac{d}{d\tau_0}H^{\alpha\beta} - f^{\alpha(\mu}\varepsilon^{\nu)\beta\gamma\delta}u_\beta\nabla_\gamma E_{\alpha\delta} - 2u_\alpha a_\beta E_\gamma{}^{(\mu}\varepsilon^{\nu)\alpha\beta\gamma} \\ &\qquad + \Theta H^{\mu\nu} + f^{\mu\nu}(\sigma^{\alpha\beta}H_{\alpha\beta}) - 3H^{\alpha(\mu}\sigma^{\nu)}_\alpha + H^{\alpha(\mu}\omega^{\nu)}_\alpha = 0 \ , \end{aligned} \tag{1.92}$$

where $\varepsilon^{\mu\nu\alpha\beta} = \epsilon^{\mu\nu\alpha\beta} / \sqrt{|^{(4)}g|}$.

In the rest-frameof the fluid, where $u^\mu = (1, 0, 0, 0)$, for a dust fluid without vorticity, the last set of equations becomes:

$$E^k{}_{i\|k} - g_{ik}\varepsilon^{kmn}\Theta_{ml}H^l{}_n = \frac{8\pi G}{3}\frac{\mathring{J}}{J}\mathring{\varrho}_{|i} \ , \tag{1.93}$$

$$H^k{}_{i\|k} + g_{ik}\varepsilon^{kmn}\Theta_{ml}E^l{}_n = 0 \ . \tag{1.94}$$

$$\begin{aligned}\dot{E}_{ij} \ &+ \ 2\Theta E_{ij} - 3\Theta_{k(i}E^k{}_{j)} - \Theta^k{}_l E^l{}_k g_{ij} - g_{m(i}\varepsilon^{mkl}H_{j)l\|k} \\ &= -4\pi G\frac{\mathring{J}}{J}\mathring{\varrho}\Big(\Theta_{ij} - \frac{1}{3}\Theta g_{ij}\Big),\end{aligned} \tag{1.95}$$

$$\dot{H}_{ij} \ + \ 2\Theta H_{ij} - 3\Theta_{k(i}H^k{}_{j)} - \Theta^k{}_l H^l{}_k g_{ij} + g_{m(i}\varepsilon^{mkl}E_{j)l\|k} = 0\,. \tag{1.96}$$

We determine in our foliation the components of the electric and magnetic parts of the Weyl tensors. The (00), $(0i)$ and $(i0)$ components of both the electric and the magnetic tensors vanish in our foliation since the velocity field has then vanishing spatial components. We thus only have to determine the spatial components E_{ij} and H_{ij}.

It is possible to show that:

$$E^i{}_j := {}^{(4)}R^i{}_{0j0} - \frac{1}{2}{}^{(4)}R_{00}\ \delta^i_j + \frac{1}{2}{}^{(4)}R^i{}_j - \frac{1}{6}{}^{(4)}R\ \delta^i_j \ , \tag{1.97}$$

$$H^i{}_j := g^{ik}\ \frac{\epsilon^{lsn}}{2J}\ g_{lr}g_{n(k}\,{}^{(4)}R^r{}_{sj)0} \ . \tag{1.98}$$

We now replace the curvature terms by their expression in terms of the kinematical expansion tensor Θ_{ij}. The electric part becomes:

$$\begin{aligned}E^i{}_j = -\frac{1}{2}\left(\dot{\Theta}^i{}_j - \frac{\delta^i_j}{3}\dot{\Theta}\right) - \left(\Theta^i{}_k\Theta^k{}_j - \frac{\delta^i_j}{3}\Theta^l{}_k\Theta^k{}_l\right) + \\ \frac{1}{2}\theta\left(\Theta^i{}_j - \frac{\delta^i_j}{3}\Theta\right) + \frac{c^2}{2}\left(\mathcal{R}^i_j - \frac{\delta^i_j}{3}\mathcal{R}\right)\end{aligned} \tag{1.99}$$

and the magnetic part is:

$$H^i{}_j = g^{ik}\ \frac{\epsilon^{lns}}{J}\ g_{n(k}\,\Theta_{lj)\|s} \ . \tag{1.100}$$

If we assume at the same time that the Einstein equations are satisfied, we have from Raychaudhuri equation:

$${}^{(4)}R_{00} := -\dot{\theta} - \Theta^l{}_k\Theta^k{}_l = 4\pi G\rho - \Lambda \ , \tag{1.101}$$

and from the evolution equation for the extrinsic curvature:

$${}^{(4)}R^i{}_j := \mathcal{R}^i{}_j + \dot{\Theta}^i{}_j + \theta\Theta^i{}_j = (4\pi G\rho + \Lambda)\,\delta^i_j \ . \tag{1.102}$$

We can follow the same idea as the one presented in II.1.3 and replace in the definitions of $E^i{}_j$ (1.97) the curvature terms ${}^{(4)}R_{00}$ and ${}^{(4)}R^i{}_j$ by their expression in terms of the sources, obtained from the Einstein equations (1.101) and (1.102). This new tensor that we can call the Einstein-electric part,

$$ {}^{\mathbf{GR}}E^i{}_j := -\dot{\Theta}^i{}_j - \Theta^i{}_k\Theta^k{}_j - \frac{1}{3}\left(4\pi G\rho - \Lambda\right)\delta^i_j \ , \tag{1.103}$$

will then coincide with the real electric part of the Weyl tensor $E^i{}_j$ only if the Raychaudhuri and the absence of vorticity equations are satisfied:

$$ {}^{\mathbf{GR}}E^k{}_k = 0 \quad \Leftrightarrow \quad (3.20) \quad ; \quad {}^{\mathbf{GR}}E_{[ij]} = 0 \quad \Leftrightarrow \quad (1.41) \ , \tag{1.104}$$

In the same way, we can encode into the antisymmetric part of some Einstein-magnetic tensor:

$$ {}^{\mathbf{GR}}H^i{}_j := g^{ik}\,\frac{\epsilon^{lns}}{J}\,g_{nk}\,\Theta_{lj\|s} \ , \tag{1.105}$$

the momentum constraints equation:

$$ {}^{\mathbf{GR}}H_{[ij]} = 0 \quad \Leftrightarrow \quad (3.14) \ . \tag{1.106}$$

In Section II.1.5, we will focus on the gravitoelectric part of the Einstein equations, i.e. on the equations that can be obtained from the absence of trace and the symmetry of the Einstein-electric tensor (1.104).

1.4.4 Newtonian limit of the electric and magnetic parts

In [14] the authors consider first-order perturbations on a flat FLRW background. The line element is

$$ ds^2 = a(\tau)^2\left(-(1+2\psi)d\tau^2 + 2w_i d\tau dx^i + [(1-2\phi)g_{ij} + 2h_{ij}]dx^i dx^j\right) \ , \tag{1.107}$$

where ψ and ϕ are scalar perturbations, w_i are vector perturbations and h_{ij} are tensor perturbations satisfying $g^{ij}h_{ij} = 0$ and $g^{jk}\nabla_k h_{ij} = 0$. We define $D_{ij} := \partial_i\partial_j - \delta_{ij}\Delta/3$ and get:

$$ E_{ij} = \frac{1}{2}D_{ij}(\phi+\psi) + \frac{1}{2}\nabla_{(i}\dot{w}_{j)} - \frac{1}{2}(\ddot{h}_{ij} + \Delta h_{ij}) \ , \tag{1.108}$$

$$ H_{ij} = -\frac{1}{2}\nabla_{(i}\nabla_m w_n \epsilon_{j)mn} + \nabla_k \epsilon^{kl}{}_{(i}\dot{h}_{j)l} \ . \tag{1.109}$$

According to [14], in the Newtonian limit, $\phi = \psi$, the vector and the tensor modes are zero. The magnetic part vanishes and the electric part now coincides with (1.74) since $g_i = -\nabla_i\phi$. This is also what is claimed in [58], where the authors give a clearcut definition of the Newtonian limit of General Relativity. When $\lambda = 1/c^2$ goes to zero, Newtonian theory is recovered whereas in the opposite limit, we obtain Einstein's theory. The magnetic part is then interpreted as the rotation of the nearby free-falling gyroscopes, which is zero in Euclidean Newtonian theory.

Nevertheless, in [14], the authors show that it is possible to build from the Newtonian quantities some electric and magnetic parts that will fulfill the (1.93) (1.94) (1.95)(1.96) equations. In [89], an expansion is done around the Newtonian electric and magnetic parts and the non-local aspects of the equations are discussed in detail. The authors show that in the Maxwell-Weyl equations, the magnetic part should not be set to zero. Indeed, the first post-newtonian term $\frac{1}{c^3}{}^{(PN)}H_{ij}$ has to be taken into account for the decomposition to be consistent. Then, the Newtonian equations can be recovered from the Newtonian limit of these equations.

1.5 Analogies between the gravitoelectric system and the Lagrange-Newton-System

In this section, we will highlight the similarities between the gravitoelectric part of the Einstein equations for an irrotational dust fluid, obtained in the Strong Lagrangian approach for a flow orthogonal foliation, and the Lagrange-Newton-System. The Einstein equations that will be considered are thus the ones established in Section II.1.1.4, namely the Lagrange-Einstein-System for this matter model. They will be compared to the Newtonian equations formulated in the Lagrangian frame: the Lagrange-Newton-System. We will show that a mathematical operation, the Minkowski Restriction, can be applied to the gravitoelectric part of the Einstein equations to get the Lagrange-Newton-System. This interesting result will be used in the next chapter in order to build the gravitoelectric perturbations at any order from the Newtonian perturbative solutions.

1.5.1 Gravitoelectric part of the Einstein equations

In Section II.1.4.3, we have introduced the Einstein-electric tensor, from which some of the Einstein equations can be recovered. From now on, we drop the $^{\mathbf{GR}}$ superscript when we refer to this tensor. We also gave the components of this tensor in the coordinate basis $\{\mathbf{d}X^i\}$ in terms of the expansion tensor. This tensor can also be represented by the 3 one–form fields $\mathbf{E}^a$ (see [35] Eq. (A23)), functions of the coframes:

$$\mathbf{E}^a = -\ddot{\boldsymbol{\eta}}^a + \frac{1}{3}(\Lambda - 4\pi G\varrho)\,\boldsymbol{\eta}^a \ . \tag{1.110}$$

Then, the irrotationality condition (1.47) and the trace equation of motion (1.51) are generated by

$$G_{ab}\,\mathbf{E}^a \wedge \boldsymbol{\eta}^b = \mathbf{0} \quad ; \quad \epsilon_{abc}\,\mathbf{E}^a \wedge \boldsymbol{\eta}^b \wedge \boldsymbol{\eta}^c = \mathbf{0} \ . \tag{1.111}$$

These two equations are therefore referred to as the *gravitoelectric part* of the Einstein equations. A projection of the gravitoelectric one–form fields and Equations (1.111), using the Hodge star operator, yields to their coefficient representation:

$$E^i{}_j = -\tfrac{1}{2J}\epsilon_{abc}\epsilon^{ikl}\ddot{\eta}^a{}_j\eta^b{}_k\eta^c{}_l + \tfrac{1}{3}\,(\Lambda - 4\pi G\varrho)\,\delta^i{}_j \ ; \tag{1.112}$$

$$E_{[ij]} = 0 \quad ; \quad E^k{}_k = 0 \ . \tag{1.113}$$

These equations are equivalent to

$$\delta_{ab}\ddot{\eta}^a{}_{[i}\eta^b{}_{j]} \;=\; 0 \ , \tag{1.114}$$

$$\frac{1}{2}\epsilon_{abc}\epsilon^{ikl}\ddot{\eta}^a{}_i\eta^b{}_k\eta^c{}_l \;=\; \Lambda J - 4\pi G\mathring{J}\mathring{\varrho} \ , \tag{1.115}$$

which we have already derived in Section II.1.1.4. They are formally very close to the Lagrange-Newton-System. This formal analogy between the two sets of equations will be used in the next chapter, where relativistic perturbative solutions will be built from the Newtonian perturbation scheme.

1.5.2 Minkowski Restriction of the gravitoelectric system

Definition of the Minkowski Restriction

We will now discuss the gravitoelectric part of the Einstein equations, and the full Newtonian system. Formally, this link is provided by the *Minkowski Restriction*. Let $\tilde{\boldsymbol{\eta}}^\alpha$ be Cartan one–form fields in a 4−dimensional manifold (Greek letters are used in 4 dimensions). A set of forms $\tilde{\boldsymbol{\eta}}^\alpha$ is said to be *exact*, if there exist functions f^α such that $\tilde{\boldsymbol{\eta}}^\alpha = \mathbf{d}f^\alpha$, where $\mathbf{d}$ denotes the exterior derivative operator, acting on forms and functions. The *Minkowski Restriction* (henceforth MR) consists in the replacement of the non-integrable coefficients by integrable ones, $\tilde{\eta}^\alpha_{\ \nu} \rightarrow f^{\alpha\to\mu}_{\ \ |\nu}$, keeping the speed of light c finite. With this restriction, the Cartan orthonormal coframe coefficients yield the Newtonian deformation gradient, and the local tangent spaces all become identical and form the global Minkowski space-time. The *Newtonian limit* could be defined as MR of Einstein's theory and additionally sending c to infinity.

In the flow–orthogonal foliation the 4−dimensional orthonormal coframes reduce to $\tilde{\boldsymbol{\eta}}^\alpha = (\mathbf{d}t, \tilde{\boldsymbol{\eta}}^a)$, and their MR reads $\mathbf{d}f^\alpha = (\mathbf{d}t, \mathbf{d}f^{a\to i})$. Sending the spatial Cartan coframes to exact forms, i.e. executing the MR , their coefficients $\eta^a_{\ i}$ are restricted to the Newtonian deformation gradient $f^a_{\ |i}$. Note that c and the signature are carried by the 4−dimensional metric coefficients; c is set to 1 throughout this work.

Equivalence of the integrability of the orthonormal and adapted coframes and the flatness of space

The standard choice of *orthonormal coframes* $\tilde{\boldsymbol{\eta}}^a$ in the Cartan formalism implies for the spatial metric coefficients $\tilde{g}_{ij} = \delta_{ab}\,\tilde{\eta}^a_{\ i}\,\tilde{\eta}^b_{\ j}$, with $\tilde{\eta}^a_{\ i}(t_i) \neq \delta^a_{\ i}$ at initial time, in order to have an initially nontrivial metric.

The alternative choice of *adapted coframes* $\boldsymbol{\eta}^a$, used in the thesis and presented in Section I.2.3.2, represents the metric coefficients as $g_{ij} = G_{ab}\,\eta^a_{\ i}\,\eta^b_{\ j}$, where we are entitled to require $\eta^a_{\ i}(t_i) = \delta^a_{\ i}$ at initial time, encoding the initial metric into the coefficients G_{ab}, i.e. $G_{ij} = G_{ab}\,\delta^a_{\ i}\,\delta^b_{\ j}$. This makes the comparison with the Newtonian choice of Lagrangian coordinates to coincide with the Eulerian ones at some initial time more direct.

As will be discussed in (2.3), the basic assumption is that both coframe types describe the same metric form, i.e. $\mathbf{g} = \delta_{cd}\,\tilde{\boldsymbol{\eta}}^c \otimes \tilde{\boldsymbol{\eta}}^d = G_{ab}\,\boldsymbol{\eta}^a \otimes \boldsymbol{\eta}^b$, from which we infer:

$$G_{ab} = \delta_{cd}\,\tilde{\eta}^c_{\ a}\tilde{\eta}^d_{\ b}\ , \tag{1.116}$$

where we denote with $\tilde{\eta}^c_{\ a} = e_c^{\ i}\,\tilde{\eta}^c_i$ the coefficients of the projection of $\tilde{\boldsymbol{\eta}}^c$ onto the basis $\boldsymbol{\eta}^a$.

The *MR* applied to either of these coframes requires them to be exact forms, $\tilde{\boldsymbol{\eta}}^a = \mathbf{d}\tilde{f}^a$ or $\boldsymbol{\eta}^a = \mathbf{d}f^a$. They then define some global Eulerian coordinates, $\tilde{x}^a$ and x^a, respectively. In the *MR* , Eq. (1.116) is equivalent to

$$G_{ab} = \delta_{cd} \frac{\partial \tilde{f}^c}{\partial x^a} \frac{\partial \tilde{f}^d}{\partial x^b} \ . \tag{1.117}$$

We infer from (1.117) that the coefficients G_{ab} just depend on initial vector displacements after executing the *MR* . They are related to the initial deformation gradient in the orthonormal description, as can be seen by looking at the metric equivalence relation in an exact Lagrangian basis, $\mathbf{g} = \tilde{g}_{ij}\ \mathbf{d}\tilde{X}^i \otimes \mathbf{d}\tilde{X}^j = g_{ij}\ \mathbf{d}X^i \otimes \mathbf{d}X^j$:

$$\begin{aligned} \mathbf{g}(X^k, t_i) &= \delta_{ab}\tilde{f}^a{}_{|\tilde{X}^i}(\tilde{X}^k, t_i)\tilde{f}^b{}_{|\tilde{X}^j}(\tilde{X}^k, t_i)\mathbf{d}\tilde{X}^i \otimes \mathbf{d}\tilde{X}^j \\ &= \delta_{ab}\tilde{f}^a{}_{|i}(X^k, t_i)\tilde{f}^b{}_{|j}(X^k, t_i)\mathbf{d}X^i \otimes \mathbf{d}X^j \\ &= G_{ab}(X^k)\delta^a{}_i\delta^b{}_j\mathbf{d}X^i \otimes \mathbf{d}X^j \ , \end{aligned} \tag{1.118}$$

where a slash denotes derivative with respect to the coordinates X^i, as in the main text, and it is explicitly noted otherwise. From (1.117) we conclude that

$$\mathbf{g} = G_{ab}\ \boldsymbol{\eta}^a \otimes \boldsymbol{\eta}^b = \delta_{cd}\ \frac{\partial \tilde{f}^c}{\partial x^a}\frac{\partial \tilde{f}^d}{\partial x^b}\mathbf{d}x^a \otimes \mathbf{d}x^b = \delta_{cd}\ \mathbf{d}\tilde{x}^c \otimes \mathbf{d}\tilde{x}^d \,, \tag{1.119}$$

which is the Euclidean metric.

Summarizing: execution of the *MR* leads, in either of the chosen coframes, to a metric that is equivalent to the Euclidean metric. The coefficients G_{ab} can then be expressed in terms of initial vector displacements, *cf.* Eq. (1.118).

Minkowski Restriction of the gravitoelectric part of the Einstein equations

In the *MR* , (1.114) becomes

$$\delta_{ab}\ddot{f}^a{}_{|[i}\, f^b{}_{|j]} = 0 \ , \tag{1.120}$$

i.e. is equal to (2.48). Since, for a flat space-time $\mathring{J} = 1$, (1.115) becomes

$$\frac{1}{2}\epsilon_{abc}\epsilon^{ikl}\ddot{f}^a{}_{|i}\, f^b{}_{|k}\, f^c{}_{|l} = \Lambda J - 4\pi G\mathring{\varrho} \tag{1.121}$$

i.e. is equal to (2.47). So, the gravitoelectric part of the Einstein equations (1.114) (1.115) then reduces to the Lagrange-Newton-System. Moreover, we obtained the Lagrange-Newton-System expressed in the inertial frame, i.e. for $\ddot{\mathbf{f}} = \mathbf{g}$. Therefore, $\ddot{\mathbf{f}}$ is then solution of the following equations:

$$\nabla \times \ddot{\mathbf{f}} = \mathbf{0} \,, \tag{1.122}$$

$$\nabla \cdot \ddot{\mathbf{f}} = \Lambda - 4\pi G\varrho \ . \tag{1.123}$$

(1.122) implies that $\ddot{\mathbf{f}} = -\boldsymbol{\nabla}\phi$, where ϕ is a scalar potential solution of the Poisson equation.

The *MR* operation closes the system, reducing the number of free functions from nine ($\eta^a{}_i(X^k,t)$) to three ($f^i(X^k,t)$). A discussion of the *MR* for the remaining equations, yielding nontrivial Newtonian analogs, will be done in Section II.1.5.3. Considering only the gravitoelectric equations is not enough to determine the nine functions of the coframe coefficients. The relativistic aspects contained in the remaining equations will lead to a richer structure of the solutions and also to constraints on solutions of the gravitoelectric system. A follow–up work will explicitly consider both parts in the framework of first–order solutions. To conclude, the Lagrange–Einstein gravitoelectric equations are (up to non-integrability) equivalent to their Newtonian analogue but the remaining equations do not have an obvious Newtonian counterpart.

1.5.3 Minkowski Restriction of the other Einstein equations

The equations that we left to be interpreted are the momentum constraints, the one containing the Ricci scalar (1.125) and the one containing the traceless part of the Ricci tensor (1.127) $\tau^i{}_j$, obtained from the traceless part of the evolution equation for the extrinsic curvature (1.42):

$$
\begin{aligned}
\left(\epsilon_{abc}\epsilon^{ikl}\dot{\eta}^a{}_j\eta^b{}_k\eta^c{}_l\right)_{\|i} &= \left(\epsilon_{abc}\epsilon^{ikl}\dot{\eta}^a{}_i\eta^b{}_k\eta^c{}_l\right)_{\|j} \ , && (1.124)\\
\epsilon_{abc}\epsilon^{mkl}\dot{\eta}^a{}_m\dot{\eta}^b{}_k\eta^c{}_l &= 16\pi G\mathring{J}\mathring{\varrho} + 2\Lambda J - c^2\, JR \ , && (1.125)\\
\frac{1}{2}\Big(\epsilon_{abc}\epsilon^{ikl}\ddot{\eta}^a{}_j\eta^b{}_k\eta^c{}_l &- \frac{1}{3}\epsilon_{abc}\epsilon^{mkl}\ddot{\eta}^a{}_m\eta^b{}_k\eta^c{}_l\delta^i{}_j\Big) && (1.126)\\
+\Big(\epsilon_{abc}\epsilon^{ikl}\dot{\eta}^a{}_j\dot{\eta}^b{}_k\eta^c{}_l &- \frac{1}{3}\epsilon_{abc}\epsilon^{mkl}\dot{\eta}^a{}_m\dot{\eta}^b{}_k\eta^c{}_l\delta^i{}_j\Big) = -c^2\, J\tau^i{}_j \ .
\end{aligned}
$$

Considering a flat space-time in the frame of General Relativity would automatically lead to a zero curvature $\mathcal{R}^i{}_j = 0$. Here, we no longer work in the frame of General Relativity since we decouple the geometry of space-time and the dynamics of the fluid. In this context, $\mathcal{R}^i{}_j$ is no longer a geometrical term but should be reinterpreted.

To have an intuition of the new meaning of $\mathcal{R}^i_j$, we first consider the Newtonian case for a homogeneous isotropic universe. Newton's second law combined with Poisson equation leads to (1.9). Integrating it gives the equation (1.9) that we remind here:

$$
\left(\frac{\dot{a}}{a}\right)^2 - \frac{8\pi G}{3}\rho_H - \frac{\Lambda}{3} + \frac{k}{a^2} = 0 \ , \tag{1.127}
$$

By identifying this equation, called Friedmann's equation, to Hamiltonian constraint for a Universe with constant curvature ${}^N\mathcal{R}$, we can show that:

$$
\frac{k}{a^2} = c^2\frac{{}^N\mathcal{R}}{6} \ . \tag{1.128}
$$

We have shown that the equations (1.125) and (1.127), contain, in the frame of General Relativity, some information that has no Newtonian counterpart. Here, these supplementary equations should not be interpreted as equalities but rather as some kinematical definitions for the Minkowskian analogue of curvature: ${}^\mathcal{M}\mathcal{R}^i{}_j$. The following equations are general but their interpretation is specific to our approach.

The Raychaudhuri equation (1.115) can be rewritten:

$$\dot{\theta} + \frac{1}{3}\theta^2 + 2\sigma^2 + 4\pi G\rho - \Lambda = 0 \ . \tag{1.129}$$

If we define $l = J^{1/3}$, it becomes:

$$3\frac{\ddot{l}}{l} + 2\sigma^2 + 4\pi G\rho - \Lambda = 0 \ . \tag{1.130}$$

This equation is equivalent to:

$$\dot{\sigma^2} + 2\theta\sigma^2 = \frac{1}{2}\,{}^{\mathcal{M}}\dot{\mathcal{R}} + \frac{1}{3}\,{}^{\mathcal{M}}\mathcal{R}\;\theta \ , \tag{1.131}$$

which can be rewritten as:

$$6(\sigma^2\,{}^{\mathcal{M}}\mathcal{R})^{1/2}\,(J[\sigma^2]^{1/2})^{\cdot} = (J\,{}^{\mathcal{M}}\mathcal{R}^{3/2})^{\cdot} \ . \tag{1.132}$$

Since the integral of (1.130) has to be the Hamiltonian constraint, a ‘Minkowskian curvature’ term can be defined form integration constants and kinematical quantities:

$$^{\mathcal{M}}\mathcal{R} := 2\sigma^2 - \frac{8}{l^2}\int \sigma^2 l\,\dot{l}\mathrm{d}t - 2\frac{(\mathring{\sigma}^2 - \frac{1}{2}\,{}^{\mathcal{M}}\mathring{\mathcal{R}})}{l^2} \ . \tag{1.133}$$

Finally, we obtained an evolution equation for $^{\mathcal{M}}\mathcal{R}$ as a function of the shear. We can check that, in the case of a homogeneous isotropic flow, we recover the Newtonian result (1.128) since then $l(t) = a(t)$. From (1.127) and Hamiltonian constraint we can define $^{\mathcal{M}}\mathcal{R}^i{}_j$ from kinematical quantities (shear and expansion) and integration constants[6]:

$$\begin{aligned} {}^{\mathcal{M}}\mathcal{R}^i{}_j &:= \frac{2}{3}\delta^i_j\,[\sigma^2 - \frac{1}{3}\theta^2 + 8\pi G\rho + \Lambda] - \dot{\sigma^i_j} - \theta\,\sigma^i_j \ , && (1.134)\\ {}^{\mathcal{M}}\mathcal{R}^i{}_j &:= \frac{1}{3}\delta^i_j\,{}^{\mathcal{M}}\mathcal{R} - \dot{\sigma^i_j} - \theta\,\sigma^i_j \ . && (1.135) \end{aligned}$$

1.6 Concluding remarks

In this chapter we presented various ways to approach the GEM analogy. We first considered the similarities between the Newtonian theory of gravity and electrodynamics. We then built a generalization of the field equations for the gravitational field and for Newton’s second law. We have then shown that the Euler-Newton-System could be obtained in the limit where the speed c goes to infinity. Afterwards, we turned to General Relativity and developed the GEM approach based on the decomposition of the Weyl tensor into an electric and a magnetic part. As was discussed, these fields satisfy equations that exhibit similarities with the Maxwell equations. Nevertheless, contrary to electrodynamics, the electric and the magnetic parts of the Weyl tensor do not play similar roles. The electric

6. Setting $^{\mathcal{M}}\mathcal{R}^i{}_j$ to zero would have led to a conservation equation for σ^i_j which would have restricted the problem to a self similar flow.

part is the relativistic generalization of the Newtonian tidal tensor whereas the magnetic part encodes the dynamics of gravitational waves. A Newtonian limit of the electric and magnetic parts has also been discussed in order to better understand what they contain in the relativistic case.

In this chapter, we also discussed the analogies between the gravitoelectric part of the Einstein equations and the Lagrange-Newton-System. The Minkowski Restriction, which is the mathematical operation that enables us to go from the gravitoelectric part of the Einstein equations to the Lagrange-Newton-System, was also applied to the other Einstein equations. Nevertheless, since the Minkowski Restriction decouples the geometry of space-time from the dynamics of the fluid (the geometrical Ricci curvature tensor being then zero), an alternative interpretation of the curvature terms in terms of the kinematical properties of the fluid has then been formulated.

Chapter 2

Gravitoelectric Perturbation and Solution Schemes at Any Order

This chapter is based on the paper by A. Alles, T. Buchert, F. Al Roumi and A. Wiegand [4].

Contents

In Section II.1.1.3, we presented the Einstein's equations in the $3+1$ form for the Cartan coframe variable. In previous work, the first–order solution was investigated for the trace and antisymmetric parts. The solution then obtained was extrapolated in the spirit of Zel'dovich's approximation in Newtonian cosmology. Moreover, a definition of a nonperturbative scheme of structure formation [35] was also provided. The average properties of the latter in relation to the Dark Energy and Dark Matter problems were studied by T. Buchert, C. Nayet and A. Wiegand in [36]. Here, we proceed by providing the gravitoelectric subclass of relativistic nth–order perturbation and solution schemes. As in previous work we restrict our attention to irrotational dust continua for simplicity.

The problem of perturbation solutions in general relativity has been addressed by many works. In cosmology the 'standard approach' is based on the gauge invariant 'Bardeen formalism' (for a selection of key references on standard perturbation theory see Refs. [10], [112], [88], [51]). A covariant and gauge–invariant approach has been proposed [62, 63]. The reason for the existence of various approaches is due to an ambiguity of the choice of perturbation variable, the choice of a 'background', but also due to different philosophies; e.g. the standard gauge–invariant approach compares the physical manifold with a reference 'background manifold', while others solely operate on the physical manifold.

The conceptual difference of our framework lies in the fact that we no longer consider a reference background manifold. All the quantities are now defined on the physical space section. All orders of the perturbations are defined on the physical manifold, not with respect to a zero–order manifold (that was interpreted as the background manifold in standard perturbation theory). Moreover, we are perturbing a single dynamical variable, the Cartan coframes. As a consequence, the issue of gauge invariance does not arise; covariance or diffeomorphism invariance is guaranteed for a given foliation of spacetime by using Cartan differential forms.

A similar point of view has also been taken in previous work, i.e. the pioneering work by Kasai presents a relativistic generalization of the 'Zel'dovich approximation' [161], and followup works with his collaborators present a class of second–order perturbation solutions [85, 131]; see also the earlier papers by Tomita [146, 147, 148], the paper by Salopek et al. [132] as well as the series of papers by Matarrese, Pantano and Saez [105, 106, 107], considerations of so–called 'silent universe models' [11, 89, 14, 19, 66], and the recent paper [122]. These works are all in a wider sense concerned with the relativistic Lagrangian perturbation theory and concentrate on an intrinsic, covariant description of perturbations. Still, the present work takes another angle and goes beyond some concepts of these latter works, as we now explain. In this work, we consider, as presented in Section II.1.1.4, the Einstein equations formulated within a flow–orthogonal foliation with a single dynamical variable: the spatial Cartan coframe fields. As we have seen in Section II.1.5, they generalize the Lagrangian deformation gradient being the single dynamical variable in the Newtonian theory. One advantage of this approach is that only perturbations of this variable are considered, which entitles us to express all other physical quantities as functionals of this variable. Thus, it is possible to leave the strictly perturbative framework and to construct nonperturbative models inserting the deformation solutions at a given order of expansion of the Einstein equations into the functional definitions of these fields, without *a posteriori* expanding the functional expressions. This in turn provides highly nonlinear approximations for structure formation (e.g., the density field is known through an exact integral of the perturbation variable; the metric as a bilinear form maintains its role as a measure of distance, i.e. as a quadratic expression; the curvatures are the general defining functionals for the given perturbed space, etc.).

Moreover, we provide construction rules to derive relativistic perturbative solutions from the known Newtonian solutions at any order of the perturbations: we have to additionally study the traceless symmetric part of the equations having no obvious Newtonian analog, and which is fundamentally linked to the traceless Ricci tensor and the physics of gravitational waves. Then, we give the perturbation and solution schemes to any order of the perturbations for the gravitoelectric part of the Lagrange–Einstein system. These schemes cover the full Newtonian hierarchy of the Lagrangian perturbation theory using a restriction rule that we will define. Thus, the results of this work allow us to construct the relativistic counterpart of all Newtonian results, where higher–order information is needed, e.g., to construct the bispectrum of the perturbations (cf. Refs. [120, 121]).

We perform a strictly intrinsic derivation, i.e., without reference to an external background space. The perturbations are described locally (in coordinates of the tangent spaces at the physical manifold at each order of the perturbations). There is no need for a diffeomorphism to a global background manifold. Furthermore, the existence of such a global diffeomorphism depends on the global topology of the physical manifold which, in general, needs several coordinate charts to cover it.

Einstein's equations within a flow–orthogonal foliation of spacetime can be formulated in terms of equations for the gravitoelectric and gravitomagnetic parts of the spatially projected Weyl tensor, as we have shown in Section II.1.4. Subjecting the gravitoelectric subsystem of equations to a *MR* , i.e. by sending the Cartan coframes to exact forms, we obtain the Newtonian system in Lagrangian form (*cf* Section II.1.5 and [35]). In this chapter, we investigate the reverse process, i.e. the transposition from integrable to nonintegrable deformations, which enables us to construct a gravitoelectric subclass of the relativistic perturbation and solution schemes that corresponds to the Newtonian perturbation and solution schemes.

While the Newtonian system furnishes a vector theory, where the gravitational field strength is determined by its divergence and its curl (the trace and antisymmetric parts of the Eulerian field strength gradient), the so generalized schemes deliver nontrivial solutions for the trace–free symmetric part that is connected to the gravitoelectric part of the spatially projected Weyl tensor, the Newtonian counterpart of which is the tidal field tensor.

This section is structured as follows. In Section II.2.1 we investigate perturbation and solution schemes at any order n of the perturbations by explicitly paraphrasing the Newtonian schemes. Section II.2.2 explains the reconstruction rules and provides explicit examples. Finally, Section II.2.3 sums up and discusses perspectives.

2.1 Construction schemes for relativistic perturbations and solutions at any order

We now turn to the main part of this part and construct the gravitoelectric subclass of n^{th}–order relativistic perturbation and solution schemes through generalization of the known Newtonian schemes. This allows furnishing relativistic inhomogeneous models for large–scale structure formation in the Universe. The successful Lagrangian perturbation theory in Newtonian cosmology is well–developed. We will here generalize the perturbation and solution schemes of Newtonian cosmology given in the review [55], whose essential steps will be recalled in this section, followed by their relativistic counterparts.

All schemes are applied to the matter model 'irrotational dust'. It is possible to extend the present schemes by employing the framework for more general fluids in a Lagrangian description that will be developed in forthcoming work. Most of the known representations are focused on writing equations in terms of tensor or form coefficients. Our investigation will be guided by the compact differential forms formalism as before. However, we will also project to the coefficient form in parallel to ease reading.

2.1.1 General n–th order perturbation scheme

As in standard perturbation theories, we decompose the perturbed quantity into a Friedmann–Lemaître–Robertson–Walker (FLRW) solution and deviations thereof, which are expanded up to a chosen order n of the perturbations. Contrary to the standard perturbation theory, we do not perturb the metric globally at the background space, but we perturb the Cartan coframes locally:

$$\boldsymbol{\eta}^a = \eta^a_{\ i}\mathbf{d}X^i = a(t)\left(\delta^a_{\ i} + \sum_n P^{a(n)}_{\ \ i}\right)\mathbf{d}X^i \ , \tag{2.1}$$

in the local exact basis $\mathbf{d}X^i$. Notice that with this ansatz we choose to perturb a zero–curvature FLRW model, but it is possible to encode an initial first–order constant curvature in the coefficient functions G_{ab} in the following local metric coefficients, which can be calculated from the above coframe ansatz:

$$g_{ij} = G_{ab}\eta^a_{\ i}\eta^b_{\ j} \ . \tag{2.2}$$

We remind that, in order to obtain equations that are formally closer to the Newtonian ones, we do not choose orthonormal (Cartan) coframes $\tilde{\boldsymbol{\eta}}^a$ as is common in the literature, but the ones called *adapted coframes* $\boldsymbol{\eta}^a$. Furthermore, we can link these results to the ones obtained for the orthonormal coframes $\tilde{\boldsymbol{\eta}}^c$ (compare also corresponding remarks in [40] and [74]). Indeed, the metric bilinear form can be written as:

$$\mathbf{g} = \delta_{cd}\ \tilde{\boldsymbol{\eta}}^c \otimes \tilde{\boldsymbol{\eta}}^d = G_{ab}\ \boldsymbol{\eta}^a \otimes \boldsymbol{\eta}^b \ . \tag{2.3}$$

From this identity, we conclude:

$$G_{ab} = \delta_{cd}\ \tilde{\eta}^c_{\ a}\tilde{\eta}^d_{\ b} \ , \tag{2.4}$$

where the $\tilde{\eta}^c{}_a$ are the coefficients of the projection of $\tilde{\boldsymbol{\eta}}^c$ onto the basis $\boldsymbol{\eta}^a$. In the next subsection, we will specify the coframes we consider in such a way that the initial coframe perturbations vanish. From now on, we will call these coframes *adapted coframes* to distinguish them from the orthonormal ones.

2.1.2 Initial data for the perturbation scheme

We choose initial data in formal correspondence with the Lagrangian theory in Newtonian cosmology and generalize these initial fields to the relativistic stage. This has obvious advantages with regard to the aim to give construction rules that translate the known Newtonian solutions to general relativity. For the initial data setting in the Newtonian case see [55].

General initial data setting for the perturbations

Let the three one–form fields $\mathbf{U}^a = U^a_i \mathbf{d}X^i$ be the initial one–form generalization of the Newtonian peculiar velocity–gradient, obtained by the inverse *MR* . Accordingly, let $\mathbf{W}^a = W^a_i \mathbf{d}X^i$ be the initial one–form generalization of the Newtonian peculiar–acceleration gradient. Our solutions will be written in terms of these initial data. We summarize them together with the constraints at the end of this paragraph.

By generalizing the Newtonian initial data, the initial data for the comoving perturbation form coefficients read (we denote $P^a_i(t_i) =: \mathscr{P}^a_{\ i}$, and correspondingly for its time–derivatives):

$$\mathscr{P}^a_{\ i} = 0 \; , \tag{2.5}$$
$$\dot{\mathscr{P}}^a_{\ i} = U^a_{\ i} \; , \tag{2.6}$$
$$\ddot{\mathscr{P}}^a_{\ i} = W^a_{\ i} - 2H_{\mathbf{i}} U^a_{\ i} \; . \tag{2.7}$$

We assume, without loss of generality [55], that the initial data are first–order. As shown in Paragraph II.2.1.2, the initial density contrast $\delta_{\mathbf{i}} := (\varrho_{\mathbf{i}} - \varrho_{H\mathbf{i}})/\varrho_{H\mathbf{i}}$ satisfies the equality:

$$\delta\varrho_{\mathbf{i}}{}^{(1)} = \delta\varrho_{\mathbf{i}} = \varrho_{H\mathbf{i}}\delta_{\mathbf{i}} = -\frac{1}{4\pi G}\delta^k_{\ a} W^a_{\ k} \; . \tag{2.8}$$

Equation (2.5) implies that the coframes we will work with from now on are initially equal to the exact Lagrangian coordinate basis: $\boldsymbol{\eta}^a(t_{\mathbf{i}}) = \delta^a_{\ i}\, \mathbf{d}X^i$. This in turn provides the initial metric coefficients in the form:

$$G_{ij} = g_{ij}(t_{\mathbf{i}}) = G_{ab}\delta^a_{\ i}\delta^b_{\ j} \quad . \tag{2.9}$$

In view of the flow–orthogonal foliation, we have the irrotationality constraint:

$$\boldsymbol{\omega} = G_{ab}\dot{\boldsymbol{\eta}}^a \wedge \boldsymbol{\eta}^b = \mathbf{0} \implies G_{ab}\mathbf{U}^a \wedge \delta^b_{\ j}\mathbf{d}X^j = \mathbf{0} \; . \tag{2.10}$$

This implies for the coefficient functions: $U_{[ij]} = 0$. (We used the implicit definition $U_{ij} := \delta^b_{\ i} G_{ba} U^a_{\ j}$.)

Remark:
From (2.4) and (2.5), it is interesting to notice the following relations that hold to zeroth and first order (the full initial data are considered to be first order, as was also the choice in the Newtonian schemes [55]):

$$\begin{cases} G^{(0)}_{ij} = \delta_{ij} \; ; \\ G^{(1)}_{ij} = 2\,\tilde{\mathscr{P}}_{ij} \; ; \\ 2\tilde{P}_{(ij)} = G^{(1)}_{ij} + 2P_{(ij)} \; ; \end{cases} \tag{2.11}$$

where $\tilde{\mathscr{P}}_{ij} = \tilde{P}_{ij}(t_{\mathbf{i}})$. We are thus able to rederive some results from the ones obtained in previous works that used orthonormal coframes. For example, the Ricci curvature tensor at first–order can be obtained by inserting the identities (2.11) into (93) of [35]. We can so obtain the adapted coframes from the orthonormal ones and vice–versa.

Relativistic counterpart of the Poisson equation and consequences for $\mathbf{W}^a$

In the Newtonian approach the initial peculiar–acceleration and the density inhomogeneities are linked through the Poisson equation. In order to generalize this equation to the relativistic case, we note the following relativistic generalization of the Newtonian field strength gradient that follows from inspection of the Lagrange–Einstein system (for details the reader can always consult [35]):

$$\mathcal{F}^i_{\;j} := \dot{\Theta}^i_{\;j} + \Theta^i_{\;k}\Theta^k_{\;j} \tag{2.12}$$
$$= -\mathcal{R}^i_{\;j} - \Theta\Theta^i_{\;j} + (4\pi G\varrho - \Lambda)\,\delta^i_{\;j} + \Theta^i_{\;k}\Theta^k_{\;j}\;, \tag{2.13}$$

with the 3−Ricci tensor coefficients $\mathcal{R}_{ij}$ whose trace is the Ricci scalar $\mathcal{R}$, and Θ_{ij} the expansion tensor coefficients. According to the energy constraint, $\mathcal{R} + \Theta^2 - \Theta^k_{\;\ell}\Theta^\ell_{\;k} = 6\pi G\varrho + 2\Lambda$, the symmetry of the expansion tensor and Ricci curvature, it is straightforward to show that the relativistic gravitational field coefficients $\mathcal{F}_{ij}$ respect the following field equations:

$$\mathcal{F}^k_{\;k} = \Lambda - 4\pi G\varrho \quad ; \quad \mathcal{F}_{[ij]} = 0\;. \tag{2.14}$$

In terms of the coframe fields, the relativistic gravitational field can be written as follows:

$$\mathcal{F}^i_{\;j} = \frac{1}{2J}\epsilon_{abc}\epsilon^{ikl}\ddot{\eta}^a_{\;j}\eta^b_{\;k}\eta^c_{\;\ell}\;\;. \tag{2.15}$$

Hence, inserting the coframe perturbations and evaluating this expression at initial time, we get the following relations (note that the zero–order fields trivially satisfy the second constraint):

$$\mathcal{F}^k_{\;k}(t_{\mathbf{i}}) = \Lambda - 4\pi G\varrho_{\mathbf{i}} = \tag{2.16}$$
$$\Lambda - 4\pi G\varrho_{H\mathbf{i}}(1+\delta_{\mathbf{i}}) = 3\ddot{a}_{\mathbf{i}} + \delta^k_{\;a}W^a_{\;k}\;; \tag{2.17}$$
$$\mathcal{F}_{[ij]}(t_{\mathbf{i}}) = \delta^b_{\;[i}G_{ba}W^a_{\;j]} = W_{[ij]} = 0\;. \qquad , \tag{2.18}$$

with the initial density contrast $\delta_{\mathbf{i}}$. Thus, the deviation one–form fields $\mathbf{W}^a$ obey the following equations that generalize the Poisson equation for the inhomogeneous deviations off the zero–order solution:

$$*\frac{1}{2}\epsilon_{abc}\mathbf{W}^a\wedge\delta^b_{\;j}\mathbf{d}X^j\wedge\delta^c_{\;k}\mathbf{d}X^k = -4\pi G\delta\varrho_{\mathbf{i}}\;;\; G_{ab}\mathbf{W}^a\wedge\delta^b_{\;j}\mathbf{d}X^j = \mathbf{0}\;,$$

with $\delta\varrho_{\mathbf{i}} = \varrho_{\mathbf{i}} - \varrho_{H\mathbf{i}}$, implying for the coefficient functions:

$$-\frac{1}{4\pi G}\delta^k_{\ a} W^a_{\ k} \quad = \quad \delta\varrho_{\mathbf{i}} = \varrho_{H\mathbf{i}}\delta_{\mathbf{i}} \quad ; \quad W_{[ij]} = 0 \ . \tag{2.19}$$

Summary of initial data

We summarize the set of initial data, determined by our choice of the basis and subjected to the constraints. We assume in perturbative expansions, without loss of generality [55], that the initial data $\{(2.20)-(2.22)\}$ are first order. We drop the index $^{(1)}$ for notational ease and denote the initial data for the comoving perturbation form coefficients by $P^a_{\ i}(t_i) =: \mathscr{P}^a_{\ i}$. We set:

— for the initial deformation and the initial generalizations of the Newtonian velocity and acceleration gradients:

$$\begin{cases} \mathscr{P}^{a(n)} = \mathbf{0} \ \forall n \ , \\ \mathbf{U}^{a(1)} = \mathbf{U}^a, \ U_{[ij]} = 0 \ ; \\ \mathbf{W}^{a(1)} = \mathbf{W}^a, \ W_{[ij]} = 0 \ , \end{cases} \tag{2.20}$$

— where the coefficients are related via the initial values of the time–derivatives of the deformation:

$$\begin{cases} \dot{\mathscr{P}}^a_{\ i} = U^a_{\ i} \ ; \\ \ddot{\mathscr{P}}^a_{\ i} = W^a_{\ i} - 2H_{\mathbf{i}} U^a_{\ i} \ , \end{cases} \tag{2.21}$$

— together with additional initial constraints that are to be respected (a relation to the initial metric, to the initial density contrast, and the four ADM constraint equations evaluated at initial time):

$$\begin{cases} G_{ij} = G_{ab}\, \eta^a_{\ i}(t_{\mathbf{i}})\eta^b_{\ j}(t_{\mathbf{i}}) = G_{ab}\delta^a_{\ i}\delta^b_{\ j} \ ; \\ 4\pi G \delta\varrho_{\mathbf{i}}^{\ (1)} = -W \ ; \\ H_{\mathbf{i}} U = -\frac{\mathcal{R}(t_{\mathbf{i}})}{4} - W \ ; \\ \left(U^a_{\ j}\delta_a^{\ i}\right)_{||i} = \left(U^a_{\ i}\delta_a^{\ i}\right)_{|j} \ ; \end{cases} \tag{2.22}$$

Here and in the following we use the abbreviations $\delta^k_{\ a} U^a_{\ k} =: U$, $\delta^k_{\ a} W^a_{\ k} =: W$ for the trace expressions.

— the initial Ricci curvature as found from the equation of motion (1.42):

$$\begin{aligned} \mathcal{R}^i_j(t_{\mathbf{i}}) = -(W^i_j + H_{\mathbf{i}} U^i_j) - \delta^i_j (W + H_{\mathbf{i}} U) \\ -\epsilon_{abc}\epsilon^{ilk} U^a_{\ j} U^b_{\ l} \delta^c_{\ k} \ ; \end{aligned} \tag{2.23}$$

— equating this expression with the initial Ricci tensor as calculated from the initial metric,

$$\begin{aligned} \mathcal{R}^i_{\ j}(t_{\mathbf{i}}) = {} & G^{\,i(1)}_{[j|b]} G_a^{\,b|a(1)} + G_j^{\,b|a(1)} G^{\,i(1)}_{[b|a]} + G^{\,a(1)}_{b|j} G_a^{\,[b|i](1)} + \frac{1}{2} G^{\,a(1)}_{[a|b]} G_j^{\,b|i(1)} - \frac{1}{2} G_a^{\,a|b(1)}\, G^{\,i(1)}_{[j|b]} \\ & + \frac{1}{2} G^{(1)\,a}_{b|[j} G^{(1)\,b|i}_{a]} + 2G^{(1)\,[a|i]}_{[j|a]} + 2G^{(2)\,[a|i]}_{[j|a]} - 2G^{(1)\,a}_{b} G^{[b|i](1)}_{[j|a]} - 2G^{(1)\,i}_{a} G^{[b|a](1)}_{[j|b]} , \end{aligned} \tag{2.24}$$

we determine the first–order part of the initial metric (which is a derived quantity),

$$2G^{(1)\,[i|k]}_{\;\;[k|j]} = -H_{\mathbf{i}}U^i_{\;j} - W^i_{\;j} - (H_{\mathbf{i}}U + W)\,\delta^i_{\;j} \ , \tag{2.25}$$

— as well as the second–order part of the initial metric (which later appears in the perturbation and solution schemes):

$$2G^{(2)\,[i|k]}_{\;\;[k|j]} = f(U^i_{\;j}, W^i_{\;j}) \ , \tag{2.26}$$

where the function f can again be derived by equating (2.24) and (2.13). All further orders vanish.

The initial data given in (2.20) are exhaustive: in our ADM split, the system of equations $\{(1.41) - (1.44)\}$ contains 9 second–order equations of motion for the coframes subjected to 4 constraints. A general solution therefore contains 18 coefficient functions encoded in U_{ij} and W_{ij} that reduce to 12 functions for solutions of the irrotationality conditions (1.41), which these latter are represented by the 6 constraints $U_{[ij]} = 0$ and $W_{[ij]} = 0$. The general solution is further subjected to the 4 ADM constraints resulting in corresponding constraints on U_{ij} and W_{ij}.

2.1.3 Gravitoelectric perturbation scheme

We now recall the general Lagrangian perturbation scheme of Newtonian cosmology and generalize it to a gravitoelectric scheme in relativistic cosmology. By construction, this latter will already contain the known Lagrangian perturbation scheme at any order in the geometrical limit of exact deformation one–forms.

Recap: Newtonian theory

The general perturbation scheme has been fully developed in [55]. Our approach only slightly differs in terms of the initial conditions: we formulate them such that they are formally closer to the relativistic approach. Following the general ansatz (2.1), we introduce three comoving perturbation forms $\mathbf{d}P^i$ of the three components of the comoving vector perturbation fields $P^i(X^i, t)$:

$$\mathbf{d}f^i(\vec{X}, t) =: a(t)\mathbf{d}F^i(\vec{X}, t) = a(t)\left(\mathbf{d}X^i + \mathbf{d}P^i(\vec{X}, t)\right) \ , \tag{2.27}$$

and decompose the perturbation gradient field on the FLRW background order by order:

$$\mathbf{d}P^i = \sum_{m=1}^{\infty} \epsilon^m \mathbf{d}P^{i(m)} \ . \tag{2.28}$$

It is, of course, possible to consider perturbations of the position fields f^i, because the Newtonian equation can be expressed in a vectorial form. The relativistic equations are, however, tensorial and we, therefore, consider the representation in terms of the gradient of the fluid's deformation.

In order to provide unique solutions of the Newtonian system, suitable boundary conditions have to be imposed. For the cosmological framework the requirement of periodic boundary conditions for field deviations from a Hubble flow is a possible choice [28]. This translates into an integral constraint on the perturbations: integration over a compact spatial domain $\mathcal{M}$ implies the following:

$$\int_{\mathcal{M}} \mathbf{d}P^i = \int_{\partial\mathcal{M}} P^i = 0 \quad ; \quad P^i = \sum_{m=1}^{\infty} \epsilon^m P^{i(m)} . \tag{2.29}$$

Recall now that $\mathbf{U}^i = \mathbf{d}U^i = U^i{}_{|j}\mathbf{d}X^j$ and $\mathbf{W}^i = \mathbf{d}W^i = W^i{}_{|j}\mathbf{d}X^j$ are the initial one–form peculiar–velocity gradient and the initial one–form peculiar–acceleration gradient. The fields W^i are determined nonlocally by the following set of equations, equivalent to Poisson's equation:

$$W^i{}_{|i} = *\frac{1}{2}\epsilon_{ijk}\mathbf{d}W^i \wedge \mathbf{d}X^j \wedge \mathbf{d}X^k = -4\pi G\delta\varrho_{\mathbf{i}} \; ;$$
$$\delta_{ij}\mathbf{d}W^i \wedge \mathbf{d}X^j = *\mathbf{d}\left(W^i\mathbf{d}X^i\right) = \mathbf{0} \, . \tag{2.30}$$

In view of the restriction to irrotational flows, we additionally impose the constraint:

$$\delta_{ij}\mathbf{d}\dot{f}^i \wedge \mathbf{d}f^j = \mathbf{0} \Longrightarrow \delta_{ij}\mathbf{d}U^i \wedge \mathbf{d}X^j = *\mathbf{d}\left(U^i\mathbf{d}X^i\right) = \mathbf{0} \, . \tag{2.31}$$

Without loss of generality, we can choose the following general set of initial data that can be obtained in the Newtonian theory or, else, from the *Minkowski Restriction* of ((2.20)–(2.22)):

— for the initial deformation, peculiar–velocity and peculiar–acceleration:

$$\begin{cases} \mathbf{d}\mathscr{P}^{i(n)} = \mathbf{0} \; \forall n \; ; \\ \mathbf{d}U^{i(1)} = \mathbf{d}U^i, \; U_{[i|j]} = 0 \; ; \\ \mathbf{d}W^{i(1)} = \mathbf{d}W^i, \; W_{[i|j]} = 0 \; , \end{cases} \tag{2.32}$$

— together with the definition of the Lagrangian metric coefficients and the initial data relation to the density perturbation:

$$\begin{cases} g_{ij} = \delta_{kl} f^k{}_{|i} f^l{}_{|j} \; ; \\ \delta\varrho_{\mathbf{i}}{}^{(1)} = \delta\varrho_{\mathbf{i}} = \varrho_{H\mathbf{i}}\delta_{\mathbf{i}} = -\frac{1}{4\pi G} W^k{}_{|k} \; . \end{cases} \tag{2.33}$$

The metric is Euclidean, since the coefficients can be transformed to the coefficients δ_{ij} with the help of the to $\mathbf{f}$ inverse coordinate transformation.

Plugging the ansatz (2.27) into the Newtonian equations for the deformation gradient expressed in terms of forms, see [55]:

$$\delta_{ij}\mathbf{d}\ddot{f}^i \wedge \mathbf{d}f^j = \mathbf{0} \, , \tag{2.34}$$

$$\frac{1}{2}\epsilon_{ijk}\mathbf{d}\ddot{f}^i \wedge \mathbf{d}f^j \wedge \mathbf{d}f^k = (\Lambda - 4\pi G\varrho)\,\mathbf{d}^3 f \, , \tag{2.35}$$

we find for the background Friedmann's equation:

$$\epsilon_{ijk}\, 3\frac{\ddot{a}}{a}\mathbf{d}X^i \wedge \mathbf{d}X^j \wedge \mathbf{d}X^k = \epsilon_{ijk}\left(\Lambda - 4\pi G\varrho_H\right)\mathbf{d}X^i \wedge \mathbf{d}X^j \wedge \mathbf{d}X^k$$
$$\Longrightarrow 3\frac{\ddot{a}}{a} = \Lambda - 4\pi G\varrho_H \, , \tag{2.36}$$

and a full hierarchy of the perturbation equations:

$$\delta_{ij} \quad \mathbf{d}\dot{P}^i \wedge \left(\mathbf{d}X^j + \mathbf{d}P^j\right) = \delta_{ij} a^{-2} \mathbf{d}U^i \wedge \mathbf{d}X^j \; ; \tag{2.37}$$

$$\begin{aligned} \epsilon_{ijk} \quad & \left[\left(\mathcal{D}_1 \mathbf{d}P^i\right) \wedge \mathbf{d}X^j \wedge \mathbf{d}X^k + \left(2\mathcal{D}_2 \mathbf{d}P^i\right) \wedge \mathbf{d}P^j \wedge \mathbf{d}X^k + \left(\mathcal{D}_3 \mathbf{d}P^i\right) \wedge \mathbf{d}P^j \wedge \mathbf{d}P^k \right] \\ = \quad & -\epsilon_{ijk} \frac{4\pi G}{3} \delta\varrho_{\mathbf{i}} a^{-3} \mathbf{d}X^i \wedge \mathbf{d}X^j \wedge \mathbf{d}X^k \; , \end{aligned} \tag{2.38}$$

where we defined the operator

$$\mathcal{D}_\ell := \frac{d^2}{dt^2} + 2H \frac{d}{dt} - \frac{4}{\ell} \pi G \varrho_H \; . \tag{2.39}$$

Projecting with the Hodge star operator to the coefficient form (and integrating Equation (2.37)), we obtain:

$$P_{[i|j]} = \int_{t_{\mathbf{i}}}^t \dot{P}_{m|[i} P^m_{\ |j]} dt' \; ; \tag{2.40}$$

$$\mathcal{D}_1 P^i_{\ |i} = -4\pi G \delta\varrho_{\mathbf{i}} a^{-3} - \frac{1}{2} \epsilon_{ijk} \epsilon^{lmn} \left[P^i_{\ |l} \ P^j_{\ |m} \mathcal{D}_3 P^k_{\ |n} + 2\delta^i_{\ |l} P^j_{\ |m} \mathcal{D}_2 P^k_{\ |n} \right] . \tag{2.41}$$

After splitting the equations (2.37) and (2.38) order by order, we obtain n sets of equations. At first–order we get:

$$\begin{aligned} \delta_{ij} \mathbf{d}\dot{P}^{i(1)} \wedge \mathbf{d}X^j &= \mathbf{0} \; ; & (2.42) \\ \epsilon_{ijk} \mathcal{D}_1 \mathbf{d}P^{i(1)} \wedge \mathbf{d}X^j \wedge \mathbf{d}X^k &= a^{-3} \epsilon_{ijk} \mathbf{d}W^i \wedge \mathbf{d}X^j \wedge \mathbf{d}X^k \; ; & (2.43) \end{aligned}$$

in coefficient form:

$$P^{(1)}_{[i|j]} = 0 \quad ; \quad \mathcal{D}_1 P^{i(1)}_{\ |i} = a^{-3} W^i_{\ |i} \; , \tag{2.44}$$

i.e. a set of linear equations. The generic n^{th}–order system of equations will be written below with an implicit summation over the order of perturbations in the source terms:

$$A^{(p)} B^{(q)} = \sum_{p+q=n} A^{(p)} B^{(q)} \; , \tag{2.45}$$

$$A^{(r)} B^{(s)} C^{(t)} = \sum_{r+s+t=n} A^{(r)} B^{(s)} C^{(t)} \; . \tag{2.46}$$

Thus, at any order $n > 1$, the perturbation equations read:

$$\begin{aligned} \delta_{ij} \mathbf{d}\dot{P}^{i(n)} \wedge \mathbf{d}X^j &= -\delta_{ij} \mathbf{d}\dot{P}^{i(p)} \wedge \mathbf{d}P^{j(q)} \; ; & (2.47) \\ \epsilon_{ijk} \mathcal{D}_1 \mathbf{d}P^{i(n)} \wedge \mathbf{d}X^j \wedge \mathbf{d}X^k &= -\epsilon_{ijk} \Big[\left(2\mathcal{D}_2 \mathbf{d}P^{i(p)}\right) \wedge \mathbf{d}P^{j(q)} \wedge \mathbf{d}X^k \\ & \quad + \left(\mathcal{D}_3 \mathbf{d}P^{i(r)}\right) \wedge \mathbf{d}P^{j(s)} \wedge \mathbf{d}P^{k(t)} \Big] \; ; & (2.48) \end{aligned}$$

in coefficient form:

$$\begin{aligned} P^{(n)}_{[i|j]} &= \int_{t_{\mathbf{i}}}^t \dot{P}^{(p)}_{m|[i} P^{m(q)}_{\ |j]} dt' \; ; & (2.49) \\ \mathcal{D}_1 P^{i(n)}_{\ |i} &= -\frac{1}{2} \epsilon_{ijk} \epsilon^{lmn} P^{j(s)}_{\ |m} P^{k(t)}_{\ |n} \mathcal{D}_3 P^{i(r)}_{\ |l} - \left(\mathcal{D}_2 P^{i(p)}_{\ |i}\right) P^{j(q)}_{\ |j} + \left(\mathcal{D}_2 P^{i(p)}_{\ |j}\right) P^{j(q)}_{\ |i} \; . & (2.50) \end{aligned}$$

The reader may consult the review [55] and references therein for further details.

Einstein's theory

Assuming the perturbation ansatz (2.1) for the coframes, and using the operator $\mathcal{D}_\ell$ as defined in (2.39), the analogous expansion is performed: the zeroth order again leads to the Friedmann equation, and the general perturbation scheme reads:

$$G_{ab} \quad \dot{\mathbf{P}}^a \wedge \delta^b{}_j \mathbf{d}X^j + G_{ab}\dot{\mathbf{P}}^a \wedge \mathbf{P}^b = \mathbf{0} \; ; \tag{2.51}$$

$$\begin{aligned} \epsilon_{abc} \quad & \left[\mathcal{D}_1 \mathbf{P}^a \wedge \delta^b{}_j \mathbf{d}X^j \wedge \delta^c{}_k \mathbf{d}X^k + (2\mathcal{D}_2 \mathbf{P}^a) \wedge \mathbf{P}^b \wedge \delta^c{}_k \mathbf{d}X^k + (\mathcal{D}_3 \mathbf{P}^a) \wedge \mathbf{P}^b \wedge \mathbf{P}^c \right] \\ = \quad & \epsilon_{abc} W \frac{1}{3} a^{-3} \delta^a{}_i \mathbf{d}X^i \wedge \delta^b{}_j \mathbf{d}X^j \wedge \delta^c{}_k \mathbf{d}X^k \; . \end{aligned} \tag{2.52}$$

In coefficient form and integrating (2.51) they become:

$$P_{[ij]} \;=\; G_{ab} \int_{t_\mathrm{i}}^{t} \dot{P}^a_{[i} P^b{}_{j]} dt' \; ; \tag{2.53}$$

$$\mathcal{D}_1 P^i{}_i \;=\; -\left(\left(\mathcal{D}_2 P^i{}_i \right) P^j{}_j - \left(\mathcal{D}_2 P^i{}_j \right) P^j{}_i \right) - \frac{1}{2} \epsilon_{ijk} \epsilon^{lmn} \left(\mathcal{D}_3 P^i{}_{|l} \right) P^j{}_{|m} P^k{}_{|n} + W a^{-3} \tag{2.54}$$

Expansion order by order leads to the first–order gravitoelectric equations:

$$G^{(0)}_{ab} \dot{\mathbf{P}}^{a(1)} \wedge \mathbf{d}X^b = \mathbf{0} \; ; \tag{2.55}$$

$$\epsilon_{abc} \mathcal{D}_1 \mathbf{P}^{a(1)} \wedge \delta^b{}_j \mathbf{d}X^j \wedge \delta^c{}_k \mathbf{d}X^k = a^{-3} \epsilon_{abc} \mathbf{W}^a \wedge \delta^b{}_j \mathbf{d}X^j \wedge \delta^c{}_k \mathbf{d}X^k \; ; \tag{2.56}$$

and the general n^{th}–order, $n > 1$, set of nonlinear equations:

$$G_{ab} \dot{\mathbf{P}}^{a(n)} \wedge \delta^b{}_j \mathbf{d}X^j = -G_{ab} \dot{\mathbf{P}}^{a(p)} \wedge \mathbf{P}^{b(q)} \; ; \tag{2.57}$$

$$\begin{aligned} & \epsilon_{abc} \mathcal{D}_1 \mathbf{P}^{a(n)} \wedge \delta^b{}_j \mathbf{d}X^j \wedge \delta^c{}_k \mathbf{d}X^k = \\ & -\epsilon_{abc} \Big[2 \left(\mathcal{D}_2 \mathbf{P}^{a(p)} \right) \wedge \mathbf{P}^{b(q)} \wedge \delta^c{}_k \mathbf{d}X^k \\ & \qquad + \left(\mathcal{D}_3 \mathbf{P}^{a(r)} \right) \wedge \mathbf{P}^{b(s)} \wedge \mathbf{P}^{c(t)} \Big] \; . \end{aligned} \tag{2.58}$$

In coefficient form, this reads:

$$P^{(1)}_{[ij]} = 0 \quad ; \quad \mathcal{D}_1 P^{i(1)}_{i} = W a^{-3} \; , \tag{2.59}$$

and

$$P^{(n)}_{[ij]} \;=\; G^{(r)}_{ab} \int_{t_\mathrm{i}}^{t} \dot{P}^{a(s)}_{[i} P^{b(t)}_{j]} dt' \; ; \tag{2.60}$$

$$\mathcal{D}_1 P^{i(n)}_{i} \;=\; -\frac{1}{2} \epsilon_{ijk} \epsilon^{lmn} P^{j(s)}_{m} P^{k(t)}_{n} \left(\mathcal{D}_3 P^{i(r)}_{l} \right) - \left(\mathcal{D}_2 P^{i(p)}_{i} \right) P^{j(q)}_{j} + \left(\mathcal{D}_2 P^{i(p)}_{j} \right) P^{j(q)}_{i} \; . \tag{2.61}$$

This provides equations for the perturbation fields at any order n from solutions of order $n - 1$.

Comparing $\{(2.57),(2.58)\}$ to the Newtonian equations $\{(2.47),(2.48)\}$, we see (not surprisingly) that we arrive at two equivalent sets of equations if we link the perturbations $\mathbf{P}^a$ and $\mathbf{d}P^i$ at any order via the *MR* – recall that the construction was done by inversion of the *MR* : $\mathbf{d}P^i = P^i{}_{|j}\mathbf{d}X^j \mapsto P^a{}_j\mathbf{d}X^j = \mathbf{P}^a$; for the initial data: $\mathbf{d}U^i = U^i{}_{|j}\mathbf{d}X^j \mapsto U^a{}_j\mathbf{d}X^j = \mathbf{U}^a$ and $\mathbf{d}W^i = W^i{}_{|j}\mathbf{d}X^j \mapsto W^a{}_j\mathbf{d}X^j = \mathbf{W}^a$. Therefore, we can simply translate the formal solution scheme for the trace–parts and the antisymmetric parts of the perturbations. However, note already here that the inversion of the *MR* produces a symmetric traceless component that is represented in Newtonian theory by the tidal tensor.

2.1.4 Gravitoelectric solution scheme

Recap: Newtonian theory

We first recall the general solution scheme given in [55], written for the perturbation gradients only.

The hierarchy begins with the first–order equations $\{(2.42),(2.43)\}$ which are uniquely determined by the constraint initial data (2.32). The general n^{th}–order, $n > 1$, solution scheme from Eqs. $\{(2.37),(2.38)\}$, reads:

$$\delta_{ij}\mathbf{d}P^{i(n)} \wedge \mathbf{d}X^j \;=\; {}^N\boldsymbol{\mathcal{S}}^{(n)} \; ; \tag{2.62}$$

$$\epsilon_{ijk}\mathcal{D}_1\mathbf{d}P^{i(n)} \wedge \mathbf{d}X^j \wedge \mathbf{d}X^k \;=\; {}^N\boldsymbol{\mathcal{T}}^{(n)} , \tag{2.63}$$

uniquely determined by the source terms:

$${}^N\boldsymbol{\mathcal{S}}^{(n)} \;:=\; -\delta_{ij}\int_{t_0}^{t} \mathbf{d}\dot{P}^{i(p)} \wedge \mathbf{d}P^{j(q)} dt' \; ; \tag{2.64}$$

$${}^N\boldsymbol{\mathcal{T}}^{(n)} \;:=\; -\epsilon_{ijk}\left[2\left(\mathcal{D}_2\mathbf{d}P^{i(p)}\right) \wedge \mathbf{d}P^{j(q)} \wedge \mathbf{d}X^k + \left(\mathcal{D}_3\mathbf{d}P^{i(r)}\right) \wedge \mathbf{d}P^{j(s)} \wedge \mathbf{d}P^{k(t)}\right] \; . \tag{2.65}$$

We have earlier demonstrated the formal equivalence between the Newtonian equations and the relativistic gravitoelectric equations. The generalization of the Newtonian solution scheme to obtain the corresponding relativistic scheme is now straightforward.

Einstein's Theory

The perturbative gravitoelectric Lagrange–Einstein system starts at $n = 1$ with the equations $\{(2.55),(2.56)\}$, uniquely determined by the corresponding constraint initial data (2.20). The n^{th}–order, $n > 1$, gravitoelectric solution scheme reads:

$$G_{ab}\mathbf{P}^{a(n)} \wedge \delta^b{}_j\mathbf{d}X^j \;=\; \boldsymbol{\mathcal{S}}^{(n)} \; ; \tag{2.66}$$

$$\epsilon_{abc}\mathcal{D}_1\mathbf{P}^{a(n)} \wedge \delta^b{}_j\mathbf{d}X^j \wedge \delta^c{}_k\mathbf{d}X^k \;=\; \boldsymbol{\mathcal{T}}^{(n)} \; , \tag{2.67}$$

which is uniquely determined by the source terms:

$$\boldsymbol{\mathcal{S}}^{(n)} \;:=\; G^{(r)}_{ab}\int_{t_0}^{t}\left(-\dot{\mathbf{P}}^{a(s)} \wedge \mathbf{P}^{b(t)}\right) dt' \; ; \tag{2.68}$$

$$\boldsymbol{\mathcal{T}}^{(n)} \;:=\; -\epsilon_{abc}\Big(2\left(\mathcal{D}_2\mathbf{P}^{a(p)}\right) \wedge \mathbf{P}^{b(q)} \wedge \delta^c{}_k\mathbf{d}X^k + \left(\mathcal{D}_3\mathbf{P}^{a(r)}\right) \wedge \mathbf{P}^{b(s)} \wedge \mathbf{P}^{c(t)}\Big) \; . \tag{2.69}$$

The coefficient form of these equations is given by (2.59)–(2.61).

2.2 Application of the solution scheme

In order to illustrate the use of the scheme {(2.66),(2.67)} in practice, we will in what follows explicitly explain the construction of relativistic solutions from Newtonian ones for the general procedure and through examples, in Subsections II.2.2.3 and II.2.2.4, respectively. Before we do so we explain the general systematics of solution scheme.

2.2.1 Systematics of the solutions

The n–th order scheme is a hierarchy of ordinary second–order differential equations, sourced by an inhomogeneity resulting from combinations of lower–order terms. Thanks to the linearity of the ordinary differential equations (ODE), the solution is, at any order n, a linear superposition of modes that we will label by l:

$$P^{i(n)}_{\;j} = \sum_{l} P^{i\;\,(n,l)}_{\;j} \quad . \tag{2.70}$$

In the Newtonian case, and for the gravitoelectric relativistic part, the modes can be further separated into spatial and temporal parts: $P^{i\;\,(n,l)}_{\;j} = \xi^{(n,l)}(t) P^{i\;\,(n,l)}_{\;j}(X_k)$. This is due to the fact that (2.67) is an ODE and that its coefficients only depend on time.

From the theory of second–order ODE's it is known (see, e.g., Section 2.1.1 of [119]), that an equation of the form

$$f_2\left(a\right)y'' + f_1\left(a\right)y' + f_0\left(a\right)y = g\left(a\right) \ , \tag{2.71}$$

will have as the general solution:

$$y\left(a\right) = C_1 y_1\left(a\right) + C_2 y_2\left(a\right) + \int_{a_{\mathrm{i}}}^{a} G\left(a,s\right)\frac{g\left(s\right)}{f_2\left(s\right)}ds \ , \tag{2.72}$$

where Green's function $G\left(a,s\right)$ is defined by

$$G\left(a,s\right) = \frac{y_2\left(a\right)y_1\left(s\right) - y_1\left(a\right)y_2\left(s\right)}{y_1\left(s\right)y_2'\left(s\right) - y_1'\left(s\right)y_2\left(s\right)} \ . \tag{2.73}$$

Therefore, at any order, the solution will have two modes l that are given by the homogeneous solution, known for a given background model (in the examples we will explicitly give the solutions for the Einstein–de Sitter case, henceforth EdS, and the Cold Dark Matter background with a cosmological constant, henceforth ΛCDM). The different modes of the particular solution can be calculated from the integral in (2.72) by setting $g = \mathcal{T}^{(n)}$. As integration is linear, the particular solution can be computed for each subpart of the source separately, and those parts appear as a $P^{i\;\,(n,l)}_{\;j}$ in the sum (2.78).

In order to study these subparts, we split the perturbations into their trace, their symmetric tracefree part and their antisymmetric part:

$$\mathbf{P}^a = \frac{1}{3}P\delta^a_{\;j}\mathbf{d}X^j + \mathbf{\Pi}^a + \mathfrak{P}^a \ . \tag{2.74}$$

Then, Equations $\{(2.60), (2.61)\}$ read:

$$\begin{aligned}\mathfrak{P}^{(n)}_{ij} = \int_{t_i}^{t} \frac{1}{3}\left(G^{(r)}_{a[i}\Pi^{a(t)}_{\ \ j]}\dot{P}^{(s)} - G^{(r)}_{a[i}\dot{\Pi}^{a(s)}_{\ \ j]}P^{(t)}\right) + \frac{1}{3}\left(G^{(r)}_{a[i}\mathfrak{P}^{a(t)}_{\ \ j]}\dot{P}^{(s)} - G^{(r)}_{a[i}\dot{\mathfrak{P}}^{a(s)}_{\ \ j]}P^{(t)}\right) \\ + \left(G^{(r)}_{ab}\dot{\mathfrak{P}}^{a(s)}_{\ [i}\Pi^{b(t)}_{\ \ j]} - G^{(r)}_{ab}\mathfrak{P}^{b(t)}_{\ [i}\dot{\Pi}^{a(s)}_{\ \ j]}\right) + \left(G^{(r)}_{ab}\dot{\Pi}^{a(s)}_{\ [i}\Pi^{b(t)}_{\ \ j]} + G^{(r)}_{ab}\dot{\mathfrak{P}}^{a(s)}_{\ [i}\mathfrak{P}^{b(t)}_{\ \ j]}\right) dt' \ ; \end{aligned} \tag{2.75}$$

$$\begin{aligned}\mathcal{D}_1 P^{(n)} = & -\frac{2}{3}P^{(q)}\mathcal{D}_2 P^{(p)} + \Pi^{b(q)}_{\ \ a}\mathcal{D}_2\Pi^{a(p)}_{\ \ b} + \mathfrak{P}^{b(q)}_{\ \ a}\mathcal{D}_2\mathfrak{P}^{a(p)}_{\ \ b} \\ & - \frac{1}{2}\left[\frac{1}{3}\left(\frac{2}{3}P^{(t)}P^{(r)} - \Pi^{a(t)}_{\ \ b}\Pi^{b(r)}_{\ \ a} - \mathfrak{P}^{a(t)}_{\ \ b}\mathfrak{P}^{b(r)}_{\ \ a}\right)\mathcal{D}_3 P^{(s)}\right. \\ & + \frac{1}{3}\left(-P^{(t)}\mathfrak{P}^{a(r)}_{\ \ b} - \mathfrak{P}^{a(t)}_{\ \ b}P^{(r)}\right)\mathcal{D}_3\mathfrak{P}^{b(s)}_{\ \ a} \\ & + \frac{1}{3}\left(-P^{(t)}\Pi^{a(r)}_{\ \ b} - \Pi^{a(t)}_{\ \ b}P^{(r)}\right)\mathcal{D}_3\Pi^{b(s)}_{\ \ a} \\ & + \left(\Pi^{a(t)}_{\ \ c}\Pi^{c(r)}_{\ \ b} + \Pi^{c(t)}_{\ \ b}\Pi^{a(r)}_{\ \ c} + \Pi^{a(t)}_{\ \ c}\mathfrak{P}^{c(r)}_{\ \ b} + \Pi^{c(t)}_{\ \ b}\mathfrak{P}^{a(r)}_{\ \ c}\right. \\ & + \left.\mathfrak{P}^{a(t)}_{\ \ c}\Pi^{c(r)}_{\ \ b} + \mathfrak{P}^{c(t)}_{\ \ b}\Pi^{a(r)}_{\ \ c} + \mathfrak{P}^{a(t)}_{\ \ c}\mathfrak{P}^{c(r)}_{\ \ b} + \mathfrak{P}^{c(t)}_{\ \ b}\mathfrak{P}^{a(r)}_{\ \ c}\right) \\ & \left.\left(\mathcal{D}_3\Pi^{b(s)}_{\ \ a} + \mathcal{D}_3\mathfrak{P}^{b(s)}_{\ \ a}\right)\right] . \end{aligned} \tag{2.76}$$

Hence, the trace and the antisymmetric parts are completely determined by the lower–order expressions of all parts (four equations for four components of $P^i_{\ j}$). What is missing is an equation for the five components of the tracefree symmetric term $\Pi^{i(n)}_j$. Recall that the gravitoelectric system is only closed after imposing the *MR* , which then couples the tracefree symmetric time–evolution to the one of the trace and encodes the spatial dependence in a Poisson equation.

2.2.2 Reconstruction of the relativistic solutions

In order to illustrate the scheme for the relativistic case, we will discuss here how to reconstruct the full n–th order solution from the recursive equations $\{(2.66),(2.67)\}$.

Trace part

The trace part is the main part that is given by the hierarchy. In the absence of the tracefree symmetric term $\Pi^{i(n)}_j$, there is no antisymmetric term emerging and we are left with a recursion relation for the trace:

$$\mathcal{D}_1 P^{(n)} = -\frac{2}{3}P^{(q)}\mathcal{D}_2 P^{(p)} - \frac{1}{9}P^{(t)}P^{(r)}\mathcal{D}_3 P^{(s)} \ . \tag{2.77}$$

Antisymmetric part

It may appear counterintuitive that a nonvanishing antisymmetric part arises (starting from second order), given our assumption of irrotationality due to the given foliation of spacetime. However, this fact is known from the Newtonian Lagrangian perturbation theory, where antisymmetric parts arise, starting at second order, in Lagrangian space, while no vorticity is created in Eulerian space [24]. Our comoving setting corresponds to the Lagrangian picture of fluid motion, and the antisymmetric terms at order n satisfy and follow from the irrotationality condition (2.66), given all subleading terms $p = 1 \dots n-1$. However, we need to reconstruct a part of the tracefree symmetric term to recover all the Newtonian modes that have antisymmetric components, a problem to which we turn now.

Tracefree symmetric part

As our scheme does not separately provide a relation that determines the five coefficients of the tracefree symmetric part (these equations are part of the gravitomagnetic scheme), we have to reconstruct the relevant part that complies with the Newtonian solutions. In order to achieve this it suffices to realize that the one–form fields $\mathbf{P}^a(X^k,t)$ become integrable in the *MR* , $\mathbf{d}P^i(X^k,t)$, and so also the tracefree symmetric part. Hence, in the *MR* , the tracefree symmetric part of $\mathbf{d}P^i(X^k,t)$ inherits the time–evolution from the trace. With this in mind, and due to the superposition property of our solution scheme, we are entitled to split the general tracefree symmetric coefficients Π_{ij} into a part that reproduces the tracefree symmetric part of $\mathbf{P}^a(X^k,t)$ in the *MR* , denoted by ${}^E\Pi_{ij}$, and another part ${}^H\Pi_{ij}$. This is possible at any order:

$$\Pi_{ij}^{(n)} = \sum_{l\,m} \xi^{(n,l)}(t)\, {}^E\Pi_{ij}^{(n,l)}(X^k) + {}^H\Pi_{ij}^{(n,m)}(X^k,t) \ . \tag{2.78}$$

The temporal coefficients $\xi^{(n,l)}$ are the same for the trace and the tracefree symmetric gravitoelectric parts. For the full relativistic solution there is in addition a contribution, denoted by ${}^H\Pi_{ij}$, which is related to gravitational waves. For the time being we note that the superposition property discussed above assures that the resulting individual terms in the decomposition (2.78) are correct, if we use only this gravitoelectric part of the tracefree symmetric tensor in the hierarchy. Thus, even though the scheme does not determine all the components of $P^{i(n)}_{\ j}$ without solving the gravitomagnetic equations, it is consistent for the terms it delivers. Moreover, by inspection of corresponding perturbation and solution schemes that we derived for the gravitomagnetic part [4], we can conclude that the so–reconstructed solutions provide the leading–order modes of the relativistic solutions at any order. Of course, inserting the reconstructed solution into the full set of Einstein equations will result in constraints on initial data in addition to the standard constraints. As an example we will discuss the constraints in the first–order scheme given below.

2.2.3 Example 1: recovering parts of the general first–order solution

In order to illustrate the hierarchy we begin with the first–order equations of the scheme {(2.66),(2.67)}, i.e. in coefficient form (2.59). With the split in space and time coefficients, the latter are the well–known solutions of the equation (equivalent to the equation in the Newtonian scheme [21, 16, 22]):

$$\ddot{\xi} + 2H\dot{\xi} - \frac{3}{2}{H_{\mathbf{i}}}^2\Omega_{\mathbf{i}m}a^{-3}\xi = W a^{-3} \ . \tag{2.79}$$

For an EdS universe the modes are proportional to a, $a^{-3/2}$ and a^0. Together with the initial conditions, the solution for the trace found from (2.59) reads:

$$P^{(1)} = \frac{3}{5}\left[(Ut_{\mathbf{i}} + \frac{3}{2}Wt_{\mathbf{i}}^2)a - \left(Ut_{\mathbf{i}} - Wt_{\mathbf{i}}^2\right)a^{-\frac{3}{2}} - \frac{5}{2}Wt_{\mathbf{i}}^2\right] \ . \tag{2.80}$$

The antisymmetric part vanishes in view of (2.59), $\mathfrak{P}^{a(1)}_{\ i} = 0$. We then need to reconstruct the tracefree symmetric part along the lines described in II.2.2.2 to complete the solution:

$$\begin{aligned} {}^E\Pi^{(1)}_{ij} = & \frac{3a}{5}\left({}^EU^{tl}_{ij}t_{\mathbf{i}} + \frac{3}{2}{}^EW^{tl}_{ij}t_{\mathbf{i}}^2\right) \\ & - \frac{3}{5a^{3/2}}\left({}^EU^{tl}_{ij}t_{\mathbf{i}} - {}^EW^{tl}_{ij}t_{\mathbf{i}}^2\right) - \frac{3}{2}{}^EW^{tl}_{ij}t_{\mathbf{i}}^2 \ . \end{aligned} \tag{2.81}$$

The notation ^{tl} stands for the traceless part. The initial fields have been split accordingly:

$$U_{ij} =: {}^EU_{ij} + {}^H U_{ij} \ ; \ W_{ij} =: {}^EW_{ij} + {}^H W_{ij} \ , \tag{2.82}$$

i.e. a part initializing the gravitoelectric, and the gravitomagnetic part, respectively.

We remark that in Newtonian theory the tidal tensor is written in terms of the gravitational potential Φ:

$$-\mathcal{E}_{ij} = \Phi_{,ij} - \frac{1}{3}\delta_{ij}\nabla^2\Phi \ , \tag{2.83}$$

where a comma denotes derivative with respect to Eulerian inertial coordinates. If we consider the first–order solution (here restricted to the growing mode solution for notational ease),

$${}^EP^{i\ (1)}_{\ j} = \frac{3}{2}W^i_{\ j}t_{\mathbf{i}}^2\,(a-1) \ , \tag{2.84}$$

the first–order gravitoelectric part of the spatially projected Weyl tensor assumes the form (note the conventional sign difference of this geometrical definition with the Newtonian (active) definition of $\mathcal{E}_{ij}$):

$$\begin{aligned} E^{i\ (1)}_{\ j} &= -\ddot{\Pi}^{i\ (1)}_{\ j} - 2H\dot{\Pi}^{i\ (1)}_{\ j} \\ &= -\frac{3}{2}t_{\mathbf{i}}^2\,(\ddot{a} + 2H\dot{a})\left(W^i_{\ j} - \frac{1}{3}W\delta^i_{\ j}\right) \\ &= -\frac{3}{2}t_{\mathbf{i}}^2 a\left(\frac{3}{2}H_{\mathbf{i}}^2\frac{1}{a^3}\right)\left(W^i_{\ j} - \frac{1}{3}W\delta^i_{\ j}\right) \\ &= -\frac{1}{a^2}\left(W^i_{\ j} - \frac{1}{3}W\delta^i_{\ j}\right) . \end{aligned} \tag{2.85}$$

We find

$$E_{ij}^{\ (1)} = -\left(W_{ij} - \frac{1}{3}W\delta_{ij}\right) . \tag{2.86}$$

The trace W does not derive from a potential due to nonintegrability of the field. After executing the *MR* , we obtain (up to the conventional sign difference), the Newtonian tidal tensor (2.83).

Summarizing: given the formal analogy of the solution schemes discussed in Section II.2.1.4, the above solution solves the gravitoelectric part of the corresponding relativistic equations (2.59). The tracefree symmetric part (2.41), however, is only a part of the solution in the relativistic case. Eq. (102) in [35] states that the first–order equation for the relativistic tracefree symmetric part reads:

$$\ddot{\Pi}^{(1)}_{ij} + 3H\dot{\Pi}^{(1)}_{ij} - a^{-2}\Pi^{|k(1)}_{ij\ \ |k} = -a^{-2}\left(\mathscr{T}_{ij} + P^{(1)}_{|ij} - \frac{1}{3}P^{|k(1)}_{\ \ |k}\delta_{ij}\right) \ , \tag{2.87}$$

where $\mathscr{T}_{ij}$ is the tracefree part of the initial Ricci tensor. Plugging (2.34) and (2.41) into (2.87), we can check whether our relativistic generalization satisfies the full equation. Three modes appear in the equation: a^{-2}, a^{-1} and $a^{-7/2}$. The equation has to be satisfied at any time, thus each mode must lead to cancellation of the coefficients. This leads to the following constraints ($H_{\mathbf{i}} := 2/3t_{\mathbf{i}}$):

$$\begin{gathered} {}^E\mathscr{T}_{ij} = -H_{\mathbf{i}}{}^E U^{tl}_{(ij)} - {}^E W^{tl}_{(ij)} \ ; \\ {}^E U^{|k}_{(ij)\ |k} = {}^E U^k{}_{k|ij} \quad ; \quad {}^E W^{|k}_{(ij)\ |k} = {}^E W^k{}_{k|ij} \ . \end{gathered} \tag{2.88}$$

The first equation corresponds to the definition of the tracefree part of the initial Ricci tensor, Eq. (2.13) in the EdS case studied here. In view of the constraints $U_{[ij]} = 0$ and $W_{[ij]} = 0$ (*cf.* (2.20)), the other two conditions are equivalent to:

$${}^E U^{|k}_{ij\ |k} = {}^E U^k{}_{k|ij} \quad ; \quad {}^E W^{|k}_{ij\ |k} = {}^E W^k{}_{k|ij} \ . \tag{2.89}$$

What we call gravitoelectric part in the decomposition of initial conditions (2.21) is therefore determined to be the one that solves (2.88). The part contributing to the propagating gravitomagnetic part is then its complement. This labelling is not completely unambiguous, because in this scheme, the gravitomagnetic part computed from the gravitoelectric part is not zero, see below for the first–order scheme. (Nevertheless, as we will show in the next part, it generates a zero dynamical Ricci curvature tensor.)

In order to check how constraining these relations are, beyond the constraints that we already have, we consider the first and second time–derivatives of the momentum constraints and evaluate them at initial time in order to obtain constraints on the initial fields. Taking the second spatial derivative of these equations and contracting them with respect to one index, we get for U_{ij}:

$$U^k{}_{j|k} = U^k{}_{k|j} \Rightarrow U^k{}_{j|ik} = U^k{}_{k|ij} \Rightarrow U^{k|i}{}_{j|ik} = U^{k|i}{}_{k|ij} \ . \tag{2.90}$$

The latter identity is solved by the gravitoelectric and the gravitomagnetic parts independently. For the gravitoelectric part, we have:

$${}^E U^{k|i}{}_{j|ik} = {}^E U^{k|i}{}_{k|ij} \ , \tag{2.91}$$

which is equal to the once contracted spatial derivative of the above constraint (2.89). We conclude that (2.89) and the momentum constraints are compatible with but not equivalent to our constraints. They have to be solved independently in order for the solution to be compatible with both the evolution equation and the momentum constraints.

What they do constrain are derivatives of the gravitomagnetic part. To derive these constraints, let us first note that the first–order expression for the magnetic part can be found from Equation (107) in [35]:

$${}^E H_{ij} = a(t)\epsilon^{sl}{}_{(i}{}^E\dot{\Pi}_{j)l|s} \ . \tag{2.92}$$

The solution for ${}^E\Pi_{ij}$, *cf.* (2.41), shows that spatial derivatives of the first–order magnetic part can be traced back to spatial derivatives of U_{ij} and W_{ij}. Together with the first–order momentum constraints, $\dot{P}^i{}_{i|j} = \dot{P}^i{}_{j|i}$, and imposing the constraints (2.88), we get:

$$\epsilon^{uri}\ \epsilon^{sl}{}_{(i}{}^E U_{j)s|lr} = 0 \ \ ; \ \ \epsilon^{uri}\ \epsilon^{sl}{}_{(i}{}^E W_{j)s|lr} = 0 \ . \tag{2.93}$$

Thus, via (2.41), this leads to

$$\epsilon^{uri}\ {}^E H_{ij|r} = 0 \ , \tag{2.94}$$

i.e., the curl of ${}^E H_{ij}$ vanishes.

For its divergence the constraints (2.88) are not necessary. Taking the divergence of (2.92), and using the momentum constraints in the form ${}^E\dot{\Pi}^i{}_{l|is} = 2/3\dot{P}_{|ls}$, we can show:

$${}^E H_{ij}{}^{|i} = 0 \ . \tag{2.95}$$

By combining (2.94) and (2.95), we conclude that

$$\Delta_0{}^E H_{ij} = 0 \ . \tag{2.96}$$

Thus, the gravitomagnetic part that is generated by the gravitoelectric part is a harmonic tensor field at first order. This harmonic field can be constrained in the initial conditions (removed) by topological conditions on the perturbations.

2.2.4 Example 2: constructing second–order solutions for 'slaved initial data'

Let us now write out the system {(2.66),(2.67)} explicitly for $n = 2$. We simplify the first–order source by imposing the so–called 'slaving condition' $U^i{}_j = W^i{}_j t_\mathbf{i}$ (as explained in [21, 22] and, for second order in [23]). This is not necessary but increases readability. The sum of (2.34) and (2.41) becomes:

$$P^{(1)}_{ij} = \frac{3}{2} W_{ij} t_\mathbf{i}{}^2 \left(a - 1\right) \ . \tag{2.97}$$

At second order (2.61) is simply

$$\mathcal{D}_1 P^{i(2)}_{i} = -\left(\mathcal{D}_2 P^{i(1)}_{i}\right) P^{j(1)}_{j} + \left(\mathcal{D}_2 P^{i(1)}_{j}\right) P^{j(1)}_{i} \ , \tag{2.98}$$

and we have the system:

$$\begin{cases} \ddot{\xi}^{(2)} + 2\dfrac{\dot{a}}{a}\dot{\xi}^{(2)} + 3\dfrac{\ddot{a}}{a}\xi^{(2)} = \dfrac{3}{4} t_\mathbf{i}{}^2 \left(a^{-1} - a^{-3}\right) \ ; \\ C^{(2)} = W^i{}_j W^j{}_i - WW \ , \end{cases} \tag{2.99}$$

with the source $g^{(2)}(t) = \frac{3}{4} t_\mathbf{i}{}^2 \left(a^{-1} - a^{-3}\right)$.

In order to systematically determine the temporal coefficients of the hierarchy, it is useful to write the operator $\mathcal{D}_1$ in terms of a. We find:

$$g\left(a\right) = \Omega_{\mathbf{i}m} H_\mathbf{i}{}^2 \times \left(\left(\frac{1}{a} + a^2 c\right) P''(a) + \frac{3}{2}\left(\frac{1}{a^2} + 2ac\right) P'(a) - \frac{3}{2a^3} P(a) \right) , \tag{2.100}$$

where $c = \Omega_{\mathbf{i}\Lambda}/\Omega_{\mathbf{i}m}$. For an EdS background, $c = 0$, the homogeneous solution is

$$D\left(a\right) = aC_1 + a^{-3/2}C_2\ ; \tag{2.101}$$

Green's function of Eq. (2.73) is

$$G\left(a,s\right) = \frac{2}{5}\frac{s\left(a^{5/2} - s^{5/2}\right)}{\Omega_{\mathbf{i}m}{H_{\mathbf{i}}}^2 a^{3/2}}\ . \tag{2.102}$$

Now, it is a matter of a simple integration and Eq. (2.72) gives the second–order trace solution:

$$P^{(2)} = {}^1C^{(2)}a + {}^2C^{(2)}a^{-3/2} + \frac{9}{8}{t_{\mathbf{i}}}^4\left(1 + \frac{3}{7}a^2\right)C^{(2)}\ . \tag{2.103}$$

To find the spatial coefficients of the solution, we use the initial values for the coframe and its time–derivative. They have been chosen to vanish for all orders higher than one in the hierarchy of solutions of Eqs. (2.61). Therefore, we find the following system:

$$\begin{aligned} P^{(2)}(t_{\mathbf{i}}) &= {}^1C + {}^2C + \frac{45}{28}C^{(2)}{t_{\mathbf{i}}}^4 = 0\ ; \\ \dot{P}^{(2)}(t_{\mathbf{i}}) &= \frac{2}{3t_{\mathbf{i}}}{}^1C - \frac{1}{t_{\mathbf{i}}}{}^2C + \frac{9}{14}C^{(2)}{t_{\mathbf{i}}}^4 = 0\ , \end{aligned} \tag{2.104}$$

which fixes all constants to be $\propto C^{(2)}$. Thus, the second–order trace solution reads:

$$\begin{aligned} P^{(2)} &= \xi_+^{(2)}\left(WW - W^i{}_jW^j{}_i\right)\ ; \\ \xi_+^{(2)} &= \frac{9}{4}{t_{\mathbf{i}}}^4\left(-\frac{3}{14}a^2 + \frac{3}{5}a - \frac{1}{2} + \frac{4}{35}a^{-3/2}\right)\ . \end{aligned} \tag{2.105}$$

After executing the *MR* this coincides with the second–order Newtonian solution of [24].

The antisymmetric equation (2.66) still delivers $\mathfrak{P}^{a(2)}_{\ i} = 0$. This is due to the restriction to 'slaved initial conditions', otherwise we would have a nonvanishing part here. Thus, we only need the tracefree symmetric part to complete the solution. The gravitoelectric part can be written as

$$^{E}\Pi^{(2)}_{ij} = \xi_+^{(2)}\mathcal{S}^{(2)}_{ij}\ , \tag{2.106}$$

where the trace of $\mathcal{S}^{(2)}_{ij}$ is given by $\left(W^2 - W^i{}_jW^j{}_i\right){t_{\mathbf{i}}}^2$. The rest of its components can be determined from the generalization $\mathcal{S}^{(2)}_{|ij} \to \mathcal{S}^{(2)}_{ij}$, where $\mathcal{S}^{(2)}$ is the solution to the Newtonian Poisson equation $\Delta_0\mathcal{S}^{(2)} = \left((W^k{}_{|k})^2 - W^i{}_{|j}W^j{}_{|i}\right){t_{\mathbf{i}}}^2$, and where Δ_0 denotes the Laplacian in local (Lagrangian) coordinates (see [24]). To avoid passing by the generalization of the Newtonian result, one can of course also insert $^{E}\Pi^{(2)}_{ij}$ into (2.106) and solve the remaining relativistic equations of the gravitomagnetic part to find the off–trace components of $\mathcal{S}^{(2)}_{ij}$.

The explicit derivation of the inhomogeneous second–order term in this subsection illustrates that, using (2.72) and (2.102), the calculation of the temporal evolution of the general relativistic trace part is straightforward and only involves the calculation of integrals. This can also be easily extended to perturbations of a ΛCDM universe model by noting that (2.101) becomes:

$$D\left(a\right) = a\,{}^{(2)}F_1\left(\frac{1}{3},1,\frac{11}{6};-ca^3\right)C_1 + \sqrt{\frac{1}{a^3}+c}\,C_2\;, \tag{2.107}$$

with the Gauss Hypergeometric function ${}^{(2)}F_1$. Greens' function reads in this case:

$$G\left(s,a\right) = \frac{2}{5}\frac{s}{\Omega_{\mathbf{i}m}{H_{\mathbf{i}}}^2}\left(D_+\left(a,c\right) - D_+\left(s,c\right)\sqrt{\frac{\left(1+ca^3\right)s^3}{\left(1+cs^3\right)a^3}}\right), \tag{2.108}$$

where $D_+\left(a,c\right)$ is the first term in (2.107).

2.3 Summary and concluding remarks

We have investigated gravitoelectric perturbation and solution schemes at any order in relativistic Lagrangian perturbation theory. These schemes cover the full hierarchy of the Newtonian Lagrangian perturbation theory if restricted to integrable Cartan coframe fields. Despite the fact that the solution scheme presented in this work gives on its own not all parts of the relativistic perturbation solutions, it delivers an important part relevant to the formation of large–scale structure. As is well–known (see e.g. discussions in [99] and [4]), the fastest growing scalar modes of the relativistic solutions correspond to the Newtonian modes, shown up to second order and, by inspection of the schemes we investigated, we showed this to hold for the gravitoelectric part also beyond second order. As we recover all the Newtonian terms with their correct temporal evolution and their constrained spatial coefficients, we also know that our solution contains all terms that become important in the Late Universe. The presented scheme is explicit enough to derive solutions at any desired order by algebraic codes along the lines of the reconstruction rules that we exemplified up to the second order. We demonstrated the close formal correspondence of the gravitoelectric Lagrange–Einstein system to the Newtonian theory furnishing construction rules that also allow to find other, nonperturbative relativistic solutions from Newtonian ones.

The role of gravitational waves, corresponding to the missing part in our scheme, has to be further explored. The missing part, which we denoted by ${}^H\Pi_{ij}$ in the coefficients of the tracefree symmetric parts of the perturbations, corresponds at first order to 'free gravitational waves', i.e. that part of gravitational radiation that does not scatter at the sources. This changes at higher orders, since this part will couple to the sources starting at second order. We shall investigate in detail the general first–order scheme including gravitational waves in the next Part of the thesis, where we also identify the transformations and restrictions that have to be imposed to obtain the known solutions of the standard perturbation theory, where perturbations are embedded into the background spacetime.

Part III

From a Local to a Global Description of First-Order Intrinsic Lagrangian Perturbations

Chapter 1

Gravitational Waves in the Standard Perturbation Theory

Contents

1.1 Propagative dynamics in the intrinsic approach: motivations and strategy

In the last part we have used the formal analogy between the gravitoelectric part of the Einstein equations and the Lagrange-Newton-System to build a relativistic generalization of the Newtonian perturbative solution to order n. These solutions exhibit the same time-dependence as the Newtonian ones and therefore do not encode propagative dynamics. Furthermore, we have seen that, at first-order, the gravitoelectric part of the initial conditions has to fulfill the equalities (2.89). As discussed in Section II.1.4.3, the magnetic part of the Weyl tensor is often thought to encode gravitational waves. It is interesting to note that the gravitoelectric solutions also generate a magnetic part that only at first order is a solution of the Laplace equation (2.96). These equations are elliptic and thus need boundary conditions to be solved. In General Relativity, if we are looking for a global solution on the manifold, these boundary conditions are provided by topology.

In this part, we will consider only the first-order perturbation theory. Gravitational waves have then only a trivial component in the gravitoelectric class of solutions. We will therefore determine where and how they are encoded in the complementary part of the solution obtained from the Newtonian perturbation theory. Moreover, we will compare our intrinsic Lagrangian perturbative approach to the standard perturbation theory, in order to highlight the similarities and identify the differences between the two. One of the main issues will be to understand under which conditions the gravitoelectric part of the solution represents the integrable part of the perturbation fields.

In the following chapter, we begin with a short presentation of the standard theory of gravitational waves. We will present the instruments that have been built to detect them and explain how they have been theoretically predicted from the linearization of the Einstein equations. Furthermore, we will discuss the gravitoelectromagnetic analogy for the linearized Einstein equations in the weak field limit. The standard treatment of gravitational waves is presented in order to better understand why our description goes beyond the standard approach, even at first-order.

The second chapter will focus on the local first-order Einstein equations and solutions. We will give the first results on the gravitomagnetic part of the solution and will carry out a comparison to the standard perturbative approach. The last chapter will treat globally the coframes and the spatial manifold. Some powerful mathematical tools and theorems, available for closed topological spaces, will be used to determine the impact of topology on the first-order solutions.

1.2 Standard description of gravitational waves

1.2.1 Observing gravitational waves in the Standard Perturbation Theory

Gravitational waves were predicted by Albert Einstein [60] and are a natural consequence of General Relativity. They propagate at the speed of light, such as the electromagnetic waves but, contrary to the electromagnetic waves, they do not propagate on space-time but are a propagating oscillation of space-time itself. Measures of time and length are thus modified by gravitational waves. Nevertheless, these effects are very small and the sensitivity of the detectors should be higher then the current one.

Indeed, being an interferometer on Earth, Virgo uses the modification of lengths by gravitational waves to detect them. A great amount of the noise in its measurements is due to some local vibrations. Overcoming this intrinsic limit is a true technical prowess. However, Virgo has not detected gravitational waves so far.

Measuring the polarization of the CMB, the BICEP 2 (Background Imaging of Cosmic Extragalactic Polarization) experiment, located in the Antarctic Amundsen-Scott base in the South Pole, claimed to have found primordial gravitational waves. Data from the BICEP2 telescope and Planck were analyzed jointly. It turned out that the signal could be entirely attributed to dust in the Milky Way rather than to the signature of some primordial gravitational waves [47].

The eLISA spatial gravitational wave detector https://www.elisascience.org , which will be the European Space Agency focus for the next two large science missions, will be a huge improvement for detection of gravitational waves. Measuring gravitational waves will not only confirm one of the predictions of General Relativity, it will furthermore provide us with some precious information in some aspects of cosmology such as the Early Universe or the large scale structure formation.

For some very good lectures on gravitational waves, the reader can refer to [73], [152] and [74].

In order to better compare our Lagrangian perturbation approach to the standard one, I here present how equations for propagation of gravitational waves are derived when the metric tensor is perturbed around a Minkowski background. Furthermore, since one of the important aspects of my research is gravitoelectromagnetism, I wish to discuss how, from the standard linearized Einstein equations, we can obtain the analogue of the Maxwell equations and even the Lorentz force. In order to simplify the comparison to electromagnetism, we will not use the $c = 1$ units in this section.

1.2.2 Linearizing the Einstein equations

When we linearize the Einstein equations according to (1.1), the gravitational field is weak, but it doesn't have to be static, and particles are allowed to move with relativistic velocities.

We will consider small perturbations around a Minkowski space-time. The metric tensor will then be decomposed as:

$$g_{\mu\nu} = \eta_{\mu\nu} + h_{\mu\nu} \quad ; \quad |h_{\mu\nu}| \ll 1 \ , \tag{1.1}$$

where $\eta_{\mu\nu}$ is the Minkowski metric: $\eta_{\mu\nu} = diag(-1,1,1,1)$. We consider the transformation of the metric for an infinitesimal coordinate transformation around point P (called gauge transformation):

$$x^{\mu'}(P) = x^{\mu}(P) + \xi^{\mu}(P) \quad ; \quad |\xi^{\mu}| \ll x^{\mu} \ , \tag{1.2}$$

then,

$$g_{\rho'\sigma'} = \frac{\partial x^{\mu}}{\partial x^{\rho'}} \frac{\partial x^{\nu}}{\partial x^{\sigma'}} g_{\mu\nu}(x^{\mu'} - \xi^{\mu}) \ . \tag{1.3}$$

If we keep only the first–order in $h_{\mu\nu}$ and ξ^{μ}, we then obtain:

$$g_{\rho'\sigma'} = \eta_{\rho'\sigma'} + h_{\rho'\sigma'} \quad \text{where} \quad h_{\rho'\sigma'} = h_{\rho\sigma} - \xi_{\rho,\sigma} - \xi_{\sigma,\rho} \ , \tag{1.4}$$

where the the comma represents the derivative with respect to x^{μ}.

In order to have gauge invariant components of the metric tensor, the coordinate transformation must be chosen such that $\xi_{\rho,\sigma} + \xi_{\sigma,\rho} = 0$.

To first order,

$$R_{\alpha\mu\beta\nu} = \Gamma_{\alpha\mu\nu,\beta} - \Gamma_{\alpha\mu\beta,\nu} \quad \text{where} \quad \Gamma_{\alpha\mu\nu} = \frac{1}{2}\left(h_{\mu\alpha,\nu} + h_{\nu\alpha,\mu} - h_{\mu\nu,\alpha}\right) \ . \tag{1.5}$$

The Ricci tensor is thus:

$$R_{\mu\nu} = \frac{1}{2}\left(h^{\alpha}{}_{\nu,\alpha\mu} + h^{\alpha}{}_{\mu,\alpha\nu} - h_{,\mu\nu} - \Box h_{\mu\nu}\right) \ , \tag{1.6}$$

where $\Box = -c^{-2}\,\partial^2/\partial t^2 + \nabla^2$ is the d'Alembert wave operator on the Minkowski space-time and $h = h^{\alpha}{}_{\alpha}$.

Now we introduce $\overline{h}_{\mu\nu} = h_{\mu\nu} - \frac{1}{2}\eta_{\mu\nu}h$ and perform the gauge transformation on it.

$$\overline{h'}_{\alpha\beta} = \overline{h}_{\alpha\beta} - \xi_{\alpha,\beta} - \xi_{\beta,\alpha} + \eta_{\alpha\beta}\xi^{\sigma}{}_{\sigma} \ . \tag{1.7}$$

Then, if we choose some harmonic coordinates such that $\Box\xi_{\alpha} = \overline{h}^{\beta}{}_{\alpha,\beta}$, and drop the prime [1], we get:

$$\overline{h}^{\beta}{}_{\alpha,\beta} = 0 \ , \tag{1.8}$$

and

$$\Box\overline{h}_{\mu\nu} = -\frac{16\pi G}{c^4}\, T_{\mu\nu} \ . \tag{1.9}$$

For an empty universe, we get the d'Alembert equation:

$$\Box\overline{h}_{\mu\nu} = 0 \ . \tag{1.10}$$

Thus, gravitational waves propagate at the speed of light.

1. This condition is called Lorenz gauge

1.2.3 Gravitoelectromagnetism in the weak field limit

The solution of (1.9) can be expressed in terms of the retarded potentials

$$\overline{h}_{\mu\nu} = \frac{4\,G}{c^4}\int \frac{T_{\mu\nu}(t - c|\mathbf{x}-\mathbf{x}'|,\mathbf{x}')}{|\mathbf{x}-\mathbf{x}'|}\mathrm{d}^3x' \ . \tag{1.11}$$

$T_{\mu\nu}$ is the analogue of the 4–current J_μ and $\overline{h}_{\mu\nu}$ is the analogue of the 4–potential A_μ. We will further assume that $|T_{00}| \gg |T_{ij}|$ and $|T_{0i}| \gg |T_{ij}|$, which, for a dust matter model, implies that the particles are moving slowly with respect to the speed of light c. We then have

$$\overline{h}_{00} = -\frac{4\phi}{c^2} \quad ; \quad \overline{h}_{0i} = \frac{2A_i}{c^2} \ . \tag{1.12}$$

The Lorenz condition $\overline{h}^{\beta}_{\ \alpha,\beta} = 0$ can now be rewritten:

$$\frac{1}{c}\frac{\partial\phi}{\partial t} + \frac{1}{2}\boldsymbol{\nabla}\cdot\mathbf{A} = 0 \ . \tag{1.13}$$

Appart from the pre-factor $\frac{1}{2}$, which comes from the fact that gravity is a spin 2 theory, this is identical to the Lorenz gauge condition in electromagnetism. If we define the gravitoelectric and the gravitomagnetic fields as follows:

$$\mathbf{E}_G = -\boldsymbol{\nabla}\phi - \frac{1}{2c}\frac{\partial\mathbf{A}}{\partial t} \quad ; \quad \mathbf{B}_G = \boldsymbol{\nabla}\times\mathbf{A} \ , \tag{1.14}$$

we then obtain the Maxwell equations:

$$\boldsymbol{\nabla}\cdot\mathbf{E}_G = -4\pi G\rho \quad ; \quad \boldsymbol{\nabla}\cdot\mathbf{B}_G = 0 \ ; \tag{1.15}$$

$$\boldsymbol{\nabla}\times\mathbf{E}_G = -\frac{1}{2c}\frac{\partial\mathbf{B}_G}{\partial t} \quad ; \quad \boldsymbol{\nabla}\times\frac{1}{2}\mathbf{B}_G = -\frac{4\pi G}{c}\mathbf{j} + \frac{1}{c}\frac{\partial\mathbf{E}_G}{\partial t} \ , \tag{1.16}$$

where $j^i = \frac{T^{0i}}{c}$. Now, for a non-relativistic particle, we have $dx^0/d\tau \simeq 1$ and $dx^i/d\tau \simeq v^i/c$. At the linear order, the geodesic equation gives:

$$\frac{d^2x^\mu}{d\tau^2} + \Gamma^\mu_{\alpha\beta}\frac{dx^\alpha}{d\tau}\frac{dx^\beta}{d\tau} = 0 \ ; \quad \frac{d\mathbf{v}}{dt} = \mathbf{E}_G + \frac{\mathbf{v}}{c}\times\mathbf{B}_G \ . \tag{1.17}$$

This is the gravitoelectromagnetic analogue of the Lorentz force law.

1.2.4 Plane gravitational waves and polarization

We now consider the plane-wave solutions of (1.10), which is also the homogeneous part of (1.9). The general solution is a superposition of these plane waves:

$$\overline{h}_{\mu\nu} = \mathrm{Re}(\epsilon_{\mu\nu}e^{-ix_\alpha k^\alpha}) \ . \tag{1.18}$$

The matrix $\epsilon_{\mu\nu}$ is symmetric and called polarization tensor. $\overline{h}_{\mu\nu}$ satisfies (1.10) and (1.8). Moreover, we can find a gauge such that

$$\overline{h}^{\alpha}_{\ \alpha} = 0 \ . \tag{1.19}$$

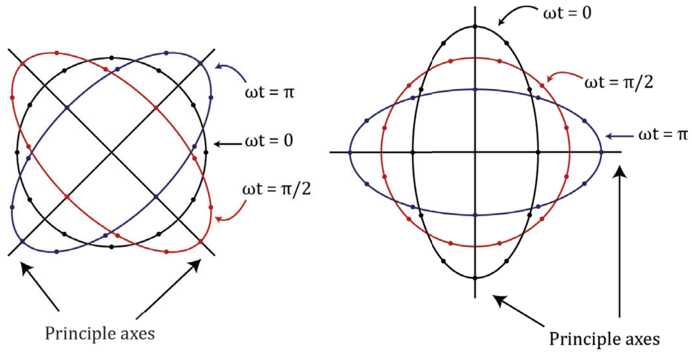

Figure 1.1: Motion of test particles for two linearly polarized states.

This implies the following relations for the wave vector and polarization tensor:

$$k_\alpha k^\alpha = 0 \quad ; \quad k^\alpha \epsilon_{\alpha\beta} = 0 \quad ; \quad \epsilon^\alpha_{\ \alpha} = 0 \ . \tag{1.20}$$

The initially 10 degrees of freedom for $\epsilon_{\mu\nu}$ become 5. The other three can be eliminated using the additional gauge transformations in the class of the harmonic coordinates. To be compatible with (1.8) and (1.19), such a coordinate transformation must satisfy

$$\Box\xi^\alpha = 0 \quad ; \quad \xi^\alpha_{\ ,\alpha} = 0 \quad . \tag{1.21}$$

For this gauge class, we have $\overline{h}_{\mu\nu} = h_{\mu\nu}$. We can choose $\xi^\alpha = \mathrm{Re}(i\varepsilon^\alpha \exp{(ik_\alpha x^\alpha)})$, the polarization tensor in the new coordinates becomes

$$\epsilon'_{\mu\nu} = \epsilon_{\mu\nu} + k_\mu \varepsilon_\nu + k_\nu \varepsilon_\mu \ . \tag{1.22}$$

$\epsilon'_{\mu\nu}$ and $\epsilon_{\mu\nu}$ represent the same physical situation for any value of ε_ν. If we consider a propagation in the $z-$ direction, then $k^\mu = (k, 0, 0, k)$, we can show, combining the different equalities (1.20), that one can choose ε^α such that only ϵ_{12} and $\epsilon_{11} = -\epsilon_{22}$ do not vanish. Thus only two degrees of freedom are left: the two possible polarizations for gravitational waves. Figure 1.1 represents, for two linearly polarized states, the motion of test particles moving about a central particle in the transverse plane. For a complete introduction on gravitational waves, the reader can refer to [152, 74, 138].

Chapter 2

Local Approach to First-Order Solutions

Contents

In [4], the Lagrangian approach to General Relativity was proven to be powerful to extract from the full solution of Einstein equation the part that has the same time dependence as the Newtonian solution. This was done in the frame of perturbation theory. In this part, we will go beyond the gravitoelectric part of the Einstein equations and consider the full set of equations up to first–order. The Cartan formalism, in the frame of the intrinsic Lagrangian approach, will be the appropriate formalism to grasp the major features of the perturbative solutions.

As we will show, the first–order gravitoelectric part of the solution, built from the Newtonian perturbative solution, does not contribute dynamically to the curvature of space sections. Its complementary part will be the one containing the free gravitational waves.

One of the main tasks of this work will be to link the standard approach to our perturbative description. We will show that, when we apply the *MR* on the first-order perturbative solution, we will get back the scalar modes of the standard approach. Nevertheless, the non-integrable first-order coframes we consider live on the perturbed manifold whereas in the standard perturbation theory, they are defined on the background space section. Therefore, the 0^{th} order space, which we will call by convenience background, will not play the same role as the background manifold, on which quantities are defined in standard perturbation theory.

Since our intrinsic approach is on curved space-times, we have to replace the Scalar-Vector-Tensor decomposition considered in the standard perturbation approach, and only available on flat space sections, by a decomposition that takes into account the geometry and topology of space. This will be done in the third chapter of this part.

2.1 Local approach and propagative dynamics

The content of this part is mostly based on the article that will be published by Al Roumi, Buchert and Wiegand. We will focus on the first–order perturbation equations and solutions and try to understand what is the physical content of the complementary part of the first–order solution obtained in [4], which is the relativistic counterpart of the first–order Newtonian solution.

We will show that the complementary part contains the first–order free gravitational waves. Moreover, we will interpret the first–order results in terms of electric and magnetic parts of Weyl tensor, which are solutions of equations that are formally analogue to Maxwell's equations (*cf* Section II.1.4.3). Moreover, we will see that the formalism used in [4] is implicitly local. In the next chapter, we will do assumptions on the topology of spatial sections in order to draw from local results some global conclusions. This local approach will enable us to compare our description to the standard one, since, in the standard perturbation theory, quantities are defined on a flat background. In this frame, Green theory can be used to build global solutions.

In this chapter, we wish first to understand the physical contents of the complementary part of the solution obtained from the Newtonian perturbation scheme. Then, we will show that the local description may hinder a full comprehension of the dynamics of the perturbation fields. To efficiently overcome the limits of the local approach, a global description will have to be considered. This will be the topic of the next chapter.

2.2 First–order perturbation scheme in a local approach

2.2.1 First–order perturbation scheme

The general perturbation scheme in the Intrinsic Lagrangian approach has been presented in Section II.2.1.1 to any order. From now on, we only consider first–order deviations. Thus, the perturbed coframes that we will consider are:

$$\eta^a_{\ i} = a(t)\,(\delta^a_{\ i} + P^a_{\ i}) \ . \tag{2.1}$$

Inserting the ansatz (2.1) into the metric tensor (2.59), we get:

$$g_{ij} = a^2(t)\left(G_{ij} + 2\,P_{(ij)} + P_{ai}P^a_{\ j}\right) \ , \tag{2.2}$$

where we have defined:

$$P_{ij} := G_{ai}P^a_{\ j} \ . \tag{2.3}$$

The aim of the next subsections is to calculate the first–order deviation fields. Note that only the zero–order metric tensor will appear in the linearized equations. Once the first–order deformation solution is computed, we are entitled to insert it into the functional expressions of the other fields, such as the metric tensor above, without truncating to first–order the expansion of the functionals. The initial conditions that we will consider have already been discussed in Section II.2.1.2.

Homogeneous equations

At zero order in the perturbation field, the metric coefficients and their inverse lead to the zero–curvature Friedmannian metric:

$$G^{(0)}_{ij} = \delta_{ij} \ \ ; \ \ g^{(0)}_{ij} = a^2(t)\delta_{ij} \ \ ; \ \ g^{ij(0)} = a^{-2}\delta^{ij} \ . \tag{2.4}$$

We remind the reader that this metric is not the one on which the perturbations propagate, as is assumed in standard perturbation approaches. As a matter of fact, the physical space in which the perturbations propagate is described by the perturbed metric.

The homogeneous (zero–order) equations read:

$$3\frac{\ddot{a}}{a} = \Lambda - 4\pi G\varrho_{H\mathbf{i}}a^{-3} \ ; \tag{2.5}$$

$$3H^2 = 8\pi G\varrho_{H\mathbf{i}}a^{-3} + \Lambda \ , \tag{2.6}$$

with the Hubble function $H := \dot{a}/a$. These equations are the well–known expansion and acceleration laws comprising the (zero–curvature) Friedmann equations. As a consequence of the definition of the orthogonal coframes, the zero–order Christoffel symbols and scalar Ricci curvature are trivially zero:

$$\Gamma^{i\ (0)}_{\ jk} = 0 \quad ; \quad \mathcal{R}^{(0)} = 0 \ . \tag{2.7}$$

2.2.2 First–order equations

In this part, we expand the Lagrange–Einstein system for the Cartan coframes to find the first–order deformation fields. As the coframes are the only dynamical quantity, we have functional definitions of all other variables like the density, the metric or the curvature in terms of their deformation. Recall, that the strategy is then to insert the first–order coframes into these functional definitions without further truncation. So even though in the linearized Lagrange–Einstein system the first–order deformation field only "sees" the first–order contribution from, for example, the curvature, we can write down the full nonlinear contributions to the curvature that are produced by the deformation at first order. In this way we are able to furnish non-perturbative approximations that will improve iteratively by going to higher order deformations.

The deformation coefficients $P^a_{\ i}$ only appear summed over the non-coordinate index in the equations, so we introduce the following tensor coefficients and their trace:

$$P^i_{\ j} \equiv \delta_a^{\ i} P^a_{\ j} \quad \text{and} \quad P \equiv P^k_{\ k} = \delta_k^{\ a} P^a_{\ k} \ , \tag{2.8}$$

and use this notation from now on.

The first–order Lagrange–Einstein equations, in the orthogonal basis, read (we omit the index (1) for the deformation field, but keep it for the Ricci curvature that is inserted according to its definition and expanded for linearizing the equations):

$$\dot{P}_{[ij]} = U_{[ij]} a^{-2} = 0 \ ; \tag{2.9}$$

$$\ddot{P}_{ij} + 3H\dot{P}_{ij} = -a^{-2}\left(\mathcal{R}^{(1)}_{ij} - \frac{\mathcal{R}^{(1)}}{4} a^2 \delta_{ij}\right) \ ; \tag{2.10}$$

$$H\dot{P} + 4\pi G \varrho_{H\mathbf{i}} a^{-3} P = -\frac{\mathcal{R}^{(1)}}{4} - a^{-3} W \ ; \tag{2.11}$$

$$\dot{P}^i_{\ [i|j]} = 0 \ . \tag{2.12}$$

Evaluating the first–order equation of motion (2.10) at initial time, we can express the initial value of the curvature tensor as a function of the chosen initial data set:

$$\mathcal{R}^{(1)}_{ij}(t_\mathbf{i}) =: \mathscr{R}_{ij} = -(W_{ij} + H_\mathbf{i} U_{ij}) - \delta_{ij}(W + H_\mathbf{i} U) \ . \tag{2.13}$$

A more transparent representation of these equations is obtained by introducing the decomposition of the deformation field into its trace, its trace-free symmetric part, and its antisymmetric part:

$$P_{ij} = P_{(ij)} + P_{[ij]} = \frac{1}{3} P \delta_{ij} + \Pi_{ij} + \mathfrak{P}_{ij} \ , \tag{2.14}$$

where we defined $\Pi_{ij} := P_{(ij)} - 1/3\ P\delta_{ij}$, $\mathfrak{P}_{ij} := P_{[ij]}$, and we introduce the trace–free symmetric part of the Ricci tensor, $\tau^{(1)}_{ij} := \mathcal{R}^{(1)}_{ij} - 1/3\ \mathcal{R}^{(1)}\delta_{ij}$. The first–order system for the deformation coefficients now reads:

$$\begin{aligned}
\dot{\mathfrak{P}}_{ij} = U_{[ij]}a^{-2} &= 0 \; ; && (2.15)\\
\ddot{P} + 3H\dot{P} &= -\frac{\mathcal{R}^{(1)}}{4} \; ; && (2.16)\\
\ddot{\Pi}_{ij} + 3H\dot{\Pi}_{ij} &= -a^{-2}\tau^{(1)}_{ij} \; ; && (2.17)\\
H\dot{P} + 4\pi G\varrho_{H\mathbf{i}}a^{-3}P &= -\frac{\mathcal{R}^{(1)}}{4} - a^{-3}W \; ; && (2.18)\\
\frac{1}{3}\dot{P}_{|j} - \frac{1}{2}\left(\dot{\Pi}^{i}{}_{j}\right)_{|i} &= 0 \; . && (2.19)
\end{aligned}$$

In order to solve the first–order trace equation and the traceless symmetric equation, it is necessary to express the first–order scalar curvature and the traceless Ricci tensor ${}^{(1)}\tau_{ij}$. To do so, we insert the metric and its inverse, truncated to first–order:

$$\begin{aligned}
g_{ij} &= a^2\left(\delta_{ij} + G^{(1)}_{ij} + 2P_{(ij)}\right) \; ; && (2.20)\\
g^{ij} &= a^{-2}\left(\delta^{ij} - G^{ij(1)} - 2P^{(ij)}\right) \; , && (2.21)
\end{aligned}$$

into the definitions of the spatial Christoffel symbol and spatial Ricci tensor to obtain:

$$\begin{aligned}
\Gamma^{k}{}_{ij}{}^{(1)} &= \frac{1}{2}\delta^{kl}\left(G^{(1)}_{li|j} + G^{(1)}_{lj|i} - G^{(1)}_{ij|l}\right) + \delta^{kl}\left(P_{(li)|j} + P_{(lj)|i} - P_{(ij)|l}\right) \; ; && (2.22)\\
\mathcal{R}^{(1)}_{ij} &= G^{(1)}_{i[k|j]}{}^{|k} + G^{k(1)}_{[j|k]i} + P_{i[k|j]}{}^{|k} + P_{j[k|i]}{}^{|k} \; ; && (2.23)\\
\mathcal{R}^{(1)} &= 2a^{-2}G^{l(1)}_{[k|l]}{}^{|k} =: \frac{\mathscr{R}}{a^2} \; . && (2.24)
\end{aligned}$$

Using the split into parts with different symmetries, we express the curvature through the parts P, Π_{ij} and $\mathfrak{P}_{ij}$. The momentum constraints allow to rewrite some terms in the curvature to obtain:

$$\begin{aligned}
\mathcal{R}^{(1)}_{ij} &= \mathscr{R}_{ij} + P_{|ij} - \frac{1}{3}P^{|k}{}_{|k}\delta_{ij} - \Pi_{ij}{}^{|k}{}_{|k} \; ; && (2.25)\\
\mathcal{R}^{(1)} &= a^{-2}\mathscr{R} \; . && (2.26)
\end{aligned}$$

We can now write the first–order traceless part of the Ricci curvature tensor as:

$$\tau^{(1)}_{ij} = \mathscr{T}_{ij} + P_{|ij} - \frac{1}{3}P^{|k}{}_{|k}\delta_{ij} - \Pi_{ij}{}^{|k}{}_{|k} \; , \qquad (2.27)$$

where we defined $\mathscr{T}_{ij} := \tau_{ij}(t_i) := \mathscr{R}_{ij} - 1/3\;\mathscr{R}\delta_{ij}$.

Now that we have the first–order scalar curvature and the traceless Ricci tensor, we can insert them into the first–order system for the deformation coefficients (2.15)–(2.19). We also perform the time–integration of the antisymmetric part and the momentum constraints, and now make use of the constraints on initial data (2.20):

$$
\begin{aligned}
\mathfrak{P}_{ij} = \mathfrak{P}_{ij}(t_{\mathbf{i}}) \ , \ \mathfrak{P}_{ij}(t_{\mathbf{i}}) &= 0 \ ; && (2.28)\\
\ddot{P} + 3H\dot{P} &= -\frac{a^{-2}\mathscr{R}}{4} \ ; && (2.29)\\
\ddot{\Pi}_{ij} + 3H\dot{\Pi}_{ij} - a^{-2}\Pi_{ij}{}^{|k}{}_{|k} &= -a^{-2}\left(\mathscr{T}_{ij} + P_{|ij} - \frac{1}{3}P^{|k}{}_{|k}\delta_{ij}\right) \ ; && (2.30)\\
H\dot{P} + 4\pi G\varrho_{Hi}a^{-3}P &= -\frac{a^{-2}\mathscr{R}}{4} - a^{-3}W \ ; && (2.31)\\
\frac{2}{3}P_{|j} &= \Pi^{k}{}_{j|k} \ . && (2.32)
\end{aligned}
$$

Note that there is no constant of integration appearing in Eq. (2.32), because we chose our initial data in (2.20) such that for $i = 1, 2, 3$, $\mathscr{P}^{a}{}_{i} = 0$. Further manipulations of this system of equations will aim at formally separating the gravitational wave tensor part from the scalar perturbations. As will be explained later, a part of the symmetric traceless deformation field is separable and has the same time dependence as the trace. We would like to isolate the dynamics of this part and show that its complementary part encodes the propagation of gravitational waves.

2.2.3 First–order master equations

We here aim at equations for the trace and symmetric traceless parts (the equation for the antisymmetric part is trivial) by combining the evolution and constraint equations, and hence by eliminating the curvature. This latter will play an important role by executing the *MR* . The result is a set of equations that allow to build solutions, we call them 'master equations'.

For the trace part we insert the Hamilton constraint (2.31) into the evolution equation (2.29) to obtain Raychauhuri's equation, which is the master equation for the trace solution:

$$
\ddot{P} + 2H\dot{P} - 4\pi G\varrho_{Hi}a^{-3}P = a^{-3}W \ . \tag{2.33}
$$

For an Einstein-de Sitter universe the modes are proportional to a, $a^{-3/2}$ and a^{0}. We obtain:

$$
P = \frac{3}{5}\left[(Ut_{\mathbf{i}} + \frac{3}{2}W{t_{\mathbf{i}}}^{2})a - \left(Ut_{\mathbf{i}} - W{t_{\mathbf{i}}}^{2}\right)a^{-\frac{3}{2}} - \frac{5}{2}W{t_{\mathbf{i}}}^{2}\right] . \tag{2.34}
$$

In the same spirit, we combine the momentum constraint (2.32) with the traceless part of the evolution equation (2.30) and replace the initial traceless curvature in favor of the initial data set, using (2.13), to obtain the following master equation:

$$
\ddot{\Pi}_{ij} + 3H\ \dot{\Pi}_{ij} - a^{-2}\left(W^{tl}_{ij} + H_{\mathbf{i}}U^{tl}_{ij}\right) = a^{-2}\left(\Pi_{ij}{}^{|k}{}_{|k} + \frac{1}{2}\delta_{ij}\ \Pi^{k}{}_{l|k}{}^{|l} - \frac{3}{2}\ \Pi^{k}{}_{j|ki}\right) \ . \tag{2.35}
$$

Splitting of the solution into ${}^E\Pi_{ij}$ and ${}^H\Pi_{ij}$

The idea is now to split the traceless part further into a component ${}^E\Pi_{ij}$ that couples to the trace part and a component ${}^H\Pi_{ij}$ that decouples from it. As was done in [4], ${}^E\Pi_{ij}$ can be built from a generalization of the Newtonian trace solution. Such a traceless solution will be separable and have the same time dependence as P. We will show that this solution built from the generalization of the Newtonian one contains the integrable part of the deformation fields. (Note that such a decoupling goes back to Einstein's Zurich notebook when he searched for gravitational wave solutions, and it is used in the standard perturbation theory in terms of the so–called SVT (Scalar–Vector–Tensor) decomposition, to which we come later.) It turns out that such a split is linked to the gravitoelectric and gravitomagnetic parts (hence our notation E and H). Indeed, we will show that ${}^E\Pi_{ij}$ generates a harmonic magnetic part of the Weyl tensor. The coupling of ${}^E\Pi_{ij}$ to the trace P can equivalently be done by considering that ${}^H\Pi^k{}_{j|k}$ is the divergence-free part. Then, the momentum constraints (2.32):

$$\frac{2}{3}P_{|j} = \Pi^k{}_{j|k} =: \left({}^E\Pi^k{}_{j|k} + {}^H\Pi^k{}_{j|k}\right) \ , \tag{2.36}$$

can be divided into two separate constraints:

$$\frac{2}{3}P_{|j} = {}^E\Pi^k{}_{j|k} \ \text{ with the definition } \ {}^H\Pi^k{}_{j|k} := 0 \ . \tag{2.37}$$

Note that, as we did for Π_{ij}, we can split the initial fields accordingly:

$$U_{ij} =: {}^E U_{ij} +^H U_{ij} \ ; \ W_{ij} =: {}^E W_{ij} +^H W_{ij} \ , \tag{2.38}$$

and hence the initial curvature:

$$W^{tl}_{ij} + H_{\mathbf{i}} U^{tl}_{ij} =: \left({}^E W^{tl}_{ij} + H_{\mathbf{i}}{}^E U^{tl}_{ij}\right) + \left({}^H W^{tl}_{ij} + H_{\mathbf{i}}{}^H U^{tl}_{ij}\right) \ , \tag{2.39}$$

where ^{tl} refers to the traceless part of the initial tensor fields. This split can be carried through to the master equation (2.35). Inserting the superposition $\Pi_{ij} = {}^E\Pi_{ij} + {}^H\Pi_{ij}$, we first extract the divergence-free part (note that the traceless initial data are not sources of the divergence-free part), which obeys the equation:

$${}^H\ddot{\Pi}_{ij} + 3H{}^H\dot{\Pi}_{ij} - a^{-2}\ {}^H\Pi_{ij}{}^{|k}{}_{|k} = a^{-2}\left({}^H W^{tl}_{ij} + H_{\mathbf{i}}{}^H U^{tl}_{ij}\right) \ , \tag{2.40}$$

Thus, the equation governing ${}^H\Pi_{ij}$ describes the propagation of gravitational waves and has the form of the d'Alembert equation with a damping term due to expansion (note that this equation assumes this form in local (Lagrangian) coordinates). The r.h.s. comes from the fact that this propagation occurs in a curved space-time.

We assumed that ${}^E\Pi_{ij}$ was built from a generalization of the Newtonian trace solution and thus had the same time dependence as P. It thus has the following expression:

$${}^E\Pi_{ij} = \frac{3a}{5}\left({}^E U^{tl}_{ij} t_{\mathbf{i}} + \frac{3}{2}{}^E W^{tl}_{ij} t_{\mathbf{i}}{}^2\right) - \frac{3}{5a^{3/2}}\left({}^E U^{tl}_{ij} t_{\mathbf{i}} - {}^E W^{tl}_{ij} t_{\mathbf{i}}{}^2\right) - \frac{3}{2}{}^E W^{tl}_{ij} t_{\mathbf{i}}{}^2 \ . \tag{2.41}$$

Plugging this expression into (2.35) and having all the different modes appearing in the equation cancel, we obtain the following conditions on the ^{E} part of the initial fields:

$$ {}^{E}U^{|k}_{ij\ |k} = U^{k}_{\ k|ij} \quad ; \quad {}^{E}W^{|k}_{ij\ |k} = W^{k}_{\ k|ij} \ . \tag{2.42} $$

These conditions are equivalent to demanding the equality:

$$ \Delta_{\mathbf{0}}{}^{E}\Pi_{ij} = \mathcal{D}_{ij}P \ , \tag{2.43} $$

Where $\Delta_{\mathbf{0}}$ is the Laplace operator for Lagrangian coordinates and $\mathcal{D}_{ij} = \partial_i\partial_j - \delta_{ij}\Delta_{\mathbf{0}}/3$. ${}^{E}\Pi_{ij}$ is now solution of

$$ {}^{E}\ddot{\Pi}_{ij} + 3H\ {}^{E}\dot{\Pi}_{ij} = a^{-2}\left({}^{E}W^{tl}_{ij} + H_{\mathbf{i}}{}^{E}U^{tl}_{ij}\right) \ . \tag{2.44} $$

Contributions of ${}^{E}\Pi_{ij}$ and ${}^{H}\Pi_{ij}$ to the Ricci curvature

If we insert the relation (2.43) into the equation that gives the first-order curvature (2.26), we see that ${}^{E}\Pi_{ij}$ compensates the curvature produced by the trace part of the perturbations in the dynamical part of the Ricci curvature. The only term that affects the dynamical part of the curvature is $\Delta_0{}^{H}\Pi_{ij}$. We conclude that ${}^{E}P_{ij}$ does not produce curvature. Nevertheless, we cannot conclude from this feature that it represents only the integrable part of the perturbation fields.

2.3 Electric and magnetic spatial parts of the Weyl tensor and the Maxwell-Weyl equations

2.3.1 Link to the electric and magnetic part of Weyl tensor

Gravitomagnetic part from ${}^{E}P_{ij}$

When we split P_{ij} into ${}^{E}P_{ij}$ and ${}^{H}\Pi_{ij}$, we obtained ${}^{E}P_{ij}$ from the generalization of the Newtonian solution. We therefore did not encode any propagative dynamics into it. Since the magnetic part of Weyl tensor is linked to gravitational waves, we expect ${}^{E}P_{ij}$ to generate a zero magnetic part. As shown in [4], all we can say is:

$$ \Delta_0 H_{ij}({}^{E}P_{ij}) = 0 \ , \tag{2.45} $$

which is again an elliptic equation that needs some global arguments to be solved.

Magnetic part of the Weyl tensor and deviations from flatness

As discussed in the definition of the Minkowski Restriction, if the coframes become integrable, the resulting metric becomes Euclidean. They then form an exact coordinate basis. Coframes, or equivalently frames, will encode deviations from flatness if their structure coefficients are non-zero. They are defined from the frames in the following way:

$$ [\mathbf{e}_a, \mathbf{e}_b] = C^{c}_{\ ab}\mathbf{e}_c \ , \tag{2.46} $$

and from the coframes in this way:

$$\mathbf{d}\,\boldsymbol{\eta}^a = -\frac{1}{2} C^a_{\ \ bc}\,\boldsymbol{\eta}^b \wedge \boldsymbol{\eta}^c \ . \tag{2.47}$$

The magnetic part and the structure coefficients are linked at first–order by the following relation:

$$H^i_{\ j} = \frac{1}{2} \epsilon_j^{\ kl} \dot{C}^i_{\ lk} \ . \tag{2.48}$$

The magnetic part thus contains the dynamical deviations from flatness.

2.4 Integrable and non-integrable solutions: comparison with the other perturbation schemes

In this section, we split the first–order deformation fields into an integrable and a non-integrable part. We show that when we execute the *MR* , we end up with the scalar solutions of the standard perturbation theory. Moreover, the trace part falls on the first scalar mode and the traceless part falls on the second scalar mode. The non-integrable mode is then by construction zero. In a second part, we will compare our results to the ones obtained in the comoving synchronous gauge.

2.4.1 Non–propagating solutions for the intrinsic Lagrangian description

Integrable and non-integrable initial conditions

We split the initial fields into their integrable and non-integrable parts:

$$U_{ij} = S_{|ij} + \tilde{U}_{ij} \ \text{ and } \ W_{ij} = -\phi_{|ij} + \tilde{W}_{ij} \ , \tag{2.49}$$

where S is the peculiar–velocity potential, and where ϕ is the peculiar–gravitational potential, which, on a flat space-time, is solution of $\Delta\phi = 4\pi G \delta\rho_{H_\mathbf{i}}$. Moreover, we split the deformation fields into an integrable and a non-integrable part:

$$P_{ij} = \Psi_{|ij} + \tilde{P}_{ij} \ . \tag{2.50}$$

In the next subsection, we determine their time-dependence.

Non–propagating separable modes

We assume that Ψ satisfies the equation

$$\Delta_\mathbf{0}\Psi = P \ , \tag{2.51}$$

i.e. that the non-integrable part of the solution (2.50) has no trace. In the Minkowski Restriction, since we have to recover the Newtonian solution, Ψ is separable:

$$\Psi(\mathbf{X}, t) = {}^\Psi C^1(\mathbf{X})\ \xi^1(t) + {}^\Psi C^2(\mathbf{X})\ \xi^2(t) + {}^\Psi C^0(\mathbf{X}) \ , \tag{2.52}$$

Einstein–de Sitter background

The trace solution is straightforward according to its formal equivalence with Newtonian solutions. Specifying an Einstein–de Sitter background we obtain:

$$\Psi(\mathbf{X},t) = {}^{\Psi}C^{-1}(\mathbf{X}) \left(\frac{t}{t_i}\right)^{-1} + {}^{\Psi}C^{2/3}(\mathbf{X}) \left(\frac{t}{t_i}\right)^{2/3} + {}^{\Psi}C^{0}(\mathbf{X}) \ , \tag{2.53}$$

where the coefficient functions are related to the chosen initial data as follows:

$$\begin{aligned} {}^{\Psi}C^{-1}(\mathbf{X}) &= -\frac{3}{5}(St_{\mathbf{i}} + \phi\, t_{\mathbf{i}}{}^2) \ ; \\ {}^{\Psi}C^{2/3}(\mathbf{X}) &= \frac{3}{5}St_{\mathbf{i}} - \frac{9}{10}\phi\, t_{\mathbf{i}}{}^2 \ ; \\ {}^{\Psi}C^{0}(\mathbf{X}) &= \frac{\phi}{4\pi G\rho_{H_{\mathbf{i}}}} \ . \end{aligned} \tag{2.54}$$

2.4.2 Propagative behavior of the non–integrable part

Particular solution for the non–integrable part

We now focus on $\tilde{\Pi}_{ij}$, which contains the non–integrable dynamics. As we will see, $\tilde{\Pi}_{ij}$ can be split into a time–independent part, which encodes the time–independent deviations to flatness and a part representing free gravitational waves. The time–independent part is the particular solution of (2.40), which satisfies the equation:

$$\Delta_{\mathbf{0}}\tilde{\Pi}^{pec}_{ij}(\mathbf{X}) = -\left(\tilde{W}^{tl}_{ij} + H_{\mathbf{i}}{}^{H}\tilde{U}^{tl}_{ij}\right) \ . \tag{2.55}$$

If we split the initial metric also into an integrable and a non-integrable part:

$$G_{ij}(\mathbf{X}) = \underline{G}_{|ij}(\mathbf{X}) + \tilde{G}_{ij}(\mathbf{X}) \ , \tag{2.56}$$

where $\tilde{G}_{ij}$ is the non–integrable part of G_{ij}, then

$$\tilde{\Pi}^{pec}_{ij}(\mathbf{X}) = -\frac{\tilde{G}^{tl}_{ij}}{2} \ . \tag{2.57}$$

This remark will make sense when we will come to the comparison with the literature.

Monochromatic solution

We first solve the homogeneous equation for $\tilde{\Pi}_{ij}$ by looking for a monochromatic (separable) solution, with frequency ω and local (Lagrangian) wave–vector $\mathbf{K}$ such that $|\mathbf{K}| =: K = \omega/c$ (where c is the speed of light),

$$\tilde{\Pi}^{\omega}{}_{ij} = \xi^{\omega}(t)\ \tilde{C}^{K}_{ij}(\mathbf{X}) \ . \tag{2.58}$$

For these local components, propagating in fibers at given points of the manifold (tangent spaces), we have two solutions of the master equation (2.40):

$$a^2\ \ddot{\xi}^{\omega\pm}(t) + 3\dot{a}a\ \dot{\xi}^{\omega\pm}(t) + \omega^2\ \xi^{\omega\pm}(t) = 0 \ . \tag{2.59}$$

We choose the plane wave basis (in the local fiber vector space) to express $\tilde{C}^K_{ij}(\mathbf{X})$:

$$\tilde{C}^K_{ij}(\mathbf{X}) = \tilde{C}^{K+}_{ij} \ \exp(i\mathbf{K}\cdot\mathbf{X}) + \tilde{C}^{K-}_{ij} \ \exp(-i\mathbf{K}\cdot\mathbf{X}) \ , \tag{2.60}$$

so that the coefficient functions obey the spatial constraints:

$$\Delta_{\mathbf{0}}\tilde{C}^K_{ij}(\mathbf{X}) + K^2 \ \tilde{C}^K_{ij}(\mathbf{X}) = 0 \ . \tag{2.61}$$

The momentum constraints, (2.37), for these modes imply:

$$\tilde{C}^{K\pm}_{ij} K^i = 0 \ , \tag{2.62}$$

which means that the projection of the propagating deviations on the direction of propagation represented by $\mathbf{K}$ is zero. This monochromatic solution has been built from a local reasoning. To build a global solution from a superposition of these modes, we will have to take into account both the local geometry and the global topology.

Minkowski Restriction and conclusions

For the set of separable solutions that we were giving in the last subsection, the *MR* only acts on the spatial coefficient functions, which become integrable tensor fields. We will explicitly show this in the following.

The *MR* assumes the integrability of the integrable coframes, which, combined with the absence of vorticity, imply that the perturbation fields can be derived from a potential Ψ:

$$P_{ij} = \Psi_{|ij} \ . \tag{2.63}$$

The trace and the traceless parts are then:

$$P = \Delta\Psi \quad \text{and} \quad \Pi_{ij} = \mathcal{D}_{ij}\Psi \ . \tag{2.64}$$

There are no longer gravitational waves since the non-integrable part is set to zero:

$$\tilde{\Pi}_{ij} = 0 \ . \tag{2.65}$$

We can thus conclude that in the *MR* , ${}^E P_{ij} = \Psi_{|ij}$ and ${}^H\Pi_{ij} = 0$. Nevertheless, we cannot conclude that, without the *MR* , ${}^E P_{ij}$ contains only the integrable part of the perturbation fields. This will be discussed in the next chapter.

2.4.3 Comparison to other perturbation schemes

In this part, we wish to highlight the links between our approach and the standard one, that uses the Scalar-Vector-Tensor decomposition for the perturbed metric in the comoving synchronous gauge.

S–V–T decomposition in the comoving synchronous gauge

In most of the literature, the perturbative approach directly works with the metric instead of using a decomposition into coframes. The synchronous metric may be decomposed as

$$ds^2 = -dt^2 + a^2(t)\gamma_{ij}(\mathbf{x},t)dx^i dx^j \; . \tag{2.66}$$

The first order corrections to a flat FLRW background are then

$$\gamma_{ij} = \delta_{ij} + \gamma^{(1)}_{\mathrm{S}ij} \; . \tag{2.67}$$

In the usual framework as used in [107], it is more common to split it into scalar vector and tensor contributions

$$\gamma^{(1)}_{\mathrm{S}ij} = -2\phi^{(1)}_{\mathrm{S}}\delta_{ij} + \mathcal{D}_{ij}\chi^{(1)\parallel}_{\mathrm{S}} + \partial_i\chi^{(1)\perp}_{\mathrm{S}j} + \partial_j\chi^{(1)\perp}_{\mathrm{S}i} + \chi^{(1)\top}_{ij} \; , \tag{2.68}$$

with the traceless derivative $\mathcal{D}_{ij} = \partial_i\partial_j - \frac{1}{3}\Delta\delta_{ij}$ and

$$\partial^i\chi^{(1)\perp}_{\mathrm{S}i} = \chi^{(1)\top i}_{\;\;i} = \partial^i\chi^{(1)\top}_{ij} = 0 \; . \tag{2.69}$$

In general there could be vector modes in the standard perturbation decomposition on the r.h.s. of (2.68) as well. However, in the irrotational case they represent gauge modes and can be set to zero [107]. In our case, we have a local coordinate system (in the tangent space at a point in the Riemannian manifold) in which there exist no vector fields. Correspondingly however, there is an antisymmetric tensor part, which also vanishes for the irrotational case. So we only need the synchronous gauge expressions for $\phi^{(1)}_{\mathrm{S}}$, $\mathcal{D}_{ij}\chi^{(1)\parallel}_{\mathrm{S}}$ and $\chi^{(1)\top}_{ij}$ as given in [107].

Let us start with the tensor part. It satisfies the equation

$$\ddot{\chi}^{(1)\top}_{ij} + 3H\dot{\chi}^{(1)\top}_{ij} - \frac{\nabla^2}{a^2}\chi^{(1)\top}_{ij} = 0 \; , \tag{2.70}$$

which corresponds to our equation (2.40) when we would subtract the contribution $\mathcal{D}_{ij}\chi^{(1)\parallel}_{\mathrm{S}}$. The solution in [107] is

$$\chi^{\top(1)}_{ij}(\mathbf{x},t) = \frac{1}{(2\pi)^3}\int d^3\mathbf{k}\,\exp(i\mathbf{k}\cdot\mathbf{x})\chi^{(1)}_{\sigma}(\mathbf{k},t)\epsilon^{\sigma}_{ij}(\hat{\mathbf{k}}), \tag{2.71}$$

where $\epsilon^{\sigma}_{ij}(\hat{\mathbf{k}})$ is the polarization tensor. σ is ranging over the polarization components $+, \times$ and $\chi^{(1)}_{\sigma}(\mathbf{k},t)$ are their corresponding amplitudes. The time evolution from (2.70) is

$$\chi^{(1)}_{\sigma}(\mathbf{k},t) = A(k)a_{\sigma}(\mathbf{k})\left(\frac{3j_1\left(3kt_i^{2/3}t^{1/3}\right)}{3kt_i^{2/3}t^{1/3}}\right) \; . \tag{2.72}$$

The first spherical Bessel function is $j_1\left(x\right) = \frac{\sin x}{x^2} - \frac{\cos x}{x}$ and $a_{\sigma}(\mathbf{k})$ is a zero mean random variable. $A(k)$ encodes the form of the spectrum of hypothetical primordial gravitational waves.

Second, we turn to the scalar sector. The solutions given in [107] are restricted to the growing mode only. In addition, the authors use the residual gauge freedom of synchronous gauge to fix $\chi_i^{(1)\parallel}$ such that $\nabla^2\chi_{\mathrm{S}i}^{(1)\parallel} = -2\delta_i$. Then, their solutions for the scalar sector are

$$\mathcal{D}_{ij}\chi_{\mathrm{S}}^{(1)\parallel} = -3t_i^2\left(\frac{t}{t_i}\right)^{\frac{2}{3}}\left(\varphi_{,ij} - \frac{1}{3}\delta_{ij}\nabla^2\varphi\right) . \tag{2.73}$$

and

$$\phi_{\mathrm{S}}^{(1)}(\mathbf{x},t) = \frac{5}{3}\varphi(\mathbf{x}) + \frac{1}{2}t_i^2\left(\frac{t}{t_i}\right)^{\frac{2}{3}}\nabla^2\varphi(\mathbf{x}) \ , \tag{2.74}$$

where φ is defined by its relation to δ_i in the cosmological Poisson equation $\nabla^2\varphi(\mathbf{x}) = \frac{2}{3t_i^2}\delta_i(\mathbf{x})$.

Relating formally the two descriptions

In our case, P_{ij} as well as the initial metric $G_{ij}^{(1)}$ appear in the decomposition of the metric perturbation:

$$\gamma_{\mathrm{S}ij}^{(1)} = G_{ij}^{(1)} + 2P_{(ij)} \ . \tag{2.75}$$

The general relation between the two sets of perturbation fields is then

$$\phi_{\mathrm{S}}^{(1)} \ \leftrightarrow \ -\frac{1}{3}\left(P + \frac{1}{2}G^{(1)}\right) \ , \tag{2.76}$$

$$\left(\Pi_{ij} + \frac{1}{2}G_{ij}^{(1)tl}\right) \ \leftrightarrow \ \frac{1}{2}\left(\mathcal{D}_{ij}\chi_{\mathrm{S}}^{(1)\parallel} + 2\partial_{(i}\chi_{\mathrm{S}j)}^{(1)\perp} + \chi_{ij}^{(1)\top}\right) \ . \tag{2.77}$$

In order to compare the standard results to ours, we modify the restrictions imposed in [107]. First, we use a different gauge choice, which is $\nabla^2\chi_{\mathrm{S}i}^{(1)\parallel} = 0$ instead of $\nabla^2\chi_{\mathrm{S}i}^{(1)\parallel} = -2\delta_i$. Second, we include the decaying mode. Then, the potential is no longer independent of time and $\nabla^2\varphi(\mathbf{x},t) = \frac{2}{3t_i^2 a}\delta(\mathbf{x},t)$. Therefore, φ now has two components φ_1 and φ_2 that are determined by $\nabla^2\varphi_1(\mathbf{x}) + a^{-5/3}\nabla^2\varphi_2(\mathbf{x}) = \frac{6}{\tau_0^2 a}\delta(\mathbf{x},t)$. Finally, we include the prefactor on the r.h.s. into the definition of a renormalized potential $\psi(\mathbf{x},t) = \psi_1(\mathbf{x}) + a^{-5/3}\psi_2(\mathbf{x})$ which then satisfies $\nabla^2\psi_1(\mathbf{x}) + a^{-5/3}\nabla^2\psi_2(\mathbf{x}) = -\delta(\mathbf{x},t)$.

With these changes the resulting metric perturbations read

$$\mathcal{D}_{ij}\chi_{\mathrm{S}}^{(1)\parallel} = 2\left(\left(\frac{t}{t_i}\right)^{\frac{2}{3}} - 1\right)\mathcal{D}_{ij}\psi_1 + 2\left(\frac{1}{\left(\frac{t}{t_i}\right)} - 1\right)\mathcal{D}_{ij}\psi_2 \ , \tag{2.78}$$

and

$$\phi_{\mathrm{S}}^{(1)}(\mathbf{x},t) \ = \ -\frac{10}{9t_i^2}\psi_1(\mathbf{x}) - \frac{1}{3}\left(\left(\frac{t}{t_i}\right)^{\frac{2}{3}} - 1\right)\Delta\psi_1 - \frac{1}{3}\left(\frac{1}{\left(\frac{t}{t_i}\right)} - 1\right)\Delta\psi_2 \ . \tag{2.79}$$

This means that first order perturbation theory in synchronous gauge gives the solutions

$$G^{(1)} \ \leftrightarrow \ \frac{20}{3t_i^2}\psi_1(\mathbf{x}) \ , \tag{2.80}$$

$$P \ \leftrightarrow \ \left(\left(\frac{t}{t_i}\right)^{\frac{2}{3}} - 1\right)\Delta\psi_1(\mathbf{x}) + \left(\left(\frac{t}{t_i}\right)^{-1} - 1\right)\Delta\psi_2(\mathbf{x}) \ , \tag{2.81}$$

and

$$G_{ij}^{(1)tl} \leftrightarrow \chi_{ij}^{\top(1)}(\mathbf{x}, t_i) \ , \tag{2.82}$$

$$\Pi_{ij} \leftrightarrow \left(\left(\frac{t}{t_i}\right)^{\frac{2}{3}} - 1\right)\mathcal{D}_{ij}\psi_1(\mathbf{x}) + \left(\left(\frac{t}{t_i}\right)^{-1} - 1\right)\mathcal{D}_{ij}\psi_2(\mathbf{x}) \tag{2.83}$$

$$+\frac{1}{2}\left(\chi_{ij}^{\top(1)}(\mathbf{x}, t) - \chi_{ij}^{\top(1)}(\mathbf{x}, t_i)\right) \ . \tag{2.84}$$

Identification of the integrable and the non-integrable part

From the last four identities, it is possible to show that the standard counterpart of ${}^E\Pi_{ij}$ is

$$\mathcal{D}_{ij}\Psi \leftrightarrow \left(\left(\frac{t}{t_i}\right)^{\frac{2}{3}} - 1\right)\mathcal{D}_{ij}\psi_1 + \left(\left(\frac{t}{t_i}\right)^{-1} - 1\right)\mathcal{D}_{ij}\psi_2 \ , \tag{2.85}$$

and for $\tilde{\Pi}_{ij}$ it is:

$$\tilde{\Pi}_{ij}^{pec} \leftrightarrow -\frac{\chi_{ij}^{\top(1)}(t_i)}{2} \ , \tag{2.86}$$

and

$$\tilde{\Pi}_{ij}^{GW} \leftrightarrow \frac{\chi_{ij}^{\top(1)}}{2} \ . \tag{2.87}$$

We here have established some formal analogies between the solutions obtained in the standard comoving synchronous approach and the ones obtained in our intrinsic approach. Even if they look very similar, some important differences exist between the intrinsic Lagrangian description and the standard comoving synchronous approach. The standard approach defines quantities on the background manifold while the tangent spaces associated to the background manifold are the same at each point.

This is not the case for the quantities we defined in the intrinsic description. Unlike the standard approach, they are functions of the Lagrangian coordinates, which have the time-feature to be transported along the fluid trajectories. They are thus defined on the perturbed manifold since Lagrangian coordinates have a basis that may be different from one point to the other on the manifold. Indeed, fluid trajectories intrinsically encode the perturbed dynamics of the fluid particles. The comoving coordinates used in the standard approach do not exhibit this non-linear feature. The transformation from the Lagrangian coordinates to the standard comoving coordinates involves non-linearities. It will be done in the upcoming article.

2.5 Conclusions and limits of the local description

In this chapter, we presented the first-order equations and solutions of the Einstein equations. The traceless part of the perturbation fields has been decomposed into $\Pi_{ij} = {}^E\Pi_{ij} + {}^H\Pi_{ij}$, where ${}^E\Pi_{ij}$ is coupled to the trace, P, via the momentum constraint equation. This is consistent with the fact that ${}^E P_{ij} = {}^E\Pi_{ij} + \frac{\delta_{ij}}{3}P$ coincides with the gravitoelectric solution obtained from the generalization of the Newtonian solution (*cf* Chapter II.2 of Part II). We have built the complementary part, ${}^{H}\Pi_{ij}$, such that it is not coupled to the trace. This part contains gravitational waves.

We have also discussed the fact that ${}^{E}P_{ij}$ does not contribute to the dynamical part of the curvature whereas ${}^{H}\Pi_{ij}$ does. Furthermore, we know that ${}^{E}P_{ij}$ encodes the integrable part of the solution. Nevertheless, in order to fully determine ${}^{E}P_{ij}$, some elliptic equations have to be solved (2.42) (2.45). In order to do so, we have to consider the topology of the spatial sections. This will be the aim of next chapter.

Chapter 3

Topology and Hodge Decomposition: a Global Approach to First-order Solutions

Contents

In last chapter III.2, we determined the first–order equations and solutions of the Einstein equations in a local approach. We considered the projection of the equations on a local coordinate basis $\{\mathbf{d}X^i\}$, thus constraining the validity of the results to the regions of the manifold that can be covered by a single coordinate chart.

This local approach did not enable us to completely determine the physical contents of ${}^E P_{ij}$ and ${}^H \Pi_{ij}$. In order to do so, some elliptic equations have to be solved (2.42) (2.45). The perturbation fields being defined on the perturbed spatial sections, only topological considerations can help us determine the boundary conditions to solve these equations.

In Section III.2.2.3, we decomposed the perturbation of the coframe into an integrable part and its complementary. We then concluded that the integrable part had to be encoded into ${}^E P_{ij}$. Nevertheless, considering closed topologies will allow us to use the powerful Hodge decomposition on Cartan coframes and have a new insight into the physics of the first-order perturbations. More precisely, it should help us determine, on the one hand, if the generalization of the Newtonian perturbation solution represents the integrable part of the perturbation fields or if it also encodes deviations from flatness. On the other hand, we will then be able to determine if the complementary part to this Newton-like solution is linked to gravitational waves.

New research results [72, 126, 114] support the closed $\mathbb{S}^3$ and quotient topologies for spatial hypersurfaces. The coframes then exhibit the interesting property to be defined globally (*cf* Section III.3.1.1). Nonetheless, at least two coordinate charts will be needed to cover this manifold (*cf* Section I.2.3.1).

In this chapter, we will first present historically how the topology of the Universe became a subject of interest for cosmologists. Topology can have indeed a strong impact on the dynamics of the Universe and on the interpretation of the observations (*cf* Section III.3.1.2). Then, we will explain why including topology to our approach will allow us to bypass the limits of the local formalism. The Hodge theorem will enable us to draw strong conclusions on the physical content of the first-order solution.

3.1 Introduction to the topology of the Cosmos

3.1.1 Why are we interested in topology?

The topological properties of a manifold are the ones that are unchanged by continuous transformations. Topology does not constrain the size or the distance: any stretching or squeezing will leave unchanged the topology. On the contrary, cutting or making holes in the manifold will affect its topology. According to these considerations, the surface of a coffee mug with a handle is topologically the same as the surface of the donut. This type of surface is called a torus.

The topology of the Universe has been ignored by cosmologists until recently. During the last decade many attempts were indeed made to determine the global shape of the Universe, i.e. geometry and topology of the its spatial comoving sections.

An aspect of topology which was neglected until recently is its impact on the dynamics of space-time. This was discussed for multiconnected space sections [127, 114], as we will explain later in this section.

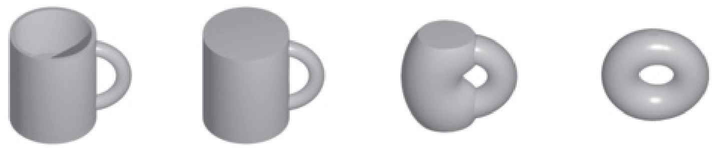

Figure 3.1: A coffee cup is topologically equivalent to a torus. The illustration has been taken from https://commons.wikimedia.org/wiki/File:Mug_and_Torus_morph.gif, credits: Lukas VB.

The coframes, that we adopted to describe the dynamics of space-time, are intimately linked to the topology of spatial sections. To illustrate this aspect, we consider the circle, $\mathbb{S}^1$, the 1-dimensional sphere. No coordinate chart can be defined globally on the whole manifold since the periodicity of $\mathbb{S}^1$ implies a coordinate singularity at an arbitrary point. Nevertheless, it is possible to build a smooth tangent vector field globally on the circle [1]. For n-dimensional manifolds, this property is called parallelizability. Indeed, a manifold $\mathcal{M}$ is parallelizable if we can build smooth vector fields $\{\mathbf{e}_1, ..., \mathbf{e}_n\}$ such that for any point P of the manifold, $\{\mathbf{e}_1(P), ..., \mathbf{e}_n(P)\}$ provides a basis of the tangent space at P. In three dimensions, we can choose the smooth vector fields to coincide with the frames. Thus, their dual, the Cartan coframes, are defined globally on a parallelizable manifold.

$\mathbb{S}^0$, $\mathbb{S}^1$, $\mathbb{S}^3$ and $\mathbb{S}^7$ are parallelizable. Furthermore, in 3-dimensions, all the orientable manifolds are parallelizable [143]. In the next sections, we will mostly focus on the topology of the 3-dimensionnal spatial sections [2]. Furthermore, we will discuss how some important properties of the coframes can be strongly constrained by the spatial topology in the case of $\mathbb{S}^3$ and its quotients.

3.1.2 Cosmic topology: from Einstein to recent times

The reader can find more material on the historical development of cosmic topology in [101], from which many of the following elements are taken.

Einstein's theory of General Relativity does not deal with topology but rather with the local geometrical properties of the Universe, such as its curvature, that can be calculated from the metric tensor. Indeed, Einstein's field equations are partial derivative equations that describe only local geometrical properties. As a consequence, if we consider a metric solution of Einstein equations, several and sometimes an infinite number of manifolds with distinct topologies of the Universe can be compatible with it.

For example, the projective space $\mathbf{P}^3$, which is obtained from the 3-dimensional hypersphere by identifying the diametrally opposite points has the same metric as the 3-dimensional hypersphere but a different topology. Indeed, it has half the volume of the 3-dimensional hypersphere. In the article [71] Friedmann highlighted the fact that General Relativity is unable to predict the topology or any global structure of space-time. Questions on the shape (e.g. existence or not of holes) of the Universe or the finite or

1. Consider for example the unit tangent field pointing clockwise.
2. Spatial topology has to be distinguished from the topology of the 4-dimensionnal spacetime

infinite nature of the Universe could not be adressed by this intrinsically local theory.

The modern problem of quantification of gravity shed a new light on the issue of the topology of space-time, which was mostly ignored until that time. Some constraints on topology came from the quantification of gravity, as in the case of the quantum gravity scenario of the birth of the Universe (which envolves quantum vacuum fluctuations). This scenario is only possible if spacelike hypersurfaces are compact.

Many topologies for the Universe have been considered throughtout time. In 1900, before Einstein invented his theory of General Relativity, Schwarzschild imagined a torus topology of space [133]: *"One could imagine that as a result of enormously extended astronomical experience, the entire universe consists of countless identical copies of our Milky Way, that the infinite space can be partitioned into cubes each containing an exactly identical copy of our Milky Way. Would we really cling on to the assumption of infinitely many identical repetitions of the same world? . . . We would be much happier with the view that these repetitions are illusory, that in reality space has peculiar connection properties so that if we leave any one cube through a side, then we immediately reenter it through the opposite side"*. Nevertheless, when Einstein applied his theory to the Universe, he assumed that space was a positively curved, finite and simply-connected space without boundary. Multiconnectedness did not attract much support until lately even if Ellis' [61] or Zeld'ovich's [162] work on topology did not exclude it. Allowing multiconnectedness, finite spatial hypersurfaces with zero or negative curvature could exist.

3.1.3 Observational evidence for multiconnected spaces?

In this part, I present and discuss some of the signatures of topology in observations. Recent work by Roukema [114, 127] is aimed at constraining and determining the topology of the comoving hypersurfaces by observational data. In [127] the author first explains how, in the Newtonian case, a torus topology $T^1 = \mathbb{S}^1 \times \mathbb{R}^2$ can generate a residual acceleration which is not predicted by usual Newtonian theory. Indeed, a mass test particle at distance x from a massive object O will be subjected to the gravitational attraction due to O but also from the one of the two nearest topological images.

These topological effects on the dynamics, usually ignored, are also discussed in the relativistic case, for the compact Schwarzschild-like solution of the Einstein equations further in [127].

As discussed in [72], CMB measurements report a first Doppler peak shifted by a few percents towards larger angular scales with respect to the peak predicted by the standard cold dark matter inflationary model, thus favoring a marginally spherical model.

Moreover, considering a multiconnected topology could be the solution for observational issues such as the lack of large angular scale correlations in the CMB. In [126], Roukema, Bulinski, Szaniewska and Gaudin discussed how the multiconnected Poincaré dodecahedron topology could explain the missing fluctuation problem in the CMB. Recent measures [92, 136] suggest an overall small positive curvature but missing fluctuations in the CMB. 3 and 5 year WMAP data estimate the chance of this lack of large angular scale correlations for the infinite and flat model to be less than $0,03\%$ [45]. By considering the multiconnected Poincaré dodecahedron 3-manifold, correlations between density perturbations should vanish above the length scale of the order of the size of the 3-manifold, thus explaining the missing fluctuation in the CMB.

This last part presented some observational evidences supporting a dodecahedron topology for the spatial hypersurfaces. It was meant to illustrate how topology may have strong implications on the dynamics of the Universe and why it has to be considered when cosmological observations are interpreted.

3.2 The Hodge decomposition and the first–order solutions

The Cartan formalism enables us to define the fields on the physical space instead of a global background. In the following, we consider that this physical space, i.e. the spatial hypersurface, is a closed 3–dimensional manifold. Then, Thurston's geometrization conjecture, that we present shortly thereafter, determines which are the possible topologies of this manifold, that may be multiconnected. Hodge theorem will then allow us to decompose the Cartan coframes into an exact, a coexact and a harmonic part. The exact part can be absorbed into a redefinition of global coordinates and, thus, defines a parametrization of a flat space section, whereas the non-exact and harmonic parts encode the true geometrical deviations from the background.

3.2.1 Thurston's geometrization conjecture

Thurston's geometrization conjecture, presented in [143], asserts that every closed 3–dimensional manifolds can be decomposed as a of 3–dimensional manifolds modeled after the 8 model geometries listed by Thurston (see also [96]). This conjecture was proved by Perelman in 2003 using Ricci flow with surgery [117] and implies Poincaré's conjecture. This conjecture asserts that any closed and simply connected 3–dimensional manifolds in homeomorphic to the hypersphere $\mathbb{S}^3$. In Section III.3.2.5, I will consider that the spatial sections are simply connected 3–dimensional manifold. As we will see, in this case, the dimension of the harmonic space of 1–forms vanishes and the Hodge decomposition is simpler.

We now give some mathematical elements that may be useful to understand the Hodge decomposition. For a very good introduction to differential geometry and Hodge decomposition, the reader can refer to [69], [113] and [9].

3.2.2 Mathematical tools for the Hodge decomposition

The volume form

On a manifold of dimension n, the volume form is defined from a set of orthonormal coframes $\{\tilde{\boldsymbol{\eta}}^i\}$, $i = 1...n$ as [3]:

$$\boldsymbol{\varepsilon} = \tilde{\boldsymbol{\eta}}^{\mathbf{1}} \wedge ... \wedge \tilde{\boldsymbol{\eta}}^n \ . \tag{3.1}$$

3. We use different notations with respect to [74]. The components of Levi-Civita tensor in a general basis are denoted by $\epsilon_{\nu_1...\nu_n}$ whereas the components of the volume form are $\varepsilon_{\nu_1...\nu_n}$.

For general coframes $\{\boldsymbol{\eta}^i\}$, $i = 1...n$, the volume form becomes:

$$\boldsymbol{\varepsilon} = \sqrt{|g|}\ \boldsymbol{\eta}^1 \wedge ... \wedge \boldsymbol{\eta}^n = \sqrt{|g|}\ \epsilon_{|\mu_1...\mu_n|}\ \boldsymbol{\eta}^{\mu_1} \wedge ... \wedge \boldsymbol{\eta}^{\mu_n} \ . \tag{3.2}$$

Where $|g|$ is the absolute value of the determinant of the metric tensor and the vertical bars denote that only components with increasing indices are included in the summation. Then,

$$\varepsilon_{\mu_1...\mu_n} = \sqrt{|g|}\ \epsilon_{\mu_1...\mu_n} \ , \tag{3.3}$$

where $\epsilon_{\mu_1...\mu_n}$ is the n–dimensional Levi-Civita tensor.

The Hodge-dual, the exterior differential and the codifferential operator $\boldsymbol{\delta} = \mathbf{d}^*$

$\mathbf{A}$ is a p–vector whose contravariant components are obtained by raising the indices of a p-form $\boldsymbol{\alpha}$. The dual of the form $\boldsymbol{\alpha}$ in an n-dimensional space is $*\boldsymbol{\alpha}$:

$$*\,\boldsymbol{\alpha} = \frac{1}{(n-p)!}\varepsilon_{\nu_1...\nu_p\ \mu_1...\mu_{n-p}}\alpha^{|\nu_1...\nu_p|}\boldsymbol{\eta}^{\mu_1} \wedge ... \wedge \boldsymbol{\eta}^{\mu_{n-p}} \ . \tag{3.4}$$

The codifferential operator $\boldsymbol{\delta} = \mathbf{d}^*$

The codifferential operator sends p-forms to $(p-1)$-forms. We will either consider closed manifolds or compact manifolds with boundaries such that the forms we consider or their Hodge-dual are zero when restricted to the boundary. Then, on a Riemannian manifold if $\boldsymbol{\beta}^p$ is a p-form:

$$\mathbf{d}^*\boldsymbol{\beta}^p = (-1)^{n(p+1)+1} * \mathbf{d} * \boldsymbol{\beta}^p \ , \tag{3.5}$$

where the exterior differential was defined in I.2.3.1.

Laplace operator on forms

If $\mathbf{A}$ is a vector field in $\mathbb{R}^n$ with Cartesian coordinates A^i, then $\nabla^2\mathbf{A}$ is the vector field whose components are $(\nabla^2\mathbf{A})^i = \sum_{j=1}^n(\partial^2 A^i/\partial X^j \partial X^j)$. These coordinates are simply the Laplacian of the coordinates of $\mathbf{A}$. In $\mathbb{R}^3$,

$$\nabla^2\mathbf{A} = grad\ div\mathbf{A} - curl\ curl\mathbf{A} \ . \tag{3.6}$$

This can be written in an intrinsic form if we consider $\boldsymbol{\alpha}^1$ the 1-form associated to $\mathbf{A}$. Then, in $\mathbb{R}^3$, this equation is equivalent to

$$\nabla^2\boldsymbol{\alpha}^1 = -\left(\mathbf{d}\mathbf{d}^* + \mathbf{d}^*\mathbf{d}\right)\boldsymbol{\alpha}^1 \ . \tag{3.7}$$

We define the Laplace-de Rham operator Δ^{dR} which is a mapping from p-forms to p-forms by the negative of the preceding:

$$\Delta^{dR} := \mathbf{d}\mathbf{d}^* + \mathbf{d}^*\mathbf{d} = \left(\mathbf{d} + \mathbf{d}^*\right)^2 \ . \tag{3.8}$$

Laplacian of a 1-form and Weizenböck formula

The Weizenböck formula gives the expression of the $\boldsymbol{\Delta}^{dR}$ applied to a 1–form $\mathbf{h}^a$. On a coordinate basis $\mathbf{d}X^i$, we have:

$$\left(\boldsymbol{\Delta}^{dR}\ \mathbf{h}^a\right)_i = -\left(\mathbf{h}^{a\|k}{}_{\|k}\right)_i + h^a{}_k\,\mathcal{R}^k{}_i\ , \tag{3.9}$$

where $_{\|}$ denotes the Lagrangian covariant derivative and $\mathcal{R}^k{}_i$ is the 3–Ricci curvature tensor. The first term involves covariant derivatives and the second one takes into account explicitly the local geometry.

If we consider the inertial coordinate system of a flat space, the coefficients of $\boldsymbol{\Delta}^{dR}$ reduce to the usual Laplacian operator, and the Riemann curvature vanishes everywhere.

Moreover, if we consider the local inertial coordinates on a given point of a manifold, $\boldsymbol{\Delta}^{dR}$ will also reduce to the usual Laplacian operator and the Ricci curvature will vanish locally.

Bochner's theorem shows that, if the oriented closed Riemannian manifold $\mathcal{M}$ has everywhere a positive Ricci curvature, then a harmonic 1–form will vanish identically. We will show later that this is also the case for any manifold that has an $\mathbb{S}^3$ topology.

3.2.3 Hodge theorem

Harmonic forms on closed manifolds

Let $\mathcal{M}$ be a closed Riemannian n-dimensionnal manifold. We define a global positive definite inner product for

$$(\boldsymbol{\alpha}^p, \boldsymbol{\beta}^p) = \int_{\mathcal{M}} \boldsymbol{\alpha} \wedge *\boldsymbol{\beta}\ . \tag{3.10}$$

Since

$$(\Delta\boldsymbol{\alpha}^p, \boldsymbol{\alpha}^p) = (\mathbf{d}\mathbf{d}^*\boldsymbol{\alpha} + \mathbf{d}^*\mathbf{d}\boldsymbol{\alpha}, \boldsymbol{\alpha}) = (\mathbf{d}^*\boldsymbol{\alpha}, \mathbf{d}^*\boldsymbol{\alpha}) + (\mathbf{d}\boldsymbol{\alpha}, \mathbf{d}\boldsymbol{\alpha}) = \|\ \mathbf{d}^*\boldsymbol{\alpha}\ \|^2 + \|\ \mathbf{d}\boldsymbol{\alpha}\ \|^2 \geq 0\ , \tag{3.11}$$

thus

$$\Delta\boldsymbol{\alpha}^p = \mathbf{0}\ \text{ iff }\ \mathbf{d}^*\boldsymbol{\alpha} = \mathbf{0}\ \text{ and }\ \mathbf{d}\boldsymbol{\alpha} = \mathbf{0}\ . \tag{3.12}$$

Thus harmonic forms are both closed and coclosed.

Hodge theorem

The vector space of harmonic p-forms:

$$\mathcal{H}^p = \{\mathbf{h}^p\ /\ \mathbf{d}\mathbf{h}^p = \mathbf{0} = \mathbf{d}^*\mathbf{h}^p\} \tag{3.13}$$

is of finite dimension and Poisson's equation

$$\boldsymbol{\Delta}^{dR}\ \boldsymbol{\alpha}^p = \boldsymbol{\rho}^p\ , \tag{3.14}$$

has a solution $\boldsymbol{\alpha}^p$ iff $\boldsymbol{\rho}^p$ is orthogonal to $\mathcal{H}^p$.

Consequence: Hodge decomposition

For any p–form $\boldsymbol{\gamma}$, we can find a p–form $\boldsymbol{\theta}$ such that $\boldsymbol{\gamma}$ can be decomposed as:

$$\boldsymbol{\gamma}^p = \mathbf{d}\boldsymbol{\alpha}^{p-1} + \mathbf{d}^*\boldsymbol{\beta}^{p+1} + \mathbf{h}^p \quad , \tag{3.15}$$

where $\boldsymbol{\alpha}^{p-1} = \mathbf{d}^*\boldsymbol{\theta}^p$, $\mathbf{d}^*\boldsymbol{\beta}^{p+1} = \mathbf{d}\boldsymbol{\theta}^p$ and $\mathbf{h}^p$ is harmonic. If $\mathbf{d}\boldsymbol{\Lambda}^{p-1}$, $\boldsymbol{\delta}\boldsymbol{\Lambda}^{p+1}$ and $\boldsymbol{\mathcal{H}}^p$ represent the vector space of, respectively, the exterior derivative of $(p-1)$–forms, the co–differential of $(p+1)$–forms and of the harmonic p–forms, all of them forming subspaces of the local co–tangent space of the Riemannian manifold, we can write this decomposition in a symbolic way:

$$\boldsymbol{\Lambda}^p = \mathbf{d}\boldsymbol{\Lambda}^{p-1} + \mathbf{d}^*\boldsymbol{\Lambda}^{p+1} + \boldsymbol{\mathcal{H}}^p \quad . \tag{3.16}$$

The decomposition (3.15) is unique:

$$\boldsymbol{\gamma}^p = \mathbf{d}\boldsymbol{\alpha}^{p-1} + \mathbf{d}^*\boldsymbol{\beta}^{p+1} + \mathbf{h}^p = \mathbf{d}\boldsymbol{\alpha}'^{p-1} + \mathbf{d}^*\boldsymbol{\beta}'^{p+1} + \mathbf{h}'^p \quad . \tag{3.17}$$

Then

$$\mathbf{d}\boldsymbol{\alpha}^{p-1} - \mathbf{d}\boldsymbol{\alpha}'^{p-1} = \mathbf{0} \quad ; \mathbf{d}^*\boldsymbol{\beta}^{p+1} - \mathbf{d}^*\boldsymbol{\beta}'^{p+1} = \mathbf{0} \quad ; \mathbf{h}^p - \mathbf{h}'^p = \mathbf{0} \quad . \tag{3.18}$$

From this we conclude that

$$\boldsymbol{\alpha}^{p-1} = \boldsymbol{\alpha}'^{p-1} + \mathbf{a}^{p-1} \ \ / \ \ \mathbf{d}\mathbf{a}^{p-1} = \mathbf{0} \quad ; \tag{3.19}$$

$$\boldsymbol{\beta}^{p+1} = \boldsymbol{\beta}'^{p+1} + \mathbf{b}^{p+1} \ \ / \ \ \mathbf{d}^*\mathbf{b}^{p+1} = \mathbf{0} \quad ; \tag{3.20}$$

$$\mathbf{h}^p = \mathbf{h}'^p \quad . \tag{3.21}$$

3.2.4 Hodge decomposition of the perturbation fields

Hodge decomposition of a 1–form

A 1–form $\mathbf{V}$ can be decomposed according to (3.15) as:

$$\mathbf{V} = \mathbf{d}\,\alpha + \mathbf{d}^*\boldsymbol{\beta} + \mathbf{h} \quad / \quad \boldsymbol{\Delta}^{dR}\,\mathbf{h} = \mathbf{0}\,, \tag{3.22}$$

where α is a scalar, $\mathbf{h}$ a 1–form and $\boldsymbol{\beta} = \beta_{ij}\ \mathbf{d}X^i \wedge \mathbf{d}X^j$ a 2–form. On the Lagrangian coordinate basis $\mathbf{d}X^i$, we get:

$$V_i\,\mathbf{d}X^i = \left(\alpha_{|i} + \frac{g_{ij}}{\sqrt{|g|}}\left(\sqrt{|g|}g^{lk}\,g^{jm}\,\beta_{km}\right)_{|l} + h_i\right)\mathbf{d}X^i \quad / \quad h_k\,R^k{}_i - \left(\mathbf{h}^{\|k}{}_{\|k}\right)_i = 0. \tag{3.23}$$

A 2–form is antisymmetric. In a 3–dimensional space, it has 3 independent coefficients. It can thus be generated from a 1−form. We define the 1–form $\mathbf{B} = B_i\ \mathbf{d}X^i$ such that

$$\beta_{km}\ \mathbf{d}X^k \wedge \mathbf{d}X^m = g^{ul}\ \varepsilon_{ukm}\ \mathrm{B}_l\ \mathbf{d}X^k \wedge \mathbf{d}X^m \quad . \tag{3.24}$$

Then, we can show that

$$\frac{g_{ij}}{\sqrt{|g|}}\left(\sqrt{|g|}g^{lk}\,g^{jm}\,\beta_{km}\right)_{|l} = g_{ij}\varepsilon^{rlj}\mathrm{B}_{r|l} \quad , \tag{3.25}$$

where we have used ε^{ijk} instead of ϵ^{ijk} in the definition of B_i in order to get a covariant object defined on the curved space. The decomposition then becomes:

$$V_i\,\mathbf{d}X^i = \left(\alpha_{|i} + g_{ij}\,\varepsilon^{ulj}\mathrm{B}_{u\,|\,l} + h_i\right)\mathbf{d}X^i \quad / \quad h_k\,R^k{}_i - \left(\mathbf{h}^{\|k}{}_{\|k}\right)_i = 0\ . \tag{3.26}$$

This decomposition is very similar to the Helmoltz-Hodge decomposition, available on flat space sections, since the first term is the divergence of a scalar potential while the second one is the generalization of the curl operator to a curved spatial section.

Helmoltz decomposition from the *MR* of the Hodge decomposition

In the *MR* , orthonormal Cartan coframes become exact forms. We can thus associate to them some global coordinates $\mathbf{x}$ such that $\boldsymbol{\eta}^a = \mathbf{d}f^a$ and $\mathbf{x} = \mathbf{f}(\mathbf{X}, t)$. Hodge decomposition in flat space in terms of global coordinates gives the Helmholtz decomposition [4]:

$$\mathbf{V} = {}^xV_i\ \mathbf{d}x^i = \left({}^x\alpha_{\ ,i} + \delta_{ij}\,\epsilon^{ulj}\,{}^x\mathrm{B}_{\,u\,,\,l} + {}^xh_{\ i}\right)\mathbf{d}x^i \quad / \quad {}^xh_i{}^{,k}{}_{,k} = 0. \tag{3.27}$$

This equation (3.27) can also be formulated as a vector identity:

$$\vec{V} = \vec{\nabla}\,{}^x\alpha + \vec{\nabla}\times{}^x\vec{\mathrm{B}} + {}^x\vec{h} \quad / \quad \Delta\,{}^x\vec{h} = \vec{0}. \tag{3.28}$$

where Δ denotes the simple Laplace operator with respect to Eulerian coordinates. In the Lagrangian coordinates, the *MR* of (3.26) gives:

$${}^XV_{\ i}\ \mathbf{d}X^i = \left({}^X\alpha_{|i} + g_{ij}\,\varepsilon^{ulj}\ {}^X\mathrm{B}_{\,u\,|\,l} + {}^Xh_{\ i}\right)\mathbf{d}X^i \quad / \quad {}^Xh_i{}^{\|k}{}_{\|k} = 0\ . \tag{3.29}$$

The Christoffel symbols that implicitly appear in the Laplace-de Rham equation for ${}^Xh_i$ are non-zero:

$$\Gamma^i{}_{kl} = \frac{1}{2\sqrt{|g|}}\epsilon_{abc}\epsilon^{imn}f^a{}_{|kl}\ f^b{}_{|m}\ f^c{}_{|n}\ . \tag{3.30}$$

From the unicity of Hodge decomposition, we conclude that ${}^X\alpha = {}^x\alpha + k$ where k is a constant.

3.2.5 Hodge decomposition of Cartan coframes for $\mathbb{S}^3$ and quotient topologies

From De-Rham and Hurewitz theorem, we can show that the dimension of the harmonic space of 1–forms on a closed oriented manifold is equal to the dimension of the first fundamental group (also called closed path group) [15] [48] [50]. For simply connected manifolds, the dimension of this group is then 0. This is the case of the $\mathbb{S}^3$ topology. The results of Hodge theorem for $\mathbb{S}^3$ can be extended to its quotients [5]. Therefore, on $\mathbb{S}^3$ there

4. The metric is $diag(1, 1, 1)$ in these global coordinates.

5. The quotients spaces $\tilde{\mathcal{M}}/\Gamma$ are built from the universal covering space $\tilde{\mathcal{M}}$ (here $\mathbb{S}^3$) and the holonomy group Γ. For example, the torus $\mathbb{T}^2$ is built from the universal covering $\mathbb{R}^2$ and the holonomy group $\Gamma = \{a\,\mathbf{e}_x + b\,\mathbf{e}_y\ \ :\ \ a, b \in \mathbb{Z}\}$: $\mathbb{T}^2 = \mathbb{R}^2/\Gamma$ whereh $\mathbf{e}_x$ and $\mathbf{e}_y$ are non-colinear vectors. For a detailed explanation of quotient spaces and equivalence classes, the reader can refer to Section 2.1.2 of [113].

exists $\boldsymbol{\gamma}^a$ such that the coframes can be decomposed as

$$\boldsymbol{\eta}^a = \mathbf{d}\alpha^a + \mathbf{d}^*\boldsymbol{\beta}^a = \boldsymbol{\Delta}^{dR}\,\boldsymbol{\gamma}^a \ , \tag{3.31}$$

where α^a is a scalar, $\boldsymbol{\beta}^a$ a 2–form and $\boldsymbol{\gamma}^a$ a 1–form.

We now assume we can encode into the first–order perturbation fields the positive curvature topology. Then, the decomposition

$$\boldsymbol{\eta}^a = a(t)\left(\mathbf{d}X^a + \mathbf{P}^a\right) \ , \tag{3.32}$$

is still available and since the harmonic space of 1–forms is of dimension 0, from (2.45) and (2.48) we conclude that structure coefficients calculated from ${}^E\mathbf{P}^a$ are constant in time. Since they are initially zero, ${}^E\mathbf{P}^a$ represents the integrable part of the perturbation fields.

First–order Hodge decomposition of the perturbation 1–form

We consider the Hodge decomposition for the perturbation field $\mathbf{P}^a$ and now denote by α^a, $\boldsymbol{\beta}^a$, $\mathbf{B}^a$ the fields that intervene in its decomposition. These fields are first–order quantities. Keeping only the first order for this equation reads:

$$P^a_{\ j} = \alpha^a_{\ |j} + \delta_{rj}\,\epsilon^{ulr}\,\mathrm{B}^a_{\ u\,|\,l} \ . \tag{3.33}$$

Note that we would have obtained the same expression if $\mathbf{P}^a$ was defined on the background space associated to the metric δ_{ij}. Nevertheless, the space section is not flat since $P^a_{\ j}$ is not in general integrable [6].

We lower the non–coordinate index of $P^a_{\ j}$ with g_{ai} which at first–order is equivalent to δ_{ai} :

$$P_{ij} = \delta_{ai}P^a_{\ j} = \alpha_{i\,|\,j} + \epsilon^{ul}_{\ \ j}\,\mathrm{B}_{iu\,|\,l} + h_{ij} \quad / \quad h_{ij}{}^{|k}{}_{|k} = 0 \ . \tag{3.34}$$

3.2.6 From SVT to Hodge decomposition

We now know that, for $\mathbb{S}^3$ and quotient topologies, ${}^E\mathbf{P}^a$ encodes the integrable part of the perturbations. Thus

$${}^E\mathbf{P}^a = \mathbf{d}\alpha^a \ . \tag{3.35}$$

As discussed at the end of Section III.2.4.3, it is thus connected to the scalar modes of the S-V-T decomposition.

The complementary part, ${}^H\boldsymbol{\Pi}^a$, is then linked to $\mathbf{d}^*\boldsymbol{\beta}^a$. Furthermore, we can show that the Hodge fields α_i and B_{ij} are defined through the following Poisson equations from the perturbation fields [7]:

$$\Delta_0\alpha_j = P_{ij}{}^{|i} \ , \tag{3.36}$$

$$\Delta_0\mathrm{B}_{ij} = \epsilon_j^{\ mr}P_{ir\,|m} \ . \tag{3.37}$$

6. This would be the case if $\epsilon^{ulr}\,\mathrm{B}^a_{\ u\,|\,l} = 0$.

7. We have set $\mathrm{B}_i{}^m{}_{|m} = 0$ since this term does not intervene in the decomposition (3.34) and thus has no physical relevance.

Equation (3.36) is consistent with the momentum equation expressed in terms of ${}^{E}\mathbf{P}^{a}$ (2.37) and here becomes trivially satisfied.

From (3.34), we know that B_{ij} represents the non-integrable part of the Cartan deformation fields. It thus contains the true deviations to the flat background. We now want to understand how the propagative part of B_{ij} can be linked to the tensor modes $\chi_{ij}^{(1)\top}$ of the perturbation fields. (3.37) can be rewritten as:

$$\Delta_0 \mathrm{B}_{ij} = \epsilon_j{}^{mr\,H}\Pi_{ir\,|m} \ , \tag{3.38}$$

which implies that the first–order magnetic part is

$$H_{ij} = \Delta_0 \dot{\mathrm{B}}_{ij} \ . \tag{3.39}$$

As we already discussed in Section III.2.4.3, ${}^{E}\mathbf{P}^{a}$ is straightforwardly related to the scalar modes. It is now possible to link the non-exact part of the Hodge decomposition to the tensor mode of the S-V-T decomposition:

$$\Delta_0 \mathrm{B}_{ij} = \frac{1}{2}\epsilon_j{}^{mr}\chi_{ir\ \ |m}^{(1)\top} \ . \tag{3.40}$$

3.3 Conclusions

In this chapter, after a historical introduction to the cosmic topology, we explained how it could have an impact on the dynamics of the Universe. My work consisted more specifically in determining how it could have an effect on the first–order solutions that were presented in the last chapter. Indeed, the topology of the spatial sections had to be considered in order to determine the physical content of the first–order solutions ${}^{E}P_{ij}$ and ${}^{H}\Pi_{ij}$. This could not be achieved with a local description of the manifold since some elliptic equations had to be solved, thus needing boundary conditions. For spatially closed hypersurfaces, we could solve the elliptic equations and use the powerful Hodge decomposition.

Furthermore, in the case of closed and simply connected (i.e. $\mathbb{S}^3$) topologies for the spatial hypersurfaces, some results on the contribution of ${}^{E}P_{ij}$ and ${}^{H}\Pi_{ij}$ to the deviations from flatness were obtained. These results can be generalized to the quotients of $\mathbb{S}^3$ topologies. To have a deeper insight into the link between the topology and the physical content of the perturbative solutions, we should now investigate the case of multiconnected spatial topologies[8], which do not have the same space of harmonic 1–forms. Moreover, we should extend our results to the perturbative solutions of higher orders to determine if the ${}^{E}\mathbf{P}^{a}$ solution will then generate deviations from flatness.

To obtain the first–order results for $\mathbb{S}^3$ topologies, we assumed that the topology of the zero–order manifold and the one defined by the first–order perturbations could be different. Then, the first one could be flat while the second one could have a spherical topology.

8. Hodge decomposition is available also for the 3–torus $\mathbb{T}^3$ which has a harmonic space of 1-forms of dimension 3.

We should precisely define the mathematical conditions on the metric tensor in order to determine if it describes a spatial manifold topologically homeomorphic [9] to $\mathbb{S}^3$. This can be achieved by the Ricci-Hamilton flow, which is available on Riemannian manifolds [10]. This geometrical flow is a process that deforms the metric in a way formally analogous to the diffusion of heat, smoothing out its irregularities. The result of this flow would then be a constant positive curvature metric.

9. The Gauss-Bonnet theorem that links the average of the curvature to the topology of the manifold (represented by its genus) for even dimensions, gives a trivial identity. This does not allow us to link geometry to topology for odd dimensions. Unfortunately, no extension to it was yet found in this case.

10. For an interesting discussion on the Ricci-Hamilton flow and the averaged inhomogeneities in a cosmological context, the reader can refer to [31].

Conclusion & Outlook

During the three years of my PhD I had the possibility to work on different projects in the frame of the Intrinsic Lagrangian description. All these projects were focused on a better description of the formation of large scale structures in an inhomogeneous approach.

In the introductory part of this thesis, I first explained how the modern representation of the Universe historically emerged. Then, I presented how Einstein elaborated Special and General Relativity in this context. In his theory of General Relativity, he abandons Newton's idea of absolute space and time. Moreover, the localization on the manifold has no longer an absolute physical meaning and is determined by the dynamical elements of the theory. Thus, the local inertial reference frames are determined by gravity.

Afterwards, I presented the *SMC* and the approximations that it implies. The *SMC* neglects the coupling between the matter content of the Universe and its geometry. Furthermore, it decouples the local from the global dynamics describing a hypothetical absolute space-time in homogeneous expansion. Nevertheless, the inhomogeneities have to be taken into account to describe accurately the average dynamics of the Universe.

In the second part of the introduction I explained in the Newtonian case why the Lagrangian approach is much more powerful then the Eulerian one. Motivated by the success of the Newtonian Lagrangian approach, we built its relativistic counterpart. The trajectory function, which is the coordinate mapping between the Lagrangian and the Eulerian coordinates, is replaced by the Cartan coframes. These coordinate–independent 1–forms enable a relativistic description of the large scale structure formation. In the third part, I discussed the consequences of the inhomogeneities on the global dynamics. In particular, I explained how a backreaction term, which contains both a kinematical and a geometrical part, arises from the non-commutation of the spatial averaging and the time evolution.

In the second part of the thesis, after a chapter on the decomposition of the Einstein equations for a $3 + 1$ foliation of space-time, I focused on the gravitoelectromagnetic analogy. I first considered the Newtonian case and then the analogy for the electric and magnetic parts of the Weyl curvature tensor. As was discussed, these fields are solutions of Maxwell-like equations.

In the Minkowski Restriction, the Cartan coframes become integrable and thus space-time becomes flat. We used the similarities between the gravitoelectric part of the Einstein equations and the Lagrange-Newton-System and inverted the Minkowski Restriction to build from the Newtonian perturbation scheme to order n the corresponding relativistic solutions.

Since Newtonian perturbative solutions do not describe propagative phenomena such as gravitational waves, their relativistic generalization is also not expected to describe them. The third part of the thesis considered, in the frame of first–order perturbation theory, the complementary part to the relativistic generalization of the Newtonian perturbation solutions. To define our perturbation fields, we used differential geometry and more precisely differential forms. We discussed the difference between this coordinate-independent approach, which intrinsically describes the perturbation fields on the curved physical spacetime, with the one adopted in the standard perturbation approach, which defines the perturbation fields on a flat background space-time. The Scalar-Vector-Tensor decomposition used in the standard approach, that is available for fields defined on a flat space section, does no longer work on curved space sections. Therefore, we considered the Hodge theory on closed oriented manifolds, that allows a decomposition of differential forms into exact, coexact and harmonic parts. We applied this decomposition to the perturbation 1–forms in the case of a simply connected topology: the $\mathbb{S}^3$ topology. For this topology, we determined which part of the solution contributed to the deviations from flatness. The ${}^E\mathbf{P}^a$ represents the integrable part of the perturbation fields and thus does not contribute to the deviations.

Furthermore, we discussed at first–order the link between the different parts of the solutions and the magnetic part of the Weyl tensor, which contains the physics of gravitational waves. Nevertheless, before investigating the physical content of ${}^E\mathbf{P}^a$ and ${}^H\mathbf{\Pi}^a$ to upper orders with the Hodge decomposition, the mathematical conditions on the metric to describe a manifold that has a globally closed topology should be first determined. This can be achieved by the Ricci-Hamilton flow. Indeed, as we have discussed in Section III.3.2.1, a 3–dimensional manifold can be decomposed as a connected sum of 3–dimensional manifolds modeled after the 8 model geometries. The Ricci-Hamilton flow is a process that, on each manifold of this connected sum, deforms the metric in a way formally analogous to the diffusion of heat, smoothing out its irregularities. The result of this flow is then a constant curvature metric.

The intrinsic perturbation scheme could be improved by defining the perturbation fields with respect to the averaged manifold in an iterative way. Nevertheless, to find this scheme we need first an accurate averaging procedure for tensors. Furthermore, to improve our description of structure formation on small scales we should take into account more realistic matter models, containing pressure and vorticity. In order to describe in a Lagrangian way a fluid with vorticity, the $3+1$ description is no longer possible. A Lagrangian description will only be possible in the frame of the $1+3$ threading approach, since the local rest-frames do no longer form global hypersurfaces.

I am very happy that during my PhD I could contribute to current research in large scale structure formation in the frame of inhomogeneous cosmology. The different projects I had the pleasure to work on will contribute to the evaluation of the backreaction term for different cosmological systems. Determining the impact of the inhomogeneities on the dynamics of different cosmological systems will be crucial to build the accurate description of relativistic large scale structure formation.

List of Figures

Appendix A

First Results for the Lagrangian Perturbation Theory for Perfect Fluids in the Strong Lagrangian Description

In this chapter, we no longer consider the dust fluid matter model and describe a perfect fluid flow. I here present the first results that I obtained for this matter model, in the Strong Lagrangian description. This work was carried out in order to obtain the relativistic generalization of the results presented in [3], for a Newtonian Lagrangian description of a perfect fluid. Indeed, we have shown that the Lagrangian description is the most relevant when we study nonlinear structure formation in the expanding Universe. The Lagrangian formulation of Einstein equations has already been proposed in [30] for dust cosmologies, explored by H. Asada and M. Kasai in [7] for a dust fluid with vorticity and by H. Asada for a fluid with pressure [8].

We here develop a formalism that will enable us to describe both the radiation dominated era in the Early Universe and the collapsing regions with large velocity dispersion. Allowing pressure in the matter model is a step towards a better description of the dynamics of structure formation.

In this work, we will focus on perfect fluid cosmologies, thus neglecting all irreversible phenomena. We will assume that there is no vorticity in the fluid flow.

A.1 Perfect fluid thermodynamics in the Strong Lagrangian description

A.1.1 Matter models

The perfect fluid description that we develop in this chapter enables us to investigate the dynamics of the Universe in many different situations and epochs. Indeed, a barotropic equation of state can be assumed for either a radiation fluid, which dominates the total energy density at early stages of structure formation, or for fundamental scalar fields.

This description is not only relevant for matter models which are supported by thermodynamical pressure. A Newtonian insight in the dynamics of collisionless systems indicates that a dynamical pressure force arises due to the formation of multi-stream flows when shell-crossing singularities in the fluid flow develop. The multi-stream force prevents a fraction of the fluid to escape from high density regions. As a result, this fraction falls onto the central region creating an internal hierarchy of caustics, as was explained in Section I.2.1.2. Such a force, which is tightly related to the velocity dispersion, is not in general isotropic. Furthermore, the evolution equations governing the anisotropic stresses involve all velocity moments of the distribution function. Yet, in this work, when we will describe such a system, we will assume that the multi-stream force acts isotropically.

A.1.2 Thermodynamics of the perfect fluid

We remind that ρ is the positive rest-mass proper density, ε is the energy density and $u = \varepsilon/\rho$ the specific internal energy. The first thermodynamical identity becomes:

$$du + p\,dv = T\,ds \tag{A.1}$$

where $v = 1/\rho$ and s is the specific entropy.

An entropy balance equation can be obtained from the conservation equations of the stress-energy tensor:

$$S^{\alpha}_{;\alpha} = \eta(\pi_{\alpha\beta}, q_{\xi}, T) \ , \tag{A.2}$$

where $S^{\alpha} = \rho s u^{\alpha} + q^{\alpha}/T$.

We here neglect all irreversible phenomena. Therefore, $q_{\alpha} = 0$ and $\pi_{\alpha\beta} = 0$. We then obtain the stress-energy tensor we formerly postulated. Since $\eta(\pi_{\alpha\beta}, q_{\alpha}, T)$ is then null, the entropy is constant along the flow lines.

We define the specific enthalpy as:

$$h(s, P) := u + pv = \frac{\varepsilon + P}{\rho} \ . \tag{A.3}$$

It can be considered as a thermodynamical potential. Then, $\left.\frac{\partial h}{\partial s}\right)_P =: T$ and $\left.\frac{\partial h}{\partial p}\right)_s =: v$. Therefore, for an isentropic evolution, since $dh/h = dP/(\varepsilon + P)$:

$$h(s, p) = h(s, P_0) \ \exp(\int_{P_0}^{P} \frac{dP}{\varepsilon + P}) \ . \tag{A.4}$$

A.1.3 Stress-energy tensor conservation and shift vector

The conservation of rest-mass density gives:

$$\nabla_{\alpha}(\rho u^{\alpha}) = 0 \Rightarrow \frac{\dot{\rho}}{\rho} = -\theta \ , \tag{A.5}$$

and the stress-energy tensor conservation equation projected along $\mathbf{u}$ leads to

$$\dot{\varepsilon} - \frac{\dot{\rho}}{\rho}(\varepsilon + p) = 0. \tag{A.6}$$

We can therefore conclude that:

$$d\varepsilon = h \, d\rho \tag{A.7}$$

The contracted Bianchi identities result in the conservation of the stress-energy tensor: $\nabla_{\beta} T^{\alpha\beta} = 0$. If we combine this equation with expressions (1.18), we derive the following energy and momentum conservation laws:

$$u_{\alpha} \nabla_{\beta} T^{\alpha\beta} = 0 \ \Leftrightarrow \dot{\epsilon} + \theta(\epsilon + p) = 0 \ \text{where} \ \theta = \nabla_{\alpha} u^{\alpha} \tag{A.8}$$

$$f_{\mu\alpha} \nabla_{\beta} T^{\alpha\beta} = 0 \ \ \Leftrightarrow u^{\alpha} \nabla_{\alpha} u_{\mu} = -\frac{f^{\alpha}_{\mu} \nabla_{\alpha} p}{\epsilon + p} \ . \tag{A.9}$$

The stress-energy tensor conservation equation projected on the rest-frames gives the equation of dynamics of the fluid:

$$\dot{u}_{\alpha} = -f^{\beta}_{\alpha} (\ln h)_{,\beta} \ . \tag{A.10}$$

For a Lagrangian flux orthogonal foliation such that $\mathbf{u} = \mathbf{n}$ and $\boldsymbol{\beta} = \mathbf{0}$ since $\mathbf{V} = \mathbf{0}$, it is possible to show from the geometrical relation:

$$n^\alpha \nabla_\alpha n_\mu = \frac{\alpha_{|\mu}}{\alpha} \quad , \tag{A.11}$$

that (A.10) becomes a relation between the lapse α and the pressure gradient [30]. $\dot{u_\alpha}$ is then equal to $n^\alpha \nabla_\alpha n^\nu$. In the Strong Lagrangian description, (A.10) relates the shift to the enthalpy state function. Indeed, we can show that (A.10) is equivalent to:

$$\dot{\beta}_i + \beta_i \frac{\dot{p}}{\epsilon + p} = -\frac{p_{|i}}{\epsilon + p} \tag{A.12}$$

which can be expressed as:

$$\dot{\beta}_i + \beta_i \,(\ln h)^{\dot{}} = -(\ln h)_{|i} \ . \tag{A.13}$$

To show this, we remind that in the Strong Lagrangian description, $\mathbf{V} = \mathbf{0}$ and $\alpha = \gamma$. Therefore, $u^\mu = (1, 0)$ and $u_\mu = (-1, \beta_i)$

$$f^\alpha_{\ \mu} \nabla_\alpha p = (\nabla_\mu p + u_\mu \nabla_0 p) \quad \Rightarrow \quad f^\alpha_{\ i} \ \nabla_\alpha p = p_{|i} + \beta_i \dot{p} \ . \tag{A.14}$$

Furthermore,

$$\begin{aligned} h^\nu_i u^\mu \nabla_\mu u_\nu = \delta^\nu_i u^\mu \nabla_\mu u_\nu &= u^\mu u_{i,\mu} - \frac{u^\mu u^\rho}{2}(g_{i\rho|\mu} + g_{\mu\rho|i} - g_{i\mu|\rho}) \\ &= \dot{\beta}_i - \frac{1}{2}(\alpha^2 + \beta_k \beta^k)_{|i} = \dot{\beta}_i \quad , \end{aligned} \tag{A.15}$$

since $n_i = 0$ and $\alpha^2 - \beta_k \beta^k = 1$. Thus, since the spatial and time derivative commute in the Strong Lagrangian description, we integrate (A.12) to obtain:

$$\beta_i(\mathbf{X}, t) = -\frac{1}{h(\mathbf{X}, t)} \left(\int^t h(\mathbf{X}, t') \, \mathrm{d}t' \right)_{|i} \ . \tag{A.16}$$

A.2 First-order scheme in the Strong Lagrangian description for a radiation fluid

A.2.1 First–order shift vector for a radiation fluid

The equation of state for a radiation fluid is:

$$P(\varepsilon) = \frac{1}{3}\varepsilon \ . \tag{A.17}$$

The enthalpy expressed in terms of the energy density and the mass density is

$$h(\varepsilon) = h_0 \varepsilon^{1/4} \quad ; \quad h(\rho) = H_0 \rho^{1/3} \ , \tag{A.18}$$

since $\rho = \frac{4}{3}\varepsilon^{3/4}$. The shift vector can thus be rewritten as:

$$\beta_i = \rho^{-1/3}(\mathbf{X}, t) \left(\int_{t_\mathrm{i}}^t \rho^{1/3}(\mathbf{X}, t') dt' \right)_{|i} \ . \tag{A.19}$$

At first order, the mass density can be expanded as:

$$\rho = \frac{\rho_{H_\mathrm{i}}}{a^3}\left(1 - \frac{W}{4\pi G} - P\right) \ . \tag{A.20}$$

We conclude that β_i is a first–order vector that has the following expression:

$$\beta_i = \Psi_{|i} \quad \text{where} \quad \Psi = -\frac{a(t)}{3}\left(\frac{W}{4\pi G}\int_{t_\mathrm{i}}^{t}\frac{dt'}{a(t')} + \int_{t_\mathrm{i}}^{t}\frac{P(\mathbf{X},t')}{a(t')}dt'\right) \ . \tag{A.21}$$

A.2.2 Zero and first–order Einstein equations

Zero–order Einstein equations

At zero–order, the Hamilton constraint equation (1.30) gives:

$$6H^2 = 16\pi G^{(0)}\epsilon + 2\Lambda \ , \tag{A.22}$$

while the evolution equation for the extrinsic curvature (1.29) reads:

$$\frac{\ddot{a}}{a} = \Lambda + 4\pi G({}^{(0)}\epsilon - {}^{(0)}p) - 2H^2 \ . \tag{A.23}$$

If we insert (A.22) into (A.23), we get the Raychaudhuri equation:

$$\frac{\ddot{a}}{a} = \Lambda - 4\pi G({}^{(0)}\epsilon + 3\ {}^{(0)}p) \ . \tag{A.24}$$

To obtain these equations, we determined the zero–order for the extrinsic curvature ${}^{(0)}\mathcal{K}^i_j = -H\ \delta^i{}_j$ and for the lapse function. Since the shift function is of order 1, the lapse function is up to first–order equal to 1.

We then inserted these quantities into the Einstein equations (1.29), (1.31) and (1.30). Furthermore, we used the fact that, as in the irrotational dust fluid case, ${}^{(0)}\Gamma^r_{kj} = 0$ and ${}^{(0)}\mathcal{R} = 0$.

Einstein equations to first–order

The first–order term of the extrinsic curvature is:

$${}^{(1)}\mathcal{K}^i{}_j = \frac{1}{2}\left({}^{(1)}\beta^i_{|j} + {}^{(1)}\beta_j^{|i} - {}^{(1)}\ h^{ik}\dot{h}_{kj}\right) = {}^{(1)}\beta^i_{|j} - \dot{P}^i{}_j \ , \tag{A.25}$$

where we have assumed that there is no vorticity and where we have inserted the metric (2.59). The trace of this first–order term is:

$${}^{(1)}\mathcal{K} = \beta_k^{|k} - \dot{P} \ . \tag{A.26}$$

The Hamilton constraint at first order gives:

$$H\left(\dot{P} - \beta_k^{|k}\right) - 4\,\pi G\ {}^{(1)}\epsilon = -\frac{{}^{(1)}\mathcal{R}}{4} \ . \tag{A.27}$$

The evolution equation for the extrinsic curvature becomes:

$$ {}^{(1)}\mathcal{R}^i{}_j + \left(\dot{P}^i{}_j - \beta^i{}_{|j}\right)^{\cdot} + 3H\left(\dot{P}^i{}_j - \beta^i{}_{|j}\right) - H\,\delta^i_j\,\left(\beta_k{}^{|k} - \dot{P}\right) + 4\pi G({}^{(1)}p - {}^{(1)}\epsilon)\delta^i_j = 0\ . \quad (A.28) $$

Finally, the momentum constraint equation becomes:

$$ \left(\beta^k{}_{|j} - \dot{P}^k{}_j\right)_{|k} - \left(\beta^k{}_{|k} - \dot{P}\right)_{|j} = 8\pi G({}^{(1)}p + {}^{(1)}\epsilon)\beta_j\ . \quad (A.29) $$

The Raychaudhuri equation at first–order is:

$$ \left(\dot{P} - \beta_k{}^{|k}\right)^{\cdot} + 2H\left(\dot{P} - \beta_k{}^{|k}\right) + 4\,\pi G\left({}^{(1)}\epsilon + 3\ {}^{(1)}p\right) = 0\ . \quad (A.30) $$

First–order Einstein equations for a radiation fluid

If we decompose ϵ and the pressure p to zero and first–order, we get:

$$ {}^{(0)}\epsilon = \epsilon_0 \frac{\rho_{H\,\mathbf{i}}^{4/3}}{a^4} \quad \text{and} \quad {}^{(1)}\epsilon = -\epsilon_0 \frac{4\,\rho_{H\,\mathbf{i}}^{4/3}}{3\,a^4}\left(\frac{W}{4\pi G} + P\right)\ . \quad (A.31) $$

Equations (A.27), (A.28), (A.29) and (A.30) then become:

$$ H\left(\dot{P} - \beta_k^{|k}\right) + \frac{2}{3}\left(\Lambda - 3\frac{\ddot{a}}{a}\right)\left(\frac{W}{4\pi G} + P\right) = -\frac{{}^{(1)}\mathcal{R}}{4}\ ; \quad (A.32) $$

$$ {}^{(1)}\mathcal{R}^i{}_j + \left(\dot{P}^i{}_j - \beta^i{}_{|j}\right)^{\cdot} + 3H\left(\dot{P}^i{}_j - \beta^i{}_{|j}\right) = \quad (A.33) $$

$$ H\,\left(\beta_k{}^{|k} - \dot{P}\right)\,\delta^i_j\, + \,\frac{4}{9}\left(3\frac{\ddot{a}}{a} - \Lambda\right)\left(\frac{W}{4\pi G} + P\right)\,\delta^i_j\ ; $$

$$ \left(\beta^k{}_{|j} - \dot{P}^k{}_j\right)_{|k} - \left(\beta^k{}_{|k} - \dot{P}\right)_{|j} = \frac{16}{9}\left(3\frac{\ddot{a}}{a} - \Lambda\right)\left(\frac{W}{4\pi G} + P\right)\beta_j\ ; \quad (A.34) $$

$$ \left(\dot{P} - \beta_k{}^{|k}\right)^{\cdot} + 2H\left(\dot{P} - \beta_k{}^{|k}\right) = \frac{4}{3}\left(\Lambda - 3\frac{\ddot{a}}{a}\right)\left(\frac{W}{4\pi G} + P\right)\ ; \quad (A.35) $$

and

$$ \beta_k{}^{|k} = \Psi_{|k}{}^{|k} = -\frac{1}{3a(t)}\left(\frac{W_{|k}{}^{|k}}{4\pi G}\int_{t_\mathbf{i}}^{t}\frac{dt'}{a(t')} + \int_{t_\mathbf{i}}^{t}\frac{P(\mathbf{X},t')_{|k}{}^{|k}}{a(t')}dt'\right)\ . \quad (A.36) $$

Expressing W from the initial conditions

If we evaluate (A.30) at $t = t_\mathbf{i}$, we get the following equation, since $\beta_k{}^{|k}(t_\mathbf{i}) = 0$:

$$ \ddot{P}(t_\mathbf{i},\mathbf{X}) + 2H\dot{P}(t_\mathbf{i},\mathbf{X}) = \frac{8}{3}\epsilon_{H\,\mathbf{i}}W(\mathbf{X})\ . \quad (A.37) $$

It is thus possible, from initial conditions, to build $W_{|k}{}^{|k}$.

First–order trace equations

We combine the previous equations in such a way that no integral over the time appears. To do so, we formulate the trace equations such that the shift vector will appear with the scale factor in front of it. Then, the time derivative of $a(t) \times \beta^{i}{}_{|j}$ gives:

$$\left(a\beta^{i}{}_{|j}\right)^{\cdot} = -\frac{1}{3a(t)}\left(\frac{W^{|i}{}_{|j}}{4\pi G} + P^{|i}{}_{|j}\right) \quad . \tag{A.38}$$

The first–order Hamilton equation (A.32) can be written:

$$a\left(\dot{P} - \beta_{k}^{|k}\right) - 4\,\pi G\;^{(1)}\epsilon\frac{a^2}{\dot{a}} = -\frac{a^2}{\dot{a}}\frac{^{(1)}\mathcal{R}}{4} \quad . \tag{A.39}$$

The time derivative of this equation gives:

$$\ddot{P}a + \dot{P}\left(\dot{a} + \frac{16\,\pi G}{3\,a^2\dot{a}}\epsilon_{H\,\mathbf{i}}\right) + \left(\frac{16\,\pi G}{3\,a^2\dot{a}}\epsilon_{H\,\mathbf{i}}\left(\frac{2}{a^3} - \frac{\ddot{a}}{a^2\dot{a}^2}\right) + \frac{1}{3a(t)}\Delta_0\right)\left(\frac{W}{4\pi G} + P\right) = \left(\frac{\ddot{a}a^2}{\dot{a}^2} - 2a\right)\frac{^{(1)}\mathcal{R}}{4} - \frac{^{(1)}\dot{\mathcal{R}}}{4}\frac{a^2}{\dot{a}} \quad , \tag{A.40}$$

where Δ_0 is the Lagrangian Laplacian operator: ${}^{|k}{}_{|k}$. If we now combine the Hamilton constraint and the trace of the evolution equation for the extrinsic curvature, we get the following equation:

$$\frac{a\,9}{4}{}^{(1)}\mathcal{R} + \left(a\left(\dot{P} - \beta_{k}^{|k}\right)\right)^{\cdot} + 4\,\pi G\;({}^{(1)}p - 4^{(1)}\epsilon)\,a = 0 \quad . \tag{A.41}$$

We insert (A.38) into this equation and get:

$$\left(\dot{P}a + \frac{9}{4}a^{(1)}\mathcal{R}\right)^{\cdot} + \frac{1}{3a(t)}\Delta_0\left(\frac{W}{4\pi G} + P\right) + \frac{176\,\pi G}{9}\epsilon_{H\,\mathbf{i}}\left(\frac{\dot{P}}{a^3} - \frac{3\dot{a}}{a^4}\left(\frac{W}{4\pi G} + P\right)\right) = 0 \quad . \tag{A.42}$$

A.3 Concluding remarks

The equation that we obtain for the trace is a wave equation, since it both implies some spatial and time derivatives. The wave that propagates is a pressure wave. In order to solve this equation, we can use the fact that the Ricci scalar can be expressed as: $\mathcal{R} = \frac{1}{a^2}\mathcal{R}(t_{\mathbf{i}})$, where $\mathcal{R}(t_{\mathbf{i}})$ can be determined by the initial data for the comoving perturbation fields (2.6) and (2.7).

Bibliography

[1] P. A. R. Ade *et al.* [Planck Collaboration], "Planck 2013 results. XV. CMB power spectra and likelihood," Astron. Astrophys. **571** (2014) A15 [arXiv:1303.5075 [astro-ph.CO]]. 20

[2] P. A. R. Ade *et al.* [Planck Collaboration], "Planck 2015 results. XIII. Cosmological parameters," [arXiv:1502.01589 [astro-ph.CO]]. 16

[3] S. Adler and T. Buchert, "Lagrangian theory of structure formation in pressure supported cosmological fluids," Astron. Astrophys. **343** (1999) 317 [arXiv:9806320 [astro-ph]]. 131

[4] A. Alles, T. Buchert, F. Al Roumi and A. Wiegand, "Lagrangian theory of structure formation in relativistic cosmology. III. Gravitoelectric perturbation and solution schemes at any order," Phys. Rev. D **92** (2015) 2, 023512 [arXiv:1503.02566 [gr-qc]]. 2, 56, 72, 86, 91, 101, 106, 107

[5] A. Alles: Inhomogeneous Cosmology: an answer to the Dark Matter and Dark Energy problems? *Ph.D. thesis*, Université Lyon 1 (2014).

[6] R. L. Arnowitt, S. Deser and C. W. Misner, "The Dynamics of general relativity," Gen. Rel. Grav. **40** (2008) 1997 [arXiv:0405109 [gr-qc]]. 34, 39

[7] H. Asada and M. Kasai, "Lagrangian description of the fluid flow with vorticity in the relativistic cosmology," Phys. Rev. D **59** (1999) 123515 [arXiv:9904005 [astro-ph]]. 53, 131

[8] H. Asada, "Lagrangian description of fluid flow with pressure in relativistic cosmology," Phys. Rev. D **62** (2000) 127301 [arXiv:0010349 [astro-ph]]. 131

[9] T. Aubin, "Some Nonlinear Problems in Riemannian Geometry," Springer, New York (1998) 398 pp. 119

[10] J. M. Bardeen, "Gauge–invariant cosmological perturbations," Phys. Rev. D, **22** (1982). 73

[11] A. Barnes and R. R. Rowlingson, "Irrotational perfect fluids with a purely electric Weyl tensor," Class. Quant. Grav. **6**, 949 (1989). 73

[12] J. D. Bekenstein, "Relativistic gravitation theory for the MOND paradigm," Phys. Rev. D **70** (2004) 083509 [Phys. Rev. D **71** (2005) 069901] [arXiv:0403694 [astro-ph]]. 1

[13] F. Bernardeau, S. Colombi, E. Gaztanaga and R. Scoccimarro, "Large scale structure of the universe and cosmological perturbation theory," Phys. Rept. **367** (2002) 1 [arXiv:0112551 [astro-ph]]. 22, 28

[14] E. Bertschinger and A. J. S. Hamilton, "Lagrangian evolution of the Weyl tensor," Astrophys. J. **435** (1994) 1 [arXiv:9403016 [astro-ph]]. 63, 65, 73

[15] H. Brezis, "Analyse fonctionnelle : Théorie et applications " Dunod, Paris (2005) *ISBN-13 978-2100043149* 123

[16] S. Bildhauer, T. Buchert and M. Kasai, "Solutions in Newtonian cosmology – the pancake theory with cosmological constant," Astron Astrophys. **263**, 23 (1992). 86

[17] V. R. Bouillot, J. M. Alimi, P. S. Corasaniti and Y. Rasera, "Probing dark energy models with extreme pairwise velocities of galaxy clusters from the DEUS-FUR simulations," Mon. Not. Roy. Astron. Soc. **450** (2015) 145 [arXiv:1405.6679 [astro-ph.CO]]. 27

[18] V. B. Braginsky, C. M. Caves and K. S. Thorne, "Laboratory Experiments to Test Relativistic Gravity," Phys. Rev. D **15** (1977) 2047.

[19] M. Bruni, S. Matarrese and O. Pantano: " Dynamics of silent universes," Astrophys. J. **445** (1995) 958 [arXiv:9406068[astro-ph.CO]]. 73

[20] T. Buchert and G. Götz, " A class of solutions for self–gravitating dust in Newtonian gravity," J. Math. Phys. **28**, (1987) 2714.

[21] T. Buchert, "A class of solutions in Newtonian cosmology and the pancake theory," Astron. Astrophys. **223** (1989) 9. 30, 86, 89

[22] T. Buchert, "Lagrangian theory of gravitational instability of Friedmann–Lemaître cosmologies and the 'Zel'dovich approximation'," Mon. Not. Roy. Astr. Soc. **254** (1992) 729 . 86, 89

[23] T. Buchert, "Lagrangian perturbation theory – a key–model for large–scale structure," Astron Astrophys. **267** (1993) L51 . 89

[24] T. Buchert and J. Ehlers, " Lagrangian theory of gravitational instability of Friedmann–Lemaître cosmologies – second order approach: an improved model for nonlinear clustering," Mon. Not. Roy. Astron. Soc. **264** (1993) 375 . 86, 90

[25] T. Buchert, " Lagrangian theory of gravitational instability of Friedmann-Lemaître cosmologies: generic third–order model," for nonlinear clustering. Mon. Not. Roy. Astron. Soc. **267** (1994) 811 [arXiv:9309055 [astro-ph]].

[26] T. Buchert, "Lagrangian perturbation approach to the formation of large scale structure," In Varenna 1995, Dark matter in the universe* 543-564 [arXiv:9509005 [astro-ph]]. 28, 31

[27] T. Buchert: Lagrangian Perturbation Approach to the Formation of Large–scale Structure. In *Proceedings of the international school of physics Enrico Fermi. Course CXXXII: Dark matter in the Universe*, edited by S. Bonometto, J. Primack and A. Provenzale (Società Italiana di Fisica, Varenna sul Lago di Como, 1996). 31

[28] T. Buchert and J. Ehlers, " Averaging inhomogeneous Newtonian cosmologies," Astron. Astrophys. **320** (1997) 1. [arXiv:9510056 [astro-ph]]. 80

[29] T. Buchert, "On average properties of inhomogeneous fluids in general relativity. 1. Dust cosmologies," Gen. Rel. Grav. **32** (2000) 105 [arXiv:9906015 [gr-qc]]. 2, 41

[30] T. Buchert, "On average properties of inhomogeneous fluids in general relativity: Perfect fluid cosmologies," Gen. Rel. Grav. **33** (2001) 1381 [arXiv:0102049 [gr-qc]]. 2, 131, 133

[31] T. Buchert and M. Carfora, "Regional averaging and scaling in relativistic cosmology," Class. Quant. Grav. **19** (2002) 6109 [arXiv:0210037 [gr-qc]]. 126

[32] T. Buchert and A. Dominguez, "Adhesive gravitational clustering," Astron. Astrophys. **438** (2005) 443 [arXiv:0502318 [astro-ph]]. 28

[33] T. Buchert, "An Exact Lagrangian integral for the Newtonian gravitational field strength," Phys. Lett. A **354** (2006) 8 [arXiv:0508059 [gr-qc]]. 58

[34] T. Buchert, " Toward physical cosmology: focus on inhomogeneous geometry and its nonperturbative effects," Class. Quant. Grav. **28** (2011) 164007. [arXiv:1103.2016 [gr-qc]] 43

[35] T. Buchert and M. Ostermann, "Lagrangian theory of structure formation in relativistic cosmology I: Lagrangian framework and definition of a non-perturbative approximation," Phys. Rev. D **86** (2012) 023520 [arXiv:1203.6263 [gr-qc]]. 2, 31, 55, 66, 73, 74, 77, 88

[36] T. Buchert, C. Nayet and A. Wiegand, "Lagrangian theory of structure formation in relativistic cosmology II: average properties of a generic evolution model," Phys. Rev. D **87** (2013) 12, 123503 [arXiv:1303.6193 [gr-qc]]. 2, 55, 73

[37] T. Buchert, "Introduction to Gravitation Theories, 2013 Master 1 ENS Lyon lecture notes"

[38] T. Buchert, "Cosmology and Gravitational Systems, 2013 Master 2 ENS Lyon lecture notes" 22, 28, 58

[39] M. N. Celerier, K. Bolejko and A. Krasinski, “A (giant) void is not mandatory to explain away dark energy with a Lemaitre – Tolman model,” Astron. Astrophys. **518** (2010) A21 [arXiv:0906.0905 [astro-ph.CO]].

[40] S. Chandrasekhar, “The Mathematical Theory of Black Holes,” Oxford University Press (1998) *ISBN 978-0198503705* 75

[41] S. Nadkarni–Ghosh and D. F. Chernoff, “ Extending the domain of validity of the Lagrangian approximation,” Mon. Not. Roy. Astron. Soc. **410**, (2011) 1454 [arXiv:1005.1217 [gr-qc]].

[42] S. Nadkarni–Ghosh and D. F. Chernoff, “ Modelling non–linear evolution using Lagrangian perturbation theory re–expansions,” Mon. Not. Roy. Astron. Soc. **431** (2013) 799 [arXiv:1211.5777 [gr-qc]].

[43] C. Clarkson, G. Ellis, J. Larena and O. Umeh, “Does the growth of structure affect our dynamical models of the universe? The averaging, backreaction and fitting problems in cosmology,” Rept. Prog. Phys. **74** (2011) 112901 [arXiv:1109.2314 [astro-ph.CO]]. 40, 43

[44] A. Conley *et al.* [SNLS Collaboration], “Supernova Constraints and Systematic Uncertainties from the First 3 Years of the Supernova Legacy Survey,” Astrophys. J. Suppl. **192** (2011) 1 [arXiv:1104.1443 [astro-ph.CO]].

[45] C. J. Copi, D. Huterer, D. J. Schwarz and G. D. Starkman, “No large-angle correlations on the non-Galactic microwave sky,” Mon. Not. Roy. Astron. Soc. **399** (2009) 295 [arXiv:0808.3767 [astro-ph]]. 118

[46] L. F. O. Costa and J. Natario, “Gravito-electromagnetic analogies,” Gen. Rel. Grav. **46** (2014) 1792 [arXiv:1207.0465 [gr-qc]]. 58

[47] R. Cowen, “ Full-Galaxy dust map muddles search for gravitational waves,” Nature news, Sep. 22, (2014) 96

[48] G. De Rham, “ Sur la théorie des formes différentielles harmoniques ,” Annales de l’Universite de Grenoble **22** (1946) 135-152 123

[49] R. H. Dicke, P. J. E. Peebles, P. G. Roll and D. T. Wilkinson, “Cosmic Black-Body Radiation,” Astrophys. J. **142** (1965) 41 19

[50] J. Dieudonné, “ Eléments d’analyse réelle ,” Tome 1 **22** (1966) 123

[51] R. Durrer, “ Gauge invariant cosmological perturbation theory ,” Fund. Cosmic Phys. **15** (1994) 209. [arXiv:9311041 [astro-ph]]. 73

[52] J. S. Dowker, “A gravitational Aharonov-Bohm effect,” Il Nuovo Cimento B Series 10 **52** (1967) 129-135 57

[53] J. Ehlers, “Contributions to the relativistic mechanics of continuous media,” Gen. Rel. Grav. **25** (1993) 1225 [Abh. Akad. Wiss. Lit. Mainz. Nat. Kl. **11** (1961) 793].

[54] J. Ehlers, “Examples of Newtonian limits of relativistic spacetimes,” Class. Quant. Grav. **14** (1997) 119

[55] J. Ehlers and T. Buchert, “Newtonian cosmology in Lagrangian formulation: foundations and perturbation theory,” Gen. Rel. Grav. **29** (1997) 733 [arXiv:9609036 [astro-ph]]. 31, 75, 76, 77, 78, 79, 80, 81, 83

[56] J. Ehlers, I. Ozsvath, E. L. Schücking and Y. Shang, “Pressure as a source of gravity,” Phys. Rev. D **72** (2005) 124003 [arXiv:0510041 [gr-qc]]. 61

[57] J. Ehlers, I. Ozsvath and E. L. Schucking, “Active mass under pressure,” Am. J. Phys. **74** (2006) 607 [arXiv:0505040 [gr-qc]].

[58] J. Ehlers and T. Buchert, “On the Newtonian Limit of the Weyl Tensor,” Gen. Rel. Grav. **41** (2009) 2153 [arXiv:0907.2645 [gr-qc]]. 65

[59] A. Einstein, “Die Grundlage der allgemeinen Relativitatstheorie,” Ann. Phys. **49** (1916) 769-822 11

[60] A. Einstein, “ Über Gravitationswellen,” Preussische Akamedie der Wissenschaften, Sitzungsberichte, (1918), 154. 96

[61] G. F. R. Ellis, “Topology and cosmology,” Gen. Rel. Grav. **2** (1971) 7. 118

[62] G. F. R. Ellis, M. Bruni, “ Covariant and gauge–invariant approach to cosmological density fluctuations,” Phys. Rev. D **40** (1989) 1804. 73

[63] G. F. R. Ellis, J. Hwang, M. Bruni: Covariant and gauge–independent perfect fluid Robertson–Walker perturbations,” Phys. Rev. D **40** (1989) 1819. 73

[64] G. F. R. Ellis and H. van Elst, “Cosmological models: Cargese lectures 1998,” NATO Sci. Ser. C **541** (1999) 1 [arXiv:9812046]. 62

[65] G. F. R. Ellis, “Inhomogeneity effects in Cosmology,” Class. Quant. Grav. **28** (2011) 164001 [arXiv:1103.2335 [astro-ph.CO]]. 39, 40, 43

[66] H. van Elst, C. Uggla, W. M. Lesame, G. F. R. Ellis and R. Maartens:, “Integrability of irrotational silent cosmological models,” Class. Quant. Grav. **14** (1997) 1151 [arXiv:9611002 [gr-qc]]. 73

[67] H. van Elst and G. F. R. Ellis, “The Covariant approach to LRS perfect fluid space-time geometries,” Class. Quant. Grav. **13** (1996) 1099 [arXiv:9510044 [gr-qc]]. 40

[68] H. van Elst and C. Uggla, “General relativistic (1+3) orthonormal frame approach revisited,” Class. Quant. Grav. **14** (1997) 2673 [arXiv:9603026 [gr-qc]]. 54

[69] T. Frankel, "The geometry of physics: An introduction," Cambridge, UK: Univ. Pr. (1997) 654 p 119

[70] A. Friedmann, "Über die Krummung des Raumes," Zeits. Phys. **10**, (1922), 377-386 13

[71] A. Friedmann, " The Universe as Space and Time" Petrograd, Akademiya (1923) 117

[72] E. Gausmann, R. Lehoucq, J. P. Luminet, J. P. Uzan and J. Weeks, "Topological lensing in spherical spaces," Class. Quant. Grav. **18** (2001) 5155 [arXiv:0106033 [gr-qc]]. 116, 118

[73] E. Gourgoulhon, "3+1 formalism and bases of numerical relativity," [arXiv:0703035 [gr-qc]]. 34, 35, 49, 53, 96

[74] O. Gron, and H. Sigbjorn, " Einstein's General Theory of Relativity," Springer, New York (2007) *ISBN 978-0-387-692005* 9, 32, 62, 75, 96, 99, 119

[75] A.Hamilton : General Relativity, Black Holes, and Cosmology. `http://jila.colorado.edu/~ajsh/astr5770_14/grbook.pdf`, (2014). 19, 32

[76] O. Heaviside, " A Gravitational and Electromagnetic Analogy," Part I, The Electrician, **31**, (1893), 281-282. 57, 61

[77] C. Hikage, J. Schmalzing, T. Buchert, Y. Suto, I. Kayo, A. Taruya, M. S. Vogeley, F. Hoyle, J. R. Gott, III, and J. Brinkmann, " Minkowski Functionals of SDSS Galaxies I : Analysis of Excursion Sets," Publications of the Astronomical Society of Japan, **55**, (2003), 911-931 [arXiv:astro-ph/0304455]. 12

[78] G. Holzmüller, " Minkowski Functionals of SDSS Galaxies I : Analysis of Excursion Sets," Z. Math. Phys. , **15**, (1870), 69. 57

[79] F. Hoyle, Fiona, M.Vogeley, " Voids in the Point Source Catalogue Survey and the Updated Zwicky Catalog," The Astrophysical Journal, **566**, 1 (2002), 641-651 [arXiv:astro-ph/0109357]. 38

[80] F. Hoyle, Fiona, M.Vogeley, " Voids in the Two-Degree Field Galaxy Redshift Survey," The Astrophysical Journal, **607**, 1 (2004), 751-764. 38

[81] E. P. Hubble, " Cepheids in Spiral Nebulae," Popular Astronomy, **33** (1925), 252. 8

[82] E. P. Hubble, " NGC 6822, a remote stellar system," Astrophysical Journal, **62** (1925), 409-433. 8

[83] X. Jaen and A. Molina, "Rigid motions and generalized Newtonian gravitation," Gen. Rel. Grav. **45** (2013) 1531 [arXiv:1210.1137 [gr-qc]].

[84] R. Jantzen, P. Carini, D. Bini, " GEM: The User Manual–Understanding Spacetime Splittings and their Relationships," URL:www.homepage.villanova.edu/robert.jantzen/gem, (2004). 58

[85] M. Kasai, "Tetrad-based perturbative approach to inhomogeneous universes: A general relativistic version of the Zel'dovich approximation," Phys. Rev. D **52** (1995) 5605. 31, 73

[86] R. P. Kerr, "Gravitational field of a spinning mass as an example of algebraically special metrics," Phys. Rev. Lett. **11** (1963), 237-238. 11

[87] M. Kerscher, K. Mecke, J. Schmalzing, C. Beisbart, T. Buchert, and H. Wagner, " Morphological fluctuations of large-scale structure: The PSCz survey," Astronomy and Astrophysics, **373**, (2001), 1-11 [arXiv:0101238 [astro-ph]]. 12

[88] H. Kodama and M. Sasaki, " Cosmological Perturbation Theory," Progress of Theoretical Physics Supplement **78** (1984) 1. 73

[89] L. Kofman and D. Pogosian, "Equations of gravitational instability are nonlocal," Astrophys. J. **442** (1995) 30 [arXiv:9403029 [astro-ph]]. 65, 73

[90] E. W. Kolb and M. S. Turner, "The Early universe," Front. Phys. **69** (1990) 1. 11

[91] E. W. Kolb, "Backreaction of inhomogeneities can mimic dark energy," Class. Quant. Grav. **28** (2011) 164009. 43

[92] E. Komatsu *et al.* [WMAP Collaboration], "Five-Year Wilkinson Microwave Anisotropy Probe (WMAP) Observations: Cosmological Interpretation," Astrophys. J. Suppl. **180** (2009) 330 [arXiv:0803.0547 [astro-ph]]. 118

[93] S. M. Kopeikin, A. N. Petrov, " Dynamic field theory and equations of motion in cosmology," Ann. of Phys. **350** (2014) 379 [arXiv:1407.3846 [gr-qc]].

[94] M. Kuhlen, M. Vogelsberger, R.. Angulo, "Numerical simulations of the dark universe: State of the art and the next decade," Physics of the Dark Universe, **1** (2012) 50 [arXiv:1209.5745 [astro-ph]]. 28

[95] F. S. Labini, "Inhomogeneities in the universe," Class. Quant. Grav. **28** (2011) 164003 [arXiv:1103.5974 [astro-ph.CO]]. 12

[96] M. Lachieze-Rey and J. P. Luminet, "Cosmic topology," Phys. Rept. **254** (1995) 135 [arXiv:9605010 [gr-qc]]. 119

[97] G. Lemaitre, "Un univers homogene de masse constante et de rayon croissant, rendant compte de la vitesse radiale des nebuleuses extra-galactiques," Ann. Soc. Sci. Bruxelles A **46**, (1927), 49-59. 13

[98] J. Lesgourgues, "Cosmology, ENS Lyon lecture notes',' available on "http://lesgourg.web.cern.ch/lesgourg/courses.html" 11, 16

[99] N. Li and D.J. Schwarz: On the onset of cosmological backreaction. Phys. Rev. D **76**, 083011 (2007) [arXiv:0702043 [gr-qc]]. 91

[100] J. P. Luminet and B. F. Roukema, "Topology of the universe: Theory and observation," [arXiv:9901364].

[101] J. P. Luminet, "Past and future of cosmic topology," Acta Cosmologica **24** (1998) 105 [arXiv:9804006 [gr-qc]]. 117

[102] R. Maartens, G. F. R. Ellis and W. R. Stoeger, S.J., "Limits on anisotropy and inhomogeneity from the cosmic background radiation," Phys. Rev. D **51** (1995) 1525 [arXiv:9501016 [astro-ph]]. 1, 39

[103] R. Maartens, G. F. R. Ellis and W. R. Stoeger, S.J., "Anisotropy and inhomogeneity of the universe from Delta(T) / T," Astron. Astrophys. **309** (1996) L7 [arXiv:9510126 [astro-ph]]. 1, 39

[104] B. Mashhoon, F. W. Hehl and D. S. Theiss, "On the Gravitational effects of rotating masses - The Thirring-Lense Papers," Gen. Rel. Grav. **16** (1984) 711. 57

[105] S. Matarrese, O. Pantano and D. Saez, " General relativistic dynamics of irrotational dust: Cosmological implications," Physical Review Letters (1994) **72** 320–323 [arXiv:9310036 [astro-ph]]. 73

[106] S. Matarrese, O. Pantano and D. Saez, " A relativistic approach to gravitational instability in the expanding Universe – Second–order Lagrangian solutions," Monthly Notices of the Royal Astronomical Society (1994) **271**513 [arXiv:9403032 [astro-ph]]. 73

[107] S. Matarrese, S. Mollerach, and M. Bruni, " Relativistic second–order perturbations of the Einstein–de Sitter Universe," Phys. Rev. D **58** (1998) [arXiv:9707278 [astro-ph]]. 73, 111, 112

[108] A. L. Melott, B. S. Sathyaprakash and V. Sahni, "Evolution of the potential in cosmological gravitational clustering," Astrophys. J. **456** (1996) 65 [arXiv:9504087 [astro-ph]]. 31

[109] A. L. Melott, T. Buchert and A. G. Weiss, "Testing higher order Lagrangian perturbation theory against numerical simulations. 2: Hierarchical models," Astron. Astrophys. **294** (1995) 345 [arXiv:9404018 [astro-ph]]. 31

[110] A.A. Michelson and E.W. Morley, "On the Relative Motion of the Earth and the Luminiferous Ether," Philos. Mag. S 5 **24** (1887) 151 [arXiv:1108.0548 [hep-ph]]. 9

[111] M. Milgrom, "A Modification of the Newtonian dynamics as a possible alternative to the hidden mass hypothesis," Astrophys. J. **270** (1983) 365. 1

[112] V. F. Mukhanov, H. A. Feldman, and R. H. Brandenberger, “ Theory of cosmological perturbations,” Phys. Rep. **215** (1992) 203. 73

[113] M. Nakahara, “Geometry, topology and physics,” Boca Raton, USA: Taylor and Francis (2003) 573 p 119, 123

[114] J. J. Ostrowski, B. F. Roukema and Z. P. Bulinski, “A relativistic model of the topological acceleration effect,” Class. Quant. Grav. **29** (2012) 165006 [arXiv:1109.1596 [astro-ph.CO]]. 116, 118

[115] P. Peebles, “Large-Scale Structure of the Universe ” Princeton University Press (1980) 440 p 27

[116] A. A. Penzias and R. W. Wilson, “A Measurement of excess antenna temperature at 4080-Mc/s,” Astrophys. J. **142** (1965) 419. 19

[117] G. Perelman, “The Entropy formula for the Ricci flow and its geometric applications,” [math/0211159 [math-dg]]. 119

[118] S. Perlmutter *et al.* [Supernova Cosmology Project Collaboration], “Measurements of Omega and Lambda from 42 high redshift supernovae,” Astrophys. J. **517** (1999) 565 [arXiv:9812133[astro-ph]]. 13

[119] A. D. Polyanin and V. F. Zaitsev, “Handbook of exact solutions for ordinary differential equations,” Boca Raton: CRC Press (1995). 84

[120] C. Rampf and T. Buchert, “Lagrangian perturbations and the matter bispectrum I: fourth–order model for nonlinear clustering,” J. C. A. P. **06** (2012) 021 [arXiv:1203.4260[gr-qc]]. 74

[121] C. Rampf and Y. Y. Y. Wong, “ Lagrangian perturbations and the matter bispectrum II: the resummed one–loop correction to the matter bispectrum,” J. C. A. P. **06** (2012) 018 [arXiv:1203.4261[gr-qc]]. 74

[122] C. Rampf and G. Rigopoulos, “ Zel’dovich approximation and general relativity,” Mon. Not. Roy. Astron. Soc. **430** (2013) L54 [arXiv:1210.5446[gr-qc]]. 73

[123] S. Räsänen, “Backreaction: directions of progress,” Class. Quant. Grav. **28** (2011) 164008 [arXiv:1102.0408 [astro-ph.CO]]. 43

[124] A. G. Riess *et al.* [Supernova Search Team Collaboration], “Observational evidence from supernovae for an accelerating universe and a cosmological constant,” Astron. J. **116** (1998) 1009 [arXiv:9805201 [astro-ph]]. 13

[125] H. Robertson, “On the foundations of relativistic cosmology,” Proc. Natl. Acad. Sci. USA **15**, (1929), 822-829. 13

[126] B. F. Roukema, Z. Bulinski, A. Szaniewska and N. E. Gaudin, “The optimal phase of the generalised Poincare Dodecahedral Space hypothesis implied by the spatial cross-correlation function of the WMAP sky maps,” Astron. Astrophys. **486** (2008) 1, 55 [arXiv:0801.0006 [astro-ph]]. 116, 118

[127] B. F. Roukema, "Cosmic topology affects dynamics", Acta Physica Polonica B **42** (2011) 2273 [arXiv:1201.0971 [astro-ph.CO]]. 116, 118

[128] B. F. Roukema, T. Buchert, H. Fujii and J. J. Ostrowski, “Is the baryon acoustic oscillation peak a cosmological standard ruler?” [arXiv:1506.05478 [astro-ph.CO]]. 12

[129] X. Roy, T. Buchert, “On Average Properties of Inhomogeneous Fluids in General Relativity III: General Foliations, ” *in preparation.* 48

[130] C. Rovelli, “Quantum Gravity ” Cambridge University Press (2007) 488 p 9, 10, 32, 33

[131] H. Russ, M. Morita, M. Kasai and G. Börner, “ Zel’dovich–type approximation for an inhomogeneous universe in general relativity: second–order solutions,” Phys. Rev. D **53** (1996) 6881. [arXiv:9512071 [astro-ph]]. 73

[132] D. S. Salopek, J. M. Stewart and K. M. Croudace, “ The Zel’dovich Approximation and the relativistic Hamilton–Jacobi Equation,” Mon. Not. Roy. Astron. Soc. **271** (1994) 1005 [arXiv:9403053 [astro-ph]]. 73

[133] K. Schwarzschild, Vierteljahrschrift der Ast. Ges. **35** (1900) 67 118

[134] K. Schwarzschild, “Uber das Gravitationsfeld eines Massenpunktes nach der Einstein’schen Theorie” Sitzungsber. Preuss. Akad. Wiss. **7** (1916), 189-196. 11

[135] L. Smarr and J. W. York, Jr., “Kinematical conditions in the construction of space-time,” Phys. Rev. D **17** (1978) 2529. 49, 53

[136] D. N. Spergel *et al.* [WMAP Collaboration], “Wilkinson Microwave Anisotropy Probe (WMAP) three year results: implications for cosmology,” Astrophys. J. Suppl. **170** (2007) 377 [arXiv:0603449 [astro-ph]]. 118

[137] V. Springel, “The Cosmological simulation code GADGET-2,” Mon. Not. Roy. Astron. Soc. **364** (2005) 1105 [arXiv:0505010 [astro-ph]]. 28

[138] N. Straumann, “ General Relativity with Applications in Astrophysics,” Springer Verlag (2004) *ISBN 978-3-642-06013-7* 99

[139] R. A. Sussman, “Back-reaction and effective acceleration in generic LTB dust models,” Class. Quant. Grav. **28** (2011) 235002 doi:10.1088/0264-9381/28/23/235002 [arXiv:1102.2663 [gr-qc]]. 43

[140] R. Teyssier, “Cosmological hydrodynamics with adaptive mesh refinement: a new high resolution code called ramses,” Astron. Astrophys. **385** (2002) 337 [arXiv:0111367 [astro-ph]]. 28

[141] F. Tisserand, “Cosmological hydrodynamics with adaptive mesh refinement: a new high resolution code called ramses,” Compt. Rend. **75** (1872) 760 [arXiv:0111367 [astro-ph]]. 57

[142] R. Thieberger and M.-N. Célérier, " Scaling Regimes as obtained from the DR5 Sloan Digital Sky Survey," Classical and Quantum Gravity, **28**:164003 (2011) [arXiv:0802.0464 [astro-ph]]. 12

[143] W. Thurston, "The Geometry and Topology of Three-Manifolds " Princeton University Press (1997) 402 p 117, 119

[144] R. C. Tolman, "Relativity, Thermodynamics and Cosmology " Oxford, Clarendon Press (1934) 528 p 61

[145] R. C. Tolman, "Effect of Inhomogeneity on Cosmological Models," Proceedings of the National Academy of Science, **20** (1934), 169-176. 11

[146] K. Tomita, "Non–linear theory of gravitational instability in the expanding Universe," Prog. Theor. Phys. **37** (1967) 831 . 73

[147] K. Tomita, "Non–linear theory of gravitational instability in the expanding Universe. II. ," Prog. Theor. Phys. **45** (1971) 1747. 73

[148] K. Tomita, "Non–linear theory of gravitational instability in the expanding Universe . III.," Prog. Theor. Phys. **47** (1972) 416. 73

[149] R. Brent Tully, E. J. Shaya, I. D. Karachentsev; H. Courtois, D. Kocevski, L. Rizzi, A. Peel, " Our Peculiar Motion Away from the Local Void," The Astrophysical Journal, **676**, 1 (2008), 184-205 [arXiv:0705.4139 [astro-ph]].

[150] A. Walker, On Milne's theory of world-structure, P. Lond. Math. Soc. **42**, (1936), 90-126. 38
13

[151] S. Weinberg, "Gravitation and Cosmology: principles and applications of the general theory of relativity, " Jhon Wiley and Sons, Inc. (1972) 657 p 11

[152] S. Weinberg, "Cosmology," Oxford, UK: Oxford Univ. Pr. (2008) 593 p 96, 99

[153] A. G. Weiss, S. Gottlöber and T. Buchert, "Optimizing higher order Lagrangian perturbation theory for cold dark matter models," Mon. Not. Roy. Astron. Soc. **278**, 4 (1996), 953-964 [arXiv:9512106 [astro-ph]]. 31

[154] A. Wiegand and T. Buchert, "Multi-scale cosmology and structure-emerging Dark Energy: a plausibility analysis," Phys. Rev. D **82** (2010) 023523 [arXiv:1002.3912 [astro-ph.CO]]. 43

[155] A. Wiegand and T. Buchert, "Multiscale approach to inhomogeneous cosmologies," J. Cosmol. **15** (2011) 6100 [arXiv:1103.1531 [astro-ph.CO]]. 2

[156] A. Wiegand, T. Buchert and M. Ostermann, "Direct Minkowski Functional analysis of large redshift surveys: a new high–speed code tested on the luminous red galaxy Sloan Digital Sky Survey-DR7 catalogue," Mon. Not. Roy. Astron. Soc. **443** (2014) 1, 241 [arXiv:1311.3661 [astro-ph.CO]]. 12

[157] I. Ciufolini, J.A. Wheeler, "Gravitation and Inertia" Princeton Series in Physics (1995) 512 p 58

[158] D. L. Wiltshire, "What is dust? - Physical foundations of the averaging problem in cosmology," Class. Quant. Grav. **28** (2011) 164006 [arXiv:1106.1693 [gr-qc]]. 40, 43

[159] J. Yadav, S. Bharadwaj, B. Pandey, and T. Seshadri, "Testing homogeneity on large scales in the Sloan Digital Sky Survey Data Release One," Mon. Not. Roy. Astron. Soc. **364** (2005), 601-606. [arXiv:0504315 [astro-ph]]. 12

[160] R. M. Zalaletdinov, "Averaging problem in general relativity, macroscopic gravity and using Einstein's equations in cosmology," Bull. Astron. Soc. India **25** (1997) 401 [arXiv:9703016 [gr-qc]]. 40

[161] Y. B. Zeldovich, "Gravitational instability: An Approximate theory for large density perturbations," Astron. Astrophys. **5** (1970) 84. 2, 30, 73

[162] I. B. Zel'dovich and L. Grishchuk, "Structure and future of the 'new' universe," Mon. Not. Roy. Astron. Soc. , **15** (1984) 207 118